AN ASSESSMENT OF BREAST CANCER CELL INVASION INTO THE BONE MARROW

Thomas Laverty

MRes, BSc

Submitted in fulfilment of requirements for the degree of Doctor of Philosophy (PhD)

Centre for the Cellular Microenvironment

Institute of Molecular, Cell and Systems Biology

College of Medical, Veterinary and Life Sciences

University of Glasgow
Glasgow
G12 8QQ

December 2022

Abstract

Breast cancer is the most commonly diagnosed cancer in women. With the largest clinical problem coming in the form of metastasis. Breast cancer is known to metastasise to secondary tumour sites within the body, namely the liver, brain, lungs and bone marrow. Upon colonisation of the bone marrow, disseminated breast cancer cells (DBCC) interact with resident bone marrow niche cells such as mesenchymal stem cells (MSCs). These interactions are partly responsible for the phenomenon of dormancy observed in DBCCs. In time DBCCs can reawaken, resulting in recurrence and aggressive secondary metastasis, with a very poor clinical outcome for patients. In order for further investigation into this phenomenon, an in vitro dormant breast cancer cell model was developed using the breast cancer cell line MCF7. This model was then used to investigate the triggers of dormant breast cancer cell reawakening.

A hallmark of cancer is an altered metabolic profile, as such the model described above was utilised in order to investigate the influence of secreted factors likely present within the bone marrow niche, on the behaviour of dormant breast cancer cells. Conditioned media from both adipogenic and osteogenic lineage MSCs was shown to be capable of triggering proliferation in the dormant breast cancer cell model. Investigation into the contents of the secretome revealed several pathways shown to be upregulated. These pathways may have an effect on the reawakening of the dormant breast cancer cells. The most interesting pathways revealed by this analysis were the arginine and proline metabolism pathway along with citrulline metabolism, with both providing interesting avenues of exploration.

In this thesis a dormant breast cancer cell model is described and utilised in order to investigate potential triggers of reactivation. Using this model to screen various potential activators of the dormant cancer, the secretome of both adipogenic and osteogenic lineage MSCs was shown to cause an upregulation in the proliferation of dormant MCF7 cells. Specific metabolites of interest were identified such as ornithine, an intermediary molecule in the urea cycle, capable of generating arginine necessary for cellular proliferation. This model thus, can

be used for future experiments in order to further investigate the causes behind breast cancer cell dormancy and reawakening.

Table of Contents

List of Tables

List of Figures

Acknowledgements

Throughout my PhD I have received heaps of support from the both the CeMi and MeMi groups and am so grateful. I would like to thank my supervisor Prof Matt Dalby for all the help and guidance over the last 4 years, and for letting me undertake the project in the first place. Thank you also to Dr Catherine Berry and Prof Manuel Salmeron-Sanchez for guidance and sound advice throughout my work. Without the guidance and aid of my supervisors I wouldn't even have known where to start, I am forever grateful for their time and effort they have expended helping both with the creation of this thesis but also my own personal development.

I have greatly enjoyed working within our lab group. My express thanks go out Dr Monica Tsimbouri, Dr Alistair MacDonald, Dr Vineetha Jayawarna, Dr Mark Sprott, Dr Sara Bartlome, Carol-Anne Smith and Dr Udesh Dhawan. With special thanks to Monica and Al, without your input I would have certainly not completed my work (and lost my mind), I am forever grateful for your help and guidance. I would also like to thank all members of CeMi as well as those who have moved on for making this a truly enjoyable experience. I would also like to thank the University of Glasgow for their award of a studentship and ultimately allowing me to pursue this endeavour.

Outside of the lab, I would like to thank my parents Andrew and Catherine for always supporting me and encouraging me to pursue what I wanted. I am forever grateful for all the help and support you have given me throughout my life. I would also like to thank my grandparents for being so loving and supportive all throughout my life. You are all amazing and I wouldn't be here without your support. I am eternally grateful to my partner, Emily, not only for supporting me though my project but also for putting up with me (especially during the write up). I feel so lucky to be with you. You are thoughtful, smart and funny, without you I would surely not have gotten this far. Thank you so much

I would like to dedicate this work to my late grandad John Laverty an amazing person taken to soon.

Author's Declaration

I hereby declare that the research reported within this thesis is my own work unless otherwise stated, and at the time of submission is not being considered for any other academic qualification.

Thomas Laverty

December 22nd 2022

Abbreviations

A-2-P	Ascorbate 2 phosphate
AFM	Atomic force microscopy
ALI	Alanine
ALIX	Programmed cell death 6-interacting protein
ASC	Apoptosis-associated speck-like protein containing card
ATP	Adenosine triphosphate
BM	Bone marrow
BMP2	Bone morphogenic protein 2
BMPR	Bone morphogenic protein receptor
BMU	Bone Remodelling unit
BSA	Bovine serum albumin
CAF	Cancer associated fibroblast
CAR	Carnitine
CE	Capillary electrophoresis
CNS	Central nervous system
Col D	Collagenase D
Col I	Collagen I
Col IV	Collagen IV
Conc.	Concentration
CSC	Cancer stem cells
CTC	Circulating tumour cells
CXCL12	C-X-C motif chemokine ligand 12
CXCR4	C-X-C motif chemokine receptor type 4
DBCC	Disseminated breast cancer cells
DCIS	Ductal carcinoma in situ
DMEM	Dulbecco's modified eagle medium
DNA	Deoxyribonucleic acid
DTC	Disseminated tumour cells
EA	Ethyl acrylate
ECM	Extra cellular matrix
ELISA	Enzyme linked immunosorbent assay
EMT	Epithelial to mesenchymal transition

ERK	Extracellular signal-related kinases
ESCRT	Endosomal sorting complex required for transport
ETC	Electron transport chain
EV	Extracellular Vesicle
FBS	Foetal bovine serum
FCS	Foetal calf serum
FGF	Fibroblast growth factor
FH	Fumarate hydrogenase
FN	Fibronectin
GC	Gas chromatography
GF	Growth factor
GOF	Gain of function
HFN7.1	Fibronectin Antibody (HFN7.1)
HRP	Horse radish peroxidase
HSPC	Hematopoietic Stem and Progenitor Cells
HSC	Haemopoietic stem cell
ICW	In cell western
IGF	Intrinsic growth factor
ILC	Invasive lobular carcinoma
LA	Low adhesion
LC	Liquid chromatography
LDH	Lactate dehydrogenase
LOF	Loss of function
MAPK	Mitogen-activated protein kinase
MCF-7	Breast cancer cell line
M-CSF	Macrophage colony stimulation factor
MCTS	Monocarboxylate transporter
MET	Mesenchymal to epithelial transition
MHC	Major histocompatibility complex
MS	Mass spectrometry
MSC	Mesenchymal stem cell
MTT	3-(4,5-dimethylthiazol-2-yl)-2,5-diphenyltetrazolium bromide
MVB	Multi vesicular bodies
NADH	Nicotinamide adenine dinucleotide

NADPH	Nicotinamide adenine dinucleotide phosphate
NST	No specific type
OPN	Osteopontin
ORN	Ornithine
OSX	Osterix
P5F3	Fibronectin Antibody (P5F3)
PBS	Phosphate buffered saline
PCA	Principle component analysis
PCR	Polymerase chain reaction
PEA	Poly (ethyl acrylate)
POSTN	Periostin
pPEA	Plasma poly (ethyl acrylate)
RAB-7	Ras-related protein
RANKL	Receptor activator of nuclear factor kappa-B ligand
RGD	Arginylglycylaspartic acid
ROS	Reactive oxygen species
RUNX2	Runt-related transcription factor 2
SDH	Succinate dehydrogenase
SEM	Scanning electron microscope
T-evs	Tumour derived evs
TA-MSC	Tumour associated MSC
TCA	Tricarboxylic acid
TCP	Tissue culture plastic
TGF	Transforming growth factor
TSP1	Thrombospondin 1
ULA	Ultra-low adhesion
XPS	X-ray photoelectron spectroscopy

Chapter 1 Introduction

1.1 Cancer

The emergence of cancer is slow and ordered, and dependent on numerous factors. Cancer is a complex disease with an assortment of features that differ from case to case. The origin of cancer begins with healthy cells undergoing various genetic and phenotypic changes, influenced by external stimuli as well as changes to the microenvironment (Grange et al. 2011)(Jabalee, Towle, and Garnis 2018). Fibroblasts make up the majority of the tumour stroma and are particularly susceptible to phenotypic alteration in response to certain cues. Fibroblasts are known to undergo changes to their morphology dependant on a particular tumour environment, these changes lead to the adoption of a phenotype similar to that of myofibroblasts (Y. H. Song et al. 2017). As well as the phenotypic transformation of fibroblasts into myofibroblasts, tumour evs (T-EVs) have been shown to cause fibroblasts to transform into activated cancer-associated fibroblasts (CAFs) (Paggetti et al. 2015). The capacity for the transformation of fibroblasts into CAFs was found to directly correlate with the aggressiveness of the tumour cells. EVs (extracellular vesicles) derived from aggressive cancer cells correlated with high CAFs expression and conversely less aggressive cancer cells associated with a lower expression of CAFs (Giusti et al. 2018). Further research into role EVs play in tumorigenesis revealed that, CAFs secrete EVs that influence tumour progression, causing increased proliferation, epithelial to mesenchymal transition (EMT), motility and migration (Richards et al. 2017) (Donnarumma et al. 2017).

The induction of angiogenesis by cancers is well documented, this hallmark process however may be regulated at least in part by extracellular vesicles (Todorova et al. 2017). This is achieved through the horizontal transfer of pro-angiogenic molecules to resident epithelial cells, triggering tumour vascularisation (O'Loghlen 2018). T- EVs have been shown to increase tumour cell migration, tube formation, cell-cell adhesion as well increasing proliferation (Zhou et al. 2019). T- EVs secretion has been shown to be increased in hypoxic environments. As well as increased production of EVs, T- EVs derived from

hypoxic environments have been associated with increased angiogenesis compared with those derived from non-hypoxic environments (Umezu et al. 2014) (Grange et al. 2011).

Along with angiogenesis and fibroblast-differentiation, extracellular vesicles are highly involved in immunomodulation (Fatima and Nawaz 2017). EVs act as cell communication molecules for cells within the immune system (Isola and Chen 2017). Conversely to the effect of T-EVs, EVs have been shown to convey anti-cancer signalling to the immune system (Gilligan and Dwyer 2020). An example of this is EVs derived from dendritic cells trigger an anti-cancer immune response (H. Lee et al. 2019). These findings have caused excitement within the scientific community as their potential for anti-cancer therapeutics has become evident (Gilligan and Dwyer 2020).

1.1.1 Breast Cancer

Breast cancer is the most common form of cancer, followed by prostate and lung cancer, with around 55,000 new cases each year in the UK (Smittenaar et al. 2016). Breast cancer accounts for the second highest number of deaths relating to cancer in women, and the incidence rate is increasing both in developed and developing countries (Smittenaar et al. 2016). Many factors have been attributed to this rise in breast cancer incidences, such as: increased coverage of screening programmes, lifestyle changes and improvements in treatments, thus leading to an increasing number of women presenting with the disease.

Several tissue types are present within the breast including, mammary tissue containing lobules, ducts and glands along with fat and connective tissue (Boyd et al. 2010). Epithelial cells in ducts, lobules or within the connective tissue of the breast can manifest into a tumour, acquiring cancerous traits such uncontrollable growth, forming a noticeable lump on the breast (Chan and Lim 2010). These lumps formed are either benign or malignant, with benign meaning there is no metastatic spread from the regional tumour site, and malignant indicating that the cancer has metastasized to distant sites within the body. Despite extensive research efforts, the exact mechanism for the initiation of breast cancer is not completely understood.

Malignant breast tumours first invade the myoepithelial cell layer and basement membrane (Morrissey, Hagedorn, and Sherwood 2013). There has been a progression system from non-malignant to pre-malignant described in the literature, in this there are several stages in the development of a pre-malignant breast carcinoma (Scully et al. 2012). These steps include but are not limited to hyperplasia, atypical hyperplasia and cancer in situ. However, breast cancer is more complex than previously thought and this model of cancer progression doesn't accurately describe the progression of breast cell into malignant breast carcinoma. It has been shown that not all pre-malignant lesions result in breast cancer and that it is not essential for all lesions to be present to result in breast cancer. Specific pre-malignant lesions however have been shown to increase the risk factor for developing breast cancer (Scully et al. 2012).

Breast cancers are loosely split into two categories: invasive and non-invasive breast cell carcinoma. Non-invasive breast cancers are known as in situ carcinomas, with ductal carcinoma in situ (DCIS) being the most common (Chan and Lim 2010). As the name suggests DCIS form from epithelial cells in the ductal cell lining and since they have not invaded through the basement membrane they are described as pre-malignant (Sharma, Kelly, and Jones 2009). DCIS can be separated into 3 distinct categories; low, intermediate, and high grade with differing prognoses based on the classification (Hüsemann et al. 2008). It has been shown that the developmental mechanisms that lead to the formation of each DCIS category are markedly different. For example, high-grade DCIS is associated with a 17q gain, whereas low-grade DCIS has been linked to a 16q loss. A non-invasive DCIS isn't life-threatening, however a higher grade of DCIS is associated with higher instances of invasive cancer diagnoses, with DCIS being classified as a pre-cursor lesion (Chan and Lim 2010).

Invasive breast cancer, however, describes cells that are able to penetrate the basement membrane and spread to other tissues, most notably the lymph nodes and from there to distant sites within the body (Green et al. 2015). The most common type of invasive breast cancer is referred to as invasive carcinoma of no specific type (NST) while second is invasive lobular carcinoma (ILC). Together these subcategories make up about 95% of invasive breast cancers (Sinn and Kreipe 2013). The spread of invasive carcinoma to other tissues and distant sites

is known as metastasis, this is known to drastically worsen patient's prognoses as treatment options are limited.

1.1.2 Breast Cancer Metastasis

Metastasis is the complex, sequential process by which cancer cell dissemination occurs. This process is ordered by numerous steps leading ultimately to the colonisation of distant sites by cancer cells. These steps consist of; primary tumour growth, angiogenesis, intravasation, circulation, extravasation and ultimately colonisation(Langley and Fidler 2007). Primary tumours prior to dissemination undergo a process known as EMT, this process sees the cancer cells lose epithelial like traits such as cell adhesion and expression of E-cadherin and gain mesenchymal like traits, increasing their motility allowing for intravasation (Scheel and Weinberg 2012).

In order for cancerous cells to spread through the basement membrane, the extracellular matrix (ECM) is degraded, so that the cells originating from the primary tumour are able to invade the surrounding stroma through the basement membrane. Within the stroma, cells such as mesenchymal cells and fibroblasts have the potential to support the invading cancer cells, dependent on certain cell-cell signalling mechanisms (Khamis, Sahab, and Sang 2012). Following invasion into the stroma, cancer cells and the surrounding cells that make up the niche are modified, allowing intravasation into the blood and lymphatic circulatory systems (Kim et al. 2019). Following intravasation, the cancer cells are altered in order to survive, allowing them to evade immune surveillance(Scully et al. 2012). After these steps the cells extravasate (leave the circulatory system) and invade the parenchyma of distant sites (Sosnoski et al. 2015). Colonisation is the final step of metastasis, whereby cancerous cells originating from the primary tumour invade a secondary site and finally undergo mesenchymal to epithelial transition, whereby the cancer cells lose traits associated with mesenchymal cells such as motility and re-gain epithelial traits such as cell adhesion (Scully et al. 2012).

Upon completion of the metastatic cascade, disseminated tumour cells reside at the secondary niche, but despite extensive research into the metastasis and

dissemination of breast cancer cells little is known about this post-metastatic stage of breast cancer. Recent findings suggest that after dissemination many breast cancers undergo a period of dormancy(Clements and Johnson 2019a). Cancer cells in this dormant state resist traditional anti-cancer drugs, it is theorized that this is because the majority of therapeutic anti-cancer drugs work by interfering with the cell cycle, but due to these cells undergoing period of cell-cycle arrest they are able to evade these traditional treatments and reside within the post-metastatic niche(Cosentino et al. 2021). Due to this acquired ability to resist treatment these disseminated breast cancer cells (DBCCs) are the pre-cursor and cause of secondary tumour growth and metastasis, causing disease recurrence. The clinical problem that needs to be addressed in this disease is to develop a treatment capable of addressing dormant BCCs, however as little is known about the mechanisms of BBC dormancy further investigation is essential.

1.1.3 Breast cancer dormancy

Tumour cells disseminate and metastasize to distant sites. However, the majority of disseminated breast cancer cells do not survive to colonise the secondary site (Scully et al. 2012). Most of the disseminated breast cancer cells die in circulation or are unable to interact with resident cells at the secondary site. Cell-cell communication is essential to prime the microenvironment prior to the invading cancer cell arrival, this is to ensure the colonisation site is able to support the invading cancer cells (Dominiak et al. 2020).

Metastatic breast cancer cells have been shown to have an affinity for the bone marrow, where they interact with various niches via essential cell-cell communication pathways (see figure 1.2) (Walker et al. 2016). The colonising tumour cells adapt to their new microenvironment in order to survive and grow, these invading cancer cells evade immune detection and enter a state of prolonged dormancy (Bushnell et al. 2021a). In this state of dormancy, the cancer cells evade immune detection as well as traditional cancer therapeutics (see figure 1.2), this is due to most anti-cancer drugs influencing the cell cycle, thus in a state of dormancy the cancer cells resit these anti-cycling drugs (Bliss et al. 2016). In a state of dormancy, the invading cancer cells reside and survive

(See figure 1.1). However, upon escape from dormancy, these cancer cells form micro-metastases which have the potential to proliferate uncontrollably (Phan and Croucher 2020). This can lead to many complications including secondary tumours and also bone structure injury (Tsuzuki et al. 2016).

Traditionally metastasis was believed to be a relatively late event in tumour development. Recent studies, however, focused on identifying disseminated tumour cells (DTCs), revealing that DTCs are present in patients that show no evidence of metastatic disease (Bragado et al. 2013) (Cieślikowski et al. 2020)(Lerouge, Decruppe, and Humbert 1998). These findings, therefore, indicate that metastasis is in fact an early event in the development of certain tumours. This is shown in several clinical studies whereby disseminated tumour cells were identified in the bone marrow of breast cancer patients in the early stages of the disease (Hüsemann et al. 2008). Thus, this has emerged as a potential screening method for metastatic disease.

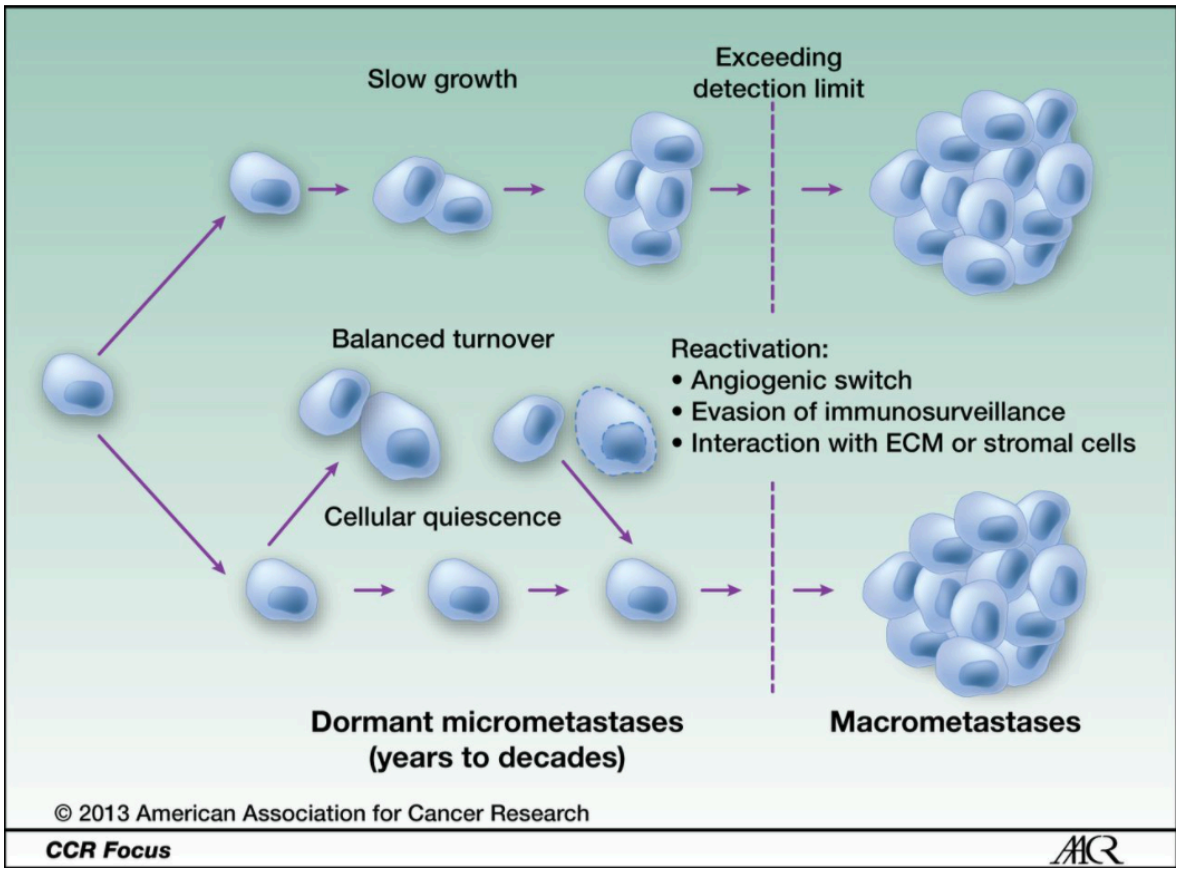

Figure 1.1 Mechanism of cancer dormancy after metastasis. Dormancy and reawakening will be investigated during this thesis. Cancer cells may grow slowly after dormancy eventually leading to a micrometastases after growing large enough to be detected. Cancer cells may also undergo a stage of death and synthesis which balances the live and dead cells, they

may also undergo cell cycle arrest in the G0/G1 phase. Image depicts potential routes for disseminated breast cancer cells Obtained from (X. H. F. Zhang et al. 2013).

Despite the potential of this screening method, there are some apparent drawbacks, namely patients testing positive for disseminated tumour cells but not presenting with metastatic disease (Cieślikowski et al. 2020). This is due to the ability disseminated tumour cells possess to remain silent or dormant for prolonged periods of time. These tumour cells can remain dormant in two distinctive states, either as mass tumour dormancy or tumour cell dormancy (Endo and Inoue 2019). Mass tumour dormancy describes a state whereby proliferation and cell death of the tumour mass is in equilibrium (Gimbrone et al. 1972). This is usually because of certain external influences such as the inability to evade immune surveillance, resulting in a constantly changing but dormant tumour mass. Tumour cell dormancy, however, is characterised by a state of cell cycle arrest in the G_0/G_1 phase. This state of dormancy is reversible, and proliferation can be re-activated though numerous means, such as exposure to cytokines, growth factors and response to changes in the microenvironment (Graham and Qian 2018). The mechanisms for both dormancy and the emergence from it are poorly understood, however certain stresses are known to play a pivotal role, these include hypoxia, drug treatment and starvation (Umezu et al. 2014). Along with these extrinsic factors various intrinsic factors are also important, such as epigenetic modifications(Sharma, Kelly, and Jones 2009). Despite the clinical significance of dormant cancer cells, there is little understanding of tumour cell dormancy, this is due to difficulties in detection, imaging and analysis of dormant cancer cells.

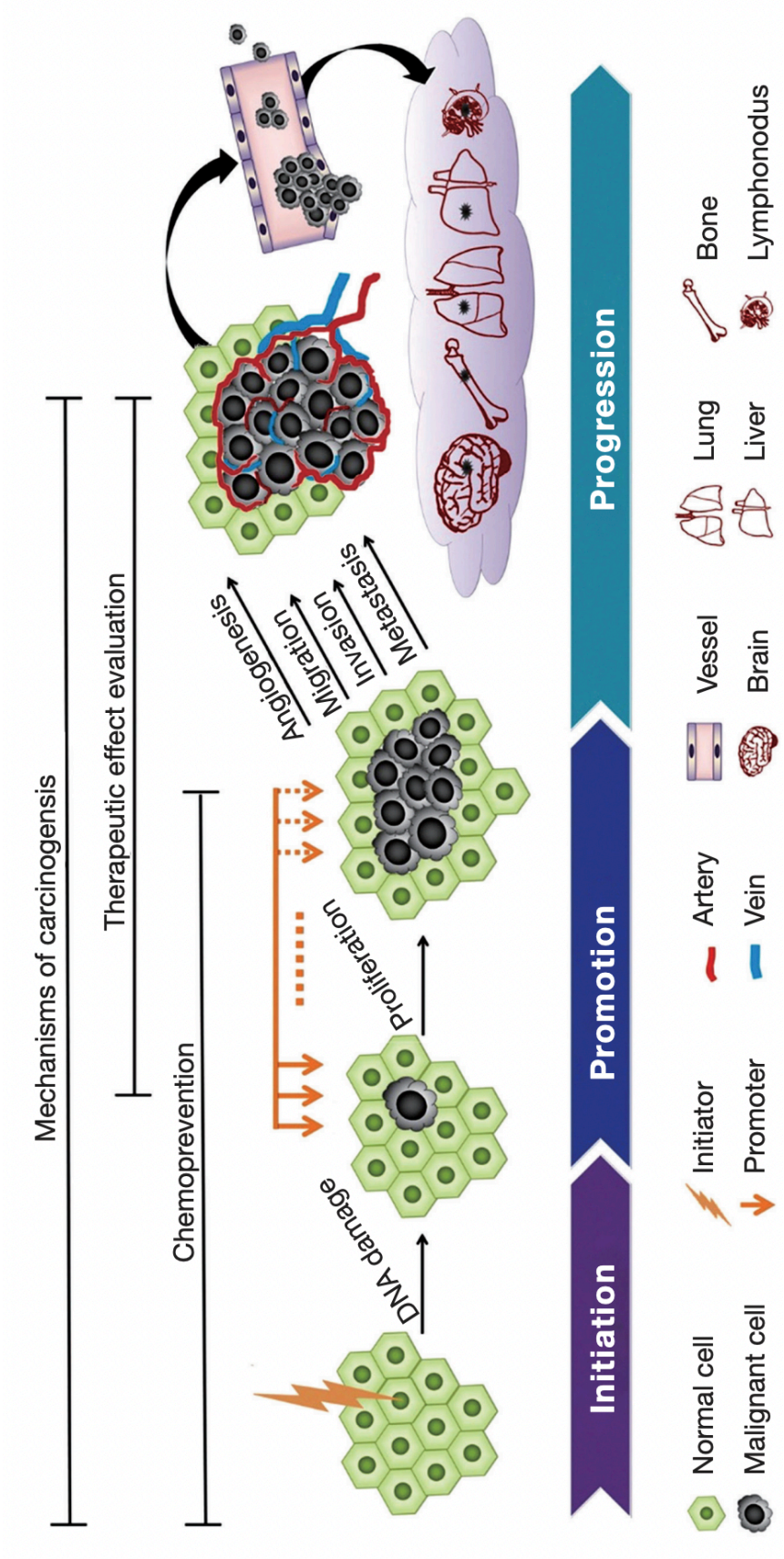

Figure 1.2 Tumour Development: cancer progression begins with DNA damage causing genetic mutation. This is followed by proliferation of cancerous cells. Some cells in the primary tumour then can detach undergoing EMT and gain motility. Disseminated cells then enter the circulatory system and spread to secondary sites within the body. Obtained from Liu et al (Yewei Liu et al. 2015).

1.2 The tumour microenvironment

Although the mechanisms involved in tumour cell dormancy are poorly understood, it is well known that both intrinsic and extrinsic factors are influential (Blache et al. 2019). This interaction between tumour cell and microenvironment is described as the 'seed and soil' hypothesis. Whereby the tumour cells (seeds) are capable of survival and growth in specific microenvironments (soil) (Fluegen et al. 2017). Thus, the capacity of a disseminated tumour cell to survive and prosper in a new site is dependent on the ability of the cell to communicate effectively with resident cells at the secondary site. The interaction between seed and soil is essential for tumour dormancy as it is tightly regulated via intrinsic and extrinsic factors (Bragado et al. 2013).

Disseminated tumour cells have the ability to colonise different sites in the body, thus demonstrating the plasticity of DTCs, as different colonisation sites would require different methods of adaptation for the DTCs due to differing selective pressures in specific niches. Disseminated breast cancer cells are most commonly found in bone, however, they have also been observed in the brain, liver and lung (Braun et al. 2000). Detection of DTCs in the bone marrow reservoir is now being used as a prognostic marker for metastatic disease in other organs (Rameshwar 2010). This is due to the fact that the blood circulating DTCs have a preference for the bone marrow, as here the DTCs can lie dormant evading the immune response and can re-disseminate to other organs once re-activated (H. Wang and Gires 2019).

1.2.1 The bone microenvironment

Bone is a dynamic organ, undergoing degradation and generation throughout life. This bone metabolism is essential for its role, maintaining the structure of the bone while also serving as a store of calcium as well as stem cells. Bone metabolism is regulated largely through two types of bone cell; osteoclasts and osteoblasts, which degrade and re-build bone respectively (Hadjidakis and Androulakis 2006). Osteoblasts are cells responsible for the creation of new bone tissue, they are derived from MSCs following the differentiation of said MSCs into

osteoblast precursors, maturation and mineralisation (L. Hu et al. 2018). Osteoclasts on the other hand are members of the monocyte/macrophage lineage, they differentiate depending on two essential cytokines: osteoblast derived receptor activator of nuclear factor kappa-beta ligand (RANKL) and macrophage colony-stimulating factor (M-CSF) (Boyle, Simonet, and Lacey 2003). Osteoclasts are known to release proteolytic enzymes that degrade the bone matrix, this in turn facilitates the release growth factors stored within the bone matrix. These growth factors have been shown to influence osteoblasts as well as cancer cells (see figure 1.3) (Shupp et al. 2018).

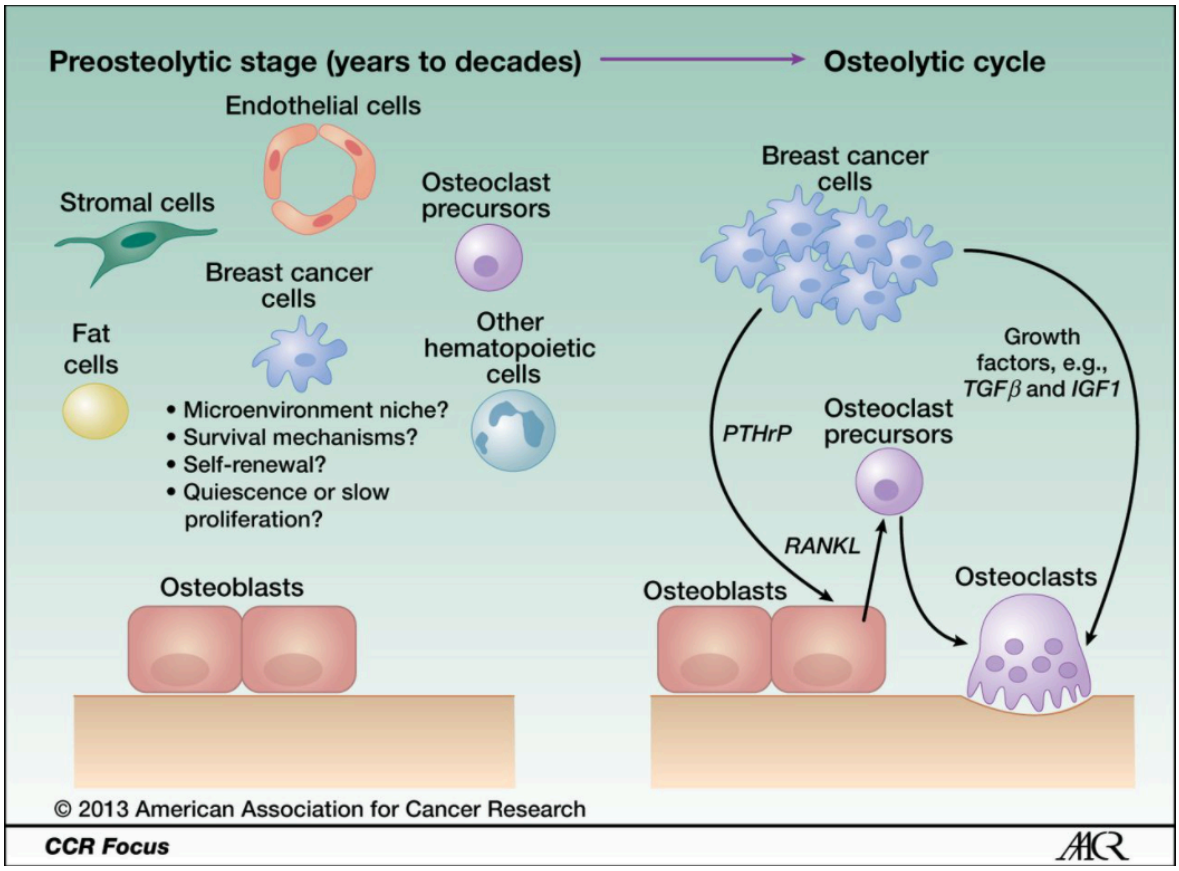

Figure 1.3 Depiction of cancer cells, along with other cells associated with the bone microenvironment before initiation of the 'vicious cycle'. This thesis will investigate the relationship between bone cells and dormant breast cancer. Right: Cell types involved with the viscous cycle, along with important signalling molecules. This image demonstrates the complex nature of bone remodelling and its relevance to disseminated breast cancer cells Obtained from (X. H. F. Zhang et al. 2013).

1.2.2 Bone remodelling

The constant state of change within the bone microenvironment is essential for proper bone function and for maintaining the quality of the bone. The basic multicellular unit (BMU) is the name given to the temporary structure responsible for the remodelling of bone. BMUs are found at various sites and are tightly regulated by the function of the main types of bone cells, osteoblasts, osteoclasts, osteocytes, and the bone lining cells. (Parfitt 2002) (Rucci 2008). With particular emphasis focused on osteocytes as key players in the complex process of bone remodelling. The constant degradation and synthesis of bone plays a key role in bone metastasis, this is emphasised by the 'vicious cycle' of bone metastasis (see figure 2) (Cook et al. 2014). This is characterised by the manipulation of osteoblasts and osteoclasts in order to obtain growth factors necessary for growth and invasion.

1.2.3 The Bone microenvironment supports tumour cell dormancy

Although the BMU is essential for bone remodelling, it does not represent the majority of the bone surface, with approximately only 20% of the bone surface undergoing active remodelling (Martin 2014). The vast majority of the bone surfaces however consist of bone lining cells, that are largely quiescent (Martin 2014). Osteoblasts, the bone cell responsible for the synthesis of bone tissue are known to produce a plethora of growth factors that are subsequently stored within the bone matrix (Rosenberg, Rosenberg, and Soudry 2012). These growth factors are then released into the bone microenvironment as osteoclasts degrade bone, the growth factors released are in active form (Neve, Corrado, and Cantatore 2011). They include bone morphogenetic protein 2 (BMP2), fibroblast growth factors (FGFs), insulin-like growth factors (IGFs) and transforming growth factors (TGFs), all of which can influence invading metastatic cancer cells, aiding the metastases (Xu and Teitelbaum 2013). Thus, the destination for a migrating tumour cell is essential for deciding its fate. If the circulating tumour cell were to arrive at a BMU, this microenvironment would be rich with growth factors that could trigger proliferation and growth. Conversely, if the tumour cell were to arrive at a site where no active BMUs are present and cells are

quiescent, this microenvironment may support tumour cell dormancy (Bragado et al. 2013). These highly specified microenvironments are essential for determining the fate of DTCs.

Stem cells within the bone microenvironment have been shown to highly influential in tumour cell dormancy, with the behaviour of invading DTCs having been shown to be comparable to the behaviour of the resident haematopoietic stem cells (HSCs) (Graham and Qian 2018). Regular function of HSCs is mediated by signals present within the HSC niche, particularly osteoblasts and endothelial cells within the niche. Homing of HSCs to osteoblast rich regions of the bone has been observed (Huang et al. 2017) (Yin and Li 2006). As well as HSCs, there is increasing evidence that DTCs localise to osteoblast rich regions of the bone, interacting directly with osteoblasts, supporting survival and tumour cell dormancy (Lawson et al. 2015). There is now increasing evidence that dormancy is a reversible process, with osteoblast and quiescent bone-lining cells interaction with DTCs switching it 'on' and interaction with osteoclasts switching it 'off' again, likely due to the release of bone-stored growth factors by osteoclasts (Lawson et al. 2015).

Although osteoblasts have been implicated in the survival and dormancy of DTCs, other cell types such as perivascular cells have been identified as important factors in tumour cell dormancy (Jahanban-Esfahlan et al. 2019). With increasing evidence showing DTCs homing and grafting to vascular areas within the bone. Breast cancer specifically has been shown to home to the bone vasculature, where signalling factors such as thrombospondin-1 promote tumour cell dormancy (Ghajar et al. 2013). However, along with factors promoting dormancy, within the bone vasculature, novel blood vessels secrete TGF-B1 (transforming growth factor-beta 1) and periostin, known to trigger the reverse of tumour cell dormancy and cause secondary tumour growth (Ghajar 2015).

Cells are recruited to the niche via the use of chemo-attractive signals and retained due to surface attachment proteins as well as extracellular matrix (ECM) proteins (Bushnell et al. 2021a). Growth factors and chemokines are also influential in the recruitment and retention of cells to this niche. However, the mechanisms that support the survival of DTCs and the reversal of tumour cell

dormancy are not well understood. Currently it is unknown whether tumour cell dormancy occurs as a consequence of signalling in the metastatic niche or signalling from the DTCs causes changes in the target microenvironment priming it for the introduction of DTCs.

1.3 Stem Cells

Stem cells are undifferentiated cells with the capacity for self-renewal. These cells can differentiate into a plethora of different cell lineages. Stem cells are further sub-categorised into different levels of developmental potency, with cells such as embryonic stem cells (pluripotent) having the potential to differentiate into any embryonic cell linage. Other cells such as adult stem cells (ASC) have a narrower scope for differentiation being unable to differentiate into any lineage, these cells are lineage specific (multipotent)(Sobhani et al. 2017). Stem cells are found throughout the body in distinct niches, the niches that stem cells reside in dictate the future of the stem cells, as the niche can either retain stem like characteristics via cycling quiescence or trigger differentiation via cell-cell signalling (C. Lee et al. 2021). Stem cell behaviour is regulated by the highly specialised stem cell niche, within the niche are a range of factors that control stem cell differentiation and quiescence (see figure 1.4) (Godoy et al. 2018).

These niches are specialised and distinct, with different categories of ASCs residing in specific niches. MSCs for example are perivascular and reside in the centre of the bone marrow (Ehninger and Trumpp 2011). Another example being epithelial stem cells residing in the budge of hair follicles. Stem cells in these niches are either maintained by the niche supporting quiescence or driven to differentiate into specific cell lineages(Sobhani et al. 2017). Although stem cell niches are specialised to certain stem cells, there are conserved properties in most stem cell microenvironments. These include specific cell-cell interactions, response to tissue damage and shared mechanistic properties dictated by the ECM Through the use of this tightly regulated niche-dependent regulation, the body can make use of localised stem cell population to repair damaged tissue, while when unused they reside in quiescence(Sobhani et al. 2017).

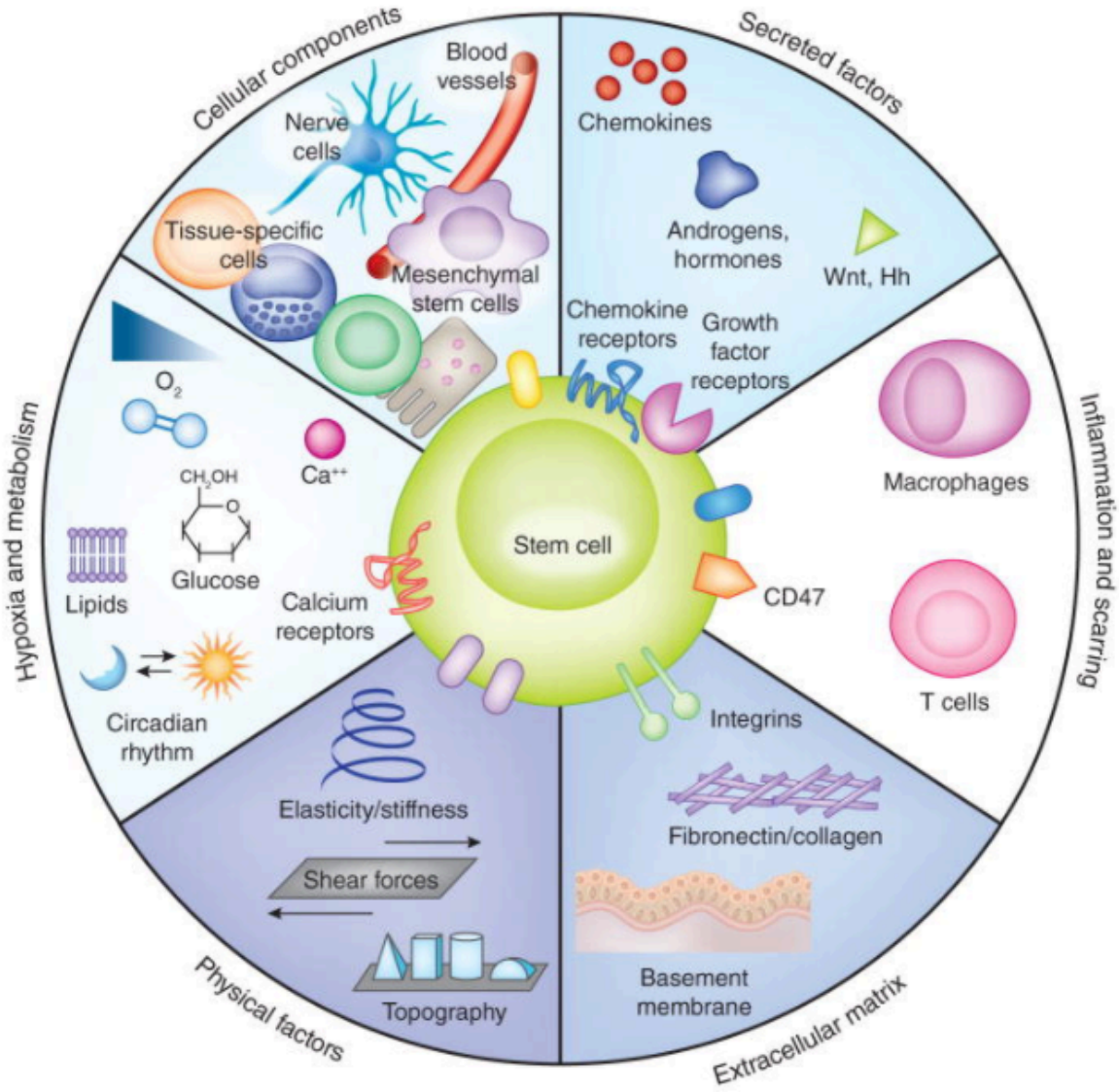

Figure 1.4 Factors that comprise the stem cell niche. Stem cell niches are comprised of heterotypic, dynamic structures. Stem cell maintenance and differentiation are strictly controlled by the inhabited niches. Stem cells and their niches communicate with each other in order to determine cell fate. Image describes factors known to influence the behaviour of stem cells Obtained from: (Lane, Williams, and Watt 2014).

1.3.1 Mesenchymal stem cells

MSCs are ASCs found in several different stem cell niches, such as the bone marrow and adipose tissue. They are characterised by their capability of differentiating into skeletal tissues along with their ability to self-renew (Donnelly, Salmeron-Sanchez, and Dalby 2018). MSCs must strike a balance between specialised differentiation in response to stimuli and maintenance of the stem cell pool, this balance is maintained by the stem cell niche.

MSCs are multipotent and capable of differentiating into a variety of different cell types, these include osteoblasts, chondrocytes, fibroblasts and adipocytes, the lineage of differentiation is dictated by the stem cell niche (Donnelly, Salmeron-Sanchez, and Dalby 2018). These cells are essential for tissue repair and synthesis of novel tissue; however, MSCs have been shown to be key contributors to the tumour microenvironment (Blache et al. 2019). MSCs have been shown to communicate with invading DTCs, promoting cancer progression, either through signals instructing DTCs to proliferate or conversely signals that drive the DTCs into dormancy via cycling quiescence in the G_0/G_1 phase of the cell cycle (Blache et al. 2019). It has been suggested that the interaction between resident MSCs and invading DTCs results in the conversion of MSCs into tumour associated mesenchymal stem cells (TA-MSCs) (Cappariello and Rucci 2019).

The isolation of MSCs is somewhat complex as they are present in various tissues and several subset groups exist, each with slightly different biological function. A group known as the International Society for Cellular Therapy has issued guidelines to define the minimum criteria for MSC classification. These include the ability to adhere to tissue culture plastic under regular tissue culture conditions. The cells must be positive for CD105, CD73 and CD90 while also being negative for various other markers including CD45, CD14, CD34 and HLA-DR surface molecules, and they also must be able to differentiate into osteoblasts, adipocytes and chondrocytes in vitro (Dominici et al. 2006). There are several methods of analysing the properties of MSCs in order to properly define them, these include analysis of the protein secretome, quantitative RNA analysis and flow cytometry analysis of surface markers (see table 1.1) (Galipeau et al. 2015). Despite these methodologies for identification of MSCs, there is no single marker that is associated with MSC stemness, however there exists a group of markers that can be used to identify specific subsets of MSCs with various biological functions. The resident cells in the BM are known to facilitate the function of other cells within the niche. Specifically, MSC like cells in the niche have been implicated in haematopoietic function (C. Lee et al. 2021).

Table 1.1 Table showing subpopulations of MSCs and marker used for identification. Details of the biological function of each subpopulation. BM: Bone marrow. (Lv et al. 2014; Galipeau et al. 2015; Dominici et al. 2006)

MSC Subpopulation	Location	Biological Properties
STRO-1+	BM	Enhanced Trafficking and tissue repair abilities. Promotes angiogenesis
CD271+	BM Adipose Tissue	Express higher level of differentiation related genes, Higher capability for tri-lineage differentiation
CD105+	BM Umbilical cord blood	Superior Myogenic potential
CD146+	BM Skeletal Muscle	Myogenic, capable of regenerating muscle cells Enhanced osteogenic differentiation
CD44+	BM	Increased proliferation, increased cell survival, modulation of cytoskeletal changes and enhances cellular motility
Nestin+	BM	Involved in HSC support and the formation of fibrotic lesions
CXCR4+	BM	Increased migration and engraftment Involved in the repair of ischemic injuries Enhances tissue repair capabilities
PDGFRα+	Foetal BM	Pro fibrotic Involved in tissue revascularisation
CD51+	Foetal BM	Capable of tri-lineage differentiation Higher proliferative capacity
CD49F+	BM	Involved in the maintenance of pluripotency Knockdown associated with differentiation

1.3.2 Haematopoietic Stem Cells

HSCs are responsible for the generation of all mature blood cells; they are multipotent and also capable of self-renewal. The process by which these cells generate blood cells is known as haematopoiesis. The function of HSCs is very tightly controlled to achieve haematopoietic homeostasis, this is done through a variety of means relying on specialized cells and signalling factors that ultimately regulate the HSC niche/microenvironment(L. D. Wang and Wagers 2011). As HSCs are multipotent, they are capable of differentiating into multiple cell types (these are limited however), one such cell type; oligopotent progenitor cells (greater limitation on differentiation potential) are ultimately

responsible for the production of mature human blood cells. This collection of multipotent and oligopotent progenitors is referred to as HSPCs (haematopoietic stem and progenitor cells), most cells present in this group with the exception of one subset of HSCs can be identified using the surface marker CD34 on the cell surface (Crane, Jeffery, and Morrison 2017).

1.3.3 Osteoblasts

Osteoblasts are extremely important in the maintenance and creation of bone tissue; they are responsible for the deposition of the bone matrix and also the regulation of osteoclast formation (Rosenberg, Rosenberg, and Soudry 2012). These cells are mononuclear specialized cells, while active they have a large cuboidal shape, enlarged endoplasmic reticulum and Golgi, and have the capability to secrete calcium containing vesicles. These cells are known to form tight cell junctions and develop specialised plasma membrane in order for higher efficiency vesicular trafficking and secretion (Rosenberg, Rosenberg, and Soudry 2012). Ultimately, after bone formation, osteoblasts are known to either apoptose or become osteocytes. Osteocytes are the most abundant cell type in the bone and are known to act as mechanosensors, instructing osteoblasts where and when to form bone and osteoclasts where and when to reabsorb bone tissue, this medium is essential for bone homeostasis (Neve, Corrado, and Cantatore 2011).

1.3.4 Endothelial Cells

Endothelial cells make up the lining of all blood vessels (arteries, veins and capillaries), they are known to form a sheet known as the endothelium and are responsible for the exchange between blood and the surrounding tissue (Krüger-Genge et al. 2019). The endothelium acts as an endocrine organ, the activity of which is responsible for controlling the level of vascular relaxation and constriction. The endothelium is also responsible for the extravasation of various molecules and proteins including macromolecules and hormones (Krüger-Genge

et al. 2019). As endothelial cells are present in capillary and sinusoids, and these structures are abundant in the bone marrow, endothelial cells play an integral role in the bone marrow microenvironment (Ito et al. 2017). The endothelial cells present in the bone marrow are physiologically distinct from those found in other areas of the body. Endothelial cells within the bone marrow are shown to express adhesion molecules and cytokines at a higher rate for those found in other tissues. Endothelial cells have also been shown to have a particular affinity for binding both CD44+ progenitors and megakaryocytes, thus bone marrow derived endothelial cells exhibit a regulatory role in haematopoiesis(Suzuki et al. 2010; Ito et al. 2017; Krüger-Genge et al. 2019).

1.3.5 Megakaryocytes

Megakaryocytes are present in the bone marrow niche and are responsible for platelet production. After maturation megakaryocytes are known to become polyploid (more than one pair of homologous chromosomes). In a process driven by cytoskeletal structures megakaryocytes extend long branch like structures into the sinusoidal blood vessels to release the platelets(Machlus and Italiano 2013).

1.3.6 Nerve Cells

Nerve cells, specifically those associated with the SNS (sympathetic nervous system) are implicated in the maintenance, structure, and function of the bone marrow(Morrison and Scadden 2014). The SNS is shown to regulate both the proliferation and differentiation of HSPCs, along with controlling the migration of cells between the bone marrow and extramedullary sites(Méndez-Ferrer and Fielding 2020). Large bundles of nerves are shown to enter the bone marrow with arteries, however the contact between the nerve terminals and the bone marrow is somewhat limited. The SNS is active and located in every area of the bone marrow(Méndez-Ferrer and Fielding 2020; Hanoun et al. 2015).

1.4 Secretome and Metabolism

1.4.1 Secretome

The term secretome is used to describe the total released molecules that are secreted from cells, tissues, organs, and microorganisms into the extracellular space. The term was first introduced by Tjalsma et al in 2000 and later revised by Agrawal et al to encompass all proteins secreted from a cell (Agrawal et al. 2010; Tjalsma et al. 2000). This definition however has been tweaked throughout the years as further research into the field allowed for a greater understanding surrounding the topic.

In the conventional protein secretion pathway, the secreted proteins usually contain N-terminus peptides which act as a guide allowing them to be transported to the Golgi apparatus from the endoplasmic reticulum. Following this, the Golgi then fuse with the plasma membrane allowing for the release of proteins (Malhotra 2013). There is however an unconventional pathway utilised within cells that includes Golgi-independent transport of integral proteins(Malhotra 2013). Along with proteins secreted from cells, the secretome is also known to encompass microRNAs, mRNA, DNA, lipids and metabolites. These secreted molecules are usually contained within specialist small membrane-bound vesicles known as extracellular vesicles. The secretome itself is highly dynamic and extremely sensitive to changes in the cellular environment, being able to alter the secreted molecules from the surrounding cells. This means that cells respond to changes in the environment by changing their own secretory pathways ultimately leading to further changes in the microenvironment (Blache et al. 2019). Many cancers are shown to take advantage of this in order to develop the microenvironment to allow for tumour growth. A functional secretome is essential for the homeostasis of the body, thus changes to this may lead to various systemic issues, including cancer (M. Wang and Kaufman 2016).

1.4.2 The Secretome in Cancer

The secretome of cancer stem cells (CSCs) has been implicated in the regulation of various different hallmarks of cancer such as: tumour growth and survival, angiogenesis, metastasis, drug resistance and immune dysregulation(López de Andrés et al. 2020). CSCs are able to communicate with and influence the tumour microenvironment through the release of micro-vesicles and exosomes along with a variety of soluble factors including metabolites, cytokines, growth factors, hormones and chemokines(Ye et al. 2014).

1.4.3 Extracellular Vesicles

Extracellular vesicles (see figure 1.5), originally believed to be largely unimportant machinery involved in cellular waste disposal, have been gaining great interest from the scientific community. This increased interest into these membrane bound vesicles came about after investigation into EVs revealed they are secreted by almost every cell in the body. Along with this, they were also found to be enriched for intracellular components (Johnstone et al. 1987). The first instances of cellular secretion of vesicles were observed in maturing reticulocytes, where the vesicles were being utilised to remove obsolete cargo and catabolites (Harding, Heuser, and Stahl 1983). However, it was not until later where research showed that these vesicles, named exosomes, have the capability to horizontality transfer cargo between donor and recipient cell(Dioufa et al. 2017). This was observed in the immune system, where exosomes, released from B-lymphocytes, acted as antigen presenters (Raposo et al. 1996). Since then, it is now widely accepted that exosomes are an integral part of cell-cell communication, and therefore potentially very important in the progression of diseases.

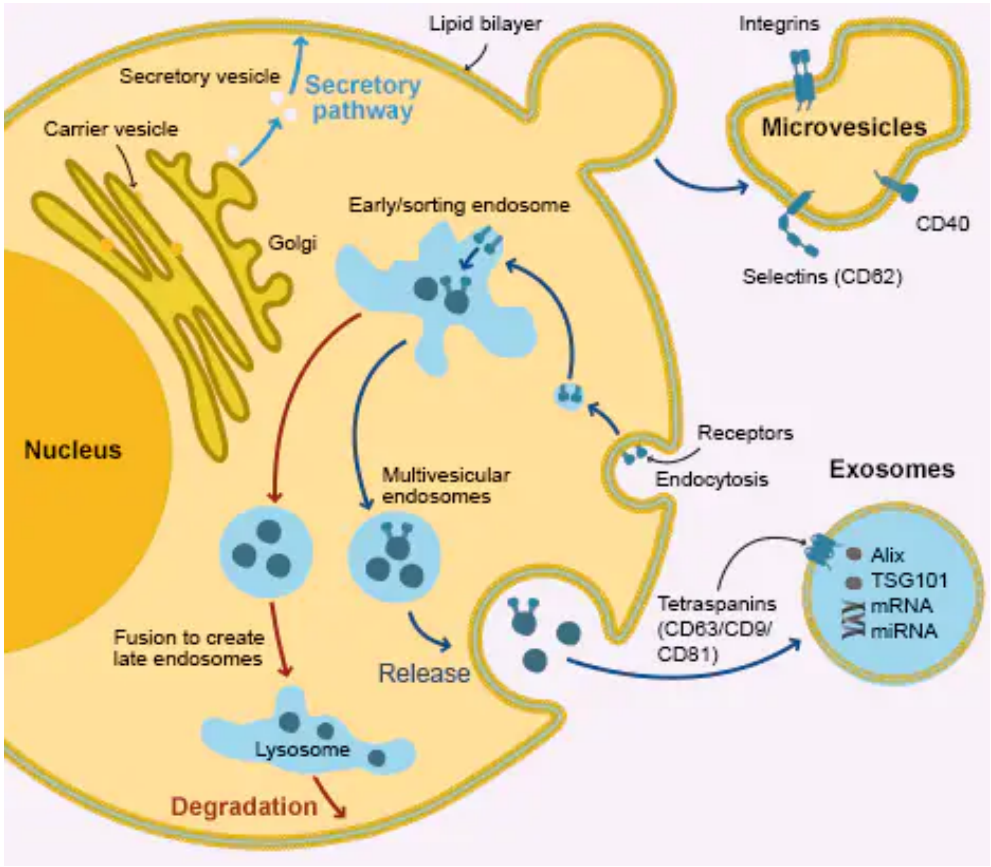

Figure 1.5 Diagram of the formation of EVs, indicating origin and mechanism of secretion. Image obtained from abcam, Extracellular vesicles: an introduction (https://www.abcam.com/primary-antibodies/extracellular-vesicles-an-introduction)

1.4.4 Extracellular Vesicle Characterisation

One potential pitfall in the study of EVs is the limited capacity to properly characterise different sub-populations. So far, EVs have been classified based on both their size as well as sub-cellular origin site, these different sub-populations of EVs are known as exosomes, micro-vesicles (MVs) and apoptotic bodies. Exosomes are the smallest of the populations averaging 50-150nm (Konoshenko et al. 2018). These EVs are formed in the multi-vesicular bodies (MVBs) in the endosome. Micro-vesicles on the other hand are larger than exosomes (150-500nm) and unlike exosomes, bud straight from the plasma membrane, as opposed to within endosomal compartments. The final sub-population of EVs are known as apoptotic bodies, these EVs are larger than both micro-vesicles and exosomes (1000-5000nm). They are known to be released from apoptotic cells and represent the final step in the apoptotic cells dying process, these steps include cell shrinkage, chromatin condensation, nuclear fragmentation, membranous blebbing and finally the breakdown of cells into apoptotic bodies

(Reed 2000). Although these are the generally accepted classification of EVs, recently these populations have been broken down into sub-categories depending on the cellular origin of the EV (Théry, Ostrowski, and Segura 2009).

Table 2 Classification of extracellular vesicles. Summary of the features used to characterise vesicles. Adapted from (Théry, Ostrowski, and Segura 2009)

Feature	Exosomes	Micro-vesicles	Apoptotic Bodies
Size	50-150 nm	100-1000 nm	1000+ nm
Appearance	Cup Shape	ND	Heterogeneous
Sedimentation	100,000g	10,000g	2000g
Intracellular origin	Endosomes	Plasma Membrane	ND

1.4.5 Synthesis and secretion of Extracellular Vesicles

As apoptotic bodies belong to a separate secretion process, exosomes and micro-vesicles are the two main sub-populations of EVs. Although aspects of sorting mechanisms are overlapped in the synthesis/secretion pathway of exosomes and MV, they are synthesised in different areas within the cell. Mvs are generated by outward budding direct from the plasma membrane, while on the other hand exosomes are synthesised within MVBs (multi-vesicular bodies), the MVBs then fuse with the plasma membrane in order to release the exosomes contained within.

1.4.6 Synthesis and secretion of Exosomes

Synthesis of exosomes occurs within multi-vesicular bodies. Multi-vesicular bodies (MVB) are a vitally important part of the endocytic pathway. This pathway is integrally involved in cellular homeostasis and is important in many functional aspects of the cell. It is known as an intermediary to degradation, and is essential for, proper recycling of cellular materials, cell polarity, cilia synthesis, cell signalling, cytokinesis and migration. It is known that early endosomes mature into MVB, and while doing so they generate intraluminal vesicles (ILVs) (Babst 2011). The formation of ilvs involves the inward budding of the plasma membrane of endosomes. Once MVBs are formed they fuse with either the plasma membrane, triggering the release of exosomes into the extracellular space, or they fuse with lysosomes, resulting in their degradation

(Van Niel, D'Angelo, and Raposo 2018). Due to this finding, it is evident that there exists multiple distinct sup-populations of MVBs (pre-exosomes) within the cell. These sub-populations are then directed to breakdown or secretion dependant on the survival of MVBs within the cell. By default, MVBs are programmed to fuse with lysosomes and be degraded. However, mechanisms are present within this pathway that allow MVBs to evade lysosomal degradation and fuse with the plasma membrane (triggering the release of exosomes) (Van Niel, D'Angelo, and Raposo 2018).

Exosomes are synthesised first as ilvs, this occurs during the maturation of endosomes to MVBs. This synthesis of exosomes is reliant on specific sorting mechanisms, these processes first designate cargo destination on the limiting membrane of MVBs, then cause the membrane to bud inward, forming ILVs (Piper and Katzmann 2007). The ESCRT (Endosomal Sorting Complex Required for Transport) machinery was identified as a key regulator of membrane shaping and scission, therefore this machinery is important in the synthesis of MVBs and ILVs. However, studies have shown that molecular mechanisms are in place for ilvs to be generated in an ESCRT independent manner (van Niel et al. 2011). The ESCRT complex executes its role in the formation of ILVs in a sequential manner and is comprised of four complexes (ESCRT-0, -I, -II, -III) (see figure 1.6). This machinery is also associated with several proteins ALIX (ALG-2-interacting protein X), VTA1 (Vesicle Trafficking 1) and VPS4 (Vacuolar protein sorting-associated protein)) that are required for the correct operation of this machinery (Hanson and Cashikar 2012).

Members of the ESCRT pathway are distinct from one another and operate collectively to cause the synthesis of ilvs. ESCRT-0 is a heterodimer consisting of HRS-STAM (Van Niel, D'Angelo, and Raposo 2018), this heterodimer binds specifically to enriched PI3P proteins on the MVB membrane where it organises ubiquitinated cargo. ESCRT-0 then recruits ESCRT-1, a hetero-tetramer comprising of VPS37A-D, TSG101, VPS28 and UBAP1 or MVB12A/B (Van Niel, D'Angelo, and Raposo 2018). ESCRT-1 binds ESCRT-0 and the clustered cargo forming a rod like shape, as well as recruiting the complex involved in the next step; ESCRT-II. ESCRT-II is another hetero-tetramer comprised of VPS36, VPS22 and two VPS25s. Through VPS36, ESCRT-II is able to interact with the complex as

is, binding ESCRT-1 and PI3P (Hanson and Cashikar 2012). ESCRT-II then recruits ESCRT-III, a hetero-tetramer comprised of CHMP2A-B, CMP3, CHMP6 and CHMP4A-C (Hanson and Cashikar 2012), this final component of the ESCRT machinery causes the membrane to bud inward and ultimately forms vesicles within the MVB. After the formation of the MVB contained vesicle, VPS4 causes triggers the degradation of the ESCRT complex finalising the vesicle generation (Caillat et al. 2019).

These findings suggest that vesicle formation is reliant of ESCRT-0 as that heterodimer triggers the cascade of the ESCRT pathway. Alterations in the ESCRT machinery effects the biogenesis and secretion of vesicles, but also can alter the cargo contained within said vesicles (Van Niel, D'Angelo, and Raposo 2018). As previously mentioned, exosomes can be generated by an ESCRT independent manner, this was discovered when parts of the ESCRT machinery were depleted and exosomes where still observed (Van Niel, D'Angelo, and Raposo 2018). One mechanism by which ILVs are formed in an ESCRT independent manner, requires the synthesis of ceramide via the hydrolysis of sphingomyelin by natural type-II sphingomyelinase (Trajkovic 2008). Ceramide, in this ESCRT independent pathway is metabolised into sphingosine-1-phosphate which in turn activates G1-protein-coupled sphingosine-1-phosphate receptor. This short pathway allows for the sorting of cargo onto the limiting membrane of MVBs (the first step of vesicle formation) (Kajimoto et al. 2013). Along with ceramide being essential in the ESCRT independent formation of vesicles, several tetraspanins have been shown to regulate the sorting of endosomal cargo. Most notably CD63, which has been shown to be enriched on the surface of exosomes, as well as being identified as essential for cargo sorting in exosomes associated with several diseases including Down syndrome (Gauthier et al. 2017) and melanoma (van Niel et al. 2015). Other tetraspanins including CD9, CD81 and CD82 have been implicated in the sorting of vesicular cargo. These tetraspanins form clusters and membrane platforms that recruit other tetraspanins, this is likely the formation of the micro-domains that will eventually bud inward forming the vesicles (Charrin et al. 2014). It is therefore evident that both ESCRT dependant and ESCRT independent mechanisms are responsible for the formation of ilvs and thus exosomes, however it is likely that the contributions of each member of either pathway may vary dependent on the

cell of origin, recruitment method and cargo contents (Van Niel, D'Angelo, and Raposo 2018).

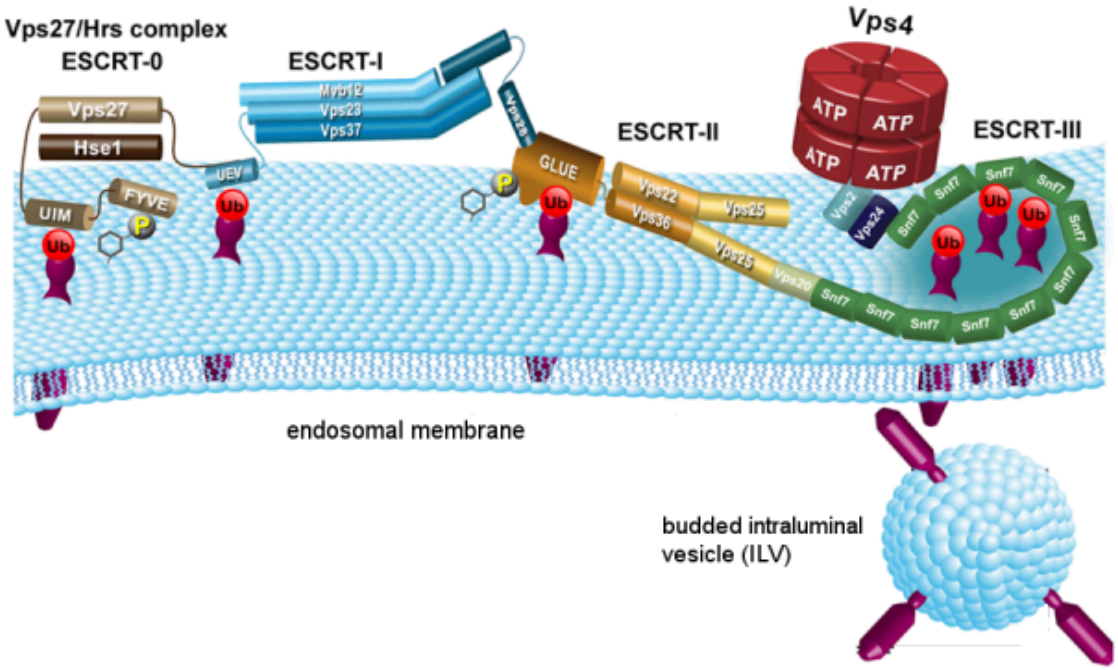

Figure 1.6 Schematic of the ESCRT Machinery. Four components of the machinery are recruited to endosomes though interactions with each other, membranes and ubiquitinated cargo. All but ESCRT III bind ubiquitinated cargo, however ESCRT III modulates the final steps of the machinery removing the ubiquitin and dissembling the complex. Budding from the membrane is facilitated by a curvature-inducing factor. Obtained from (Pakdel 2014).

Upon the synthesis of ilvs, the containing MVBs are directed to one of two outcomes, either degradation by lysosomal fusing or secretion by fusing with the plasma membrane. There exists a balance between the secretion and degradation of MVBs with sorting machinery and modifications to cargo playing an influential role in the outcome of MVBs. Both outcomes rely on a two-step process involving the transport and fusion of MVBs, however the protein involved in this trafficking are clearly distinct (Van Niel, D'Angelo, and Raposo 2018). Several processes are involved in intercellular transport, namely: the action of actin and microtubules, the action of important molecular motors and their interaction with molecular switches such as small GTPases (Bonifacino and Glick 2004). Lysosomal targeting is achieved by retrograde (reverse) transport on

microtubules via the use of dynein (retrograde molecular motor) recruited by RAB-GTPase RAB-7. Shockingly RAB-7 is also influential in the release (secretion) of exosomes, with the ubiquitylation status of RAB-7 dictating the outcome (P. Song et al. 2016).

The RAB family of proteins have been shown to be involved in endosomal sorting, with specific family members undertaking different roles (Wandinger-Ness and Zerial 2014). Along with RAB-7 being essential for maintaining the balance between secretion and degradation of exosomes, RAB27A and RAB27B are also essential for the secretion of exosomes (Bobrie et al. 2012). With RAB27B regulating the transport of MVBs to the plasma membrane, both RAB27 isoforms are involved in the docking of MVBs to the plasma membrane, promoting fusion. Thus, an increase in these RAB27 isoforms leads to increased exosome secretion (Van Niel, D'Angelo, and Raposo 2018). Other RAB proteins have been implicated as modulators of exosome secretion through either direct regulation or the priming of MVB secretion, these include RAB 35 and RAB11 (Hsu et al. 2010) (Savina et al. 2003). The ultimate steps that lead to the fusion of MVB with the plasma membrane are still largely unknown; however, it has been postulated that this process involves mediation by SNARE and synaptotagmin proteins (Jahn and Scheller 2006).

1.4.7 Synthesis and secretion of Micro-vesicles

As MVs are formed from the budding of the plasma membrane, the mechanisms by which the synthesis and secretion of MVs is completed, overlap. Also interesting is the observation that formation of MVs from the plasma membrane seems to have relationship to the formation of other structures generated from the plasma membrane (Tricarico, Clancy, and D'Souza-Schorey 2017). The secretion/formation of micro-vesicles relies on the fission of the plasma membrane, this is known to be regulated by the interaction of actin and myosin followed by an ATP-dependant contraction (D'Souza-Schorey Crislyn and Clancy 2012). Due to this activation of GTP binding proteins, namely, ARF6 and ARF1 results in actomyosin contraction (Muralidharan-Chari et al. 2009). This contraction is achieved through the phosphorylation of the myosin light chain,

the result of said contraction is the budding of MV from the plasma membrane (Muralidharan-Chari et al. 2009).

GTPases are important in the regulation of general membrane dynamics, with the Rho family of GTPases being specifically implicated (Guan et al. 2020). It has been shown that RhoA and Rac1 play key roles in the regulation of micro-vesicle formation. With RhoA being linked to the formation and shedding of micro-vesicles and conversely Rac1 shown to negatively regulate this process (Sedgwick et al. 2015).

Along with these mechanisms for the formation of micro-vesicles, lipids have been shown to contribute to their synthesis (Muralidharan-Chari et al. 2010). This is evident as cholesterol rich regions within the plasma membrane have been shown to play a pivotal role in the shedding of micro-vesicles (Al-Nedawi et al. 2008). Thus, the regulation of cell membrane phospholipid asymmetry is highly influential regarding the budding of micro-vesicles, several proteins have been implicated in this regulation, including flippases/floppases and scramblases (Hankins et al. 2015). These proteins are involved in the movement of specific phospholipid species across the plasma membrane(Hankins et al. 2015), and thus may be influential in the synthesis and secretion of micro-vesicles.

1.4.8 Extracellular Vesicle Cargo

The cargo contained within extracellular vesicles is highly heterogeneous, comprising of DNA, mRNA, miRNA, lipids as well as proteins(Isola and Chen 2017; Xie et al. 2019; O'Loghlen 2018). Identifying which cargo associates with which extracellular vesicle is very difficult, this is largely due to the fact that EV isolation techniques are non-standardised, and non-specific. Upon isolation of EVs from serum or growth media, several different sub-populations of EVs will be precipitated, thus, it is challenging to draw association between cargo contents and vesicle of origin. Due to this, there is gap in knowledge regarding markers to specifically select for particular exosomes, as such further research must be conducted.

There is a great variety and abundance of vesicle cargo, the heterogeneity of these vesicles comes about due to vesicles being cell-type specific and can be influenced by several factors. These factors include the pathological or physiological state of the cell of origin, along with response to stimuli that regulate their production. Interestingly, the first regulator of extracellular vesicle formation is the cargo itself (Van Niel, D'Angelo, and Raposo 2018). It has been shown that ectopic expression of certain cargoes, such as the major histocompatibility complex class II (MHC) can trigger MVB formation and ultimately lead to the release of exosomes containing said protein (Ostrowski et al. 2010). This has been a common finding, as a large proportion of vesicle cargo has been shown to be synthesis and secretion factors. Along with these factors important for EV synthesis and secretion, proteins involved in the remodelling of the plasma membrane as well several tetraspanins (CD81 and CD9) have been purified from EVs (Doyle and Wang 2019), these proteins are currently being used as identifying markers for EVs (Anand et al. 2019).

Along with proteins and lipids, it has been shown that extracellular vesicles also contain genetic material. The first evidence of this was the detection of RNA and observation of the horizontal transfer of said RNA in mast cells (Valadi et al. 2007). After this initial finding further research into the cargo contents of extracellular vesicles was undertaken, DNA along with non-coding RNA was identified in EVs (Lázaro-Ibáñez et al. 2019) (see figure 1.7). However, very little is known about the mechanisms responsible for sorting genetic material into EVs (Anand et al. 2019), despite this, the discovery of genetic information in EVs could potentially lead to them being used a circulating biomarker. Currently there is limited understanding regarding the lipid contents and function within extracellular vesicles, however it has been shown that certain lipids (such as cholesterol) are enriched within extracellular vesicles (Pfrieger and Vitale 2018).

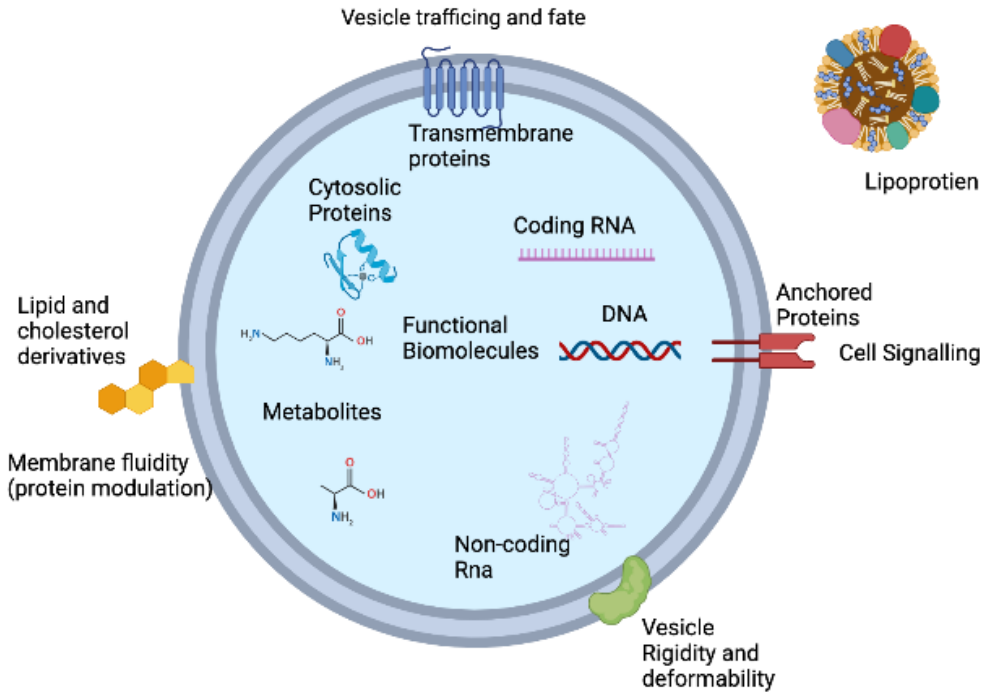

Figure 1.7 Composition of EVs. Image showing the potential contents of Extracellular Vesicles, along with membrane bound surface proteins. (created in biorender).

1.4.9 Uptake of Extracellular vesicles

After EVs have been secreted into the extracellular space, they are known to interact with other cells. As previously mentioned EVs contain a variety of cargo that can significantly alter the phenotype of the recipient cell. For this effect to take place, EVs need to transfer their cargo to the recipient cell. EVs are known to fuse with target cell membranes, either endosomal membrane after endocytic uptake or via the cell plasma membrane (Mulcahy, Pink, and Carter 2014).

It has been shown that the major method of EV uptake is endocytosis, with EVs being transported to endosomal compartments within the cell. Experimental evidence suggests that EV uptake by endocytosis is an energy dependant process that makes use of cytoskeletal proteins. Several methods of EV endocytosis have been described, such as clathrin-mediated endocytosis, caveolin-dependant endocytosis as well as others (Mulcahy, Pink, and Carter 2014).

Although endocytosis is the most common method of EV uptake, EVs can also bind directly with the cell plasma membrane, it has been postulated that the EVs bind to the external leaflet of the plasma membrane via surface interactions with resident proteins (Mulcahy, Pink, and Carter 2014). Several protein families have been identified as influential in this process, including, RAB, SNARES and SEC1/MUNC type proteins (Beer and Wehman 2017). This method of EV uptake occurs via the fusion of lipid bilayers (encasing the EV and cell), these lipid bilayers, when in close proximity, fuse and form a hemi-fusion stalk (McNeil and Steinhardt 1997). The stalk then expands to form a hemi-fusion diaphragm bilayer (Tsai, Chang, and Lee 2014), this structure then causes an opening in the membrane through a pore, the contents are then released within the cell. The two previously distinct lipid bilayers form a consistent structure due to their hydrophobicity (Chernomordik, Melikyan, and Chizmadzhev 1987).

1.4.10 Extracellular vesicles and cancer

After the revelation that extracellular vesicles are capable of horizontally transferring information to recipient cells, EVs have gained great relevance in both physiological and pathological processes. It is well known that most cell types release EVs, tumour cells are not exempt from this and are known to release tumour specific vesicles (Cappariello and Rucci 2019). This release of T-EVs is known to influence the tumour microenvironment. T- EVs have been shown to influence intercellular communication, allowing for tumour signalling to both surrounding tumour cells along with distant sites (Jabalee, Towle, and Garnis 2018)(Jabalee, Towle, and Garnis 2018).

Upon this discovery, a major focus of EV research in regard to tumours is focused on the tumour stroma, particular fibroblasts, immune cells and endothelial cells (Cappariello and Rucci 2019). These genetic and phenotypic changes lead eventually to the acquisition of traits such as uncontrolled growth and the ability to invade surrounding tissues and disseminate to distant sites (Scheel and Weinberg 2012). The interaction between cancer cells and different cell types in the tumour microenvironment further adds to the complexity of this disease(Blache et al. 2019).

Each distinct tumour will vary greatly depending on the genetic background of the original cell, site of neoplastic legion and external stimuli. However, despite this, there is known to be common, essential modifications leading to uncontrolled growth and spread (Sinn and Kreipe 2013). These essential modifications are observed in the majority if not all cancers. The common modifications leading to malignant growth involve; evasion of apoptosis, insensitivity to anti-proliferative signals, acquisition of replicative immortality, angiogenesis and intravasation (Hanahan and Weinberg, 2000).

Along with these common traits known for some time, recent research has identified other common traits associated with cancer growth and spread. These include the ability of cancer cells to reprogram metabolism and evade the immune response (Gonzalez, Hagerling, and Werb 2018). The accumulation of these traits leads ultimately to the malignant growth and spread of the tumour. However, the acquisition of these traits relies heavily on the correct genetic remodelling of the cells surrounding the initial tumorous cell (Gonzalez, Hagerling, and Werb 2018). Therefore, genetic instability has been described as a hallmark of tumour progression (Yixin Yao 2014). Along with genomic alterations, epigenetic modifications have also been implicated in the progression of tumours, via methylation and de-methylation of promoters of genetic elements influential in the development of a metastatic tumour (Sharma, Kelly, and Jones 2009).

1.5 Metabolism of quiescent and proliferating cells

The state of differentiation of normal cells controls their metabolic requirements. All live cells are somewhat metabolically active requiring different metabolites depending on state of the cell. Non- dividing or quiescent cells are metabolically active in order to achieve their physiological function and also to maintain their structure. Quiescent cells are also known to undergo redox reactions and balance energy. Proliferating cells, however, require different metabolites in order to generate the molecules required for cell growth, these are in the form of simple metabolites used to generate macromolecules necessary for cells growth (M. G. vander Heiden 2011). These metabolites include amino acids, fatty acids and nucleotides. Stringent control systems are in

place for all cellular processes including metabolic reactions. This control system is achieved through cell signalling molecules part of a greater cell signalling system (Zheng 2012). The networks that are involved in the regulation of metabolic reactions within the cell are comprised of several genes, including proto-oncogenes and tumour suppressors that are heavily linked to the formation of tumours. Thus, alterations in the normal signalling may result in cell cycle arrest and/or apoptosis.

Normal cells usually reside in close proximity to blood vessels. Therefore, they usually have access to the required nutrients and oxygen needed for regular cellular function. Metabolites associated with normal cells include fatty acids, sugars and amino acids; these are usually readily available and as such normal cells make use of these in their environment. The differences between normal and proliferating cells can be observed in the metabolites they require for their activity (Zhu and Thompson 2019). Although the necessary metabolites are present in the cellular environment, they must be transported across the cell membrane. This is usually achieved using specialised transporter molecules, these metabolites can also be directly catabolised in order to generate ATP (adenine triphosphate). Normal (non-proliferating) cells are known to generate their ATP using mitochondrial metabolism, which uses NADH to drive the electron transport chain (oxidative phosphorylation). Proliferating cancer cells however are known to switch from oxidative phosphorylation to glycolysis for their ATP (M. G. V. Heiden, Cantley, and Thompson 2009). NADH is recycled to NAD+ (able to accept electrons from the ETC), in normal cells this is achieved through mitochondrial respiration, however in proliferating cells this can be achieved through both mitochondrial respiration and lactate production.

1.5.1 Cellular metabolism in cancer

Cancer metabolism has been studied for quite some time, with early discoveries by Otto Warburg and his colleagues shaping the research landscape (Otto Warburg, Wind, and Negelein, 1927). He observed in the 1920s that malignant liver cells obtained from rodents used glycolysis to generate cellular ATP, this is despite the presence of oxygen (Otto Warburg, Wind, and Negelein; Erson and Brooklyn, 1927). This accompanied by increased lactate secretion observed in

cancerous cells was termed aerobic glycolysis, otherwise known as the ‘Warburg effect’. These findings therefore prompted Warburg to hypothesise that emergence of cancerous cells was due to the inhibition of mitochondrial respiration. However, this was disproven in the 60s when genetics and genetic remodelling was found to be heavily influential in cancer development. Despite this however, the phenomenon that cancer cells favour aerobic glycolysis over oxidative phosphorylation persists. One potential explanation for this is that many important metabolic processes required for the synthesis of more complex macromolecules rely on intermediates from the glycolytic pathway. However, genetic changes, not impaired mitochondrial function have been shown to drive the flux in glycolysis in cancer cells, these genetic changes include changes to proto-oncogenes and downregulation of tumour suppressors. It has also been shown that cancer cells may favour glycolysis to reduce the generation of ROS (reactive oxygen species) (Zheng 2012). Therefore, the metabolic reprogramming observed in cancer cells is essential for the synthesis of many of the metabolic ‘building blocks’ necessary for cell growth(Lunt and Vander Heiden 2011a; V. R. Fantin and Leder 2006). (See figure 1.8)

Cancer cells are known to alter their environment through various mechanisms. One method is to influence the metabolite composition of their immediate environment. As cancer cells need an increased nutrient influx and have an increased metabolic rate, the rate at which by-products are produced is also increased. Thus, tumour cells secure mechanisms of toxic by-product removal to stabilise the tumour microenvironment (Justus, Sanderlin, and Yang 2015).

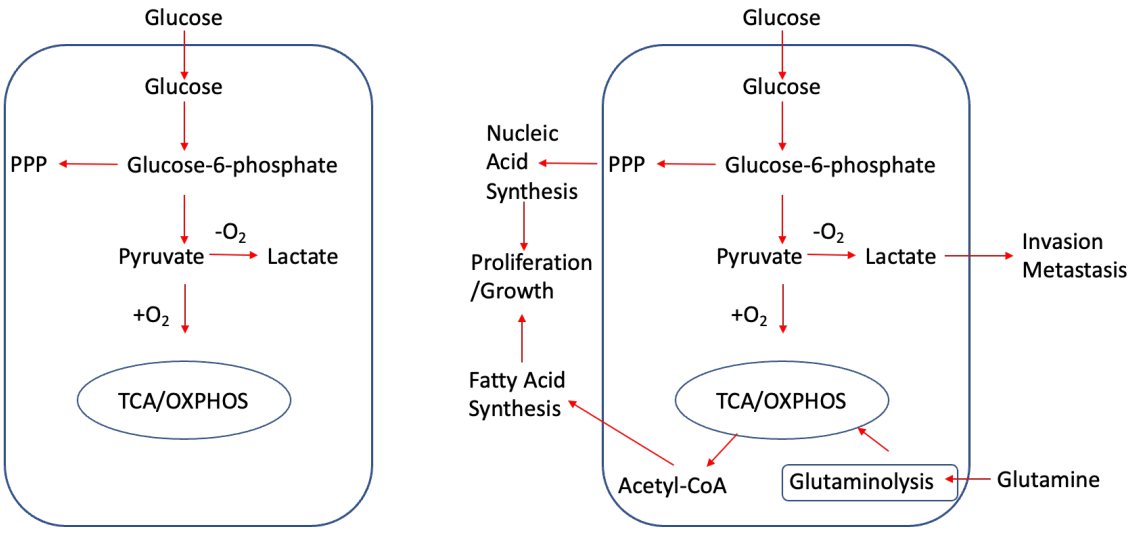

Figure 1.8 Metabolic differences between normal (left) and cancer cells (right). Normal cells are known to metabolise glucose into pyruvate which is then oxidised to CO_2 through the TCA cycle and OXPHOS. Cancer cells are known to convert glucose to lactate through anaerobic respiration, this is due to the need for metabolic intermediates for growth by cancer cells. Adapted from (Jóźwiak et al. 2014)

1.5.2 Glycolysis

Glycolysis (see figure 1.9) is part of the metabolic processes that help govern homeostasis within the cell. The process involves converting 1 mole of glucose into 2 moles of pyruvate, resulting in the generation of two moles of ATP and two moles of NADH(Yetkin-Arik et al. 2019). The cell type and environment they reside in are the determining factors in the fate of the glucose-derived pyruvate. Where oxygen is abundant, pyruvate is transported into the mitochondria and undergoes oxidation through the ETC, this produces CO_2 ultimately and results in the generation of 36 moles of ATP for each mole of glucose (Zheng 2012). In a hypoxic (oxygen deprived) environment however, the glucose-derived pyruvate is converted into lactic acid. A catalyst known as lactate dehydrogenase (LDH) is responsible for this reaction, while also replenishing NAD^+ from NADH. However, in proliferating tissue, lactate is mainly produced through pyruvate as opposed to oxidative phosphorylation. The lactate produced by anaerobic respiration is converted back into pyruvate and glucose via the liver. Pyruvate therefore is central in energy metabolism, with its fate determined by the both the energy demands of the cell as well as the anabolic processes necessary for cell growth (Zhu and Thompson 2019).

Breast cancer, among several others including lung cancer, show a high expression of the catalyst LDHA which is responsible for the regeneration of NAD^+. Inhibition of this enzyme has been shown to arrest/slow the proliferation of tumour cells while under hypoxic conditions(Valeria R. Fantin, St-Pierre, and Leder 2006). Along with this, inhibition of LDHA causes a metabolic switch from aerobic glycolysis to oxidative phosphorylation, resulting in greater ATP production. In tumours, the inhibition of this enzyme has also been shown to cause a reduction in tumour formation(Valeria R. Fantin, St-Pierre, and Leder 2006). Therefore, LDHA function is an essential part of tumour development.

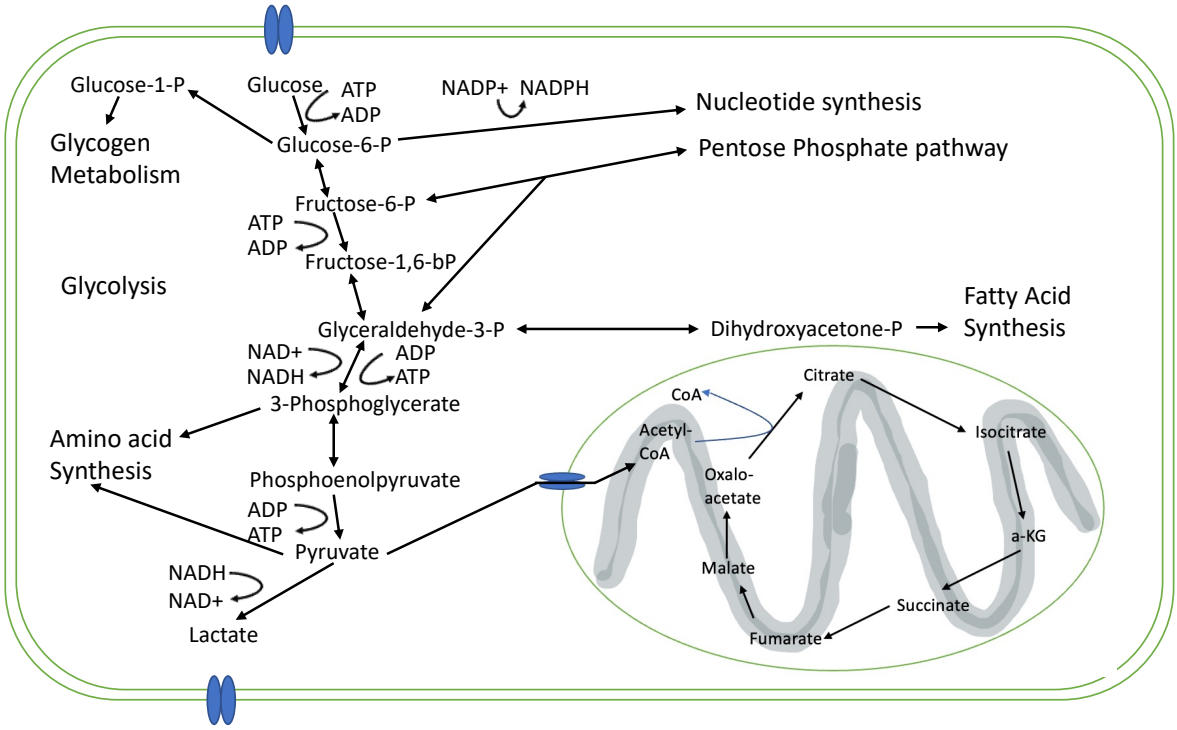

Figure 1.9 Schematic overview of the metabolic reactions responsible for the conversion of glucose into pyruvate via glycolysis. Metabolic intermediates act as precursors to various metabolic processes such as amino acid and fatty acid synthesis. Under regular conditions glucose is metabolised into CO2 by the mitochondria resulting in the production of ATP. Cancer cells however are known to utilise aerobic glycolysis by which most (>90%) of glucose molecules are converted into lactate, which is later secreted.

1.5.3 Glutaminolysis

Glutaminolysis is the process by which glutamine is converted, via glutamate, to α-ketoglutarate (see figure 1.10). Glutamine is present in the body as the highest abundance and most versatile amino acid. Glutamine is extremely important in intermediary metabolism, pH homeostasis and also nitrogen exchange pathways(Cruzat et al. 2018). In most cells in the body glutamine is used as a substrate for several metabolic pathways. These essential mechanisms include nucleotide synthesis, antioxidant synthesis, NADPH (nicotinamide adenine dinucleotide phosphate) synthesis amongst other pathways essential for maintenance of cellular function (Curi et al. 2005). Glutamine is also used to generate pyruvate through the oxidative carboxylation of malate and thus can contribute to the regeneration of NADPH(Alberghina and Gaglio 2014). An important gene known as c-MYC is shown to be a master regulator of glutaminolysis. This proto-oncogene (a gene capable of inducing cancer when mutated) is shown to be overexpressed in several cancers (D. M. Miller et al. 2012). Cells that are overexpressing c-MYC are shown to be highly dependent on glutamine for reasons mentioned above. This phenomenon is known as glutamine addiction. The effect of this ‘addiction’ can be seen in the cell’s activity, with altered transcriptional programming in order to upregulate the expression of enzymes involved in glutaminolysis as well as transporters of glutamine (Wise et al. 2008).

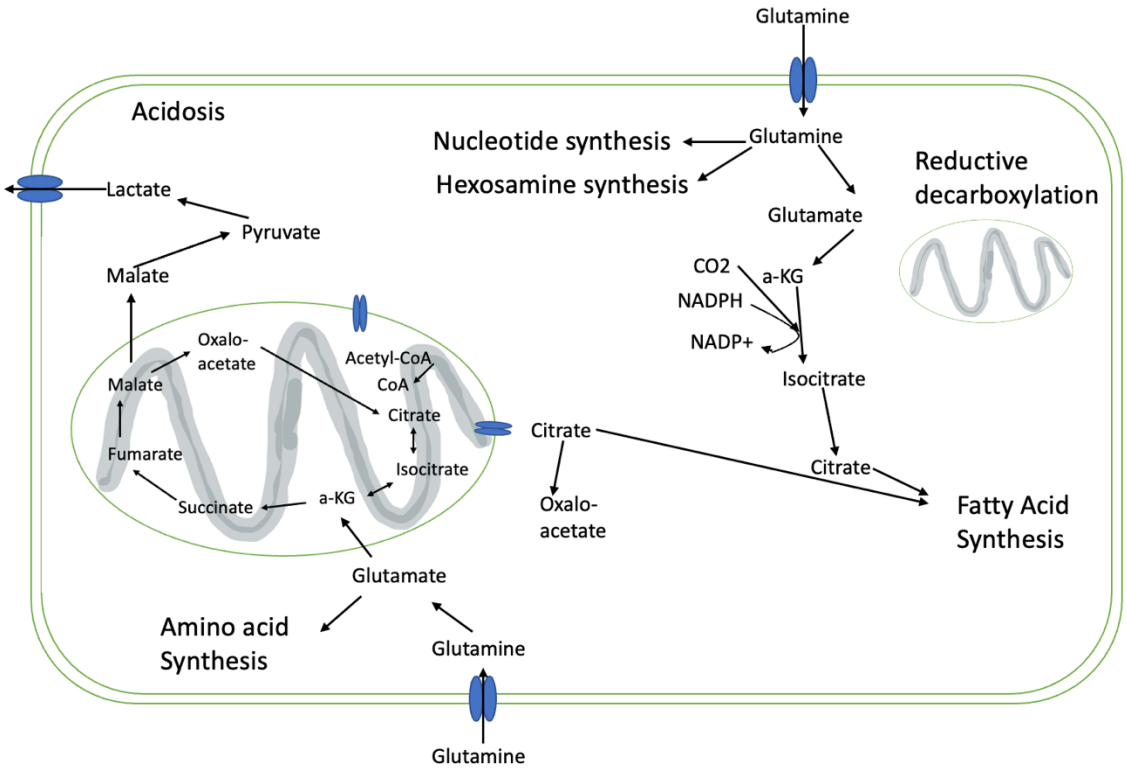

Figure 1.10 Schematic overview of glutaminolysis. Many cancer cells exhibit glutamine addiction. These cancer cells use glutamine as a substrate for anaplerosis of the TCA cycle.

1.5.4 Synthesis of Amino Acids

Amino acids are necessary for the construction of proteins, they are usually obtained from the from the cellular environment, known as essential amino acids. Some, however, are unobtainable from the environment and need to be synthesised by several intracellular reactions, known as non-essential amino acids. There are several pathways responsible for the synthesis of amino acids, these include glycolysis, the TCA cycle and glutaminolysis(Cao et al. 2019).
A specific pathway that has been implicated in the survival of cancer is the serine pathway. This pathway is known to divert from 3-phosphoglycerate during glycolysis, this has been observed as all enzymes associated with this pathway are shown to be overexpressed in cancer (L. Sun et al. 2015).

1.6 Growth factors and signalling molecules

Growth factors and signalling molecules deliver fate-determining signals to cells, the capacity for cells to respond to changes in growth factor signalling governs homeostasis. As such growth factors and other signalling molecules are important regulators of various aspects of cellular biology such as development of the microenvironment, wound healing and homeostasis. Due to their far-reaching influence, growth factors have been implicated numerous cancers (Cohen and Levi-Montalcini 1956). Alterations in regular growth factor signalling are observed in many cancers, with oncogenes being identified as potential substitutes for growth factors in order to initiate autocrine signalling in the tumour (Witsch, Sela, and Yarden 2010). The transformation of regular cells into cancerous cells involves the accumulation of a number of genetic mutations (Witsch, Sela, and Yarden 2010), however the expression of altered growth factors facilitates proliferation and progression, clonal expansion and invasive growth (Witsch, Sela, and Yarden 2010).

1.6.1 BMP2 in breast cancer

Bone morphogenetic proteins (BMPs) are a diverse set of growth factor proteins with over 20 members belonging to the TGF-B superfamily (Huang et al. 2017). It has been shown that BMP-2 induces EMT (epithelial to mesenchymal transition) leading to a loss of epithelial traits and gain of traits such as motility (M. Singh et al. 2018). Recent studies have also shown that exposure to pollutants can trigger activation of the BMP-2 pathway and thus may contribute to cancer cell stemness (Huang et al. 2017). The mechanisms by which BMP-2 promotes breast cancer metastasis are widely unknown (Huang et al. 2017).

Interestingly studies have shown that BMPs have a paradoxical effect on cancers, by both promoting and inhibiting cancer progression (Peng et al. 2016),(F. Hu et al. 2013). BMP-2 specifically has been shown to inhibit cancer growth by causing arrest in G1 phase (A. Chen et al. 2012). However, BMP-2 has also been shown to trigger EMT, migration and invasion of breast cancer cells. It has been postulated that the two roles of BMP-2 may be explained by the timing of BMP-2 expression. Early expression of BMP-2 in a cancer triggers BMP-2 induced apoptosis, as in the

early stages the number of tumour cells is relatively low, the impact of apoptosis is more severe. However, once the tumour cell numbers have increased EMT and stemness caused by BMP-2, are now more significant owing to the greater number of tumour cells (Huang et al. 2017).

Interestingly rhBMP-2 was shown to trigger the formation of tumour cell spheroids along with increasing the number of $CD44^{+}/CD24^{-}$ cells within the tumour population (Huang et al. 2017). Suggesting that rhBMP-2 induces breast cancer cell stemness. Along with this effect rhBMP-2 was found to significantly downregulate Rb and E-cadherin, Rb is a tumour suppressor, acting by inhibiting genes involved in progression through the G1-S phase of the cell cycle (Vélez-Cruz and Johnson 2017).

BMP-2 promotes breast cancer stemness and EMT via CD44 and Rb signalling pathways as both CD44 and Rb are key mediators of the rhBMP-2 pathway (C. Chen et al. 2018). Also implicated in these pathways, namely the regulators of Rb and CD44, are the Smad and PI3K/AKT pathways (Delston et al. 2011) ultimately leading to breast cancer metastasis and stemness.

1.6.2 CXCR4/CXCL12 axis

The CXCR4/CXCL12 axis has been shown to be instrumental in the metastasis of breast cancer to specific areas of the body. The chemokine receptor CXCR4 and its ligand CXCL12 have been shown to induce proliferation, survival and invasion of cancer cells (Y. Sun et al. 2014). High levels of CXCR4 expression have been observed in breast cancer cells, this along with high levels of expression of the CXCR4 ligand CXCL12 in target tissues leads to the direct migration of tumour cells to metastatic target tissues (Zhao et al. 2014) (Y. Sun et al. 2014). This may mean that the preference for metastatic breast cancer for the bone marrow may be dictated via mechanisms like this. This was shown by inhibition of CXCL12 in mouse stromal fibroblasts delaying the time of tumour onset along with reduction in the amount of distant metastasis (Ahirwar et al. 2018). Thus, CXCL12 expression in MSCs may lead to the migration of metastatic breast cancer to the bone marrow.

1.7 Biomaterials

Biomaterials represent a very exciting field in medicine, specifically regenerative medicine. Biomaterials have been shown to be functionally useful in the field of regenerative medicine such as the delivery of drugs to localised areas and the creation of artificial organs(Vienken J 2008; Khandare and Minko 2006). Traditionally three types of biomaterials are used, these being natural, synthetic, and ceramic. With each holding advantages and disadvantages over the others. The use of polymers is an emerging field that is gaining a lot of traction in recent years, as the applications of polymers, in regard to biomaterials, are numerous (Pradhan and Slater 2019; Leslie-Barbick et al. 2011). Both natural and synthetic polymers are currently being used in research, with each holding advantages over the other, with natural polymers such as collagen being biodegradable, biologically active and exhibiting solid cell-cell interactions(Vienken J 2008). However natural polymers such as collagen also have drawbacks, such as poor processability and reproducibility. Whereas synthetic polymers are largely the opposite. Biomaterials then provide a highly tuneable and expandable mechanism for both research and regenerative medicine(Pradhan and Slater 2019).

Biomaterials are a versatile tool to improve several aspects of cellular function, including cellular adhesion, proliferation, biocompatibility and differentiation (Elkhenany et al. 2015). Biomaterials can be synthesised in different ways; surface modification is particularly useful and can be inexpensive. Altering the surface of potential biomaterials can improve cell-cell interactions along with cell-protein interactions (Alba-Perez et al. 2020a).

Two distinct methods of coating a biomaterial onto a surface are regularly used, these being spin-coating and plasma polymerisation. The traditional method of spin-coating relies on a liquid-vapor interface on the surface being coated, then uses centrifugal force to distribute the sample in an even film over the surface (Moreira, Vale, and Alves 2021). Plasma polymerisation however relies on ionisation of an organic monomer gas through a high frequency electrical discharge (Sprott et al. 2019; Sprott 2019). Plasma polymerisation may be used to deposit layers of polymer onto various surfaces, including other polymers,

metals, and ceramics (Sprott 2019; Sprott et al. 2019). It's a relatively inexpensive and effective method to coat biomaterials in order to increase cell adhesion and presentation of various proteins (Sprott 2019). Plasma polymerisation involves cross-linking of monomeric units after fragmentation resulting in a randomly organised polymer. A benefit of using plasma polymerisation over traditional wet-solvent methods is, time efficiency, as it is significantly quicker than wet-solvent methods. The coating is also highly cross-linked structure meaning that there is a higher level of substrate to coating adhesion. Plasma is also capable of efficient deposition of polymer on 3D printed structures (porous and non-porous) (Sprott et al. 2019). There is no need for solvent-based treatments when using plasma polymerisation, thus reducing potential cytotoxicity. This is also important as plasma does not require pre-treatment of the biomaterial in question, again shortening the time needed to perform polymer coatings. A fine control of polymer thickness also gives plasma polymerisation an edge over traditional solvent-based coating techniques (Alba-Perez et al. 2020a) (Thissen 2016).

It has previously been shown that poly(ethyl acrylate) (PEA) is capable of acting as a surface biomaterial, triggering fibronectin (FN) into its open conformation (Llopis-Hernández et al. 2016), thus increasing the efficiency of growth factor presentation (Z. A. Cheng et al. 2018). Nanofibrillar FN organisation is triggered upon binding with PEA, this in turn leads to the exposure of both the growth factor (GF) and integrin binding domains (Alba-Perez et al. 2020a). It has been shown that plasma polymerised PEA is similarly able to initiate open FN conformation and GF presentation, in particular ultra-low doses of hBMP-2. This presentation of BMP-2 when interacting with MSCs triggers osteogenesis in vitro and bone formation in vivo, thus demonstrating the capability of plasma PEA (Alba-Perez et al. 2020b). Plasma PEA will therefore be used to coat tissue culture plastic for the efficient presentation of GFs and signalling molecules, in order to alter the secretome and investigate downstream effects. Before seeding with cells, various surface characterisation is necessary, such as AFM (atomic force microscopy), XPS and ELISA to determine the depth, resolution and binding site affinity of the surface coating.

1.8 3-D Culture Methods

Spheroids are described as cellular aggregates and can be generated through a variety of different techniques; these cell aggregates have been utilised more recently to generate 3D cultures of various cell types. Spheroids can facilitate cell-cell interactions replicate nutrient/oxygen gradients and are also able to generate their own ECM(Cui, Hartanto, and Zhang 2017; Gunti et al. 2021). There have been several methods of spheroid generation described including hanging drop of culture medium, restricted adhesion conditions (liquid overlay) and magnetic levitation using magnetic nanoparticles(Cui, Hartanto, and Zhang 2017).

As solid tumours grow in 3D space, they are subject to heterogeneous exposure to both oxygen and nutrients. Previously, investigations into cancers in vitro have relied on cancer cells seeded in a monolayer, though this is far from optimal due to the 3D nature of cancer cells in vivo(Cui, Hartanto, and Zhang 2017). Thus, 3D methods of culturing cancer cells in vitro have been utilised over the past few decades in order to study various cancers. The reason for this is spheroids provide a robust 3D model of cancer in order to study various aspects of cell biology including proliferation, differentiation, apoptosis and metabolism of the cells in a solid tumour model, and their response to different stimuli.

Spheroids of a large size (>500um) have been shown to be comprised of several different layers of cells, with the centre of the structure under hypoxic conditions while the outer layer of cells are active and proliferating(Nath and Devi 2016). Thus, these cell aggregates behave largely in the same manner as micro-metastases and avascular tumours in vivo. The necrotic core is surrounded by a layer of quiescent cells capable of acquiring nutrients from the environment and then compressed by a layer of proliferating cells able to migrate into the surrounding environment (Wallace and Guo 2013). Therefore, spheroid culture is optimal for studying breast cancer dormancy/recurrence in vitro.

1.9 Hypothesis and aims

In order to better understand the mechanisms behind breast cancer dormancy and recurrence, it is clear that the interplay between MSCs and invading cancer cells needs to be further investigated. This PhD aims to investigate the potential triggers for reawakening of dormant breast cancer. This will be achieved via the creation of a functional in vitro dormant breast cancer cell model, then using this model to assess various different potential triggers obtained from conditioning media using differentiating MSCs.

State of the art studies have looked at several methods of both modelling the disease and investigation into therapeutics. Namely the emergence of EVs as potential initiators of both dormancy and reawakening has been telling, with several research groups choosing to focus on this aspect of breast cancer dormancy (Sandiford et al. 2021; Hernández-Barranco, Nogués, and Peinado 2021; Al-Awsi et al. 2023). Alongside the study of EVs as a potential cause of reactivation, several research groups have decided to develop in vitro models of dormant breast cancer in order to test growth factors, metabolites and drugs ex vivo. These research groups employ different strategies to develop a dormant model, including serum deprivation (growth of breast cancer cells under serum deprived conditions mimicking nutrient-deprived environment), with another being 3D culture (utilised in this thesis) (Pranzini, Raugei, and Taddei 2022; Bushnell et al. 2021b). Ultimately both fields are developing year on year, and both are vitally important to the overall knowledge surrounding breast cancer metastasis and dormancy. This thesis will aim to further develop knowledge surrounding this area, namely in the design of an in vitro model of dormant breast cancer and investigation into the effects of the secretome of bone marrow niche cells along with post differentiation cells (adipo and osteo lineages)

The hypothesis of this study is that differentiating MSCs release factors and metabolites that influence the phenotype and behaviour of invading micro-metastases, the aims of the PhD are as follows:

- Optimisation of cell culture techniques in order to generate a stable, dormant breast cancer cell model for in vitro testing. These include a

liquid overlay method to generate MCF7 spheroids as well as a high-density seeding methodology.

- Characterisation of the MCF7 spheroid model in terms of triggering a dormant phenotype. These include as assessment of cell viability, structural characterisation through microscopy, expression of various genes associated with dormant breast cancer cells and also expression at the protein level of proliferation associated factors.

- Trigger differentiation of MSCs in vitro into osteoblast and adipocyte lineages, this will be achieved through various techniques, namely through the use of supplemented media shown to induce differentiation. This will also be achieved through the use of a biomaterials system, comprised of plasma polymerised PEA (poly(ethyl acrylate)), fibronectin and various growth factors, designed to trigger the differentiation of MSCs. Cell culture medium will then be conditioned using these differentiating cells, said media will then be used to treat the dormant breast cancer cell model.

- Investigate the factors present in conditioned media (namely metabolites), which is shown to trigger the proliferation of the dormant breast cancer cell model. Then to treat the dormant breast cancer cell model with metabolites of interest to investigate potential metabolic triggers of dormant breast cancer cell reawakening.

Chapter 2 Materials and Methods

This chapter describes the general materials and methods used to complete experiments during this project, also specific methodologies used in specific chapters (labelled). Also presented here are the lists of cell culture solutions, solution preparations, immunological reagents and website URLs used within this thesis.

2.1 Cell Culture Solutions

Table 2.1 list of cell culture reagents.

Reagents	Supplier	Further Info
4- (2-hydroxyethyl)-1-piperazine-ethanesulphonic acid	Thermo Fischer Scientific, UK	HEPES
Bone Morphogenic Protein	Sigma Aldrich, UK	BMP2
Bovine Insulin Transferrin	Stem Cell Technologies, UK	BIT
Bovine Serum Albumin	Sigma Aldrich, UK	BSA
C-X-C Motif Chemokine Ligand 12	Sigma Aldrich, UK	Human CXCL12
Dimethyl Sulfoxide	Sigma Aldrich, UK	DMSO
Dulbecco's Modified Eagle's Medium	Sigma Aldrich, UK	DMEM
Ethylenediaminetetraacetic acid	Sigma Aldrich, UK	EDTA
Fibronectin	Sigma Aldrich, UK	Human, from plasma
Foetal Bovine Serum	Sigma Aldrich, UK	FBS
Fungizone® Amphotericin B	Gibco by Life Technologies, UK	250 µg/mL
L-Glutamine	Invitrogen, UK	200 mM
Minimum Essential Medium Non-Essential Amino Acids	Sigma-Aldrich, UK	MEM-NEAA
Penicillin-Streptomycin (10 mg/mL stock)	Sigma-Aldrich, UK	P/S, 10 mg/mL
Phosphate-Buffered Saline	Sigma-Aldrich, UK	PBS
Sodium Pyruvate	Sigma-Aldrich, UK	100 mM
Stem Cell Factor	Peprotech, UK	Human SCF
Trypsin	Sigma-Aldrich, UK	10X solution
Hanks' Balanced Salt Solution	Thermo Fischer Scientific, UK	HBSS
Medium 199	Thermo Fischer Scientific, UK	

2.2 Solution Preparations

Table 2.2 list of solution preparations.

Reagents	Component	Concentration
Trypisn/Versene solution	Trypisn Versene	0.5 ml 20 ml
HEPES Saline Solution	NaCL KCL Glucose HEPES Phenol Red Solution	150 nM 5 mM 5 mM 10 mM 0.5%
10% FBS DMEM	DMEM FBS P/S L-glutamine MEM-NEAA Sodium Pyruvate	500 ml 50 ml 10 ml 5 ml 5 ml 5 ml
Fixative Buffer	PBS Formaldehyde Sucrose	90 ml 10 ml 2 g
Permeabilization Buffer	PBS NaCL MgCl2.6H2O HEPES Sucrose Triton X	100 ml 0.292 g 0.06 g 0.476 g 10.3 g 0.5 ml
IF Blocking Buffer	PBS BSA	100 ml 1 g
ICW Blocking Buffer	PBS Milk	100 ml 1 g
Wash Buffer	Tween 20 PBS	0.1 ml 100 ml
MSC Freezing Media	FBS DMEM DMSO	35 ml 10 ml 5 ml
Osteogenic Differentiation media	Dexamethasone A-2-P Glycerol Phosphate	10 μl 1.75 μl **0.0238 g**
Adipogenic Differentiation media	Dexamethasone IBMX Insulin Indomethacin	10 μl 10 μl 100 μl 20 μl

2.3 Immunological Reagents

Table 2.3 List of immunological reagents.

Reagents	Supplier	Further Info
647 anti-rabbit IgG	Thermo Fischer Scientific, UK	1:200 for IF
Biotinylated anti-mouse IgG	Vector Laboratories, UK	Produced in horse
Biotinylated anti-rabbit IgG	Vector Laboratories, UK	Produced in horse
CellTag 700	LI-COR Biosciences, UK	1:500 for ICW
Fluorescein Streptavidin	Vector Laboratories, UK	
Formaldehyde	Thermo Fischer Scientific, UK	
IRDye conjugated goat anti-mouse	LI-COR Biosciences, UK	1:800 for ICW
IRDye conjugated goat anti-rabbit	LI-COR Biosciences, UK	1:800 for ICW
Magnesium Chloride Hexahydrate	Sigma-Aldrich, UK	MgCl2.6H2O
Phalloidin 488	Molecular Probes, Life Technologies	1:100 for IF
Sodium Chloride	VWR Chemicals	
Triton X-100	Thermo Fischer Scientific, UK	
Tween 20	Sigma-Aldrich, UK	
Vectashield mounting medium with DAPI	Vector Laboratories, UK	
Nestin antibody	Abcam, UK	#ab22035, 1:200 for ICW and IF
VCAM antibody	Abcam, UK	#ab134047, 1:200 for ICW and IF
OPN antibody	Santa Cruz Biotechnology	# sc-21742, 1:50 for ICW and IF
FN antibody	Sigma-Aldrich, UK	#F7387, 1:200 for ICW
P5F3 antibody	Santa Cruz Biotechnology	#sc-18827, 1:200 for ELISA
HFN7.1 antibody	Developmental Studies Hybridoma Bank	

2.4 Website URLs

Table 2.4 Table of website URLs for online analysis software used in this project.

Website	URL
PATHOS	https://motif.gla.ac.uk/Pathos/
Metaboanalyst	https://www.metaboanalyst.ca/
Biorender	https://biorender.com/

2.5 General Methods

2.5.1 Cell Culture

MCF7 and MSC cells were cultured at 37°C with 5% CO_2 using modified DMEM (Dulbecco's modified eagle's medium) (basal medium used for culture of mammalian cells) and DMEM respectively, MCF7 cells were cultured in 400mL of DMEM, 100mL medium 199, 50mL foetal bovine solution, 10mL Penicillin/streptomycin,5mL sodium pyruvate and 5ml of non-essential amino acids. MSCs were cultured using 500mL DMEM, 50mL foetal bovine solution (FBS), 10mL Penicillin/streptomycin, 5mL sodium pyruvate and 5mL of non-essential amino acids. MSCs (cell line) were used up brought up and used at passage 1-2 and discarded after passage 4 due to limited differentiation capacity. Primary MSCs were also utilised and discarded after passage 4 for reasons stated above. Cells were maintained in either T75 or T150 tissue culture flasks and split at 90% confluence. The procedure was as follows: a HEPES wash (Thermofisher) followed by incubation at 37ºC in 5% trypsin/versene solution for 5 minutes. Cell suspension was then centrifuged at 1400rpm for 7 minutes, supernatant discarded, and cell pellet re-suspended in 5 mL culture media and counted, then re-seeded into fresh flasks, with media changed at 3-day intervals.

2.5.2 Cell Freezing/Thawing

Cells were pelleted and resuspended in 1 mL cell freezing solution before being frozen at -80°C overnight then transferred to liquid nitrogen for storage. Cells were thawed by removing from liquid nitrogen and adding the cell suspension dropwise to fresh media warmed to 37°C and centrifuging at 1400 rpm for 4 minutes. Cell pellet was resuspended in 5 mL fresh media and cells seeded in several T75 or T150 flasks containing 10 mL fresh media.

2.5.3 Monolayer Culture

Cells were lifted from the surface of T75 or T150 flasks using trypsin/versene, before seeding in a 24,48 or 96 well plate. Cells were allowed to adhere for 24 hours, incubated at 37°C with 5% CO_2.

2.5.4 Cell Treatments

Cells were treated with media conditioned on differentiated cells for 48 hours. Cells were driven to differentiation using supplemented media (see 2.6), this differentiation media was removed, and cells washed with HEPES solution. Regular DMEM (see above) was then added to the cells for 48 hours before harvesting. Conditioned media was stored at -80 °C until use.

2.5.5 Differentiation media

Media was made up as follows for osteogenic and adipogenic differentiation respectively: dexamethasone (0.01μM), ascorbate-2-phosphate (50μg/mL) and 10 mM glycerol phosphate and dexamethasone (0.1μM), IBMX (50 μM), insulin (10μM) and indomethacin (200μM) (see also table 2.1) (Vater, Kasten, and Stiehler 2011).

2.5.6 Stem Cell Differentiation

MSCs were grown to 90% confluency then split into T75 flasks. Cells were characterised before differentiation for cell viability and activity, this was done using a live/dead stain (see section 2.5.11) and Alamar blue assay (see section 2.5.13). MSCs were then treated with supplemented media (see table 2.1). Cells were encouraged to differentiate for 28 days changing the supplemented media twice a week. Cells were stained after 28 days using Oil Red O and Alizarin Red to stain for lipids and calcium deposition respectively. These stains were used to confirm lineage specific differentiation of MSCs.

2.5.7 Spheroid Generation

The Liquid overlay technique was used to generate spheroids. There are several different methodologies for generating spheroids including hanging drop, liquid overlay and high-density seeding each possessing advantages over the other. Liquid overlay however is cheap, effective, allows for long term culture and allows for the large-scale production of spheroids with studies showing viability and longevity of spheroids in culture (Costa et al. 2018). The liquid overlay technique is also the method of spheroid generation that produces the most reproducible spheroids and also allows for the size of spheroid to be stringently controlled (varying only with the number of cells used for generation) (Metzger et al. 2011).

MCF7 cells were grown to around 90% confluency, detached and counted. The cell pellet was re-suspended to make up the concertation to 10 million cells/mL. The cells were then seeded in 5 µL in the centre of the well of a 6 well tissue culture plate (Corning). Cells were left to adhere for up to 4 hours, each well was then flooded with media (high density seeding). Along with high density seeding, ultra-low adhesion plates (Corning CLS3471- 24EA) were used to generate MCF7 spheroids. Varying cell densities were used (10,000 cells, 7,500 cells, 5,000 cells and 2,500 cells) to generate spheroids of different sizes in order to assess the optimal starting seeding density. Liquid overlay technique was used following optimisation.

2.5.8 Spheroid Size Measurements

Spheroids were generated using varying cell seeding densities (2.5×10^4 cells/mL, 5×10^4 cells/mL, 7.5×10^4 cells/mL, 1×10^5cells/mL). Spheroids were then allowed to form and grow for various time points. Several images (3+ after each agitation) were then taken of each spheroid (plates were agitated prior to each image being taken to ensure morphology of spheroid was consistent). A scale image was taken, and this data imputed to ImageJ to define pixel density/length ratio. Images were then analysed in ImageJ using both diameter and circumference to ascertain the area of each spheroid.

2.5.9 Western Blotting

Cells were treated with relevant treatments, after which lysates were isolated using RIPA buffer with a protease inhibitor cocktail. RIPA buffer was added after cells were pelleted and washed, cells were then incubated on ice for 30 minutes, samples were then sonicated for 10 minutes. RIPA suspension was then centrifuged at max speed for 30 minutes to remove cell debris. Lysates were then stored at -80°C.

Lysates were separated using 10% SDS-PAGE. Using gels: Thermo NuPAGE tris-acetate (3-8%) and Bis-Tris (4-12%) depending on the size of protein (smaller proteins travel faster, so a higher concentration gel is used for more accurate separation of proteins). Loading solution was made up, consisting of protein lysates, dH20, 4x loading buffer and 10x reducing agent. This solution was denatured at 80°C for 10 mins, then protein was loaded into gel alongside molecular weight markers. The gel was then run at 150V for varying times depending on the gel used/ protein of interest (higher voltage increases the speed of protein migration through the gel, however, also causes and increase in temperature of the gel, altering its physical properties). The time of run is dependent on the size of the protein of interest and the thickness of the gel, smaller proteins move quicker than larger proteins). After resolution of proteins, they were transferred to a PVDF membrane at 25V for 2 hours. The membrane was then blocked with 5% milk/TBS Tween20 for 1 hour. Following blocking, the membrane was then incubated with required primary antibody (diluted in 5% milk/TBS Tween-20 at recommended concentrations) overnight. The membrane was then washed at room temperature in TBS-Tween-20 3x 10 mins. After washing the membrane was incubated at room temperature with secondary antibody (diluted in 5% milk/TBS-tween 20) for 1 hour while avoiding membrane exposure to light. The membrane was then treated with 1ml of ECL and exposed using Thermo-scientific myECL imager.

2.5.10 Immunostaining

Cells were fixed in fixative buffer (see above) for 15 minutes at 37°C, then permeabilized using perm buffer (see above) for 4 minutes at 4°C. Samples were then blocked using blocking buffer (see above) for 30 minutes at room

temperature and incubated with primary antibody overnight. After primary incubation samples were washed using wash buffer (see above) three times for 5 minutes and the incubated with secondary antibody for 2 hours at room temperature. Before visualization samples were stained with DAPI/PBS to stain nuclei. Images were acquired using EVOS M700 and analysis done using imageJ.

2.5.11 Live/Dead Assay

MCF7 were grown on low adhesion tissue culture plates for 48 hours, cells were then kept in suspension (changing media every 3 days) for 3,5,7, and 14 days to assess cell viability. Live dead stain was performed: adding 20 µL of 2mM EthD-1 stock solution to 10mL of sterile PBS and vortex (Solution A). Then 5 µL of calcein was added to solution A. 100 µL of Solution a was added to each well containing cells. The cells were then incubated for 15-20 minutes at 37 ^{o}C 5% CO2. Ethanol at 100% was used to treat cells for the negative control.

2.5.12 MTT metabolic activity assay

Cells were seeded at varying densities and allowed to grow/form spheroids for 48 hours. Media is then removed and replaced with various treatment media and left for 24, 48 and 72 hours. After designated time of incubation, 5-diphenyl-tetrazolium bromide (MTT) was added at 0.5mg/ml and incubated for 2 hours. After incubation, the supernatant was removed and 100 µl DMSO was added to the supernatant in order to dissolve formazan crystals. The optical density of the resulting solution was then measured at 570nm using Thermofisher Multiscan FC. This value directly correlates with the number of viable cells in the solution therefore, a percentage viability was calculated using negative control cells.

2.5.13 Alamar Blue assay (Resazurin)

Alamar blue along with other assays was used to determine cell proliferation. Alamar blue has a REDOX (reduction-oxidation) indicator that changes colour depending on cellular proliferation. Cells were seeded and grown at varying densities and allowed to grow/from spheroids for 48 hours. Media is then

removed and replaced with media containing alamar blue solution at 1:10 in cell specific medium. Cells were then incubated for 2 hours at 37C 5% CO2. After incubation supernatant is removed from wells and transferred into a fresh 96-well plate. Absorbance readings at 570 and 600 were then taken using Thermofisher Multiscan FC. Percentage reduction in alamar blue is then calculated using % reduction of alamar blue = (Eoxi600 x A570) - (Eoxi570 x A600) / Ered570 x C600) - (Ered600 x C570) where parts of this equation are defined values, please see protocol.

2.5.14 Microscopy

MCF7 spheroids were generated using above protocol. Spheroids were imaged using light, fluorescence and SEM to investigate the overall morphology of the cell masses. For light microscopy spheroids were washed using PBS 3x before imaging. Spheroids were then fixed in 2.5% glutaraldehyde/ 0.1M phosphate buffer fixative for 1 hour at room temperature. Spheroids were then rinsed in buffer 3 times. After fixation spheroids were treated with osmium tetroxide/ 0.1M phosphate buffer for 1 hour. Spheroids were then washed again 3x 10 mins before treatment with uranyl acetate avoiding light exposure for 1 hour. Samples were then dehydrated using increasing concentrations of ethanol up to ethanol absolute. Samples were then dried in hexamethyldisilazane and mounted onto stubs. Once mounted, the samples were then coated in gold/palladium up to 10nm using polaron SCS15 SEM coating system. Samples were then visualised using JOEL 6400 SEM at 10kV.

2.5.15 Plasma Polymerisation (Chapter 4)

Plasma chamber optimisation was adapted from previous research (Alba-Perez et al. 2020c). 24 well plates were placed within the chamber placed horizontally to the plasma flow. Samples were then exposed to air plasma for 5 minutes at 50W. Monomer was then polymerized to pPEA using 50W for 15 minutes. After coating AFM and XPS were used to characterise the polymer coating on the surface, identifying the depth of the coating as well as the chemical composition. Samples were sterilized under UV light for 30 minutes before use.

2.5.16 X-ray photoelectron spectroscopy (Chapter 4)

X-ray photoelectron spectroscopy was used to identify the surface chemical composition of the pPEA coated samples. All samples underwent x-ray photoelectron spectroscopy at The Harwell XPS EPSRC National Facility for X-ray Photoelectron Spectroscopy. Each sample was analysed 3 times using a K-alpha system equipped with a monochromatic Al-K-alpha source at a maximum beam size of 400 μm x 800 μm. Parameters were as follows: X-ray energy; 1491.69 eV, emission current of 15 mA, voltage; 12 kV and a power of 225 W. All spectra analysis and curve fitting performed using CasaXPS software (Casa Software Ltd).

2.5.17 Atomic Force Microscopy (Chapter 4)

Atomic force microscopy was used to confirm the conformation of ECM proteins, namely FN. AFM was used to quantify surface roughness and image the topology of samples. Prior to the adsorption of FN onto samples, samples were imaged by AFM as a control. FN was allowed to be adsorbed onto the surface of the samples for one hour, samples were then washed three times using PBS and then washed once with deionised water (dH_2O). Samples were then dried using nitrogen and stored to allow for further drying. All samples were imaged using the JPK Nanowizard 4 and all image analysis was conducted using JPK data processing software version 5. A pyramidal silicon tip was used for alternating contact mode imaging.

2.5.18 ELISA

FN was adsorbed onto pPEA, after adsorption samples were washed three times with PBS. Samples were blocked using 1% BSA/PBS for 30 minutes at room temperature on an orbital plate shaker. Block was removed and solution containing primary antibodies was added, samples were incubated for one hour at room temperature. After incubation of primary antibody, samples were washed three times for five minutes with 0.1% tween-20/PBS. Following this, samples were incubated with secondary antibody for 1 hour at room

temperature. After incubation samples were washed three times as above, and streptavidin -HRP was added and incubated for 20 minutes. Solutions were aspirated and substrate solution was added, and samples were incubated for 20 minutes at room temperature avoiding light. Stop solution was added to halt the reaction after 20 minutes, samples were then read using a Thermofisher Multiscan FC.

2.5.19 ELISA for growth factor adsorption (Chapter 4)

FN was adsorbed onto pPEA, BMP-2, CXCL12 and a combination of both proteins were adsorbed onto the FN. The solution was then aspirated and stored with the stock solution used for adsorption. These solutions would be used to assess the amount of protein adhered to the surface ECM proteins, ELISA would be used to determine specific protein concentrations in both the stock solutions and solutions used for adsorption. Capture antibody was added to high-binding 96 well plates and incubated overnight. Capture antibody was the aspirated and plate was washed three times using was buffer. Reagent diluent was added to each well to block for one hour at room temperature. Samples and standards were then added to the plate and incubated overnight at 4°C. Samples and standards were aspirated, and plates were washed three times using wash buffer. The detection antibody was then added to the relevant samples and incubated at room temperature for two hours. Samples were aging washed three time with wash buffer and then streptavidin-HRP was added, and plates were incubated for 20 minutes in the absence of light. Streptavidin was then aspirated, and samples washed, substrate solution was then added, and samples incubated for 20 minutes in the dark, after 20 minutes stop solution was added to each samples to stop the reaction and finally samples were read using a Thermofisher Multiscan FC.

2.5.20 In Cell Western for Osteogenic and Stemness Markers

After adsorption of FN onto pPEA, FN was adsorbed to the surface and allowed to bind for one hour, samples were then washed with PBS and cells at 10,000 cells/cm^2 were allowed to adhere overnight. Following adherence of the cells, media was aspirated and replaced with experimental media (1% FBS containing growth factors of interest). Cells were then grown on the model for four weeks with media being changed twice per week. After differentiation time period, media was aspirated and cells were washed three ties in PBS, then fixed in fixation buffer for fifteen minutes at 37°. Samples were then blocked in blocking buffer for a further 90 minutes. Samples were then incubated with primary antibody overnight at 4° (Anti-Osteopontin antibody (ab8448), Anti-RUNX2 Antibody (F-2): sc-390351, Recombinant Anti-CD166 antibody [EPR2759(2)] (ab109215) and Anti-Nestin antibody ab22035). After overnight incubation primary antibody was removed and samples were washed three times with washing buffer. Following three washes samples were further incubated with secondary antibody for one hour at room temperature. Finally, samples were washed with washing buffer three times and then washed with deionized water. Samples were analysed using infrared signal measurement, plates were read using an Odyssey infrared imaging system.

2.5.21 Osteo Staining (Chapter 5)

MSCs were grown/ differentiated for 28 days, media was removed from the cells, cells were then washed three times using 1x PBS. Cells were fixed in 4% formaldehyde for 15 minutes at room temperature. Fixative was removed and cells washed three times using diH_2O. Water was aspirated and 1 mL of 40 mM Alizarin Red S per well and cells were incubated at room temperature for 30 minutes with gentle shaking. Dye was aspirated and samples washed five times with diH_2O. Samples were then imaged using a phase microscope.

2.5.22 Adipo Staining (Chapter 5)

MSCs were grown/ differentiated for 28 days, media was removed from the cells, cells were then washed three times using 1x PBS. Cells were fixed in 4% formaldehyde for 15 minutes at room temperature. Fixative was removed and cells washed three times using diH_2O. After washing 60% isopropanol was added to samples and incubated for 5 minutes at room temperature. Isopropanol was aspirated and samples stained with pre-prepared oil red o working solution (see above), samples were incubated with the dye for 15 minutes at room temperature with gentle shaking. The dye was then aspirated, and samples washed five times with diH_2O to remove excess stain. Haematoxylin was then added to samples and incubated for one minute. Samples were then washed again five times with diH_2O. Samples were then covered in diH_2O and imaged under a microscope.

Chapter 3 Breast Cancer Model – Spheroid Characterisation

3.1 Introduction

In recent years, interest in the phenomenon of dormant cancer cells residing within the bone marrow niche has greatly increased. The mechanics behind this entry into quiescence as well as those involved with its re-activation need to be investigated in order to combat this deadly occurrence. If these factors can be determined, then they can potentially be employed to develop novel therapeutics(X. H. F. Zhang et al. 2013; Ono et al. 2014). Recent evidence suggests that this dormant phenotype can be adopted upon entry of DBCCs into the bone marrow. This change in phenotype, however, is not instantaneous, with DBCC developing different characteristics depending on the site of entry into the bone marrow (Walker et al. 2016) (Clements and Johnson 2019b). Along with this, as the cancer cells do not immediately become quiescent, they may form micro-metastases within the bone marrow niche.

Historically, the methodology employed to research this would have been focused on a two-dimensional condition(Weiswald, Bellet, and Dangles-Marie 2015a). Recently, however, interest has risen greatly in the application of three-dimensional models being employed to research cancer in vitro. One such method of three-dimensional investigation into cancer cells is the formation of spheroids. Due to a spheroid's unique morphology, they have risen as a very attractive model for research into cancer, due to the fact they more accurately represent in vivo tumours when compared with traditional two-dimensional culture methods (Kapałczyńska et al. 2018). As the cells amalgamate into the spheroid, distinct regions develop within the structure(Cui, Hartanto, and Zhang 2017). This is due to the diffusion gradient of oxygen, metabolites and nutrients observed in cancer spheroids(Mehta et al. 2012). These distinct zones within the spheroid are well characterised, with the centre zone consisting of a necrotic core of cells with a low pH, poor nutrient acquisition, and reduced waste removal (Chandrasekaran 2012). This necrotic core is then surrounded by both proliferating and quiescent cells(Han, Kwon, and Kim 2021). The advantages of using spheroids as opposed to traditional two-dimensional cultures is apparent, with research also showing that spheroids can be used to form both

heterogenous cell populations as well as microenvironmental cell conditions(Vinci, Box, and Eccles 2015). Although spheroids are a useful tool in the investigation of cancer in vitro, they do lack the complexity of an in vivo model, as spheroids are made up of only one cancer cell type, as opposed to the great complexity of cells present in vivo, such as immune and basement membrane cells.

3.1.1 Spheroid variation and generation

There are four categories that all spheroids fall under, these are distinguished both by their origin and by the techniques used to generate them. The subtypes of spheroid are multicellular tumour spheroid (MCTS), tumour-sphere, tissue derived tumour-sphere and organotypic multicellular spheroids (Raghavan et al,2016).

MCTS spheroids are formed using cell lines and rely on the cells used to aggregate together and bind to each other, as opposed to the tissue culture surface. There are several methodologies to form MCTS spheroids, including hanging drop, liquid overlay and a newer technique that utilises microcapsules containing membranes made of methylcellulose (Raghavan et al, 2016). The liquid overlay technique is reliable and reproduceable(Vinci, Box, and Eccles 2015), and involves the use of ultra-low adherence tissue culture vesicles. This process consists of growing single cell suspensions in low/non-adherent conditions, as adherence to the tissue culture plastic is restricted, the cells adhere to each other, resulting in the formation of an MCTS spheroid.

Tumour-spheres are formed from a single cell suspended in an ECM like matrix. Each tumour-sphere is formed by one cancer stem cell proliferating to form a round solid structure(Weiswald, Bellet, and Dangles-Marie 2015b). These spheroids are easily distinguishable from MCTS spheroids as they have a distinctive morphology. The structure of tumour-spheres is a dense solid mass with no space in between cells, MCTS spheroids therefore are larger in size as they have extracellular space in between cells(Zajac et al. 2018). Only a select number of cell line are capable of forming tumour-spheres, such as MCF7s, this

is due largely to the high expression of e-cadherin, a type of cell adhesion molecule aiding in the adherence of cells to one another (with high expression correlating with superior spheroid formation)(Manuel Iglesias et al. 2013).

Tissue-derived tumour-spheres are formed by dissociating and aggregating cancer tissue samples. Generation of tissue-derived tumour-spheres is in some ways similar to the generation of MCTS spheroids, as both methods rely on using a low-adherence cell culture vessel resulting in large, less compact spheroids compared with regular tumour-spheres.

Organotypic multicellular spheroids are generated in largely the same manner as the tissue derived spheroids, however the tumour is cultured for an extended period of 2 to 3 weeks in low percentage agar media. This model more accurately represents an in vivo tumour and therefore allows for the research of a more realistic tumour model. Despite this method relying on the enzymatic or mechanical disruption of tumours, the cancer retains heterogeneity seen in vivo. These types of spheroids contain multiple cell types including cancer cells, stromal cells and non-cancerous cells and are thus able to somewhat accurately replicate the tumour microenvironment(Gunti et al. 2021).

Another methodology employed for the generation of spheroids, is a high-density seeding method whereby cells are seeded in a small volume of media into the centre of a 96 well tissue culture plate, allowed to adhere for 4-6 hours and then the well is flooded with cell culture medium. Thus, there are several methodologies for generating cellular spheroids, with each method holding advantages over others. Therefore, investigation was undertaken in order to assess the validity and viability of the different spheroid culture methods.

3.1.2 Objectives

This chapter aims to develop an in vitro three-dimensional model, using a breast cancer cell line (MCF7), for the investigation into the phenomenon of breast cancer dormancy. The generation of a physiologically relevant model for investigation into the mechanisms responsible for the re-activation of dormant

breast cancer will facilitate further study of both dormancy and reawakening. There exist numerous methodologies for the generation of spheroids, however each have distinct advantages over each other, this chapter will attempt to determine the optimum methodology for a cheap, high-throughput model for dormant breast cancer (Gunti et al. 2021; Han, Kwon, and Kim 2021; Pulze et al. 2020a). Several methods of reducing the proliferation of the breast cancer cell line will be investigated in order to determine the optimum setup for the model used for investigation into re-awakening. The optimum model will be used for future experiments to investigate potential pathways responsible to breast cancer recurrence. This will involve investigating different methods of re-awakening and then isolating secreted metabolites and investigate them as potential triggers for reactivation.

3.1.3 Experimental Design

In order to investigate the growth of spheroids, a breast cancer cell line (MCF7) was used to generate spheroids. Cells were seeded using a variety of different methods; high-density seeding, liquid overlay technique utilising ULA (ultra-low adherence) plates and a combination of both methods. MCF-7 cells were selected as the cell line to be used in this thesis; this is due to previous research identifying MCF7 spheroids as a stable reproducible model for breast cancer (Pulze et al. 2020a; Sahana et al. 2018). MCF7 cells were seeded at varying cell densities (2.5×10^3, 5.0×10^3, 7.5×10^3 and 1×10^4 cells per well). Spheroids generated as per previous chapter (as per section 2.7). Spheroids were imaged using an Axiovert and Evos microscope and diameters and circumference measured using ImageJ this is in order to investigate the rate of growth of different sizes of spheroid. Along with this, various assays were used to assess the proliferation/metabolic activity rate of the spheroids using MTT and alamar blue assays. Further validation was conducted by investigating the expression of Ki67 (a proliferation marker, used specifically to identify dormant breast cancer cells (L. T. Li et al. 2015).

3.2 Results

3.2.1 Spheroid Generation

All results here used the MCF7 (ATCC) cell line. In order to generate this 3D cancer model, a rigid spheroid generation methodology needed to be designed in order to reproduce consistently sized spheroids. The impact of initial seeding density on the ultimate size and shape of spheroids was assessed. Spheroids were seeded at varying densities (2.5×10^3, 5.0×10^3, 7.5×10^3 and 1×10^4 cells per well). Spheroid size was then assessed using the circumference and diameter measurements after imaging on Axiovert and Evos M700 microscopes.

Herein spheroid diameter and circumference are used to calculate the area of spheroids. These measurements along with the use of resazurin reduction will be used to determine both the size and cellular activity of spheroids generated using varying seeding densities. This information will help determine the optimum seeding densities of the spheroids for further experiments.

MCF7 cells were seeded using various methods to generate low proliferative spheroids, seeded using a high-density seeding method, liquid overlay (ULA plates) method and a combination of the two.

High density seeding and liquid overlay technique were compared as methods of generating low proliferative cancer cell masses. After 7 days of culture both methods of spheroid generation showed a trend of reduction in cell proliferation when compared with the 2D controls, however the reduction of the high-density seeding samples was insignificant (see figure 1). In contrast spheroids generated using ULA plates and the combination treatment both resulted in significantly reduced cell proliferation as assessed using resazurin reduction (see figure 1). This coupled with issues faced with high density seeding, including the cell mass detached from the tissue culture plastic determined that ULA plate generation of spheroid samples would be used for future experiments.

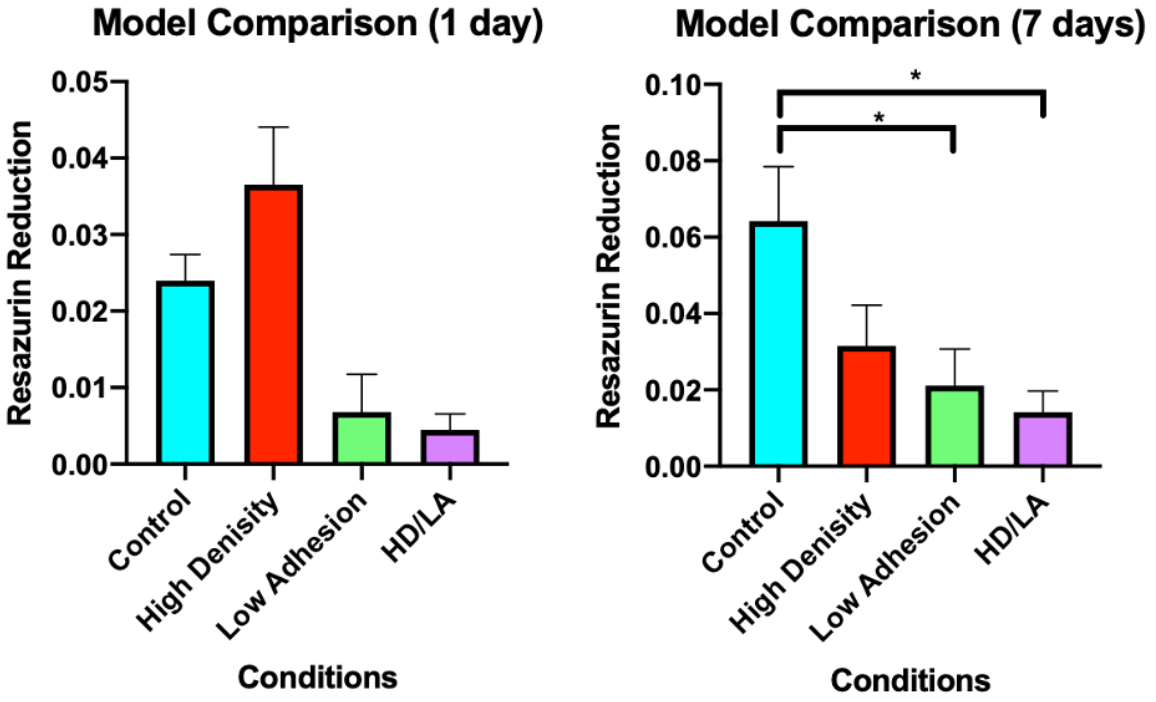

Figure 3.1 MCF7 cells seeded using different methods to restrict proliferation. MCF7 cells into cell culture plates under specific conditions (see methods). Cell proliferation was measured using Alamar Blue assay (Resazurin) after growth for 1 and 7 days. Cell proliferation was compared against 2D control. High density seeding method showed reduced proliferation compared with controls, however proliferation rates remained higher than liquid overlay protocol. Both LA and HD LA showed significantly reduced proliferation compared with 2D controls. Statistical analysis using an unpaired t-test. "*" = p < 0.05, "" = p < 0.01, "***" = p < 0.001, "****" = p < 0.0001, "ns" = non- significant. n=3.**

3.2.2 Cell Seeding Density

All results herein were generated using MCF-7 (ATCC) cells seeded in ULA 96-well plates. After deciding upon a method for generating low-proliferative spheroids, the methodology needed to be verified and characterised. Therefore, several different seeding densities were investigated, and spheroid sizes were assessed.

MCF-7 cells generated large, stable spheroids. Spheroid size increased along with cell density. The mean size of the highest cell density spheroid (1×10^4 cells/mL) were significantly different ($p<0.05$) to those seeded at the lowest cell density (2.5×10^3 cells/mL). Higher cell density seeded spheroids generated the largest spheroids with a large cross-sectional range, the range between seeding densities was also large, with great differences being observed between seeding

densities with the smallest spheroids being on average half as large as the largest (see figure 2).

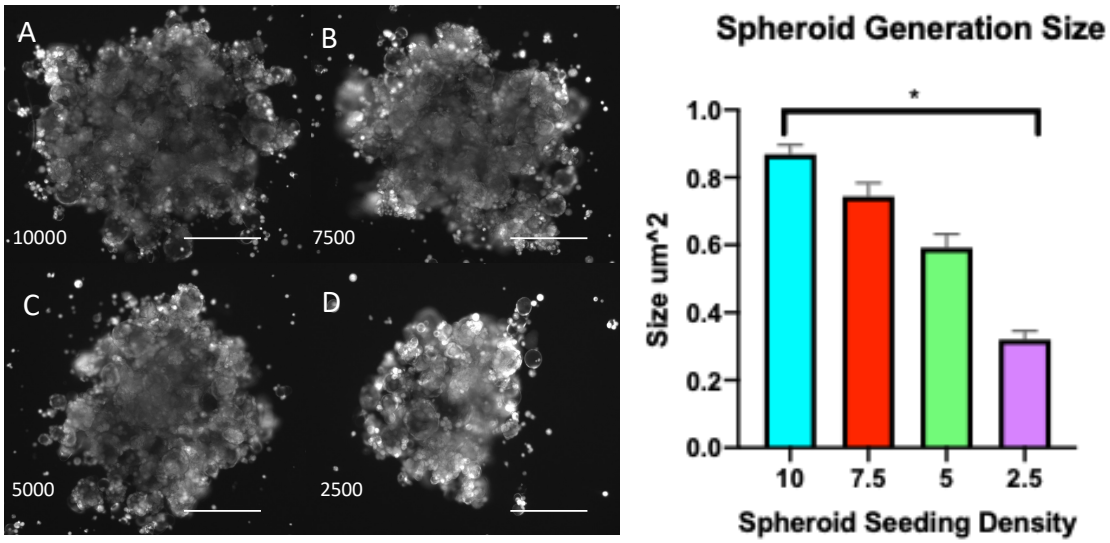

Figure 3.2 MCF7 spheroids seeded at four cell seeding densities. Spheroids were cultured for 48 hours in Ultra Low adhesion, round bottom plates (Cell Carrier Spheroid ULA 96-well Microplate, Perkin Elmer). Images acquired with Evos M700. Fluorescence derived from live cell staining (calcein AM). >10 spheroids measured at each cell seeding density. Spheroid areas measured via pixel count using ImageJ. Scale Bar = 100 μm Statistical analysis using Kruskal Wallis test. "*" = p < 0.05, "" = p < 0.01, "***" = p < 0.001, "****" = p < 0.0001, "ns" = non- significant. n=3.**

3.2.3 Spheroid Cell Viability

Spheroids were generated using the above method, incubated for 14 days and stained with calcein AM and ethidium homodimer (fluorescent dyes that bind live and dead cells respectively). After culture for 14 days, all sizes of spheroid showed many live cells with very minimal dead cells stained, thus this model was used for future experiments after showing very little cell death (see figure 3.3). Along with this, previous research into the viability of MCF7 spheroids indicated viability. This was done by transferring the MCF7 spheroids to a 2D culture plate before staining (the spheroid is shown to disassemble and fully spread over the 2D surface, thus live/dead staining is an effective method of validation) (Gong et al. 2015).

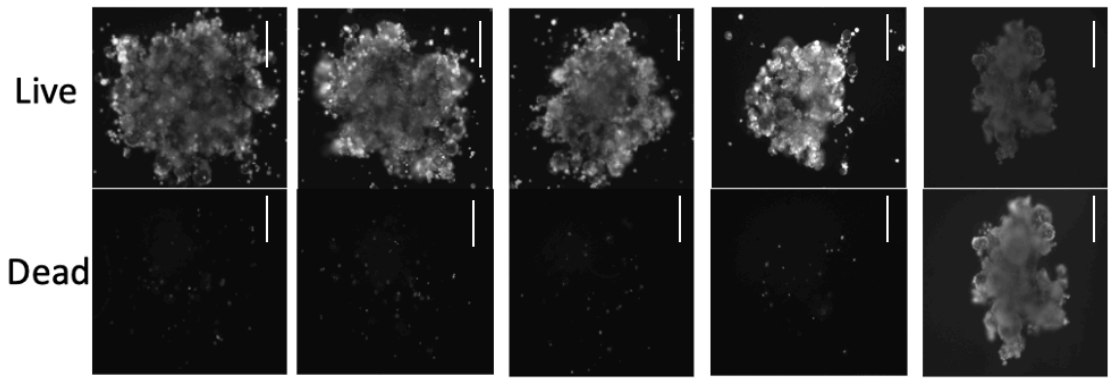

Figure 3.3 MCF7 spheroid viability. Spheroids where cultured in Ultra low adhesion round bottom 96-well plates. Spheroids were seeded at varying cell densities before staining. A) 10,000 cell seeding density, B) 7,500 cell seeding density, C) 5,000 cell seeding density, D) 2,500 cell seeding density, E) negative control MCF7 cells seeded at 5,000 cell seeding density, treated with 70% ethanol for 20 minutes prior to staining. All spheroids stained with calcein AM (live cells) and ethidium homodimer (dead cells). All spheroids allowed to grow for 7 days prior to staining. Spheroids all retained shape over time, showing their stability in this morphology. Scale Bar = 100 μm.

3.2.4 Electron Microscopy

As per the results of the cell density experiments, spheroids used in future experiments would be derived from cells seeded at 1 x 10^4 cells/mL and 5 x 10^3 cells/mL, two sizes were selected in order to investigate the effects of the size of the spheroid when treated with various factors (see chapters 5 and 6). These two sizes were chosen as both were shown to be viable after 14 days and both were shown to have markedly reduced expression levels of ki67. MCF-7 spheroids of different sizes were investigated using SEM (scanning electron microscopy). Spheroids were generated as per section 2.5.7 and prepared from SEM as per section 2.5.14.

MCF7 spheroids of different sizes were generated and allowed to form/grow for 48 hours, they were then prepped and imaged using SEM at 100x, 1000x, 1500x and 4000x magnification. Images taken at the lower magnification showed the whole spheroid, thus providing information into the morphology of the spheroids of different sizes. The larger cell density spheroid showed a diameter of around 300 μm, with the smallest spheroid diameter was around 150 μm (see figure

3.4). These data correlate with cell density experiments as the ultimate size of the spheroid is shown to be determined by the number of cells seeded. The overall area of each size of spheroid was measured using ImageJ and compared with one another, the size of spheroid was consistent with the number of cells used in spheroid generation.

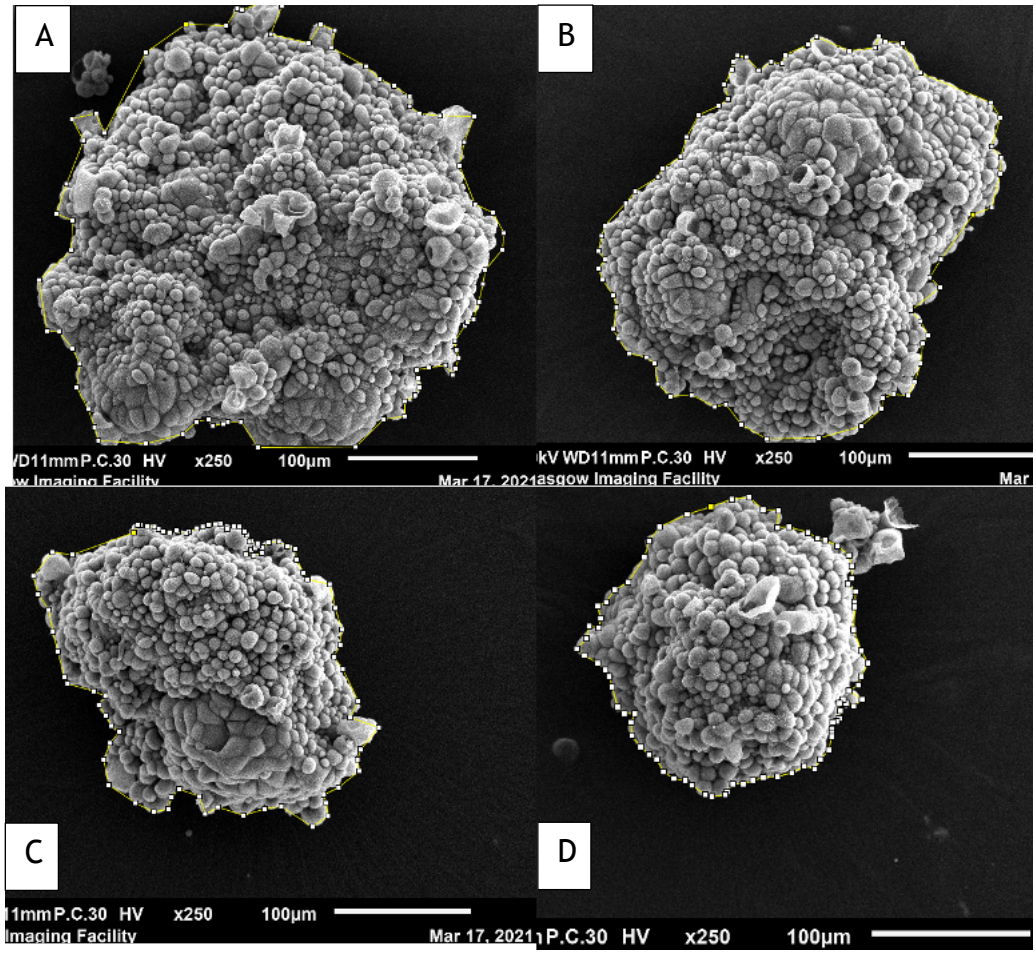

Figure 3.4 Electron microscopy of multicellular MCF7 spheroids. MCF7 spheroids seeded at four cell seeding densities A) MCF7 spheroid seeded at 50,000 cells/mL – 200 µL seeded – 10,000 cells. B) MCF7 spheroid seeded at 37,500 cells/mL (7,500 cells). C) MCF7 spheroid seeded at 25,000 cells/mL (5,000 cells). D) MCF7 spheroid seeded at 12,500 cells/mL (2,500 cells). Scale bar: 100 µm for all images. Images captured using JEOL JSM-6400 scanning electron microscope at 10kV Spheroids were cultured/generated using ultra low adhesion plates. All spheroids grown for 48 hours prior to imaging.

Increased magnification images of the spheroids show the cells are highly compacted within the spheroid mass. Cells are clearly bound to one another with the approximate cell diameter of the peripheral cells averaged around 10-12 µm. The inner cells, however, are shown to be more compacted than those at the periphery with cell diameter ranging from 3-7 µm (see figures 5 and 6).

These sizes observed correlate with literature describing spheroids generated using MCF7 cells(Pulze et al. 2020a). The variation in cell sizes within the spheroid suggest that the innermost cells experience higher pressure from the surrounding cells as compared with those on the periphery. Inner cells also appear to be more tightly bound to one another, this difference in morphology of cells within the spheroid is emphasised in the literature in that, within spheroids there are multiple zones of cells with distinct characteristics. The outer rim of cells is proliferative (proliferative rim) and the innermost cells are non-proliferative.

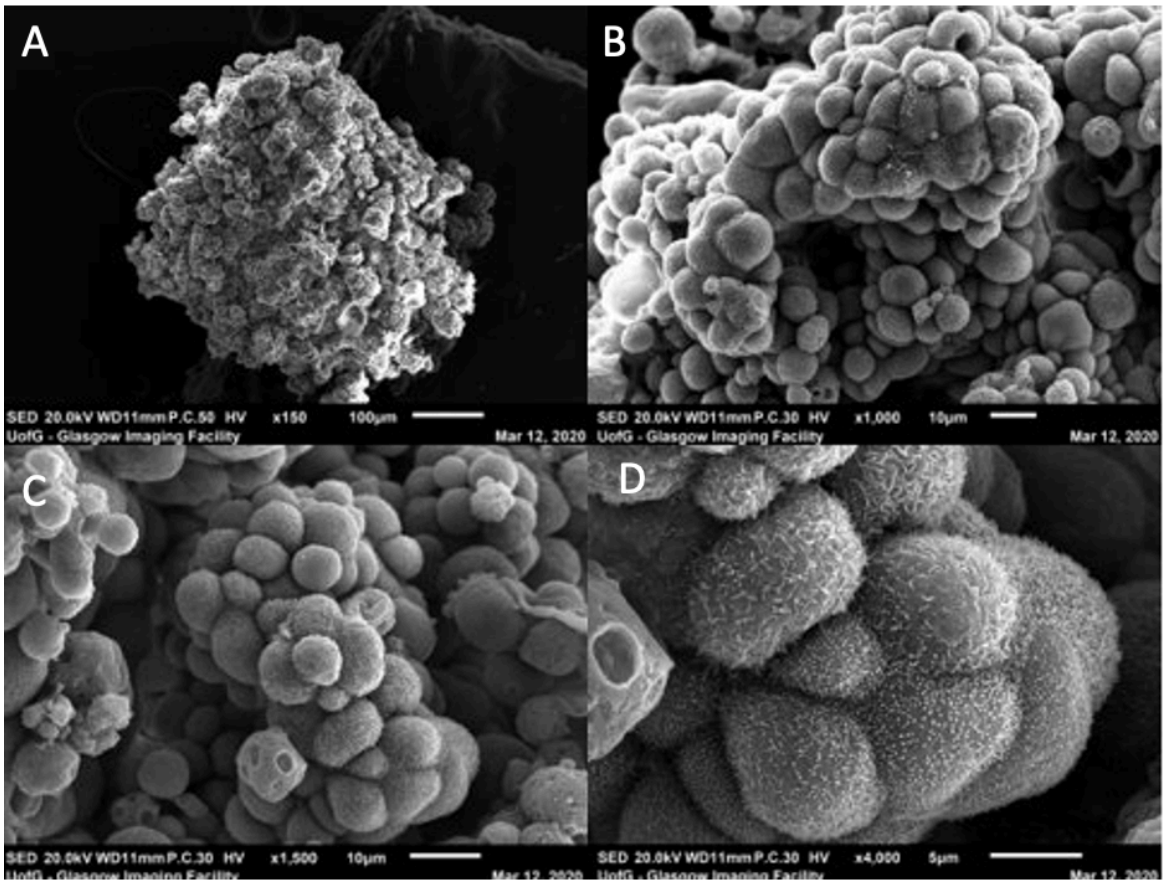

Figure 3.5 Electron microscopy of multicellular MCF7 spheroids. A) 150X magnification; scale bar 100 μm. B) 1,000X magnification; scale bar 10 μm. C) 1,500X magnification; scale bar 10 μm. D) 4,000X magnification; scale bar 5 μm. Images captured using JEOL JSM-6400 scanning electron microscope at 10kV. Spheroids cultured for 48 hours in ultra-low adhesion 96-well plates in all cases.

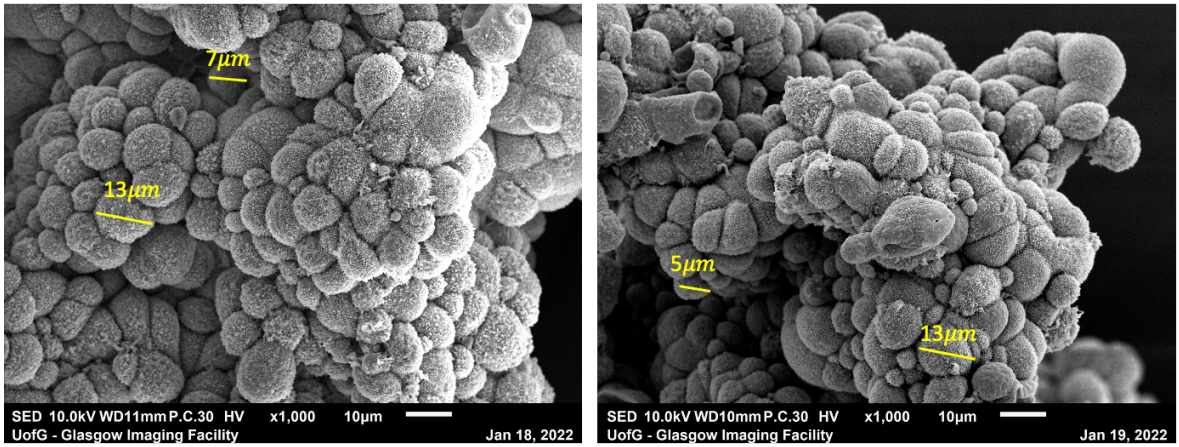

Figure 3.6 Electron Microscopy images (SEM) of multicellular MCF7 spheroids. Both images were taken at 1000x magnification. Images captured using JEOL JSM-6400 scanning electron microscope at 10kV. Images indicate the method used to determine the diameter of cells within the spheroid. A range of cells sizes are present in the outer proliferating layer of cells of the spheroid. Each spheroid was comprised of cells seeded at 1 x 10^4, spheroids were seeded and grown for 48 hours in ULA plates, prepped for SEM and imaged.

Spheroids were generated using the above-described method and allowed to grow for up to 7 days. Spheroid samples were taken 24 and 48 hours after seeding as well as at 7 days to investigate the rate growth of MCF7 spheroids. After analysis it is clear that the MCF7 spheroids do not grow significantly after 7 days, this is indicative of the lack of proliferation of MCF7 cells when in spheroid formation (see figure 3.7).

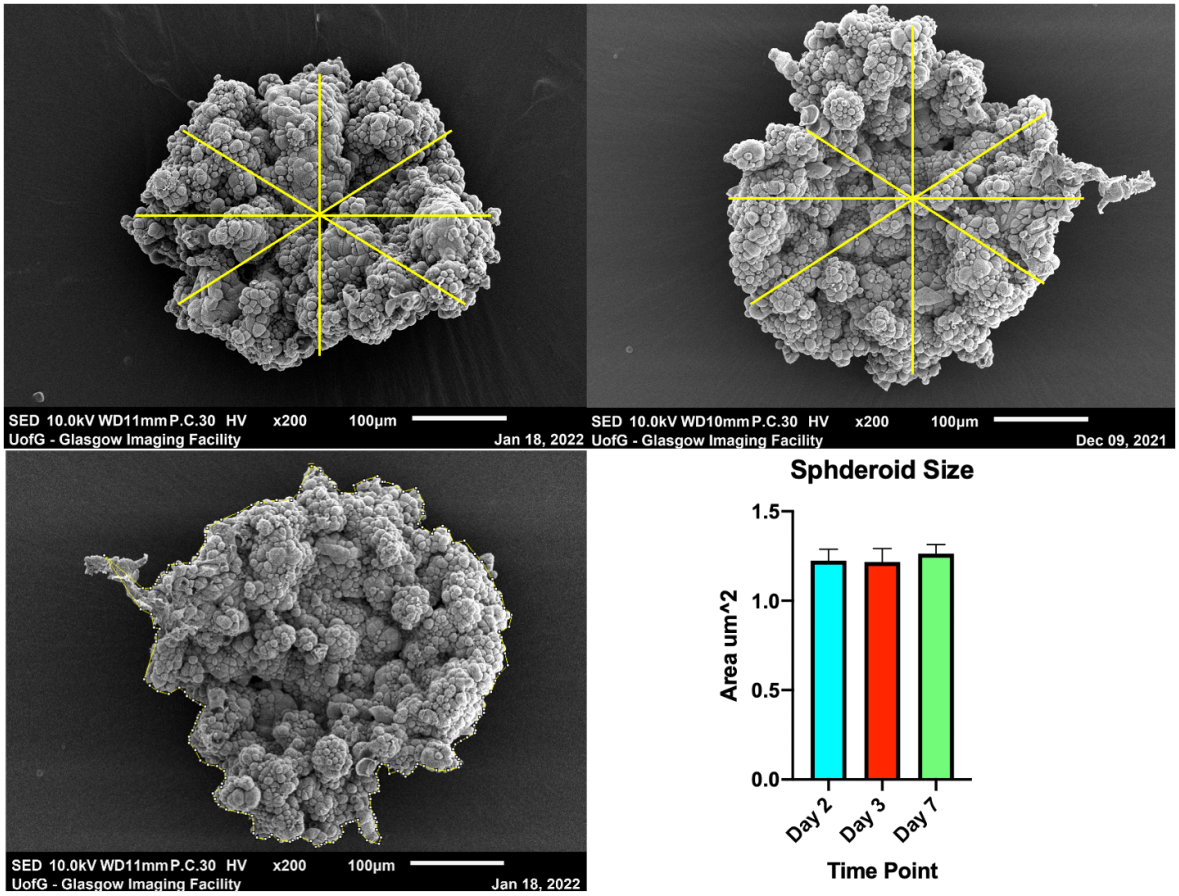

Figure 3.7 Electron Microscopy images (SEM) of multicellular MCF7 spheroids. All images were taken at 200x magnification. Images captured using JEOL JSM-6400 scanning electron microscope at 10kV. SEM software scale bar was used to determine the pixel density/µm ratio. The line measuring tool was then used to measure the diameter at several different locations of the spheroid, after this the polygonal tool (ImageJ) was used to measure the circumference of each spheroid. Each spheroid was comprised of cells seeded at 1 x 10^4, spheroids were seeded and grown for 48,72 and 120 hours. The average area of spheroid was assessed at each time point and plotted (bottom right) after 7 days of culture the average area of 10k spheroids did not significantly change, indicating that the multicellular spheroid has a reduced proliferation rate compared with that of 2D controls. Statistical analysis using Kruskal Wallis test. "*" = p < 0.05, "" = p < 0.01, "***" = p < 0.001, "****" = p < 0.0001, "ns" = non- significant. n=3.**

3.2.5 Proliferation rates of MCF7 spheroids

MCF7 cells in spheroid conformation have less proliferative potential than those in 2D culture. MCF7 spheroids were generated as per section 2.7 using varying cell seeding densities (total number of cells seeded; 2.5 x 10^3, 5.0 x 10^3, 7.5 x 10^3 and 1 x 10^4 cells per well). All spheroids were grown in 96 well ULA plates, MCF7 cells were seeded at the same density into the wells of a regular tissue culture treated 96 well plate to generate a 2D culture control. The 2D and 3D cultures were then grown and investigated at various time points in order to

assess the growth patterns of both 2D and 3D MCF7 cultures. Several methods of assessing proliferation were used including Alamar blue (resazurin reduction), MTT (3-(4,5-Dimethylthiazol-2-yl) assays and probing for expression of Ki67 (proliferation marker). A combination of all assays mentioned above were used to determine and confirm cell proliferation changes between 2D and 3D MCF7 cultures.

A large difference in the proliferation of MCF7 cells dependant on the conformation was observed. Spheroids of each size were compared against 2D controls consisting of the same number of seeded cells. MCF7 cells were grown for 14 days, and proliferation was assessed using MTT assay. At each cell seeding density a statistically significant difference ($P = <0.001$) regarding the proliferation rates of cells was observed. The proliferation rate of MCF7s was shown to be significantly reduced when in spheroid conformation, compared with 2D controls (see figure 3.8).

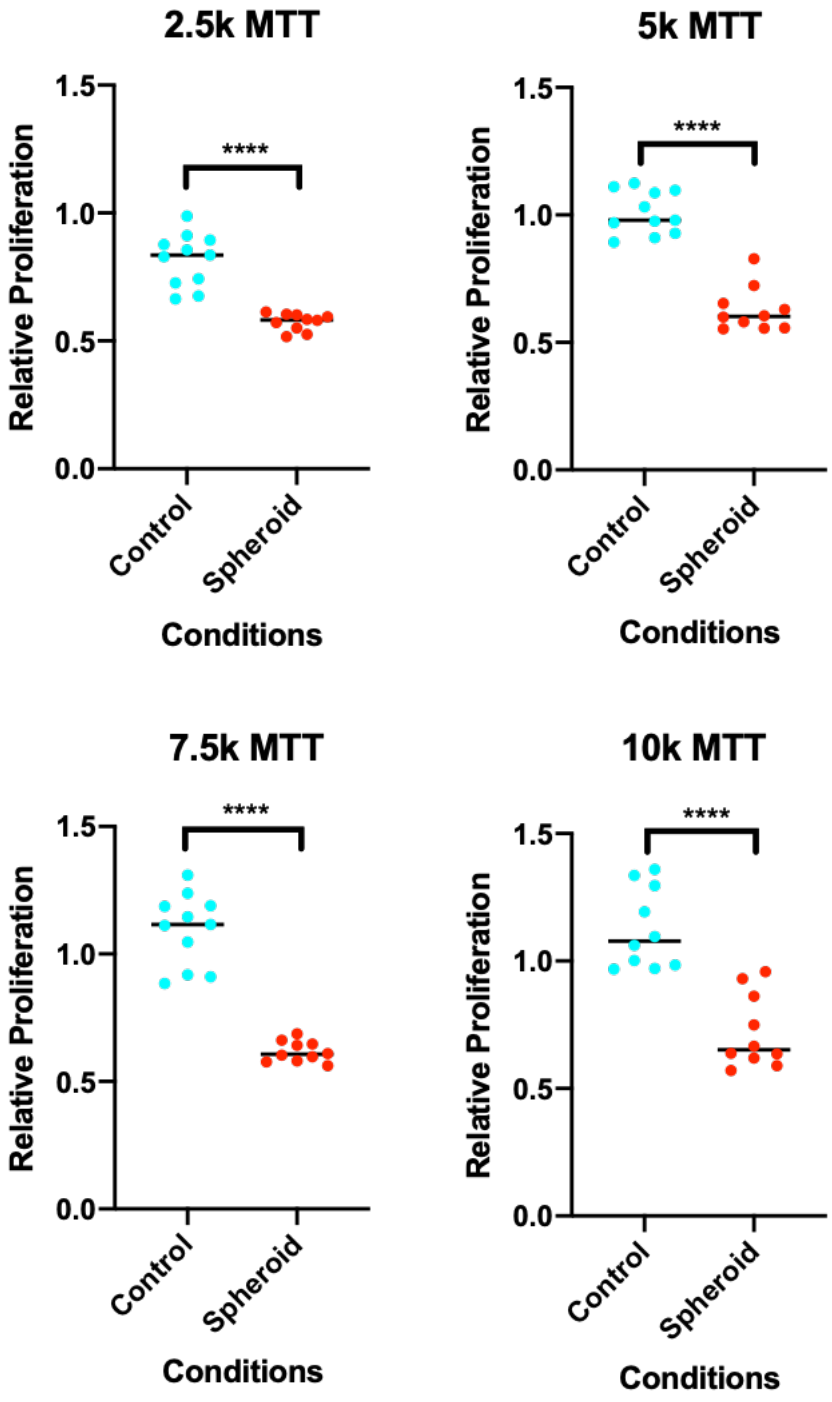

Figure 3.8 MCF7 proliferation measured using MTT (3-(4,5-Dimethylthiazol-2-yl)-2,5-Diphenyltetrazolium Bromide) assay. MTT reagent added to spheroids growing in ultra-low adhesion 96-well plates and allowed to incorporate for 4 hours. Samples then read with a Thermofisher Multiscan FC – and relative proliferation calculated. Spheroids showed significantly reduced rates of proliferation compared with 2D controls across all sizes of spheroid. Statistical analysis using Kruskal Wallis test. "*" = $p < 0.05$, "" = $p < 0.01$, "***" = $p < 0.001$, "****" = $p < 0.0001$, "ns" = non- significant. n=3.**

MTT assay indicated MCF7 cells experienced lower levels of cell proliferation in spheroid conformation versus 2D, using MTT assay. In order to further confirm these results alamar blue assay was used as this assay is shown to be more sensitive than MTT. Alamar blue assay confirmed the reduction in proliferation (see figure 3.9). Varying sizes of spheroid determined by cell seeding density were grown for 14 days along with 2D controls, the reduction in resazurin was assessed after four hours and compared with 2D controls.

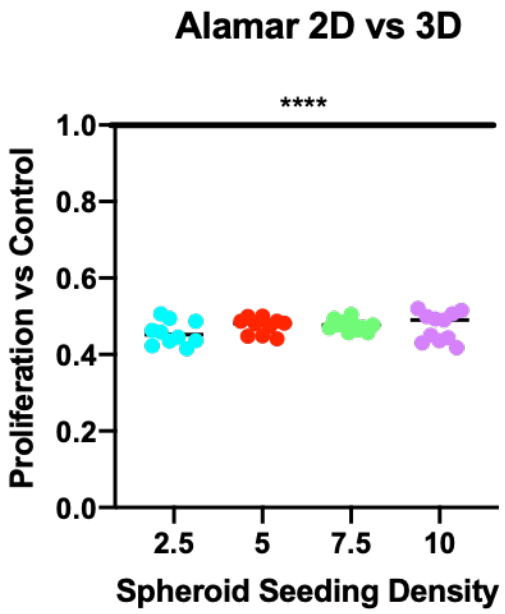

Figure 3.9 MCF7 proliferation measured using alamar blue assay (resazurin). Line at 1 is representative of the control. Resazurin was added to spheroids growing in ultra-low adhesion 96-well plates and 2D controls in regular tissue culture treated 96 well plates and allowed to incorporate for 4 hours. Samples then read with Thermofisher Multiscan FC and relative proliferation calculated. Spheroids showed significantly reduced rates of proliferation compared with 2D controls across all sizes of spheroid. Statistical analysis using Kruskal Wallis test. "*" = p < 0.05, "" = p < 0.01, "***" = p < 0.001, "****" = p < 0.0001, "ns" = non- significant. n=3.**

3.2.6 Ki67 expression in MCF7 spheroids

Ki67 is a cell proliferation marker and is constitutively expressed in proliferating mammalian cells. Ki67 is known to only be produced by actively dividing cells, and is located in the nucleus(Sobecki et al. 2016). Not only is this protein only produced by proliferating cells, but it is also essential for cycling of mammalian cells, being most highly active in G2 phase. Thus, this protein is widely used as a proliferation marker when assessing tumour growth(Sobecki et al. 2016).

Ki67 was shown to be significantly reduced in spheroids when compared with 2D controls, indicating a reduction in proliferation of MCF7 cells in spheroid conformation see figure 3.10).

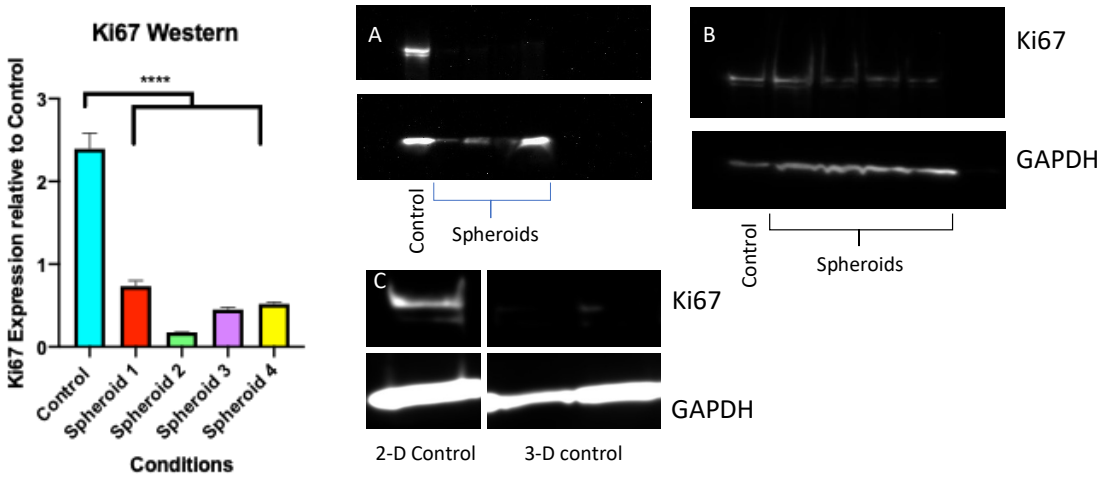

Figure 3.10 MCF7 spheroids were generated as per section 2.7. MCF7s were seeded at the same cell density in regular 96 well tissue culture treated plates as a control. Cells were allowed to grow for 14 days and then lysates were isolated (as per section 2.8) Proteins were then isolated form hey lysates using gel electrophoresis. Ki67 and GAPDH antibodies were used in order to assess total protein concentration of each target. Ki67 expression was shown to be significantly reduced in MCF7 spheroids versus 2d controls. A) Western blot image showing control sample (left) and spheroid samples (right). B) Western blot image showing control sample (left) and spheroid samples (right). C) Western blot image showing control sample (left) and spheroid samples (right). ImageJ was used to investigate the ratio between expression of GAPDH and Ki67.

3.3 Discussion

The key aim of this chapter was to establish an MCF7 model that exhibited reduced proliferation compared with 2D controls, in order to investigate the mechanisms behind breast cancer dormancy and reactivation. This was done via the generation of cancer cell spheroids. In order to validate this, the objectives were to establish spheroids and characterize spheroid formation, stability, structure and proliferation rates.

The key findings of this chapter include the following:

- MCF7 cells are highly proliferative when under 2D culture conditions, this is markedly reduced when MCF7s are forced into a 3D cell culture conformation (spheroid).

- It was shown that MCF7 cells form stable spheroids when grown in round bottom ultra-low adherence plates (liquid overlay technique). It was also demonstrated that the spheroids could be generated reliably and reproducibly.

- MCF7 spheroids have a statistically significantly reduced proliferation rate when compared with controls.

- MCF7 spheroids show a significant reduction in the expression of key proliferation marker Ki67.

-

3.3.1 Model Comparison

Both methodologies used (high-density seeding and spheroid generation) showed a reduction in cell proliferation of MCF7s when compared with 2D controls. However, the reduction of proliferation seen in spheroids generated using the liquid overlay technique was far greater than that of the high-density seeded cells. Spheroids were also more stable and reproducible than the high-density cell mass approach. Other issues arose when using the high-density cell mass, such as after growth for 3 days, often the mass of cells would become detached from the tissue culture surface rendering them unusable. For reasons stated above the spheroid model was used in place of the high-density cell mass for all future experiments.

3.3.2 Characterization of spheroid Size

Differences in the sizes of spheroids formed was shown to be uniform, showing that MCF7 cells form structurally stable, reproducible spheroids. Spheroids formed by MCF7 cells are compact, tightly bound structures. This characteristic seen in MCF7 spheroids is likely due to the noted high expression of E-cadherin associated with this cell line(Pulze et al. 2020b). E-cadherin is a key cell adherence protein, a component of the adherens junctions, responsible for cell adhesion and the maintenance of the epithelial phenotype of cells(Sahana et al.

2018). The high expression of e-cadherin has been shown in previous research by analyzing the expression of e-cadherin in MCF7 spheroids which shows the high e-cadherin expression observed in 2D MCF7 culture is maintained in 3D (Yakavets et al. 2020).

The stable, reproducible nature of MCF7 cell spheroids was also observed, notable as the cell seeding density increased, so did the overall size of the spheroid formed. Spheroid sizes were also measured over various time points, at each time point no significant growth (change in spheroid size) was observed, with spheroid area increasing on average by <5%. (See figure 3.7)

3.3.3 Characterization of spheroid Viability

MCF7 spheroids formed reliable, reproducible spheroids. In order to further verify this model, cell staining was performed in order to identify the proportion of live versus dead cells present in the cell mass. Spheroids seeded at varying cell densities (2.5×10^3, 5.0×10^3 , 7.5×10^3 and 1×10^4 cells per well), were allowed to form and grow and investigated at different time points (3, 7 and 14 days post seeding). Each sample size showed very little dead cell staining while all also showing high levels of live cell staining. This taken in conjunction with previous research conducted by Gong et al (Gong et al. 2015), showing cell viability across the spheroid, validates this cell structure as a viable breast cancer 3D model.

3.3.4 Characterization of spheroid Morphology

As previously shown, MCF7 cells generate stable spheroids, with the size and size range increasing as the number of seeded cells increased. MCF7 cells, due to their high expression of E-cadherin, possess a strong epithelial phenotype (Pulze et al. 2020b), they have been shown to form colonies in 2D monolayer culture. MCF7s high expression of E-cadherin has been shown to persist in 3D culture, thus aiding the formation of spheroids(Sahana et al. 2018).

Electron microscopy (SEM) was used in order to investigate the morphology/phenotype of MCF7 spheroids. Various sizes of spheroids were grown and investigated at different time points. SEM showed the same pattern of spheroid formation as previously indicated, with the size of spheroid ultimately dependent on the number of cells seeded. SEM showed that MCF7 cells within the spheroid retain their epithelial like phenotype, with cells being closely compacted and associated with one another. Cells were shown to be highly compacted within the spheroid mass, with cells differing in size depending on where they reside within the spheroid. Cells on the outer extremities were shown to be larger than those present within. Across all seeding densities MCF7 spheroids adopted a tightly compacted ball like structure, with cells being compacted within the spheroid. The lamellipodia, a cytoskeletal protein associated with epithelial and endothelial cells, can be seen at the protruding edges of MCF7 spheroids, further indicating the retention of MCF7 epithelial like phenotype in 3D spheroid culture (See figure 3.5).

3.3.5 MCF7 cells adopt a quiescent phenotype in 3D spheroid culture

MCF7 spheroids were grown, and their proliferative potential was assessed at various time points. Immediately after seeding, the MCF7s retain some proliferative activity. However, after the aggregation of cells into spheroid formation, the proliferation rate of MCF7 cells significantly reduces. Various methods were used to assess the proliferation of these cells, namely assays designed to assess cell viability and proliferation (Alamar blue and MTT). Along with these methods, the change in size (diameter and area) of spheroid was used to assess growth patterns over a 14-day period. Both Alamar blue and MTT staining revealed that, when compared with 2D monolayer controls (with the same initial number of cells seeded), MCF7 cells within the spheroid mass proliferate at a significantly lower rate (see figure 3.8). This was again confirmed as the change in size of spheroid over time revealed that although there is variation in the size of spheroids based on cell seeding density, the change in size of each spheroid over 14 days was insignificant. This further indicated that MCF7 cells in spheroid conformation have adopted a quiescent

phenotype. The loss of proliferation after 14 days in culture supports the use of both the cell type and methodology to investigate the cellular mechanics responsible for breast cancer dormancy within the bone marrow.

Along with the above methods of assessing cell proliferation, a proliferative marker (Ki67) heavily associated with both breast cancer and the MCF7 cell line (I. Miller et al. 2018; Yuan et al. 2016; Inwald et al. 2013), was assessed after spheroid formation and compared with 2D monolayer controls. Using western blot analysis, the ratio of Ki67 to a reference protein (GAPDH) was calculated in spheroids versus 2D monolayer controls. It was shown that expression of Ki67 was significantly reduced in MCF7 cells when in spheroid conformation. Indicating that proliferation of MCF7 cells has been significantly reduced when in spheroid conformation (see figure 3.10).

Chapter 4 Characterisation of Biomaterials

4.1 Introduction

4.1.1 Fibronectin

Fibronectin (FN) is an essential component of the ECM, shown to be highly influential in many aspects of cell biology, such as adhesion, differentiation, migration and proliferation(Int 1997). FN is known to organise and form fibrillar matrices(Int 1997). FN consists of two distinct subunits linked by two disulphide bonds at the C-terminus. The FN monomer is formed by repeating modules (I,II and III); twelve type I, two type II and between fifteen and seventeen type III domains. A single gene is known to encode all types of FN, with the gene consisting of around 50 exons: with alternative splicing giving rise to several isoforms of FN (Pankov and Yamada 2002).

The distinct functional domains contained in FN serve different functions, FN_{1-2} are known to bind collagen, while FN_{1-5} are known to interact with other molecules of FN to facilitate the formation of FN matrices(Pankov and Yamada 2002). FN is essential in the process of collagen matrix deposition. Several domains contained within FN (FNI_6, $FNII_{1-2}$ and FNI_{7-9}) (see figure 4.1) are shown to interact with collagens, collectively these domains are known as the collagen binding domain(Kadler, Hill, and Canty-Laird 2008). Along with collagen binding, FN is known to bind fibrin, gelatin and tenascin as well as certain bacterial species (Pankov and Yamada 2002; Henderson et al. 2011).

FN is heavily involved in cell binding, with its RGD domain known to be an integrin binding site. The RGD domain can be found in the $FNIII_{10}$ where it appears as a loop, and $\alpha_8\beta_1$ has been shown to bind; $\alpha_5\beta_1$, $\alpha_3\beta_1$, $\alpha_8\beta_1$ and $\alpha_v\beta_3$(Pankov and Yamada 2002). Integrin binding of cells in known to mediate fibrillogenesis in FN along with the RGD (Arg-Gly-Asp) cell attachment domain. It has been previously shown that integrins are capable of binding to FN even when the synergy domain (PHSRN – Pro-His-Ser-Arg-Asn) is not present. However, without the presence of this domain fibril assembly is restricted(Leiss et al. 2008).

FN has been shown to also bind growth factors through its $FNIII_{12-14}$ motif. Growth factors known to bind FN include BMP2, VGEF, FGF, PDGF(Pankov and Yamada 2002), and CXCL12(Martino and Hubbell 2010). The specific localisation of the binding of GF to the ECM facilitates the establishment of stable gradients of growth factors, this in turn mediates cell signalling and plays a vital role in development(Martino and Hubbell 2010). These functions, however, are only relevant if FN is present in 'open conformation', whereby FN is organised in fibrillar networks were both functional domains of FN are exposed and available to bind both cells and GF.

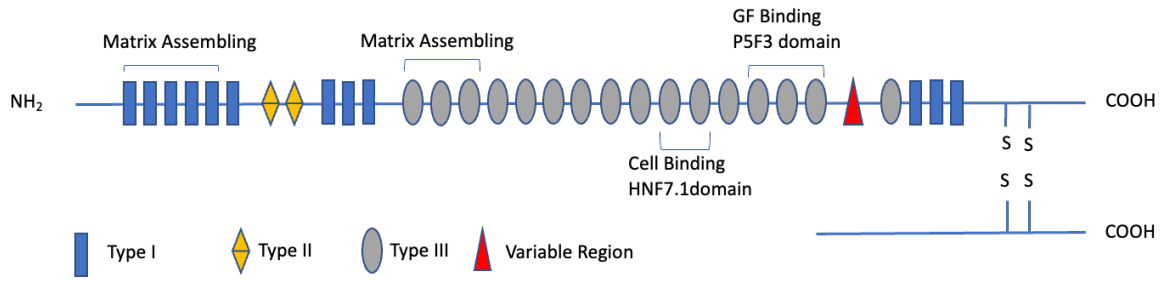

Figure 4.1 Schematic describing the structure and domains of FN. FN is made up of three domains, types I,II and III. With one domain (I-15) responsible for FN-FN assembly and interactions. Another, III9-10 containing the RGD sequence responsible for the cell adhesion and the final domain III-12-14 is responsible for the binding and presentation of growth factors.

In vivo, FN is known to present in two distinct formations, fibrillar and globular(Pankov and Yamada 2002). These formations mediate the availability of the functional domains of FN (Poi and Campbell 1996). Fibrillogenesis is the mechanism by which these FN formations are mediated in vivo(Mao and Schwarzbauer 2005), via the attachment of integrins to the RGD cell attachment domain. In vivo, cells are shown to exert contractile forces on the FN leading to conformational changes in in FN, causing exposure of other domains only available when FN is in fibrillar organisation(Gee, Ingber, and Stultz 2008). In vitro however, it is shown that FN adsorbs onto the surface and adopts a globular conformation as the cellular machinery responsible for fibrillogenesis is absent. This globular conformation restricts the binding and presentation of growth factors (P. Singh, Carraher, and Schwarzbauer 2010), thus an in vitro, cell free

methodology will be explored in order to organise FN in its fibrillar arrangement, thus exposing the previously hidden binding sites.

4.1.2 PEA

In order to drive the fibrillar organisation of FN, several methods have been developed, including the exploitation of topographical features, using hydrophobicity and also using distinct chemical composition of surfaces(Keselowsky, Collard, and García 2003). Previous work has shown that FN adsorption onto surfaces with varying properties and chemical compositions can mediate the conformation/structure of the molecule(Keselowsky, Collard, and García 2003). With cell interactions between the bound protein and integrins present on cells shown to both anchor cells to the surface as well as trigger certain aspects of cell functionality(Keselowsky, Collard, and García 2003; Mao and Schwarzbauer 2005; Dolatshahi-Pirouz et al. 2009).

PEA (poly(ethyl-acrylate) has been shown to facilitate the fibrillar organisation of FN, allowing for both the cell binding domain along with the functional domains of FN to be exposed (Llopis-Hernández et al. 2016). The exposed cell binding domain of fibrillar FN allows to for the integrin mediated binding of cells and thus the generation of focal adhesions. Thus, cells can exert force onto the FN leading to further changes to the structure and exposure of binding domains(Gee, Ingber, and Stultz 2008).

PEA is an acrylic ester polymer that is biostable in vivo and non-degradable. PEA is hydrophobic and shown to exhibit elastomeric properties (Rodríguez-Pérez et al. 2016). The ability of PEA to organise FN into its fibrillar conformation is due to the mobility and composition of functional groups within the polymer (Llopis-Hernández et al. 2016). Two methodologies have been developed in order to coat PEA onto surfaces, due to its properties both methods have been designed in order to coat a nanometrically thin layer of PEA onto the surface. These techniques are spin coating and plasma polymerisation. Both techniques of PEA coating produce very thin layers of PEA on the surface, while retaining the functionality of PEA. Specifically, plasma polymerisation of PEA has been utilised

in coating bone chips before implantation in vivo, these coated bone chips were shown to significantly enhance osteogenesis in bone defect models (Llopis-Hernández et al. 2016; Z. A. Cheng et al. 2018). This was triggered through the presentation of ultra-low doses of BMP-2 bound to the growth factor binding domain of fibrillar FN (Z. A. Cheng et al. 2018).

Therefore, PEA can be utilised in conjunction with FN in order to deliver and present ultra-low doses of growth factors to various cell types both bound to fibrillar FN.

4.1.3 Objectives

This chapter aims to characterise the materials mentioned above and optimise for use as a cell culture model to deliver ultra-low doses of BMP-2 and CXCL12. Firstly, the surface chemical properties were analysed, the organisation of FN on the tissue culture surface along with the availability of functional domains was the assessed. The binding of cells and growth factors was verified. The aim of this chapter was ultimately to generate an in vitro model capable of binding cells and presenting ultra-low doses of growth factors, leading on from the most up to date research in the field.

4.1.4 Experimental Design

In order to characterise the biomaterials model described above, serval experiments were designed to validate various aspects of the model. These include the characterisation of chemical composition on pPEA surface utilising XPS analysis, an assessment of FN conformation and investigation into the adsorption of FN onto tissue culture plastic. The availability of FN functional domains was then assessed using ELISAs specific to distinct binding domains present on FN. Growth factor binding, and release profiles were then assessed using ELISA assay to identify total protein binding at several time points. With the ultimate aim of using this model to generate differentiation specific metabolites for treatment of spheroids (see figure 4.2).

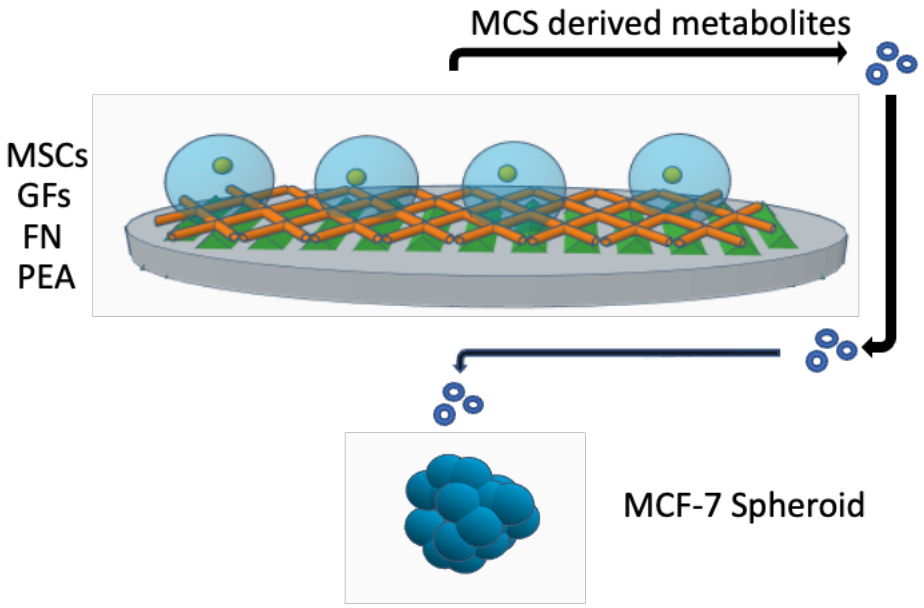

Figure 4.2 Schematic depicting the experimental design of this chapter.
A tissue culture surface will be coated using plasma PEA to deposit a thin layer (around 10 nm) of polymer on the surface. FN will then be coated onto this layer or pPEA, spontaneously triggering the fibrillar alignment of FN. The growth factors BMP2 and CXCL12 will then be coated onto the FN that will bind the P5F3 growth factor binding domain. MSCs will then be seeded onto the model and allowed to adhere to the integrin binding domain of FN. MSCs will then be grown for 28 days on the model. After 28 days growth media will be removed and cells washed, following the wash 'regular' (no additives) tissue culture media will be added and 'conditioned' for 48 hours. This media will then be harvested and used in future experiments.

4.2 Results

4.2.1 Surface Chemical characterisation

X-ray photoelectron spectroscopy was performed to characterise the surface chemical composition (top 10 nm) of samples in order to confirm the chemical motif of pPEA on tissue culture plastic. XPS confirmed the chemical composition of pPEA versus spin coated PEA, this was identified using refence to literature and previous studies conducted by this lab (Llopis-Hernández et al. 2016; Sprott 2019). Carbon and oxygen scans were obtained for pPEA (plasma PEA). The carbon and oxygen spectra were fitted with peaks indicting the binding conformations of atoms within the samples. The spectrum of pPEA indicated distinct peaks of the carbon-to-carbon bonds at 284-285 eV (as expected based on literature in which PEA is spin coated onto samples) (Alba-Perez et al. 2020c). The C=O mitotes peaked between 530 and 532 eV, whilst the C-O-C bonds peaked between 532 and 534 eV (see figure 4.3). These XPS scan data show a slight difference in the spectrum of peaks when compared to those obtained from pure PEA(Alba-Perez et al. 2020a). These small differences are likely due to the monomer fragmentation occurring when PEA is plasma coated onto tissue culture surfaces(Alba-Perez et al. 2020a).

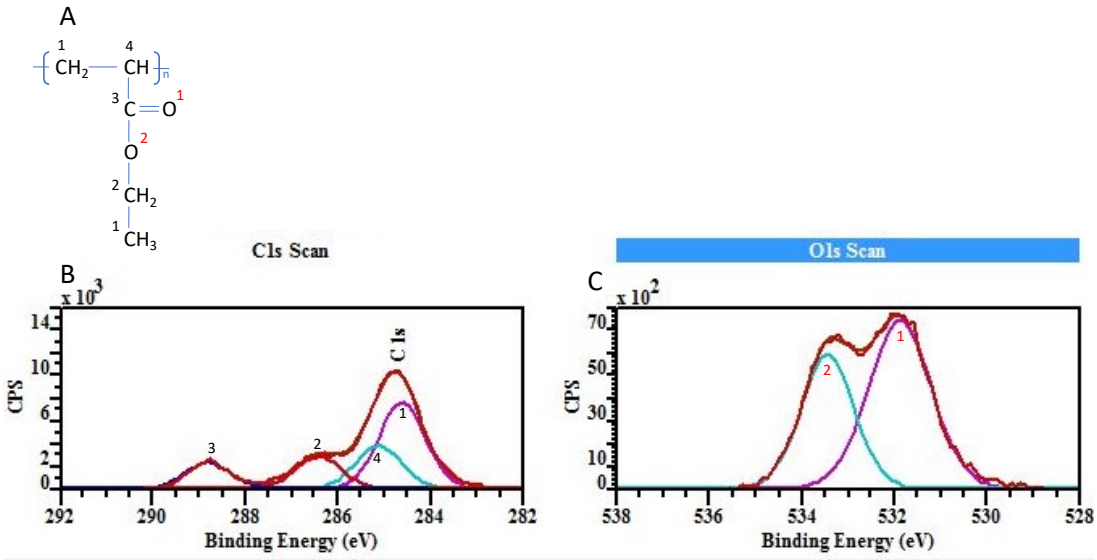

Figure 4.3 Chemical characterisation of plasma PEA via x-ray photoelectron spectroscopy analysis. A – Chemical formula for PEA, B- Carbon scan XPS, C – Oxygen scan XPS. Precise

chemical structure of PEA is depicted above with numbers indicating specific bonds within the structure. Carbon and oxygen spectra are shown above, components of the structure can be seen fitted as coloured lines. Numbers on the spectra (labelled peaks) correspond to specific bonds shown in the chemical structure seen above. Spectra shown is similar to that obtained from pure PEA(Alba-Perez et al. 2020a).

To assess the surface chemical composition of plasma polymerised PEA, a 24 well plate (corning) was coated in as described above, and x-ray photoelectron spectroscopy was performed on 3 randomly selected wells. This was performed in order to investigate how evenly pPEA is deposited over the tissue culture plastic. The total composition of each chemical bond was assessed in the three different locations (wells) and analysed (see figure 4.4). Although minor differences between the wells were observed, the spectra showed that PEA was present in its expected conformation in all wells tested.

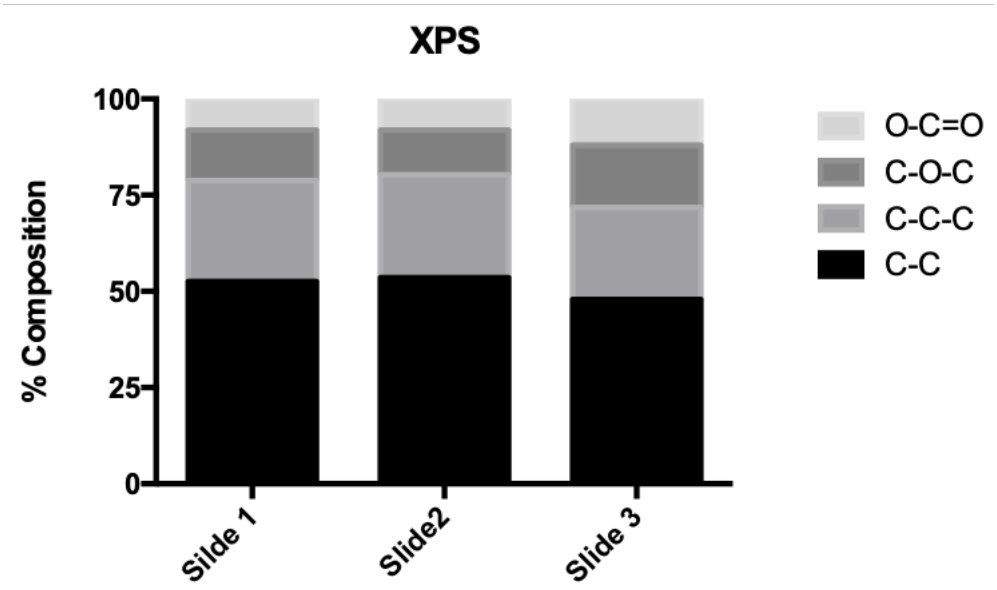

Figure 4.4 Calculated percentages of carbon composition for each selected well. In all wells peaks corresponding to PEA were observed and relative percentages of bonds were similar to that of pure PEA. Graphs are shown mean ± SEM, Statistical analysis using two-way ANOVA. "*" = p < 0.05, "" = p < 0.01, "***" = p < 0.001, "****" = p < 0.0001, "ns" = non-significant. n=3.**

4.2.2 ECM on pPEA

To confirm the presence of FN networks on the pPEA, atomic force microscopy was utilised, this allowed for the investigation into the FN surface at the nanoscale, and also allowed the roughness of the surface to be investigated. The presence of FN networks was observed and also height measurements indicated the presence of bound FN to the pPEA surface (see figure 4.4).

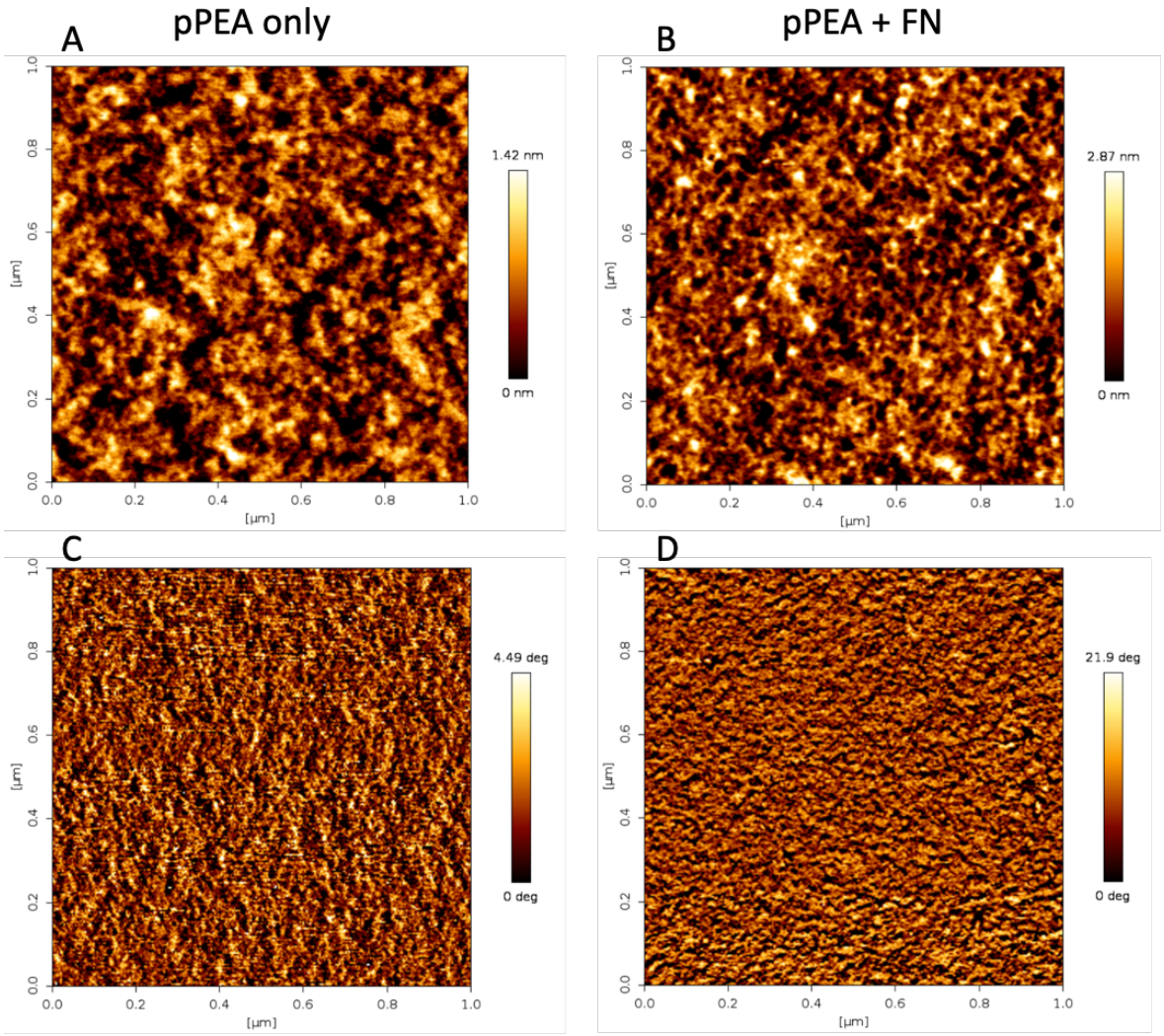

Figure 4.5 AFM imaging of adsorbed FN on pPEA samples. A- height image from tapping mode AFM of plasma coated PEA. B height image from tapping mode AFM of plasma coated PEA and FN. C- AFM phase image of plasma coated PEA. D- AFM phase image of plasma coated PEA + FN.

4.2.3 FN adsorption

To quantify the adsorption of FN to the sample surface (pPEA) a sandwich ELISA was carried out. A stock concentration of FN was made up (20 μg/mL), 100 μL FN solution was added to the pPEA coated samples and allowed to adsorb for one hour at room temperature. The stock FN solution was used as a control. After one hour the solution was aspirated and stored for future experiments.

A sandwich ELISA was carried out in order to compare the concentrations of FN present in the stock and samples, thus the difference in total protein present in control versus samples is indicative of the amount of ECM protein adsorbed onto the sample surface. Tissue culture plastic (polystyrene) was used as a control.

Both tissue culture plastic and pPEA samples were shown to bind FN, the difference in aspirated FN samples and FN stock were calculated and presented in the form of percentage adsorption. Both tissue culture plastic and pPEA were shown to adsorb significant amounts of FN onto their surface, with TCP appearing to have greater adsorption than pPEA (see figure 4.6). This observed increased ability for TCP to bind more FN than pPEA coated surfaces could potentially be due to the binding confirmations of FN, as FN bound in an open confirmation could potentially occupy more space on the surface. This could be investigated using AFM to analyse the surface prolife of pPEA and TCP bound FN and assess the networks present on the surface.

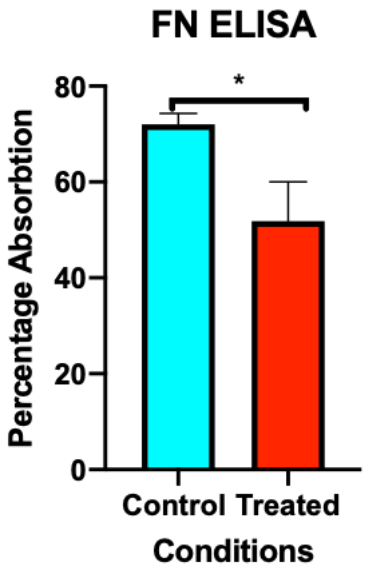

Figure 4.6 FN adsorption onto tissue culture plastic and pPEA
FN stock (20 μg/mL) was used to calculate the percentage FN adsorbed onto the surface, aspirated solutions were analysed using sandwich ELSIA. Tissue culture plastic was adsorbed significantly more of the ECM protein than pPEA coated samples. Both, however showed adsorption of FN onto the surface with TCP adsorbing around 75% of available FN and pPEA adsorbing around 50% of available FN. The discrepancy between TCP and pPEA could potentially be due to the conformation of FN after adsorption, TCP would bind FN in its globular conformation. However, pPEA would bind FN in its open conformation potentially occupying more surface area per molecule of FN causing this observed difference. Statistical analysis via an unpaired t-test Graphs is shown mean ± SEM, "*" = p < 0.05, "" = p < 0.01, "***" = p < 0.001, "****" = p < 0.0001, "ns" = non- significant. n=3.**

4.2.4 FN functional domain availability

To investigate the activity of FN bound to pPEA, an ELSIA was used to determine the availability of both the integrin and growth factor binding domains on open conformation FN. The availability of both domains were quantified using ELSIA antibodies and compared a tissue culture plastic control. The binding domains responsible for integrin (cell) and growth factors are HFN7.1 and P5F3 respectively (Llopis-Hernández et al. 2016). Upon analysis it is evident that FN coated onto pPEA is binds significantly more of each domain antibody. The availability of domains on the surface of FN indicates that FN, when adsorbed to the pPEA surface, undergoes unfolding of its structure, in turn leading to its

'open' conformation. The effect of this open conformation is observed here, as globular conformation FN was shown to bind significantly lower amount of growth factor, in contrast when coated onto pPEA the adsorption of antibodies is seen to significantly increase (see figure 4.7). This open conformation is shown to bind integrins, and also bind and present growth factors, this mechanic shown here will be utilized in this project to present growth factors to MSCs bound to FN.

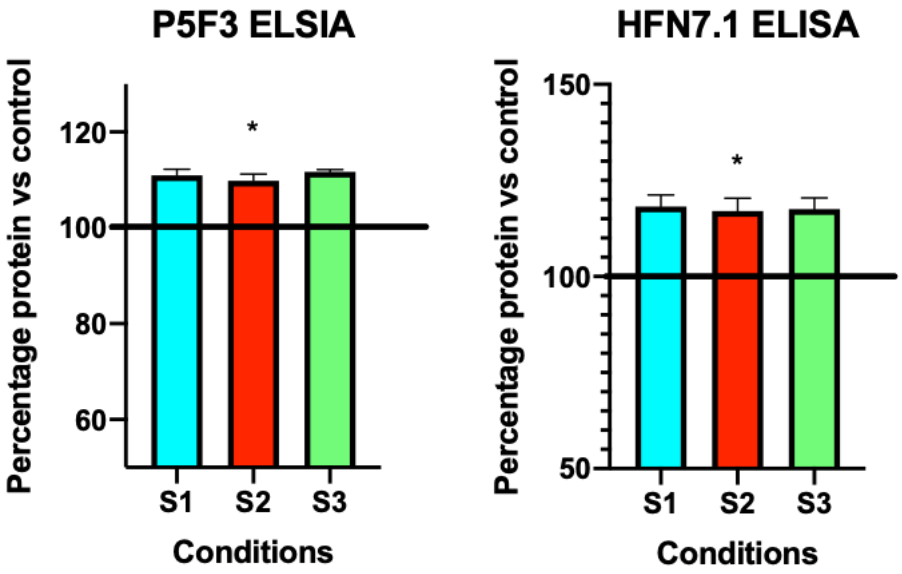

Figure 4.7 Availability of FN functional domains
The functional domain availability of FN was assessed on both tissue culture plastic (TCP) and pPEA, using ELSIA. S1, S2 and S3 represent samples 1,2 and 3 respectively. Average absorbance was calculated for each sample for both TCP and FN, the percentage difference between TCP and FN was then calculated, this represented in the above graphs. P5F3 (Growth factor binding domain) domain binding was shown to be increased on the pPEA surface when compared with TCP, with around a 10% increase in domain availability. The HFN7.1 domain (RGD-integrin binding domain) binding was also shown to increase on pPEA when compared with that of TCP. Graphs are shown mean ± SEM, Statistical analysis using two-way ANOVA. "*" = $p < 0.05$, "" = $p < 0.01$, "***" = $p < 0.001$, "****" = $p < 0.0001$, "ns" = non- significant. n=3.**

4.2.5 Confirmation of Growth factor binding

To confirm the binding of growth factors to the GF binding domain of open conformation FN, a sandwich ELISA was used in conjunction with specific protein

standards to determine the concentration of growth factor containing solutions used for the coating of samples. pPEA was investigated along with tissue culture plastic as a control, after coating with FN, samples were washed and coated with BMP2, CXCL12 or a combination of both growth factors. After incubation for one hour at room temperature the GF containing solutions were aspirated and used for future experiments.

This aspirated solution (from both FN and TCP) was used in conjunction with the stock solution of growth factors (used initially to coat sample surfaces) to determine the amount of growth factors adsorbed to the samples. These data were then analyzed and converted into percentage of protein adsorbed, based on the concentration of the growth factor stock solutions. Upon analysis of these data is it clear that FN when bound to pPEA readily binds greater amounts of growth factor protein than FN bound to TCP. The affinity of growth factor binding however is not uniform, as shown in figure 4.8, 'open conformation' FN shows a far greater affinity for binding BMP2 when compared against the TCP. However, there is less disparity in binding affinity with CXCL12 between pPEA and TCP bound FN, despite this pPEA FN is shown to bind significantly greater amount of protein than TCP bound FN.

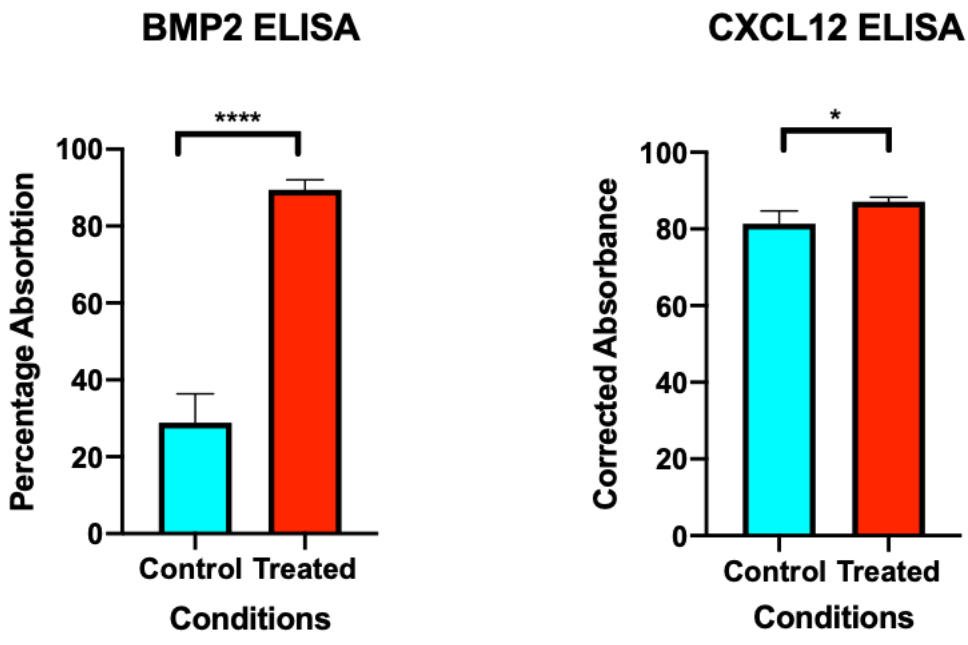

Figure 4.8 Protein adsorption onto TCP and pPEA bound FN.

The binding affinity of both BMP2 and CXCL12 to FN was assessed on both tissue culture plastic (TCP) and pPEA, using ELSIA. Average absorbance was calculated for each sample for both TCP and FN, the percentage difference between TCP and FN was then calculated, this represented in the above graphs. Control = TCP, treated = pPEA. pPEA can be seen to adsorb significantly greater amounts of BMP2 compared to TCP. The binding of CXCL12 to FN TCP and FN pPEA is more similar to that of BMP2, however FN pPEA is still shown to bind significantly more protein than FN TCP. Graphs are shown mean ± SEM, Statistical analysis using unpaired t-test. "*" = p < 0.05, "" = p < 0.01, "***" = p < 0.001, "****" = p < 0.0001, "ns" = non- significant. n=3.**

4.2.6 Biomaterial model – cell viability

Tissue culture plastic and pPEA surfaces were coated with FN, and then further coated with various growth factors (as described above). After adsorption of growth factors, MSCs were seeded onto the biomaterials surface at a density of 10,000 cells/cm^2. These cells were fed twice per week with growth factor supplemented media. In order to assess the validity of this model, cells were stained with calcein AM and ethidium homodimer to visualise live and dead cells respectively. Cells were seeded and grown for 28 days, stained, and analysed using a fluorescent microscope (Evos M700). After 28 days very little dead cells were identified on the biomaterials model, with the vast majority staining for alive cells (See figure 4.9).

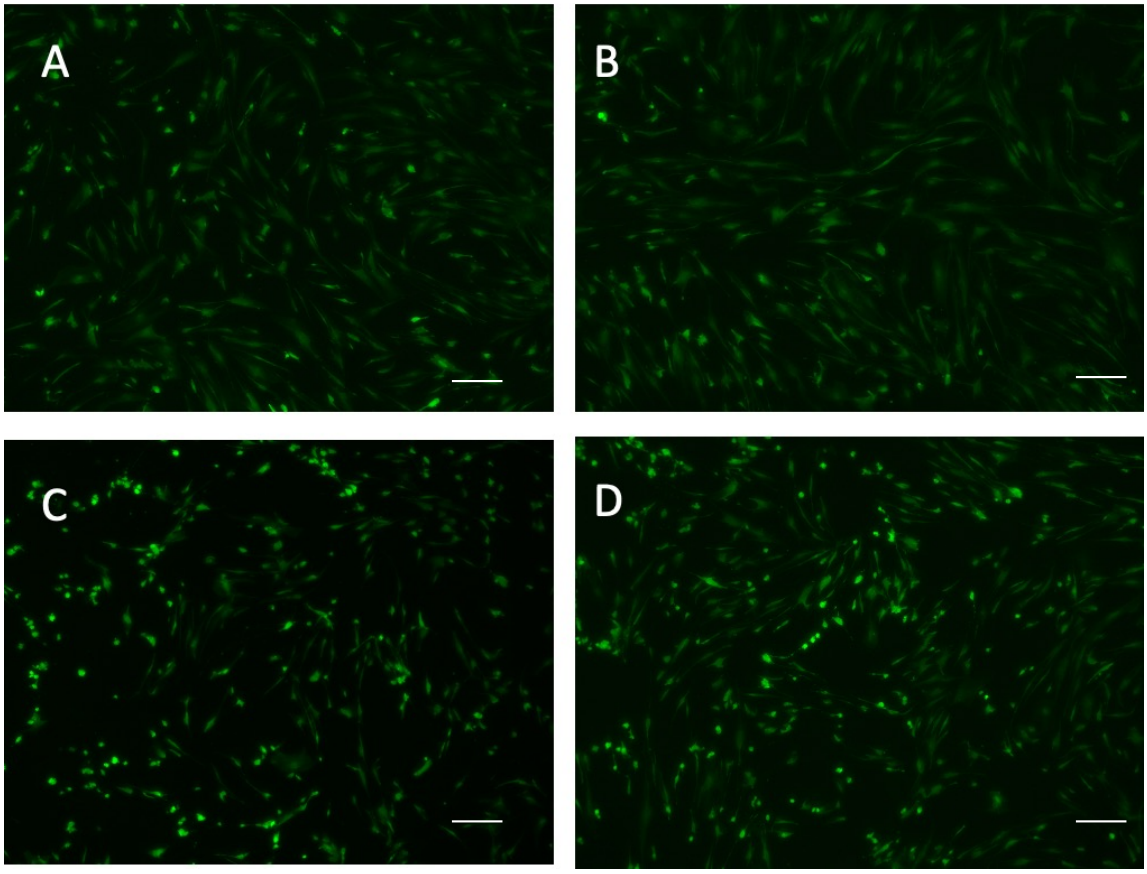

Figure 4.9 Live/dead staining of biomaterials model and control
MSCs were seeded onto TCP + FN + GF and pPEA + FN + GF at a cell density of 10,000 cells/cm2. A- Control B- BMP2 treated, C- CXCL12 treated D- BMP2 and CXCL12 treated. The MSCs were allowed to grow/differentiate for 28 days. After 28 days GF supplemented media was aspirated, and cells washed with hepes saline solution. Following the wash step calcein AM and ethidium homodimer was added to the cells (2μM and 4μM respectively) and incubated for 15 minutes at room temperature. Cells were then visualised using fluorescence microscopy. After 28 days a significant percentage of cells on the biomaterials model were alive, with the difference between samples and controls being insignificant. Scale bar = 100μm

4.2.7 Differentiation of MSCs

The aim of the biomaterials model was to trigger differentiation of MSCs using ultra-low doses of growth factors. However, after 28 days in culture differentiation markers for MSCs were shown to be insignificant when compared with MSC controls. Several methodologies were employed in order to assess the differentiation success using this model. Namely in cell western and PCR were used to assess marker expression. Antibodies for two osteogenic differentiation

markers (osteopontin and RUNX2) were used to probe the MSCs grown on the biomaterials model after 14 and 28 days. Although a trend was noticeable in the expression of these markers, no significant difference between the treated samples and controls was observed (see figure 4.10).

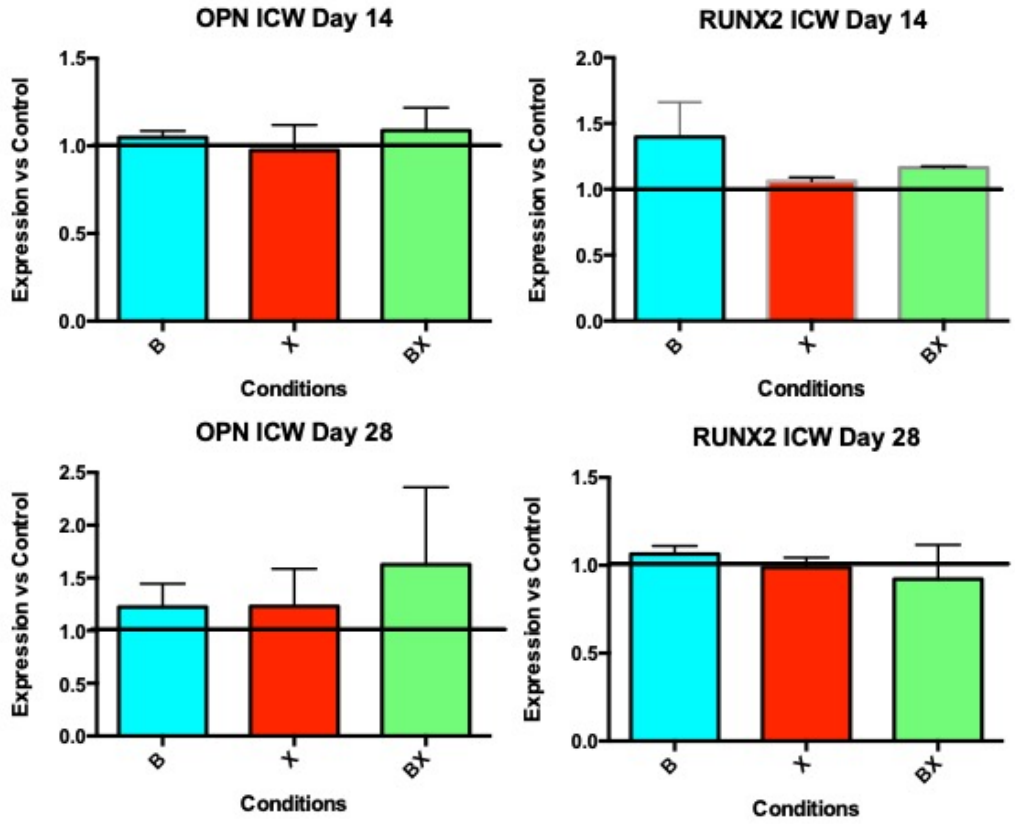

Figure 4.10 In cell western Osteopontin (left) and RUNX2 (right) expression of MSCs on biomaterials model. MSCs were seeded onto pPEA + FN + GF, media was supplemented with relent growth factor and replaced twice per week. MSCs were grown/ allowed to differentiate for 14 and **28 days. Following this period, antibodies for osteopontin and RUNX2 were used to probe for expression of these proteins in the MSCs. The relative expression of each protein was calculated using control sample as reference. A trend is visible with a slight increase in expression of OPN across all conditions and a very slight increase in RUNX2 in the BMP2 treated samples and a slight reduction in CXCL12 and BMP2/CXCL12 treated samples. Despite these trends however no significant change is observed. Graphs are shown mean ± SEM, Statistical analysis using Kruskal Wallis test. "*" = p < 0.05, "**" = p < 0.01, "***" = p < 0.001, "****" = p < 0.0001, "ns" = non- significant. n=3.**

Aside from osteogenic markers, stemness markers were also investigated in these MSCs, samples were prepared as above and stemness markers; Nestin and

CD166 were investigated. Fluorescent antibodies for the above markers were used to probe MSCs and control values were used to generate relative expression data. Similarly, to the osteogenic markers, these markers showed no significant change when compared to that of the controls (see figure 4.11).

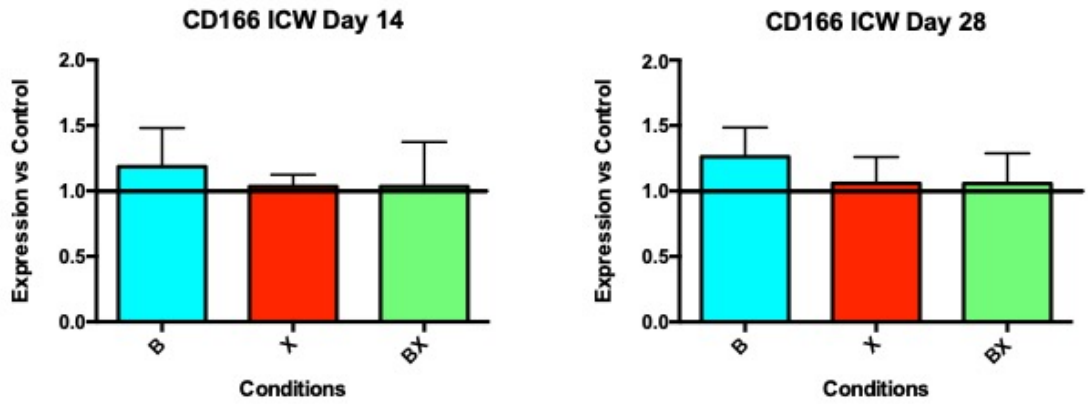

Figure 4.11 In cell western of CD166 (right) expression of MSCs on biomaterials model MSCs were seeded onto pPEA + FN + GF, media was supplemented with relent growth factor and replaced twice per week. A trend is visible with a slight increase in expression of OPN across all conditions and a very slight increase in RUNX2 in the BMP2 treated samples and a slight reduction in CXCL12 and BMP2/CXCL12 treated samples. Despite these trends however no significant change is observed. Graphs are shown mean ± SEM, Statistical analysis using Kruskal Wallis test. "*" = p < 0.05, "" = p < 0.01, "***" = p < 0.001, "****" = p < 0.0001, "ns" = non- significant. n=3.**

Despite observation of trends after in cell western analysis, no significant difference was observed regarding expression at the protein level of the markers of interest. qPCR analysis was also performed to ascertain changes in expression of certain markers at the gene level. MSCs were grown as above, after 14 and 28 days RNA was isolated from samples and quantified. Reverse transcription was then performed to generate cDNA form each sample. Primers were designed to probe for osteogenic markers; osteopontin (OPN), RUNX2 and osterix (OSX). qPCR was the performed using these primers and cDNA generated from biomaterials samples. Similar to the results of the protein expression experiments, despite a trend being observed (with BMP2 treatments showing slightly higher expression of osteogenic markers) there was no significant difference shown between the controls and treated samples (see figure 4.12).

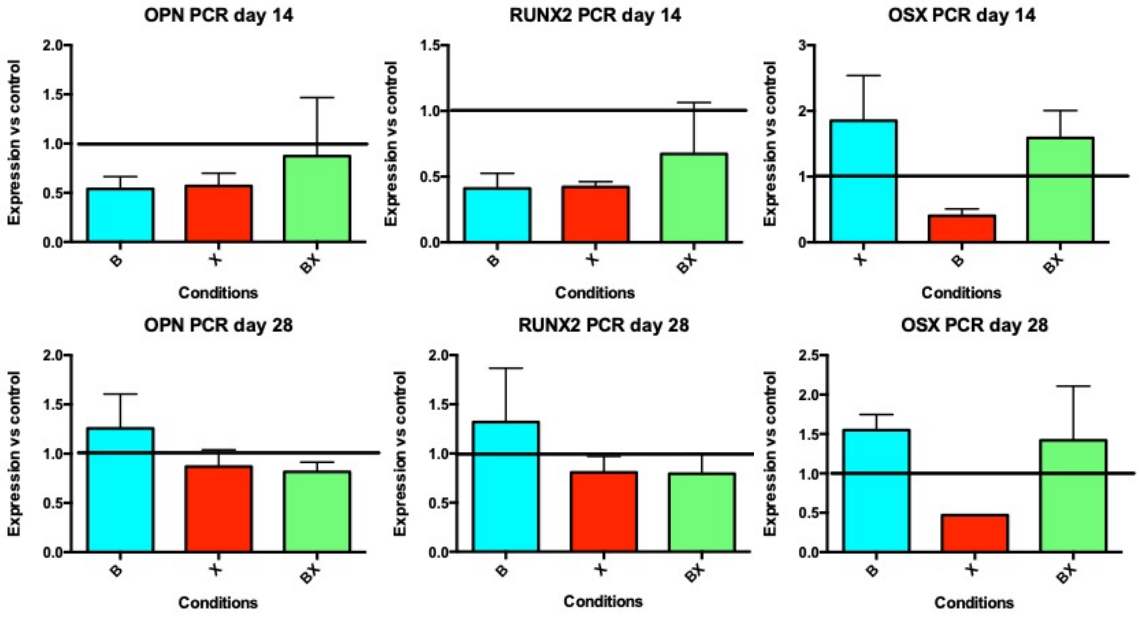

Figure 4.12 OSX (left), RUNX2 (middle) and OPN (right) qPCR expression profiles Samples were grown as above, RNA isolated and cDNA generated. Primers were designed to investigate the qPCR profiles of OSX, RUNX2 and OPN, all osteogenic markers. All samples were normalised against a control and presented as such. There was no significant difference observed in any of the genes investigated, however there does appear to be a trend with BMP2 treated cells consistently greater RNA expression of osteogenic markers investigated. Graphs are shown mean ± SEM, Statistical analysis using Kruskal Wallis test. "*" = p < 0.05, "" = p < 0.01, "***" = p < 0.001, "****" = p < 0.0001, "ns" = non- significant. n=3.**

Alizarin Red S stain was also utilised to assess the osteogenic differentiation capabilities of the model and compared against a control using osteogenic differentiation media (see methods). There was little to no difference observed between the controls and treated samples, with the positive control (osteogenic media) showing differentiation after 28 days (see figure 4.13).

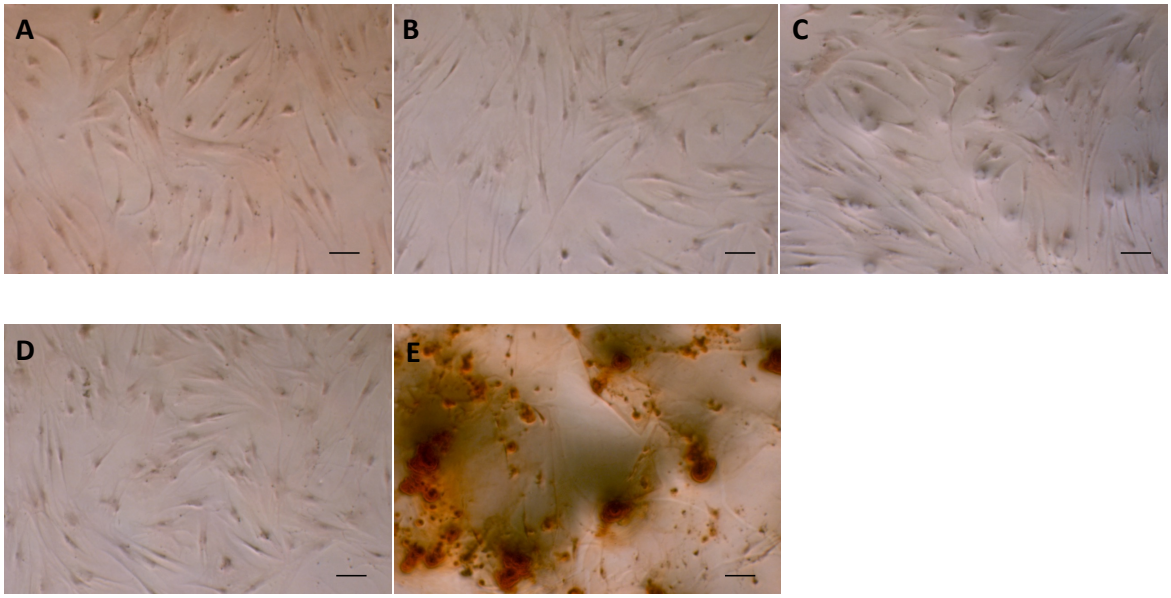

Figure 4.13 Alizarin Red S stain of 28 day cultured MSCs on the biomaterials model (pPEA + FN + GF. Conditions are as follows; A- Control (pPEA + FN), B- BMP2 (pPEA + FN + BMP2), C- CXCL12 (pPEA + FN + CXCL12), D- combination treatment (pPEA + FN + BMP2 + CXCL12), E- positive control (pPEA + FN + osteogenic media). Alizarin red s stains calcium red, thus identifies where osteogenesis has taken place, no staining is visible in treated samples, but is present in positive control, indicating a lack of osteogenic differentiation in the treated samples. Scale bar = 100 μm.

4.3 Discussion

The aim of this chapter was to develop a materials-based model in order to deliver ultra-low doses of both BMP2 and CXCL12 to MSCs, and to trigger differentiation of said MSCs. Herein we have described the characterisation of the different components of this model, with the basic structure being pPEA + FN (ECM protein) + growth factors, with cells (MSCs) being the final component in the structure.

Previous literature has described how PEA can be reliably coated onto both coverslips and biomaterials scaffolds using plasma polymerisation (Alba-Perez et al. 2020a). Using this information, this chapter aimed to generate a model of MSC differentiation using ultra low doses of growth factors. In order to increase the throughput of this model, tissue culture plates were utilized (24 well) as opposed to the use of coverslips. 24 well corning plates were coated with PEA suing the plasma polymerisation technique, these samples were then validated

using XPS. Following the surface material characterisation, the assembly of ECM networks was validated though the use of AFM (atomic force microscopy). FN was coated onto the pPEA surface and analysed using AFM. The formation of these networks, triggered by pPEA demonstrated enhanced availability of both integrin and growth factors binding domains. This enhanced availability of binding locations was confirmed through the use of ELISAs, probing specifically for these binding sites.

4.3.1 pPEA triggers spontaneous FN fibrillar organisation

The spontaneous organisation of FN into nanonetworks through the use of poly(ethyl acrylate) (PEA) has been previously described by our lab (Alba-Perez et al. 2020c; Llopis-Hernández et al. 2016; Sprott 2019; Sprott et al. 2019). This organisation into physiological like fibrils allows for the simultaneous exposure of binding motifs essential for cell adhesion and growth factor binding, specifically, the integrin binding domain (HFN7.1) and growth factor binding domain (P5F3). In order to generate the throughput necessary for this chapter, however, the standard method of coating PEA (spin coating) would be time consuming and would not be capable of coating the large volume tissue culture plates needed for high throughput. Thus, plasma polymerisation was utilised in order to coat relatively large surface areas quickly. Plasma polymerisation of PEA was investigated in this chapter, more specifically for its ability to trigger the spontaneous organisation of FN.

Firstly, XPS was used to analyse the deposition of pPEA onto tissue culture surfaces, this was validated through the analysis of the spectra, and found to be comparable to the spectra associated with spin coated (gold standard) PEA, however this method of applying PEA to surfaces could result in polymer chain modification. As well has this, plasma coated PEA has been shown to ‘peel’ whereby the thin layer of pPEA becomes detached from the surface due to the fact that the PEA is not chemically bound to the surface. Despite these drawbacks however, pPEA has been shown to trigger the spontaneous organisation of FN and consequently expose essential binding motifs. This is

demonstrated in this chapter via ELISAs, used to demonstrate the enhanced availability of both the HFN7.1 and P5F3 binding sites.

Following the characterisation of the binding site availability of pPEA bound FN, growth factor binding to the FN networks was assessed. This was achieved through the use of sandwich ELSIAs. Samples were prepared using pPEA and FN and growth factors were coated onto both pPEA and TCP samples. After one hour the growth factor containing solution was aspirated form samples, this solution was then compared against the stock solution of growth factors to determine the difference in concentration between the stock and aspirated samples. This difference would therefore indicate the amount of growth factor adsorbed to the surface. This thesis shows that FN, when coated onto pPEA, bind significantly more BMP2 and CXCL12 when compared against TCP control.

Following validation of growth factor binding, cell binding and cell viability was investigated, cells were seeded onto the biomaterials surface, allowed to adhere overnight and then treated with growth factor containing medium. After varying days of culture, cells were stained using calcein AM and ethidium homodimer to stain for live and dead cells respectively. At every time point investigated, cells were clearly seen to be adhered to the surface with also a large percentage (>80%) of cells shown to be alive.

4.3.2 Differentiation of MSCs

The capability of this model to trigger differentiation of MSCs was assessed using several methodologies including: staining using Alizarin red S, qPCR and in cell western for markers associated with differentiation and stemness. Despite observable trends in both the in cell western data along with the qPCR data, no significant difference was observed in expression of markers associated with osteogenic differentiation. Also observed, there was no significant difference between expression of stemness markers, indicating that after 28 days incubation on this system, MSCs still retain some stemness despite treatment. One potential explanation for the lack of differentiation observed is the MSCs may have remained proliferative and therefore would have resisted

differentiation, as it has been shown that although precursor differentiated cells remain proliferative, proliferation is usually halted before terminal differentiation (Ruijtenberg and van den Heuvel 2016a). These results were unexpected and unfortunate, despite this however, media used to grow these samples (conditioned) will be taken forward for use in future experiments, to investigate the metabolic changes occurring in these biomaterials treated MSCs (to potentially determine the reasoning being this observed lack of differentiation).

Chapter 5 Reactivation of dormant breast cancer cell model

5.1 Introduction

5.1.1 Breast Cancer Metastasis

Breast cancer metastasis is responsible for a very large number of deaths relating to breast cancer, with studies showing the 5-year survival rate of patients to be around only 26% (M. T. Chen et al. 2017; S. Li et al. 2012; Mariotto et al. 2017). Issues arise due to the lack of understanding around metastatic recurrence of the disease. Much progress has been made regarding the identification, diagnosis and treatment of breast cancer. However, treatments options are severely limited after metastasis, with palliative care being the single option in many cases (Miglietta et al. 2022). The major weakness in the collective understanding behind metastatic recurrence is the molecular mechanisms responsible for triggering reactivation of dormant breast cancer. The challenge here lays with the heterogeneity observed in tumours, making it difficult to predict outcomes for patients.

This recurrence is a great clinical problem with large numbers of people experiencing this issue, as patients diagnosed with small tumours have a 25-30% chance of tumour recurrence after 15 years (S. Li et al. 2012). Recently, studies have suggested and shown that residual dormant tumour cells persist in patients long after surgery and treatment (Miglietta et al. 2022; M. T. Chen et al. 2017). These micrometastases have been shown to be dormant (quiescent). The period of this dormancy has been shown to be heterogenous, with latency periods ranging from a few months to decades. Several properties can influence the period of dormancy including cancer cell type, inflammation response, lifestyle as well as a variety of other/unknown factors (Pedersen et al. 2022).

5.1.2 Tumour Dormancy

The metastatic cascade describes the phenomenon whereby cells originating from the primary tumour escape, and results in the formation of secondary

tumours at distant sites within the body (Chong Seow Khoon 2015). Tumour cells are known to invade the surrounding tissue of the primary tumour, they are then capable of intravasating from the tissue into the blood vessels and from there they can travel throughout the body using the vasculature. These cells are known as CTCs (circulating tumour cells), CTCs are then capable of extravasating at a secondary site and forming a secondary tumour (colonising). This method of tumour colonisation sees only a few CTCs forming metastases; however, this small percentage is still enough to cause severe issues for patients (Massagué and Obenauf 2016). Disseminated tumour cells or CTCs have been shown to undergo various stresses both while circulating and after secondary colonisation. The vast majority of CTCs die either in the vascular system or post-secondary colonisation (Cieślikowski et al. 2020). Systems responsible for the death of CTCs include vascular stress and immunomodulatory mechanisms, resulting in the death of CTCs in the vasculature. The small percentage of CTCs that colonise secondary sites then face further environmental stresses and immunomodulatory mechanisms, resulting in the majority of secondary metastases dying as a result of apoptosis (Cieślikowski et al. 2020).

Post invasion, there are two states of dormancy that have been described in the literature: cellular dormancy and tumour mass dormancy (Jahanban-Esfahlan et al. 2019). Cellular dormancy describes the fate of the majority of the surviving cells. Cellular dormancy is observed in the dormant niche, where singular tumour cells are thought to survive as single cells residing in the G_0 phase of the cell cycle. These cells have also been shown to have altered metabolic profiles and utilise antiapoptotic mechanisms to ensure survival (Vishnoi et al. 2015). Tumour mass dormancy describes small cell clusters that exist together in the dormant niche, these cell clusters have been shown to balance growth and cell death in a manner that results in no tumour growth. These cell clusters are comprised of cells exhibiting low proliferation and have been shown to balance pro-angiogenic and anti-angiogenic stromal and cellular cues (Miglietta et al. 2022).

Previous studies have shown that both dormant single cells and cell clusters can be triggered into forming invasive and aggressive tumours (Gomis and Gawrzak 2017). Previously noted triggers include angiogenic sprouting (growth of new

capillaries), inflammatory cytokines and changes in stromal cues (Neophytou, Kyriakou, and Papageorgis 2019). These, however, are not the only triggers; thus, more research must be conducted. This change in state, or reactivation, can cause further metastatic colonisation and is the primary cause of metastatic relapse and poor prognosis for patients (Neophytou, Kyriakou, and Papageorgis 2019).

The molecular and genetic mechanisms responsible for both dormancy and reactivation have been studied extensively (Fares et al. 2020). However, although potential causes have been suggested, no definitive explanation exists, rather a list of causes that could contribute to this phenomenon.

5.1.3 Role of the microenvironment in Tumour Dormancy

Previous studies have shown, with increasingly more evidence, that local microenvironments not only directly influence invading disseminated tumour cells (DTCs), but also have long lasting effects on the DTCs influencing the tumour homing, dormancy and chemotherapy resistance of tumour cells residing in the bone. Specifically, CXCL12 – CXCR4 signalling axis is a very well-known mechanism that supports breast cancer cell homing and colonisation to the bone (J. Wang, Loberg, and Taichman 2006). This bone homing signalling is usually a result of overexpression and presentation of CXCR4 on breast cancer cells, causing them to be more susceptible to priming by CAFs (cancer associated fibroblasts). This signalling causes colonisation of the bone marrow, where high expression of CXCL12 is noted.

Several other microenvironmental cues have been noted as potential driving factors for DTC homing and dormancy to the bone, one such example is the presence of hypoxic regions within the primary tumour (Fluegen et al. 2017). These microenvironments present within the primary tumour are known to generate ‘post-hypoxic’ DTCs (Fluegen et al. 2017). These cells, after dissemination are shown to expresses a gene expression program that favours dormancy, this is known as a NR2F1-driven pro-dormancy gene program, these cells are known to be able to avoid chemotherapy (Wu et al. 2022; Sosa et al.

2015). Thus, these findings indicate the very significant influence of the primary tumour microenvironment on the fate and survival of DBCCs.

Not only does the primary tumour microenvironment influence the dormancy phenotype/ survival of DBCCs but the microenvironment to which the cells are colonising also plays a major role. The bone marrow microenvironment in particular, as many cell types heavily associated with breast cancer metastasis and dormancy reside within said niche. The bone marrow microenvironment is heavily implicated in the homing and dormancy of DBCCs, this is largely due to the presence of two specialised stem cell niches: the endosteal 'osteoblastic' niche and the perivascular niche (Lawson et al. 2015). These niches are home to resident stem cells such as MSCs (mesenchymal stem cells) and osteoblast lineage cells, as well as endothelial cells (Crane, Jeffery, and Morrison 2017; Shiozawa et al. 2011). These resident cells are known to express several signals associated with cell-survival, quiescence and self-renewal, these signals are expressly for the maintenance of HSCs and the niche itself.

Disseminated breast cancer cells are thought to colonise these niches in order to make use of these signals in order to promote their own survival/dormancy (Shiozawa et al. 2011). The site of invasion is also shown to be important in the fate of DBCCs, in vivo imaging techniques have been employed to investigate the localisation of DBCC upon entry into the bone marrow (Price et al. 2016). These experiments have shown that DBCCs preferentially direct to the perivascular niche, this is achieved through interactions with E-selectin expressing endothelial cells (Cieślikowski et al. 2020; Fluegen et al. 2017). Further support of this was seen after analysis of patient bone marrow samples, finding that Ki67 negative breast cancer cells (dormant breast cancer cells) were more likely to be found localised to the perivascular niche as opposed to the endosteal surface (Price et al. 2016).

Experimental evidence has shown that upon colonisation of the perivascular niche, resident endothelial cells express TSP1 (thrombospondin-1), a suppressor of angiogenesis (X. Zhang et al. 2009). This molecule has been shown to promote DBCCs (Ghajar et al. 2013). Conversely, factors such as TGFβ1 (transforming growth factor beta 1) and POSTN (periostin) are shown to trigger activation

(proliferation) of DTCs. These findings indicate the fate of DBCCs is influenced by a multitude of factors relating to microenvironmental cues.

Several explanations have been postulated for tumour dormancy, including changes in gene expression, altered immune response, direct communication within the tumour microenvironment amongst others. A very well described mechanism of tumour dormancy is overactivation of the p38 MAPK stress-response pathway, resulting in the overexpression of p38 MAPK, causing an imbalance in the p38 MAPK/ ERK1/2 ratio (Clements and Johnson 2019a). Several factors such as BMP2 and TGFβ2 are known to induce $p38^{high}/ERK^{low}$ signalling, this is known to allow for maintenance of tumour cells in the dormant phenotype (Sosa et al. 2011).

5.1.4 Objectives

This chapter aims to investigate the response of dormant (Ki67 negative) breast cancer cells to various external stimuli. Along with this, investigation into the phenotype (such as size and morphology) of tumour cells mass (MCF-7 spheroid) will be carried out. These findings together will inform on the behaviour of dormant breast cancer in response to stimuli likely to be present within the bone marrow niche.

5.1.5 Experimental Design

In order to investigate the response of dormant breast cancer cells to bone marrow like stimuli, MSCs were grown in 2D and treated with differentiation media (see methods). MSCs were also grown on the previously described biomaterials model (treated with BMP2 and CXCL12). MSCs were grown/differentiated for 28 days, then washed, and fresh media (untreated) was added to the culture. Cells were incubated for 48 hours, and growth media was harvested (conditioned media). This media containing secreted factors from

MSCs and differentiated cells was used to treat dormant breast cancer cells and cell mass (Ki67 negative), the effect of which was investigated.

5.2 Results

5.2.1 MSC Differentiation

MSCs (Promocell) were differentiated using supplemented media to trigger lineage specification. Supplemented media was made up as per chapter 2, to direct the MSCs through the osteogenic and adipogenic lineages. The first step was to grow MSCs in T75 flasks until 80% confluent, cells were then washed with hepes saline solution and then supplemented media was added to the wells. Cells were then allowed to grow/differentiate for 28 days, with supplemented media changed twice per week. After 28 days MSCs were stained and imaged using Alizarin red S and Oil red O, these compounds stain for calcium deposits in the cells and lipids respectively. Supplemented media was sufficient to drive differentiation in MSCs, these differentiated cells were then used to condition media (growth media incubated with cells and harvested), this conditioned media was then used in future experiments (see figures 5.1 and 5.2).

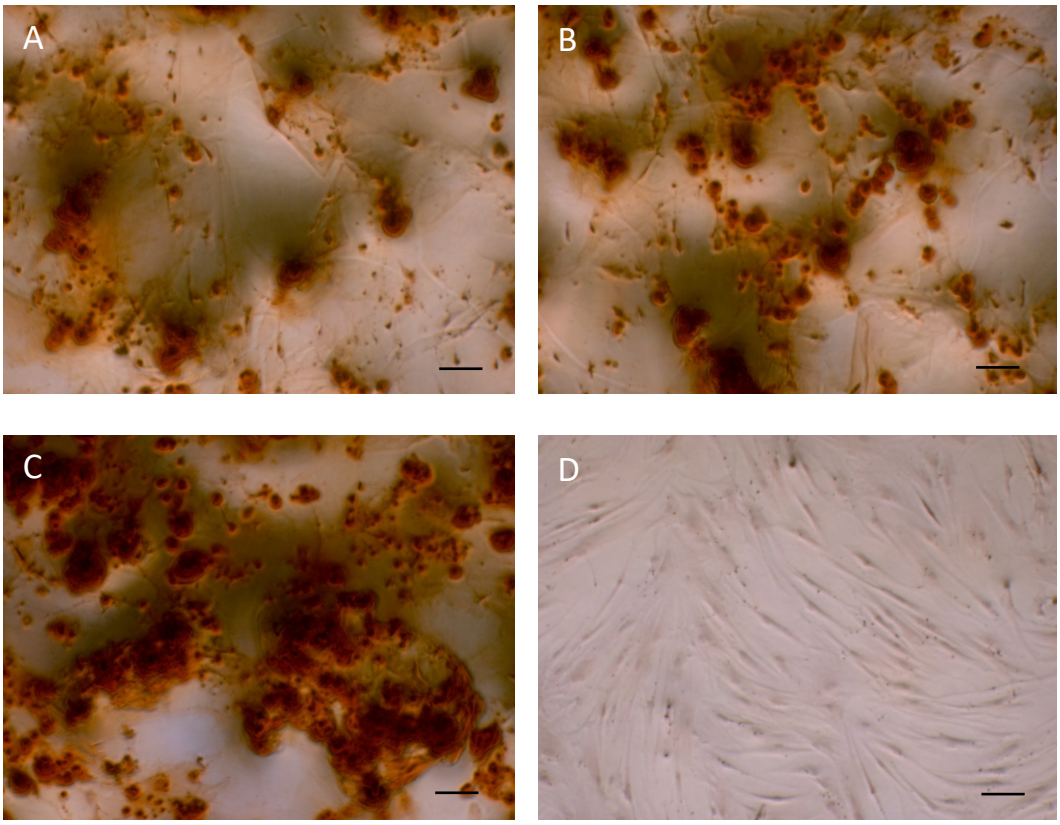

Figure 5.1 MSC differentiation into osteogenic lineage MSCs were grown until 80% confluency, then treated with osteoinductive media (see methods) for 28 days. A-C represent n=3 osteo differentiation, D represents the negative control. After 28 days samples were stained with alizarin red s, this dye stains calcium deposits (red) in the cell, thereby indicating osteogenic differentiation. Conditioned media was harvested from these samples are used for future experiments. Samples were compared against controls treated with 'regular' DMEM for the duration of the experiment. No staining was observed in control samples. Scale bar = 100 μm.

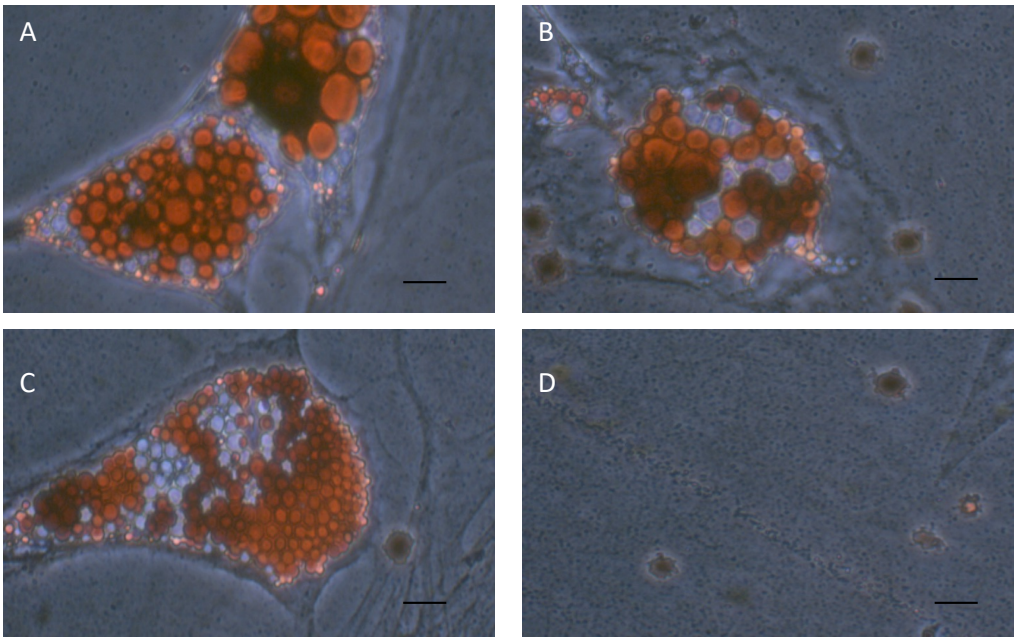

Figure 5.2 MSC differentiation into adipogenic lineage
MSCs were grown until 80% confluency, then treated with osteoinductive media (see methods) for 28 days. After 28 days samples were stained with oil red o, this dye stains lipids in the cell (red), thereby indicating adipogenic differentiation. Conditioned media was harvested from these samples are used for future experiments. Samples were compared against controls treated with 'regular' DMEM for the duration of the experiment. No staining was observed in control samples. Scale bar = 100 μm.

5.2.2 MCF7 Spheroid Morphology After Treatment with MSC Conditioned Media

MCF7 spheroids were generated as previously described (see methods). Following generation, spheroids were treated with MSC conditioned media and incubated for varying periods of time. Media was conditioned on MSCs, osteo lineage and adipo lineage cells for 48 hours, after conditioned media was used to treat MCF7 spheroids of varying size. Following treatment, spheroid morphology was investigated using microscopy and SEM.

The treatment of MCF7 spheroids with conditioned media caused various changes. Upon investigation using light microscopy (with z-stacking) it was clear that alterations were visible in treated spheroids after just 48 hours. While control spheroids along with osteo conditioned media treated spheroids appeared to be unchanged, adipo conditioned media treated spheroids displayed

a clear ‘core’ of cells and a dense ring of cells at the outermost extremities of the cell structure (see figure 5.3).

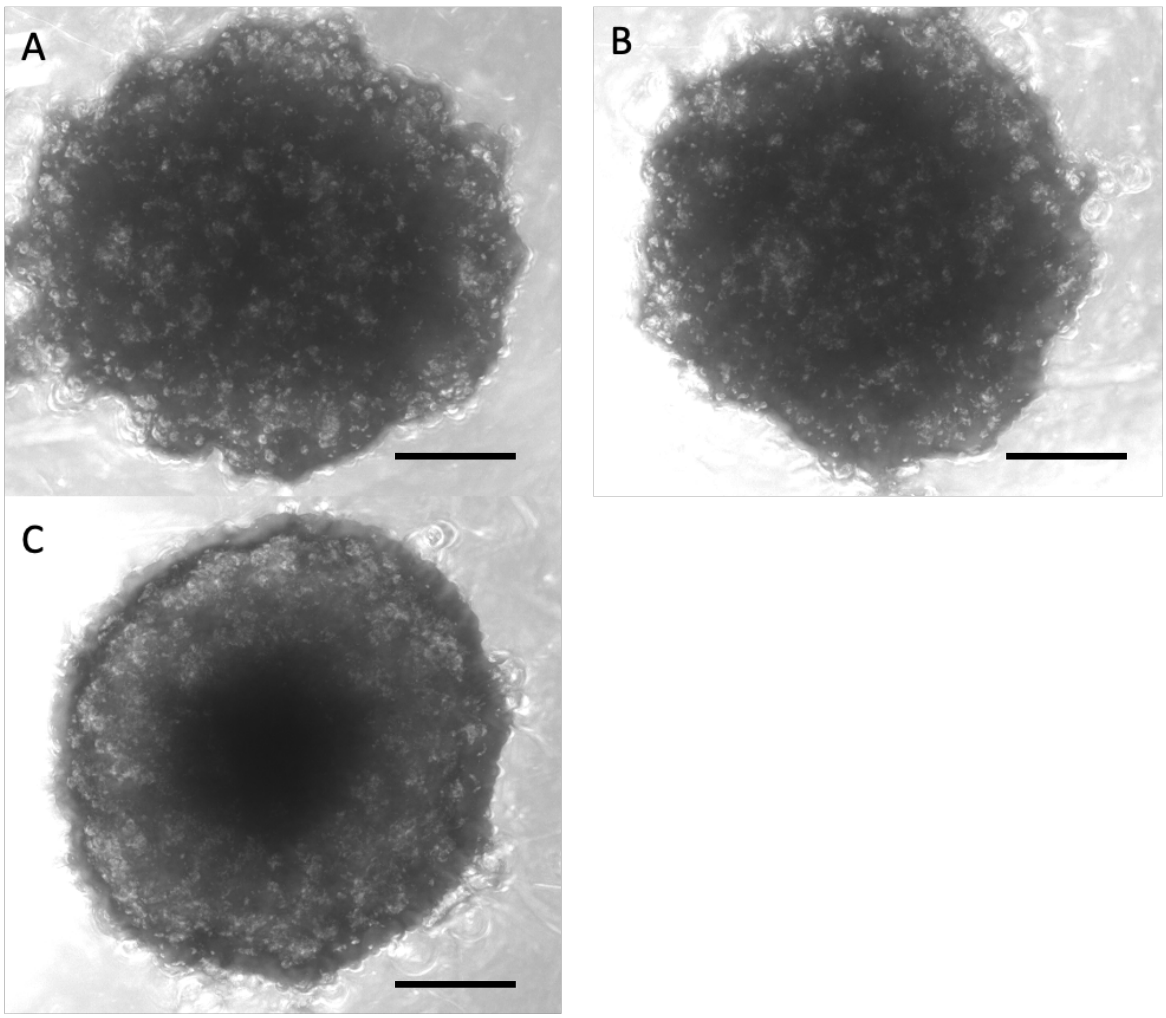

Figure 5.3 Light microscopy z-stack images of MCF7 spheroids 48 hours post treatment with conditioned media. A: Z-stack image of MCF7 spheroid treated with MSC conditioned media. B: Z-stack image of MCF7 spheroid treated with osteogenic conditioned media. C: Z-stack image of MFC7 spheroid treated with adipogenic conditioned media. All images taken on EVOS M700 microscope 10x magnification, images were taken at different planes throughout the cell structure and ‘merged’ together to for one image (z-stack). Control and MSC > osteo treated spheroids exhibit similar morphology, however adipogenic conditioned media treated spheroids clearly exhibit a dense ‘core’ of cells along with a dense ring of cell round the extremities of the cell structure, indicating adipo conditioned media is able to trigger changes in cell behaviour of MCF7 spheroids. Scale bar = 100 μm.

5.2.3 MCF7 spheroid proliferation is upregulated after treatment with conditioned media

MCF7 spheroids were generated as previously described, with four cell seeding densities investigated (2.5 x 10^3, 5.0 x 10^3, 7.5 x 10^3 and 1 x 10^4 cells per well). After formation, breast cancer cell spheroids were allowed to grow for investigation at various time points. These spheroids were used as to model dormant breast cancer cell mass and to investigate changes in tumour cell behaviour when treated with MSC secreted molecules.

MSCs were grown and differentiated into osteocyte and adipocyte lineages as described above, samples were then washed using hepes saline and fresh 'regular' (10% FBS, 2% penicillin-streptomycin, 1% sodium pyruvate and 1% non-essential amino acids) cell culture media was added. Samples were then incubated for 48 hours in this fresh medium to generate 'conditioned medium' containing secreted molecules from MSCs undergoing differentiation. This conditioned media was then used to treat 2D and 3D MCF7s, this was done to gauge the impact of bone marrow niche related signals on dormant breast cancer cell masses.

Upon incubation with MSC conditioned media, MCF7 spheroids were investigated using proliferation and cell viability assays. These assays revealed that the proliferation of 10,000 cell spheroids was significantly increased upon treatment with conditioned media. However, there was no significant difference observed between spheroids treated with adipo and osteo conditioned media. All samples were normalized to a control consisting of spheroids treated with MSC (non-differentiated) conditioned media (see figure 5.4).

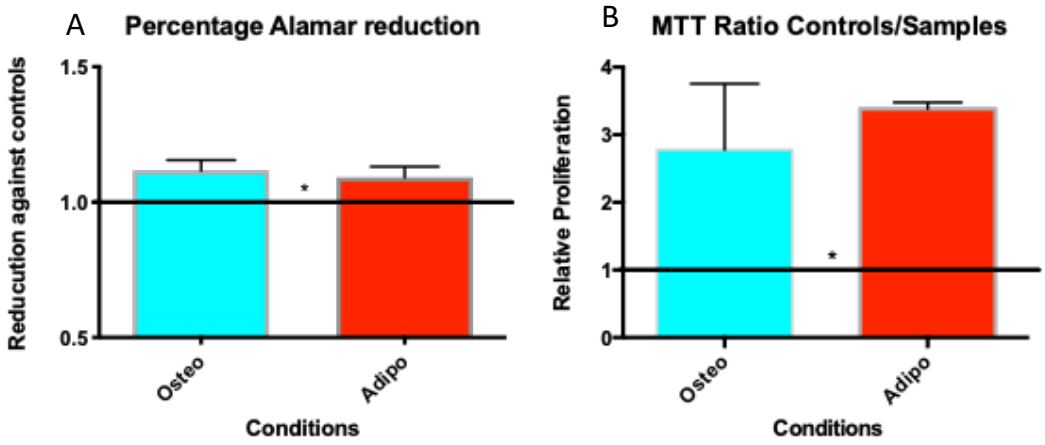

Figure 5.4 Alamar blue assay (reduction of resazurin).
Relative proliferation of spheroids (10k cells) depicted here, spheroids were grown as previously described and treated with conditioned media. A: Alamar Blue assay, B: MTT assay. Graph depicts spheroid proliferation after treatment as a factor of the control. A significant difference was observed after 48 hours for both conditioned media treatments when compared with a 'normal media' treated control. Statistical analysis using a Kruskal Wallis. "*" = $p < 0.05$, "" = $p < 0.01$, "***" = $p < 0.001$, "****" = $p < 0.0001$, "ns" = non-significant. n=3.**

It has been shown that conditioned media caused an upregulation of proliferation when used to treat spheroids made form seeding 10,000 cells into each well. Thus, further experiments were undertaken to determine the effect of spheroid size on cell proliferation after treatment with conditioned media. It was shown that across all spheroid size ranges a significant increase in proliferation was observed when compared with spheroids treated with MSC (non-differentiated) conditioned media. With greater differences observed between treated and controls in the size ranges of 7,500 and 5,000 cell spheroids. There was no significant difference observed between the adipo and osteo conditioned media treated spheroids at any size range (see figure 5.5).

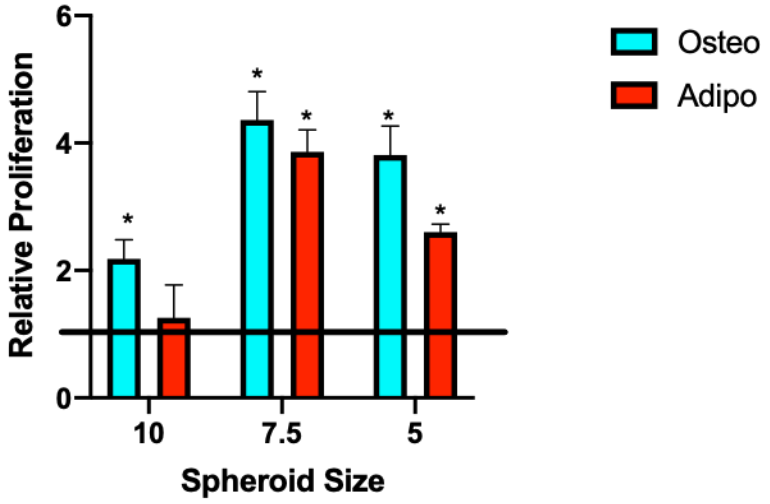

Figure 5.5 Alamar blue assay (reduction of resazurin).
Relative proliferation of spheroids of varying sizes shown here, with spheroid size across the x axis (numbers representing 10,000, 7500 and 5000 respectively). Y axis represents relative proliferation, proliferation calculated as a factor of control (MSC conditioned) treated cells. A significant difference is seen across all size ranges, however no significant difference was observed between the two treatments (osteo and adipo conditioned media). Statistical analysis using a Kruskal-Wallis test. "*" = $p < 0.05$, "" = $p < 0.01$, "***" = $p < 0.001$, "****" = $p < 0.0001$, "ns" = non- significant. n=3.**

5.2.4 MCF7 spheroid growth after treatment with conditioned media

MCF7 spheroids were generated as previously described and treated with conditioned media (see above). Spheroids were then incubated for various time periods (24h, 48h, 7 days and 14 days) with longer incubations undergoing media changes twice per week. After observation that the osteo and adipo conditioned media triggers proliferation of MCF7 cells spheroids (confirmed with Alamar blue and MTT assays (see figure 5.4), analysis of spheroid growth was undertaken. This analysis of growth was done by calculating the diameter and circumference (though the use of ImageJ and microscope scale slides) and then area of each spheroid treated with conditioned media at various time points, then comparing these data with those obtained from MSC conditioned media treated spheroids.

Spheroids were seeded and the diameter measured every 24 hours, this was done using light microscopy, each spheroid was measured 3 times. (See figure 5.6) (after light shaking to rotate the spheroid before each measurement).

Shaking was done to account for the heterologous nature of the spheroids, to allow spheroids to be measured at different orientations. An average diameter was calculated for each spheroid and then the data plotted against that of controls (see figure 5.6). The 10,000 cell MCF7 spheroids showed that post treatment the average area of spheroids significantly increased after treatment with osteo and adipo conditioned media, however the 5,000 cell spheroids only showed a significant increase in size when treated with adipo conditioned media (see figure 5.7).

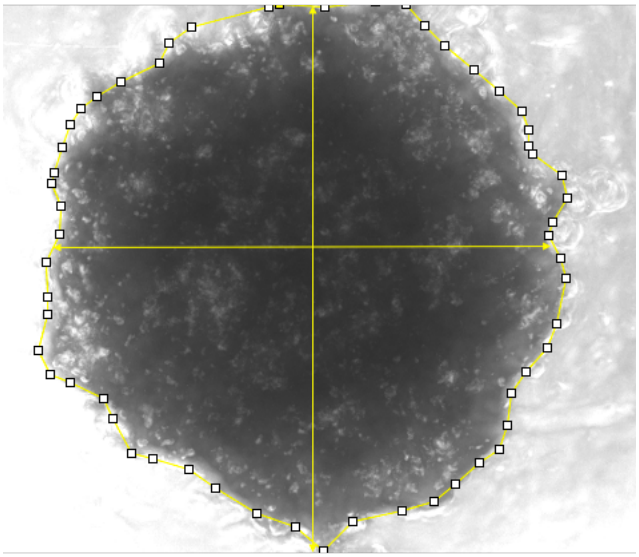

Figure 5.6 Sample image of MCF7 spheroid and methods used to measure circumference and area on ImageJ. Diameter was measured twice and averaged, and circumference measured using the 'polygonal' tool on ImageJ. Each spheroid was imaged and measured 3x and averages calculated. This was done for treated samples as well as controls, data was then plotted against controls.

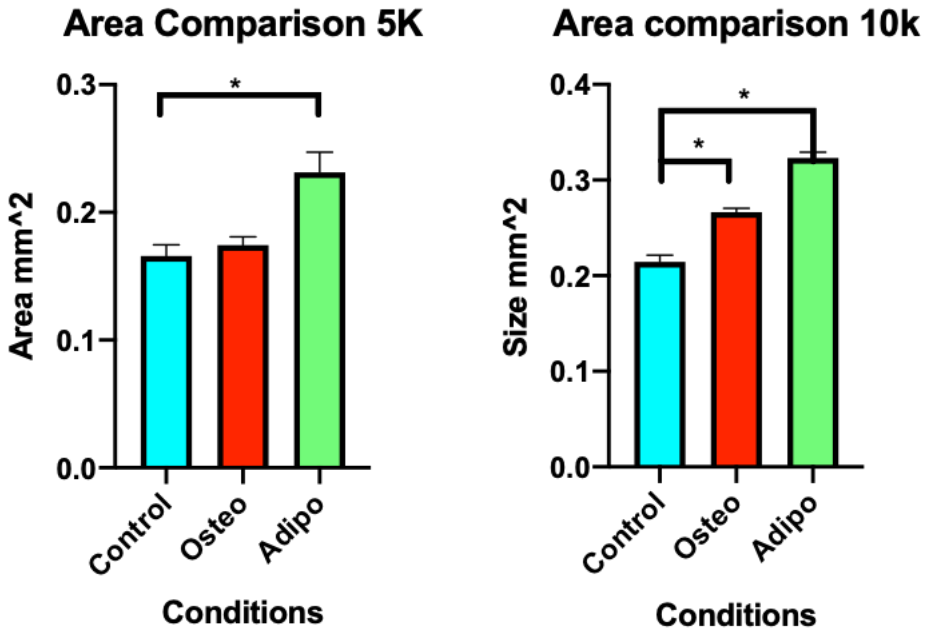

Figure 5.7 MCF7 spheroid area measurements 14 days post treatment with conditioned media. Area was calculated as above. Control samples were treated with MSC conditioned media. The 10,000 cell MCF7 spheroids showed that post treatment the average area of spheroids significantly increased after treatment with osteo and adipo conditioned media, however the 5,000 cell spheroids only showed a significant increase in size when treated with adipo conditioned media, with no significant effect observed in the osteo conditioned media treated spheroids. Statistical analysis using a Kruskal-Wallis test. "*" = p < 0.05, "" = p < 0.01, "***" = p < 0.001, "****" = p < 0.0001, "ns" = non- significant. n=3.**

As well as light microscopy, SEM was utilised to assess changes in morphology as well as overall size changes after treatment. MCF7 spheroids of different sizes were generated and allowed to form/grow for 48 hours, they were then treated using conditioned media for 14 days with media being changed twice per week (3–4-day intervals). Spheroids were then prepped and imaged using SEM at 100x, 1000x, 1500x and 4000x magnification. Images taken at the lower magnification showed the whole spheroid, thus providing information into the morphology of the spheroids undergoing different treatments.

SEM confirmed results seen after light microscopy (figures 6 and 7), with adipo conditioned media treated spheroids showing a significant overall increase in area when compared with those treated with MSC conditioned media. With adipo treated spheroids having a higher average increase in area than osteo treated spheroids (see figure 5.8).

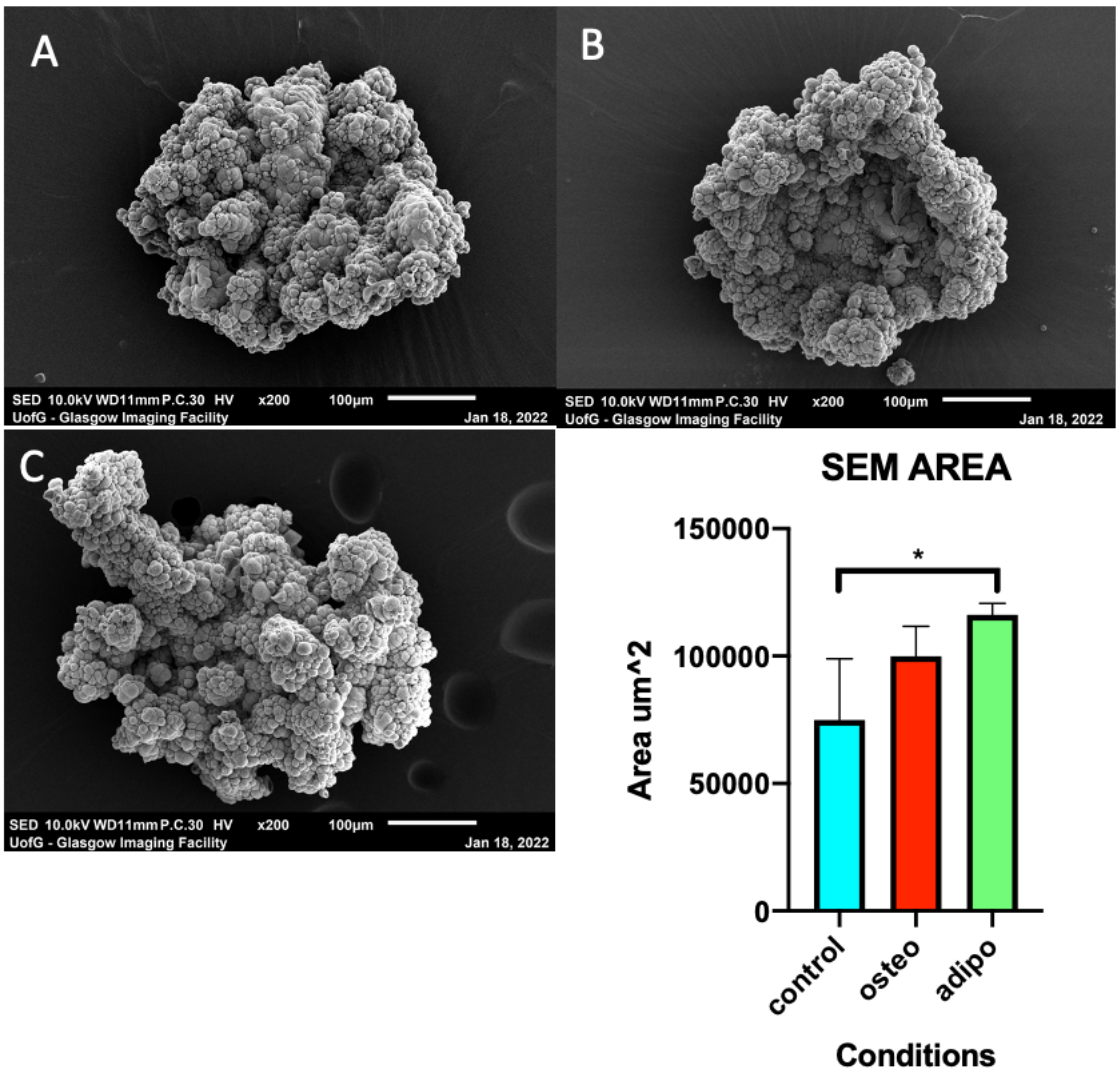

Figure 5.8 SEM images of MCF7 spheroids (10,000 cells)
Spheroids were generated (see methods), MCF7 spheroid area measurements 14 days post treatment with conditioned media. A: Control treated spheroid, B: Osteo conditioned media treated spheroid, C: Adipo conditioned media treated spheroid. A significant difference in average area of spheroids treated with adipo conditioned media was observed when compared with the average area of controls. No significant difference was observed between the control and osteo conditioned media treated spheroids. No significant difference was observed between the adipo and osteo conditioned media treated spheroids. Statistical analysis using a Kruskal-Wallis test. "*" = $p < 0.05$, "" = $p < 0.01$, "***" = $p < 0.001$, "****" = $p < 0.0001$, "ns" = non- significant. n=3.**

5.2.5 MCF7 spheroid Ki67 expression post treatment

Ki67 is a cell proliferation antigen and is constitutively expressed in proliferating mammalian cells. Ki67 is known to only be produced by actively dividing cells, located in the nucleus. Not only is this protein only produced by proliferating

cells, but it is also essential for cycling of mammalian cells, being most highly active in G2 phase. Thus, this protein is widely used as a proliferation marker when assessing tumour growth (L. T. Li et al. 2015; X. Sun and Kaufman 2018). Previous chapters have described how MCF7 cells in spheroid conformation have a significantly reduced expression of ki67, thus indicating a markedly reduced rate of proliferation. As ki67 negative cells represent dormant cells, expression, post treatment with conditioned media was investigated.

Ki67 expression was shown to be significantly increased in spheroids treated with conditioned media compared with controls (see figure 5.9). This was investigated by generating MCF7 spheroids as previously described (see methods), treating them as previously described (see above) and finally isolating cell lysates from the samples. These lysates were then analysed using gel electrophoresis, with ki67 antibodies used to probe for the proliferation marker. Ki67 was shown to be significantly overexpressed in treated spheroids when compared with untreated controls. This is indicative of re-activation on dormant breast cancer cells and correlates with previously obtained data.

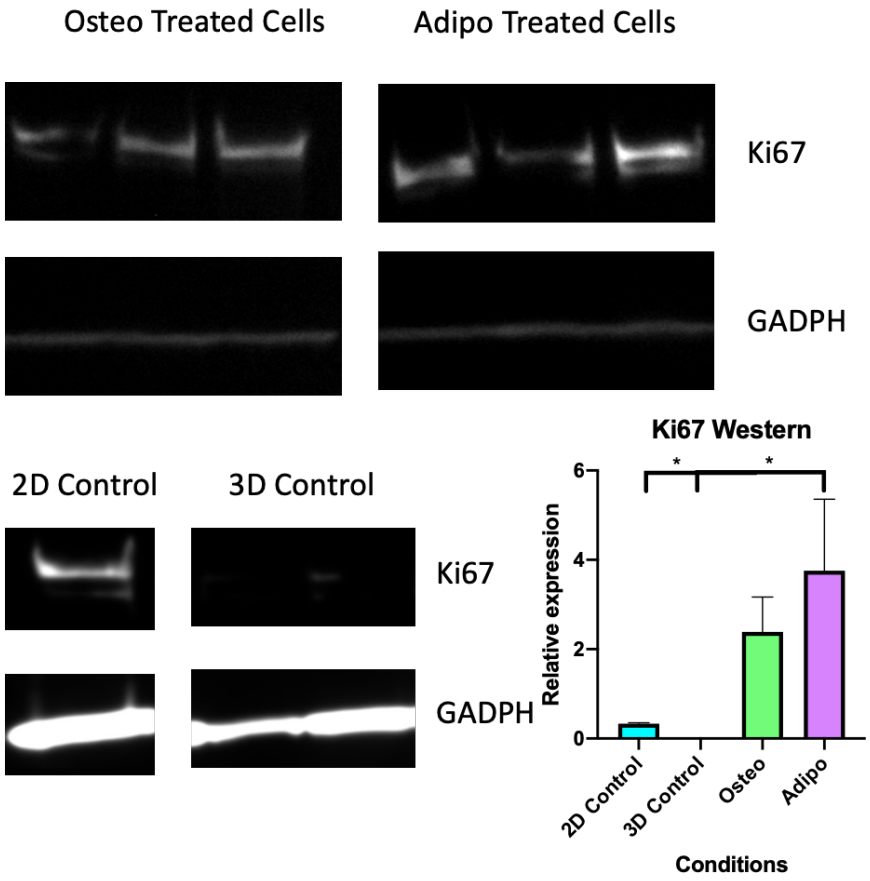

Figure 5.9 Western blot images showing expression of Ki67
Lysates were isolated from samples treated with conditioned media, lysates were also isolated from both 2D and 3D controls. Sample lysates were gel electrophoresed and probed for GAPDH and Ki67. The ratio of Ki67 to GAPDH was calculated and plotted above. A significant difference was observed in the expression of Ki67 between the adipo conditioned media treated spheroids and both the 2D and 3D controls. Statistical analysis using a Kruskal-Wallis test. "*" = $p < 0.05$, "" = $p < 0.01$, "***" = $p < 0.001$, "****" = $p < 0.0001$, "ns" = non- significant. n=3.**

5.3 Discussion

The key aim of this chapter was to investigate the potential of MSC differentiation conditioned media to trigger proliferation in the MCF7 spheroid model previously described. This was done in order to gain more insight into the potential triggers of reactivation, of dormant breast cancer cell masses in the bone marrow, specifically related to differentiation of MSCs in the bone marrow niche. This was achieved by growing MSCs in vitro until 80% confluency, then using specific media (containing various signalling molecules) designed to trigger

differentiation into specific stem cell lineages. After differentiation, the cells were then used to 'condition' normal media (DMEM as described in methods), this was done by removing the differentiation media, washing the cells and incubating them in fresh media for 48 hours. This 'conditioned' media was then used to investigate the effect of differentiated MSCs (osteoblasts, adipocytes) secretome on the previously described MCF7 spheroid model.

The key findings of this chapter include:

- Specialised differentiation media was sufficient to trigger differentiation of MSCs.
- Osteoblast and adipocyte conditioned media trigger an increase in proliferation of MCF7 spheroids as determined by cell proliferation assays.
- Conditioned media triggers growth of MCF7 cell mass as determined by light microscopy and SEM.
- Conditioned media causes upregulation of proliferation marker Ki67 correlating with previous results.

5.3.1 Characterisation of MSC differentiation

Specialised growth medium (see methods) was shown to be capable of triggering differentiation of MSC down specific lineages. This was achieved as previously described in this chapter. Post incubation with differentiation media (28 days) cells were stained with two distinct stains designed to identify bone tissue (calcium deposition) and adipose tissue (lipid stain). After 28 days of incubation differentiation into both lineages was successfully achieved and characterised through microscopy. After this differentiation period, media was conditioned; generated from the adipo and osteo lineage cells (see methods). This was done in an attempt to mimic the secretome of differentiating/differentiated MSCs in the bone marrow niche.

5.3.2 Conditioned media is capable of triggering proliferation in MCF7 spheroids

MCF7 spheroids, designed to mimic dormant tumour cell masses, after treatment with adipo and osteo conditioned media showed a significant increase in resazurin reduction. Resazurin is reduced to resorufin by viable cells, thus the more reduction observed in the assay the more viable (proliferating) cells present in the sample. Samples were compared against MSC conditioned media (conditioned in the same manner as previously described) treated controls, showing a significant increase in the number of viable cells after incubation with differentiation conditioned media.

Along with resazurin reduction, the proliferation marker (ki67) used to determine dormancy in breast cancer cells was shown to be significantly upregulated after treatment with conditioned media. This was shown by probing for GAPDH and Ki67 in MCF7 spheroid lysates, the ratio of Ki67 to GAPDH (housekeeper) was calculated for all samples and treated versus untreated was compared. Upon analysis it was evident that the ratio of Ki67 to GAPDH in treated MCF7 spheroids was significantly greater than that of both the untreated 3D controls and the 2D controls. This indicates that conditioned media is capable of triggering proliferation in the MCF7 dormant model, suggesting that MSC differentiation could potentially trigger reactivation of dormant tumour cell masses in the bone marrow niche.

5.3.3 Growth of the tumour cell mass was triggered upon treatment with conditioned media

Proliferation was shown to be upregulated through the use of assays and investigation of proliferation markers, in order to further validate this observed upregulation and to investigate how this would impact the solid tumour, microscopy was used to investigate the changes in morphology undergone by MCF7 spheroids after treatment with conditioned media. The overall size of spheroids after treatment was investigated, this revealed that treated samples (spheroids) showed a significant increase in size (area) after just 5 days incubation with conditioned media. Light microscopy was used to determine the

size of each spheroid, for further insight into morphological changes exhibited by spheroids SEM was used. SEM revealed that after treatment, spheroids generally alter in shape, this is not observed in every sample however. Some samples after treatment with adipocyte conditioned media showed a loss of the traditional spheroid ball-like shape, with cells instead growing ‘outwards’ away from the cell mass. However, this was only observed using SEM, and was not observable using light microscopy, potentially indicating that during preparation for SEM the structural integrity of the cell mas may have been disturbed, thus leading to false results. Despite this, SEM confirmed results obtained in this chapter, confirming that treated spheroids do indeed increase in size, indicating an increase in growth or exit from quiescence.

These results taken together suggest that differentiated MSCs release factors are capable of triggering reactivation of dormant breast cancer cell mass in the bone marrow niche. However further experimentation is required to confirm this observation in vivo. Following these results, further experiments were designed to investigate to contents of the adipo and osteo lineage differentiation MSC secretome. This is in order to investigate potential triggers of reactivation present in the secretome of differentiating MSCs.

Chapter 6 The relationship between secreted metabolites and reactivation of dormant breast cancer

6.1 Introduction

6.1.1 Metabolomics

Metabolomics is the analysis of small molecule metabolites in a given biological sample. The aim of this analysis is to identify intermediaries and products of metabolism such as amino acids, carbohydrates, nucleotides, organic and fatty acids, amongst others. The total set of synthesised metabolites is known as the metabolome, while total molecules secreted into the local microenvironment by particular biological samples is referred to as the secretome. There has been a recent upward trend in the use of metabolomics to coincide with the increasing need to understand disease aetiology, in particular to fill the gap in knowledge surrounding the influence of genetic and microenvironmental cues on the disease state, in this case dormant breast cancer (Bushnell et al. 2021a; L. Wang, Zhang, and Wang 2021; Zhu and Thompson 2019).

As metabolites encompass a diverse range of chemical compounds of varying size, weight and functional groups, the analysis of data generated through metabolomics requires high sensitivity and selectivity in order to discern specific metabolites in a given sample (Dunn and Ellis 2005). The most common methodologies utilised to study metabolomics are liquid chromatography (LC), gas chromatography (GC) and capillary electrophoresis (CE). These techniques are often coupled with detector modules, most commonly mass spectrometers (MS). As such, the most common metabolic analysis platforms are LC-MS and GS-MS, with both techniques capable of accurate, sensitive analysis of hundreds of metabolites in a single run (Budczies et al. 2012; Johnson et al. 2003; Takahashi et al. 2011; Dunn and Ellis 2005).

6.1.2 Metabolism of quiescent and proliferating cells

The individual metabolic requirements of specific cells depend on a multitude of factors. Specifically depending on the type, activity and differentiation state of cells. Quiescent cells are known to be metabolically active, in order to fulfil the requirements of this quiescent state and also to fulfil their physiological role and to maintain structural stability. Quiescent cells are also known to undergo redox reactions while in this state of quiescence. Contrary to quiescent cells, proliferating cells require amino acids, fatty acids and nucleotides in order to generate macromolecules needed for cell growth and division (Lunt and Vander Heiden 2011a). Like many other aspects of cell biology, metabolism is stringently controlled through regulatory networks comprised of cell signalling molecules that are part of a greater regulatory network. The networks that are involved in the regulation of metabolic reactions within the cell comprise of far-reaching genes, including proto-oncogenes and tumour suppressors that are heavily linked to the formation of tumours. These abnormal signalling cues may result in cell cycle arrest or apoptosis (Zheng 2012).

The vast majority of normal cells are known to utilise mitochondrial metabolism in order to generate ATP, this involves the generation of NADH to drive the electron transport chain and oxidative phosphorylation. In contrast, however, proliferating cells are known to make use of glycolysis in order to generate a significant amount of their ATP (Lunt and Vander Heiden 2011b; Yetkin-Arik et al. 2019). Along with using nutrients to drive glycolysis, proliferating cells have also been shown to use nutrients directly in order to synthesis macromolecules necessary for growth. In normal (non-proliferating) cells NADH is recycled to NAD+ in order to generate the necessary components to drive the electron transport chain. In this scenario then, energy (ATP) production is directly regulated by co-factor supply. In proliferating cells, however, they are known to utilise both mitochondrial respiration and lactate production to generate their energy (M. G. V. Heiden, Cantley, and Thompson 2009).

6.1.3 Cellular Metabolism in Cancer

Changes in metabolism respective to cancerous and non-cancerous cells has been extensively studied, with Otto Warburg pioneering this field. He and his colleagues observed that malignant rodent liver cells make use of glycolysis to generate ATP despite the presence of oxygen (Otto Warburg, Wind, and Negelein, 1927.; Erson and Brooklyn, 1956). This observed glycolysis was noticed along with increased lactate production from the malignant liver cells despite the availability of oxygen, this phenomenon was coined the 'Warburg effect' (Otto Warburg, Wind, and Negelein, 1927.).

This phenomenon is not completely understood. However, one hypothesis as to why this occurs is that many vital metabolic processes required for the biosynthesis of macromolecules necessary for growth rely on metabolic intermediaries generated through glycolysis (Urbano 2021). Evidence suggests that the marked increase in glycolysis observed in cancer cells is in response to activation of proto-oncogenes and the loss of expression of tumour-suppressor genes (Lunt and Vander Heiden 2011a). Data suggests that the metabolic reprogramming observed in cancer cells is essential for both generation of energy though ATP and synthesis of amino acids, fatty acids and nucleotides for the generation of the necessary macromolecules required for growth (Lebelo, Joubert, and Visagie 2019; Liberti and Locasale 2016).

Cancer cells in a given environment will exert metabolic influence over the surrounding micro-environment (Baghban et al. 2020). The increased uptake of nutrients by cancer cells coupled with increased secretion of metabolic by-products by the cancer cells causes stark changes in the metabolites present in the tumour micro-environment. These changes in metabolome constitution trigger changes in both the cancer cells and resident cells, thus tumour cells are capable of high jacking mechanisms that remove toxic by-products from their surroundings in order to stabilise the tumour micro-environment (Whiteside 2008). These metabolic alterations of cancer cells help to give them a competitive advantage over resident/normal cells, both through higher energy output and greater biomass production.

The Warburg effect phenomenon is not exclusively observed in cancer cells, with rapidly proliferating cells such as lymphocytes (Lunt and Vander Heiden 2011c) (amongst others) also observed to undergo aerobic glycolysis, as an increase in the glycolysis pathway is necessary to yield intermediaries to support branching biosynthetic pathways (L. Sun et al. 2015). Despite glycolysis being required for metabolic intermediaries, due to the increased rate of glycolysis when compared with oxidative phosphorylation, ATP production per unit time is largely unchanged, meaning proliferating cells using glycolysis are able to generate a comparable amount of ATP over the same time as cells using oxidative phosphorylation (Zheng 2012). Along with the increased requirement for glucose postulated by Warburg, further observation made (by Harry Eagle) indicated that there is a marked increase in the requirement for glutamine (Eagle et al., 1956. Since this discovery it has been shown that this increased requirements for glutamine in cancer cells in universal, while the specific requirements for glutamine with respect to cancer cells is determined by both the primary tumour and tissue of origin (Eagle et al., 1956.).

6.1.4 Regulation of Metabolism (metabolic gene mutations)

Recent studies have found that mutations in metabolic genes, be it LOF or GOF (loss of function and gain of function), can trigger alterations in the metabolome of cancer cells (Wishart 2022). These genetic alterations can cause stark changes in the phenotype of cancer cells, as they may lead to accumulations of specific metabolites depending on the location of the mutation within the gene. These accumulations may result in the selective dependency on other metabolic pathways and enzymes (Nakazawa, Keith, and Simon 2016).

Two specific LOF mutations found to highly influence the metabolic makeup of cancer cells can be found in SDH (succinate dehydrogenase) and FH (fumarate hydratase) genes (Ashrafian et al. 2010). Mutations in these genes can cause a build-up of their substrates (succinate and fumarate). These substrates have been implicated as onco-metabolites as they are able to trigger specific cellular changes and promote tumorigenesis. Other genetic alterations may cause upregulation of metabolic enzymes, this usually occurs when mutations arise

that increase the gene copy number. Overexpression of metabolic enzymes has been observed in serval cancers namely breast cancer, melanoma and prostate cancer (Sreedhar and Zhao 2018).

6.1.5 Regulation of metabolism (Microenvironment)

Alterations in the microenvironment are characteristic of tumour growth. Research has revealed that the tumour microenvironment is capable of causing changes in tumour metabolism. A strong example of the tumour microenvironment influencing the heterogeneity of tumours, is tumours exhibiting the same genetic abnormality having different metabolic activity depending on the original tissue they formed in (Reznik et al. 2018).

6.1.6 Carbon Metabolism and Breast Cancer Dormancy

As described above Warburg described the phenomenon known now as the Warburg effect, whereby cancer cells utilise the glycolysis pathway to generate ATP despite the presence of oxygen (Otto Warburg, Wind, and Negelein, 1927. Normal (non-cancer) cells under the presence of oxygen are known to utilise glycolysis to produce pyruvate from glucose, this is then oxidised to generate ATP via oxidative phosphorylation. This method of generating ATP is far more efficient than glycolysis, however normal cells lacking oxygen with undergo glycolysis to produce lactate, similar to cancer cells (Erson and Brooklyn, 1956. Cancer cells have been shown to be capable of altering their glucose metabolism so that glycolysis is used to produce lactate despite the presence of oxygen. A possible explanation is that many intermediates for growth are generated through glycolysis, thus explaining why cancer cells utilise ‘aerobic glycolysis’.

Thus, a hallmark of cancer cells is the use of ‘aerobic glycolysis’ to generate cellular energy. Glucose and lipid metabolism share a close relationship, specifically through the synthesis of glycerol and fatty acids. Recent studies have suggested that glycolysis and lipid metabolism play an integral part in breast cancer cell phenotype (Yijun Liu and Ma 2015). Specifically, a study looking into

the link between lipid metabolism and breast cancer phenotype unveiled that overexpression of an enzyme involved in lipid metabolism (Ceramide glucosyltransferase) is capable of driving proliferation of breast cancer cells. This is due to an increased capacity to replenish the TCA cycle generating intermediaries essential for growth (Schömel et al. 2019). As well as an increased capacity to utilise the TCA cycle, an increase in both glycolysis and oxidative phosphorylation was observed, indicating changes in the expression of enzymes associated with lipid metabolism, and specifically glycosphingolipid metabolism is capable of triggering alterations in breast cancer cell phenotype (Schömel et al. 2019; 2020).

Despite Warburg's hypothesis that cancer cells only switch to glycolysis when active or proliferating, several studies such as the one referenced above indicate that dormant breast cancer cells can adopt glycolysis as their primary method of energy generation for their dormant or quiescent phenotype. This is in contrast to Warburg's theory and instead suggest that an exit from glycolysis into oxidative phosphorylation during dormancy could be the trigger for dormant cancer cell activation (Schömel et al. 2019).

Oxidative phosphorylation is known to generate a higher yield of ATP when compared to glycolysis, with greater efficiency also. However, the speed at which oxidative phosphorylation is completed is far slower than that of glycolysis, meaning that per unit time the difference in ATP production is minimal (Yetkin-Arik et al. 2019).

6.2 Results

6.2.1 MSC Differentiation

MSCs (Promocell) were differentiated using supplemented media to trigger lineage specification. Supplemented media was made up as previously described (see methods). Cells were grown to 80% confluency, washed three times with hepes saline solution, then supplemented media was added to the wells. Cells were differentiated for 28 days, with supplemented media replenished twice per week. After 28 days cells were analysed and assessed for adipo and osteogenic differentiation. This was achieved through the use of dyes specific for the deposition of calcium and lipids, Alizarin red S and Oil Red O respectively. Upon analysis, it was clear from these results supplemented media (see methods) was sufficient to trigger lineage specification in MSC cells in 2D culture.

After confirmation of differentiation, supplemented media was aspirated from cells, and fresh media was added (regular DMEM - see methods) to the cells after washing with hepes saline solution. These differentiated cells were incubated with this fresh media for 48 hours to allow the secretome of differentiated MSCs to condition the media. After 48 hours the 'conditioned' media was aspirated and used for future experiments, including metabolic analysis (LC-MS).

As described in chapter 5 (see figures 5.1 and 5.2) the MSC differentiation conditioned media was shown to trigger an increase in the rate of proliferation of breast cancer cell spheroids. Thus, metabolomic analysis was performed (LC-MS) on these samples in order to identify particular metabolites and metabolic pathways that could be responsible for the observed changes in the rate of proliferation of the MCF7 spheroids.

6.2.2 Metabolic clustering of Adipo and Osteo conditioned media

In order to investigate the secretome of MSCs osteoblasts and adipocytes, media was conditioned using the methodology previously described (see methods). MSCs (Promocell) were grown until around 80% confluency then treated with either osteogenic or adipogenic media, this media was replenished twice per week, the cells were then grown/differentiated for 28 days. MSCs (Promocell) were grown in regular Corning 24 well tissue culture plates as a control. After 28 days all media was aspirated from samples and fresh media was added ad incubated for 48 hours to generate conditioned media. This conditioned media was then sent for metabolic analysis (LC-MS) in order to investigate the secretome of MSCs, osteo and adipocytes.

Upon analysis of metabolic sample data, it was evident that both the adipo and osteo conditioned media cluster together, this is likely because differentiation into different lineages often requires common metabolites. This data is interesting as previous chapters (see chapter 5) have shown both adipo and osteo conditioned media was capable of triggering proliferation in the dormant breast cancer cell mass model. This chapter will aim to offer possible explanations for the observed increased activation of breast cancer spheroids after treatment.

When all samples were compared, as mentioned above, the osteo and adipo conditioned samples cluster together, while all controls cluster separately. This appears to be concurrent with previous data obtained in this thesis, as the biomaterials conditioned media (as shown in chapter 3) was incapable of triggering proliferation in the dormant model.

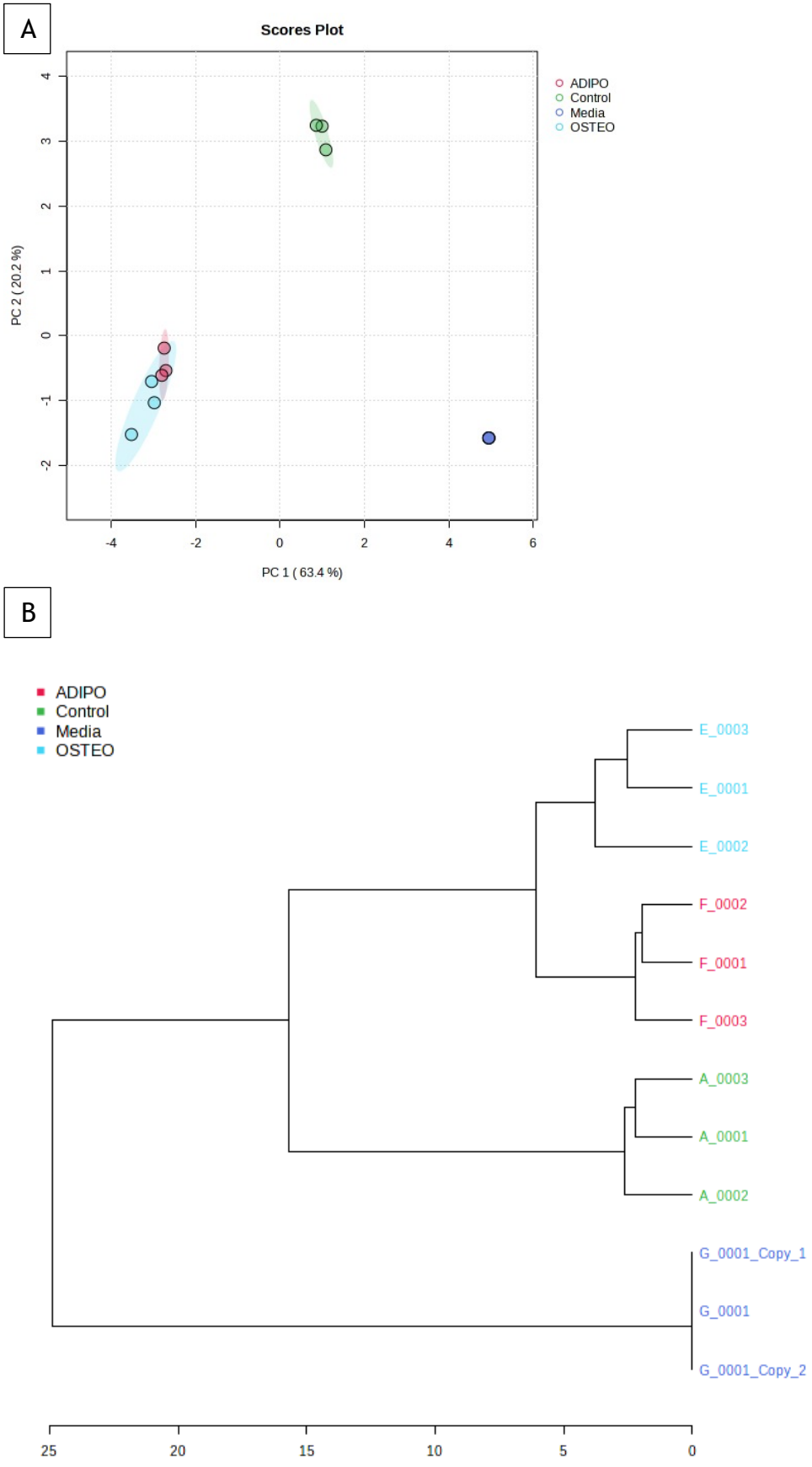

Figure 6.1 MSC cells were grown up under varying conditions (see above) in 24 well plates, media was conditioned after a 28-day incubation period. The conditioned media was analysed using LC-MS after metabolite extraction. Self-organising map (PCA) of samples (A)

showing clustering pattern of samples (B). Dendrogram depicting the relationships of similarity amongst the samples, showing that the osteo and adipo conditioned media again cluster together indicating a higher percentage of similarities in the differentiated cell conditioned media. the This analysis clearly shows that the osteo and adipo conditioned media derived metabolites cluster together and distinctly away from the remaining samples. Biomaterials conditioned media derived metabolites did not cluster away from the other samples and control.

Cells undergoing specific differentiation, namely osteogenesis and adipogenesis, release factors in the form of metabolites that could potentially trigger the reactivation of the dormant breast cancer cell mass model. Shown above the adipo and osteo conditioned media derived metabolites cluster together, meaning they have similarities in the content of the parent cell secretome. As these two conditioned mediums (adipo and osteo) were the only samples shown to trigger activation of the dormant cell mass, coupled with the fact they cluster away from the remaining samples (all of which are incapable of triggering proliferation in the dormant cell mass) potentially suggests a trigger may be present in the secretome of the differentiating cells.

Despite the observed clustering, there were noticeable differences in the secretome of these cells (see figure 6.2). As a 3rd PC value was included in the analysis, it was evident that although the adipo and osteo samples clustered away from the remaining (non-differentiated) samples, they show as 2 distinct clusters, indicating differences in the secretome of adipogenic and osteogenic cells. Along with this, differences in levels of specific metabolites may account for the observed advantage adipo media has over osteo media when used to treat MCF7 spheroids (adipo media was shown to trend toward being more effective at triggering proliferation). Levels of specific metabolites such as glycerol are shown to differ between adipo and osteo media. Previous studies have shown that glycerol can be used as a proliferative suppressor, thus the presence of higher levels of glycerol in the osteo versus the adipo media could account for the observed difference in the ‘activation potential’ of each media (Sakurai, Okada, and Mataga 2011; Wiebe and Dinsdale 1991).

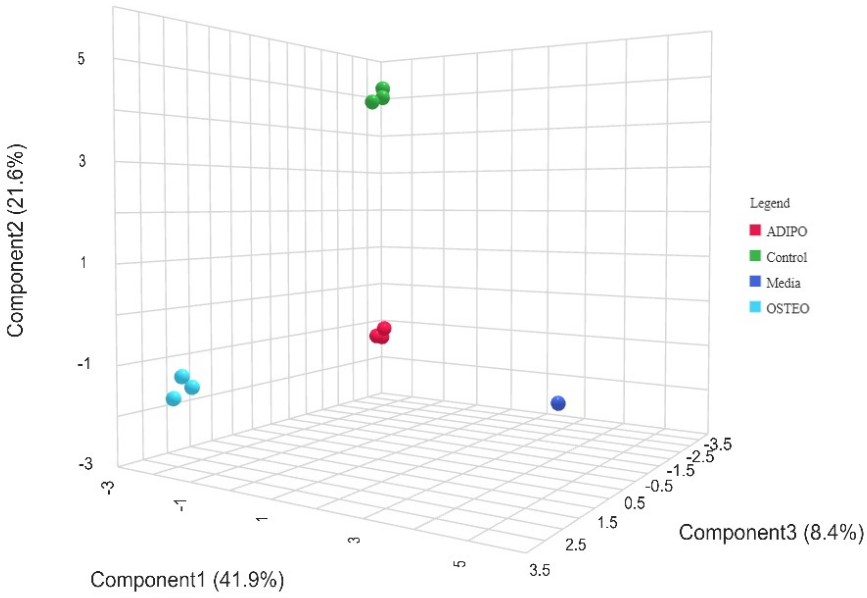

Figure 6.2 MSC cells were grown up under varying conditions (see above) in 24 well plates, media was conditioned after a 28-day incubation period. The conditioned media was analysed using LC-MS after metabolite extraction. Self-organising map (PCA) of all samples. This figure clearly shows that adipo and osteo conditioned media derived metabolites cluster away from the rest of the (non-differentiated) samples, however they do form two distinct clusters indicating differences in the secretome of their parent cells.

A heat map of up and downregulated metabolites further shows that the differentiated cell derived metabolites share many common metabolites in their secretome (see figure 6.3). The pathways most heavily associated with these metabolites of interest are arginine and proline metabolism, citrulline metabolism and tRNA charging (see figure 6.4)

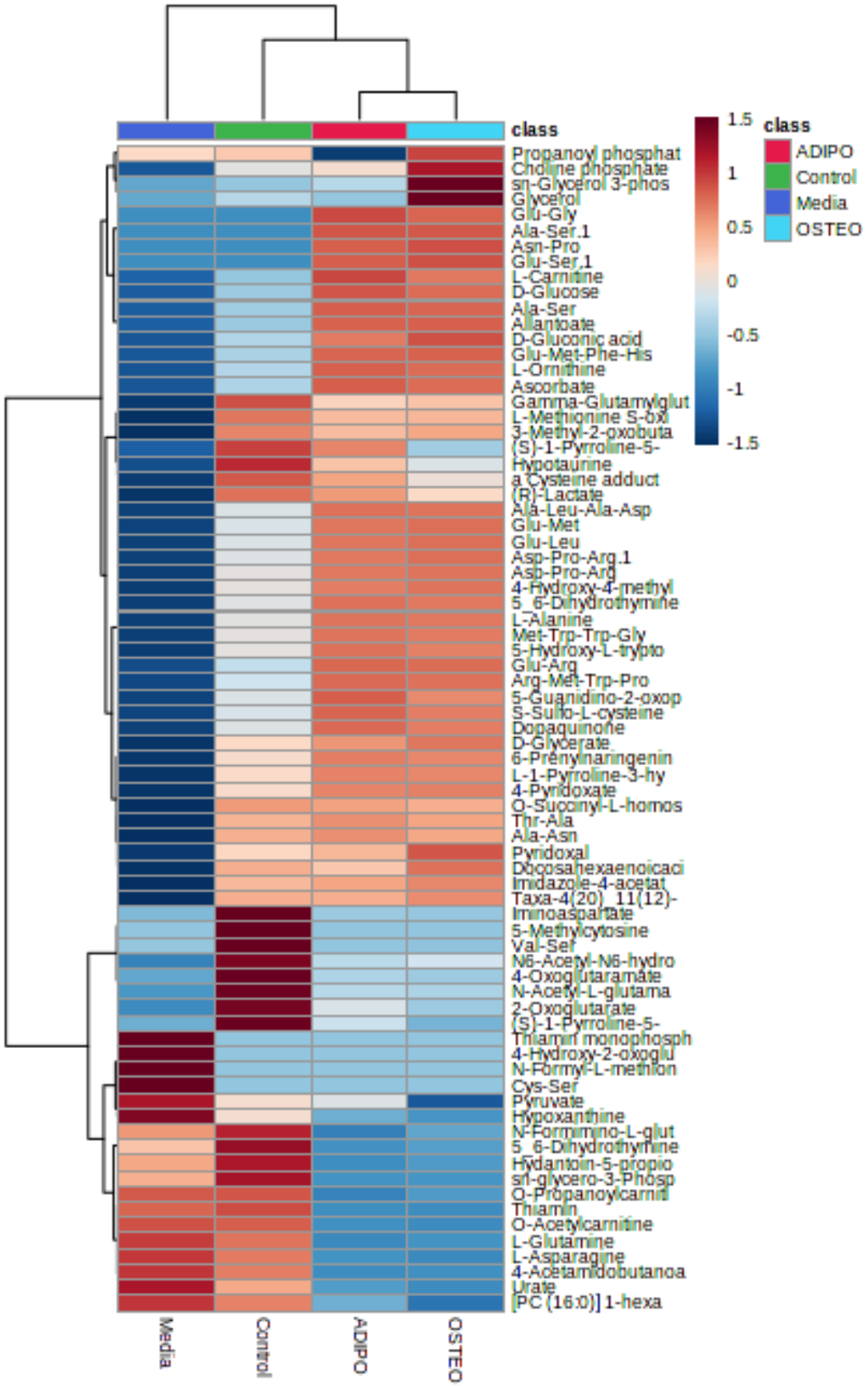

Figure 6.3 Heat Map showing the log transformed fold changes in metabolite levels in samples along with controls. Change is indicated by the colour of tile, blue indicating a downregulation and red/orange indicating an upregulation. The clustering of adipo and osteo derived metabolites is evident here, while the other samples and MSC control appear

to cluster together also. Metabolites of interest displayed here include ornithine, alanine, carnitine, N-methyl-2-pyridine-5-carboxamide and 5,6 dihydrothymine. These metabolites will be examined in further detail as to their influence on the dormant breast cancer cell mass model.

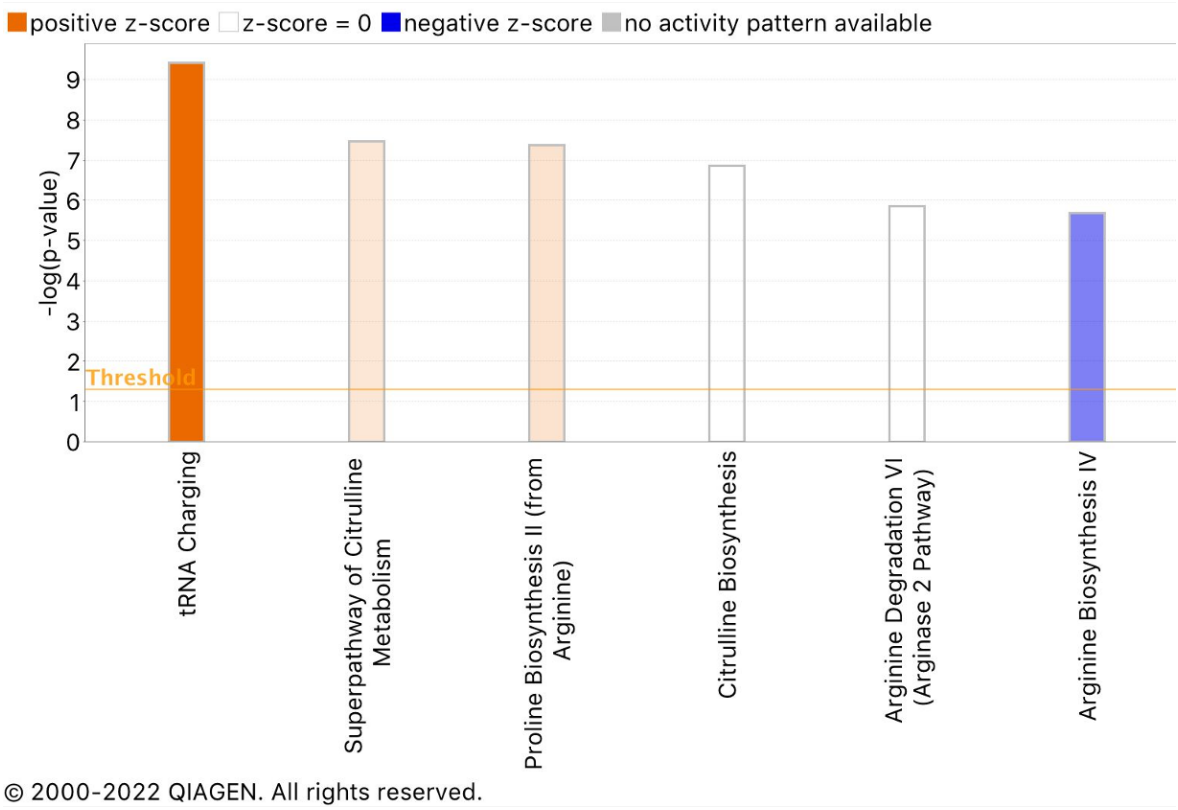

Figure 6.4 Canonical Pathways shown to be significantly altered upon metabolomic analysis. The conditioned media (adipo) was analysed using LC-MS after metabolite extraction, z-scores were calculated using IPA (see methods), image was generated using IPA.

6.2.3 Metabolites of interest

Upon analysis of the metabolomic data obtained from conditioned media of previously mentioned samples, IPA (Ingenuity pathway analysis) and PATHOS (University of Glasgow) (see methods) were used to fit the up and down regulated metabolites into their respective pathways. This analysis revealed several pathways of interest, these pathways were selected as upon analysis several important metabolites of the pathways were shown to be altered in the samples compared with the control.

Of all pathways analysed using these data, arginine and proline metabolism was found to be significantly different versus the control. This was true for both the adipo derived metabolites and osteo derived metabolites. Several metabolites in this pathway were shown to be significantly different from the control samples. Specific metabolites of interest in this pathway include arginine, proline and ornithine. As such these metabolites were analysed further, this was done by treating dormant breast cancer cell mass with media supplemented with individual metabolites of interest.

Two other metabolites of interest are 5,6 dihydrothymine and N-methyl-2-pyridine-5-carboxamide, involved in the DNA damage repair pathway and nicotine amide (NAD) pathway respectively. Both metabolites were shown to be upregulated in the samples versus the controls, as both of these molecules have been heavily implicated in various cancers (Lenglet et al. 2016; Shaul et al. 2014), they were further examined by using media supplemented with each of these molecules to treat the dormant breast cancer cell mass model.

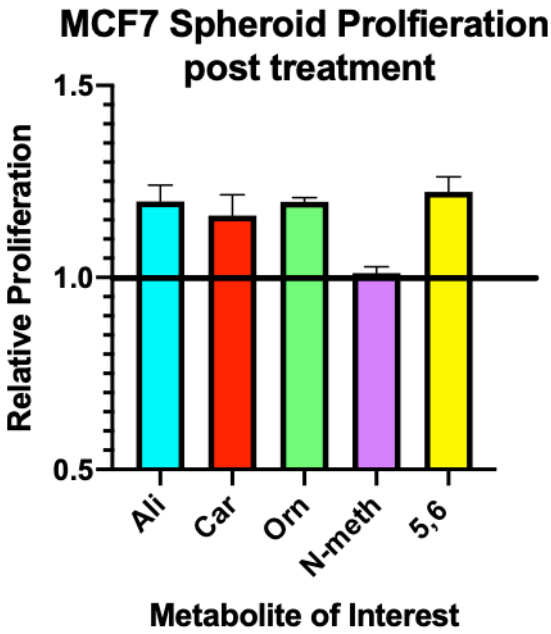

Figure 6.5 Graph showing relative proliferation of MCF7 spheroids after treatment with media supplemented with specific metabolites of interest. Determined by resazurin.All samples were compared against a control group consisting of MCF7 spheroids treated with un-supplemented media. Metabolites along the x axis are as follows: Alanine (Ali), Carnitine

Car), Ornithine (Orn), N-methyl-2-pyridine-5-carboxamide (N-meth) and 5,6 dihydrothymine (5,6) respectively. All spheroids were seeded at the same cell density (10,000 cells) and allowed to form for 48 hours. Statistical analysis using a Kruskal-Wallis test. "*" = p < 0.05, "" = p < 0.01, "***" = p < 0.001, "****" = p < 0.0001, "ns" = non- significant. n=3.**

All samples were then compared against the controls to give a factor change after treatment. No significant difference was observed across all samples; however, a trend of upregulation of proliferation was observed in several metabolite treatments. Due to this observed trend of upregulated proliferation, a more detailed analysis was carried out to investigate the effect of certain metabolites on the MCF7 spheroid model. Alanine, carnitine and ornithine were used to treat spheroids at varying concentrations. A significant difference in proliferation was observed in both alanine and ornithine treatments, indicating that DMEM supplemented with these two metabolites is sufficient to trigger proliferation in the MCF7 spheroid model (see figure 6.6).

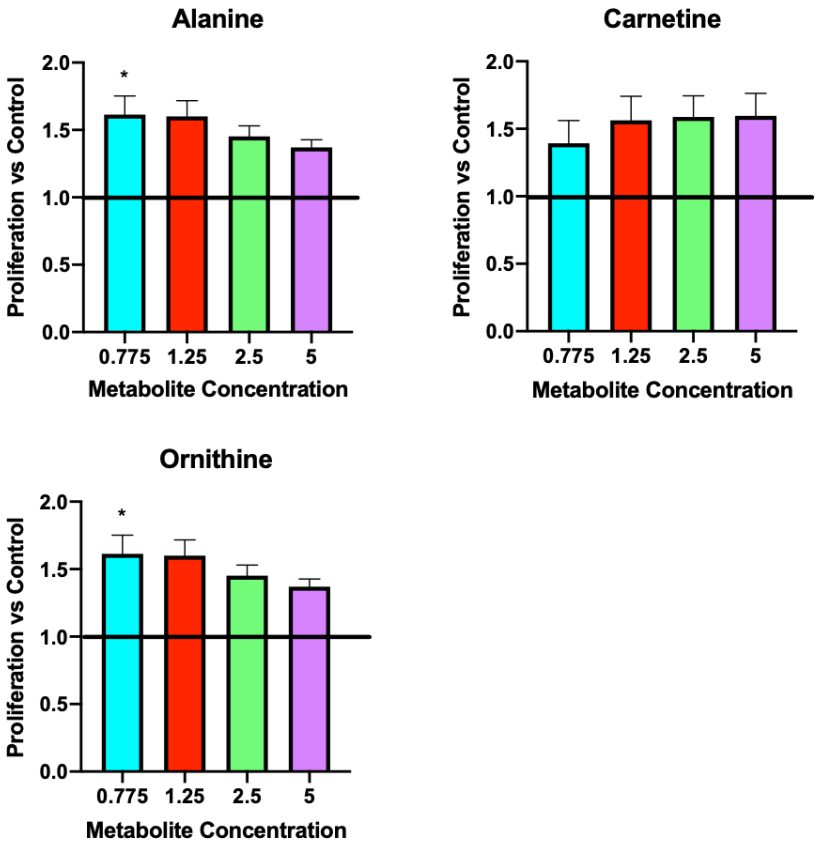

Figure 6.6 Graph showing relative proliferation of MCF7 spheroids after treatment with media supplemented with specific metabolites of interest. The proliferation of spheroid was

determined using resazurin reduction after 48 hours of treatment. Spheroids treated with alanine and ornithine show a significant difference in proliferation when compared with the control group after treatment with 0.775mM of the respective metabolite. These data shown that metabolite supplemented media is sufficient to trigger proliferation of the MCF7 spheroid model. Statistical analysis using a Kruskal-Wallis test. "*" = p < 0.05, "" = p < 0.01, "***" = p < 0.001, "****" = p < 0.0001, "ns" = non- significant. n=3. All concentrations in mM.**

6.3 Discussion

The key aim of this chapter was to investigate the metabolome of both media differentiated stem cells and 'biomaterials' treated MSCs, and to compare those with an MSC control group. This was due to the observation made in this thesis that media conditioned by differentiating MSCs was capable of triggering proliferation in the dormant breast cancer cell mass model described in this thesis (see chapter 3). As both adipo and osteo conditioned media was shown to be capable of triggering this observed proliferation, a key aim was to investigate and identify common metabolites shared by both adipo and osteo conditioned media. Along with this, an aim was to use identified metabolites to treat MCF7 spheroids to investigate the potential of metabolites, present in 'conditioned' media, to trigger proliferation in the MCF7 spheroid model. As well as identifying specific metabolites, altered pathways were analysed using these data and pathways of interest were identified.

The key findings of this chapter include:

- The secretome derived from osteo and adipo lineage MSC conditioned media share common metabolites.

- Conditioned media derived metabolites cluster together, in distinct populations versus both the control samples as well as the biomaterials conditioned samples.

- Altered metabolite concentrations in the samples versus control suggest alterations in several pathways associated with cancer growth and metabolism.

- Two metabolites common between adipo and osteo conditioned media are capable of triggering proliferation of MCF7 spheroids at <1mM.

6.3.1 Metabolic Clustering

Metabolites derived from adipo and osteo differentiated cells were shown in this chapter to largely cluster together. This is indictive that both samples share common upregulated and downregulated metabolites with one another. When analysing the clustering of all samples it was evident that the MSC control and all samples that were 'biomaterials' conditioned clustered together. This is concurrent with previous data generated in this thesis indicating that biomaterials treated MSCs showed little to no evidence of differentiation. Media conditioned with osteo and adipo cells was shown to trigger reactivation of the dormant breast cancer cell model, while all other samples were shown to be insufficient. These data taken together suggest that the common metabolites and pathways between adipo and osteo conditioned media may be responsible for the observed increase in proliferation.

6.3.2 Pathways of interest

Pathway analysis was carried out using the metabolic data obtained from conditioned media samples. This analysis identified several pathways of interest that have the potential to alter proliferation, cancer growth and the cancer microenvironment. One specific pathway that is heavily involved in cancer progression and growth is the arginine and proline metabolism pathway. Upon analysis this pathway was identified as having several changes within it, with critical metabolites such as ornithine shown to be upregulated.

Arginine is known to be a vitally important molecule that has influence over pathways essential for cell proliferation, cell signalling, immunity and biosynthesis of amino acids and growth factors(Patil et al. 2016) . Arginine is a direct resource for various essential molecules such as ornithine, NO (nitric oxide) and agmatine. Both ornithine and agmatine are precursors for putrescine,

an essential precursor for polyamines. Thus, ornithine and agmatine are vitally important molecules for cell growth. Specifically in cancers, ornithine is seen to fuel tumour cells to generate polyamine essential for growth, thus an increased concentration of ornithine used to treat dormant cells gives the cancer cell mass access to necessary precursors for the generation of putrescine for polyamine synthesis and (via the intermediary molecule of citrulline in the arginine related metabolic pathway) arginine is also produced.

Arginine has been shown to be a vitally important molecule for cell growth due to the ultimate production of NO, ornithine and agmatine(Patil et al. 2016). Cells have the intrinsic ability to synthesis arginine through the associated pathways, however many cancers become ‘arginine addicted’, a phenomenon whereby cancer cells are dependent on an external source of arginine(C. T. Cheng et al. 2018a). Starving cancer cells, specifically breast and prostate cancer cells, of arginine was shown to have far reaching effects on the cells including global transcriptional suppression of metabolic genes. The genes affected by this starvation included those involved in oxidative phosphorylation (OXPHOS), mitochondrial functions, glycolysis, and purine and pyrimidine biosynthesis. Arginine starvation triggered fragmentation of the mitochondria in cancer cells, thus arresting cell proliferation(Qiu et al. 2014; C. T. Cheng et al. 2018a).

Chapter 7 Discussion

7.1 Project Summary

The aim of this project was to investigate the phenomenon of breast cancer cell dormancy post metastasis to the bone marrow. Specifically, to investigate potential triggers of dormant breast cancer cell reawakening. This was achieved via the creation of a functional in vitro dormant breast cancer cell model, then using this model to assess various potential triggers of dormant breast cancer cell awakening. The key findings are as follows:

- MCF7 cells (breast cancer cell line) readily formed spheroids when seeded into round bottom ultra-low adherence tissue culture plates after just 48 hours. Said spheroids showed a significant reduction in cell proliferation compared with 2D counterparts.

- MCF7 spheroids were shown to be an effective model of dormant breast cancer cell mass, as significant reduction in proliferation was shown. Along with this, spheroids are shown to be effective models of solid tumours as they mimic both the nutrient gradient and hypoxic core of in vivo tumour masses (Pinto et al. 2020).

- The upscaling of biomaterials surface-based model to trigger MSC differentiation in this project was shown to be insufficient in triggering MSC differentiation.

- Media conditioned using osteogenic and adipogenic lineages of MSCs was shown to be capable of triggering proliferation in the MCF7 spheroid model.

- Metabolic analysis of differentiated cell conditioned media revealed several metabolites present in the conditioned media that are absent from the MSC control media. Several of which were shown to be capable of triggering activation when used individually to supplement regular

growth media. Potentially indicating metabolic cause of dormant tumour cell reactivation.

- Metabolic analysis also revealed potential pathways that may be responsible for reactivation of dormant breast cancer cell mass, specifically arginine and proline metabolism.

7.2 General Discussion

In conclusion the MCF7 breast cancer cell mass model described in this thesis was shown to exhibit significantly lower levels of proliferation than the controls, while also showing significant downregulation of the proliferation marker Ki67. These taken in conjunction are indicative of dormant breast cancer cell mass model, as reduced cellular proliferation and particularly the loss of ki67 expression are hallmarks of dormant breast cancer (Jahangiri and Ishola 2022). This model was then used to investigate the effect of MSC, osteoblast and adipocyte secretome on the proliferation rate of MCF-7s in spheroid formaiton. This revealed that while the secretome of MSCs was insufficient to trigger reactivation, the secretome of differentiated stem cells (adipogenic and osteogenic) were each sufficient to significantly increase cellular proliferation of the dormant cancer cell model. This therefore suggests that differentiation of MSCs within the bone marrow niche is a potential mechanism by which residing dormant breast cancer cell masses awaken.

Along with these findings metabolic analysis revealed several individual metabolites that were capable of triggering reactivation of the model when used to supplement growth media (specifically ornithine and alanine). Metabolomic analysis also revealed a pathway with a potentially important role in the reactivation of dormant breast cancer, specifically the arginine and proline metabolism pathway.

As shown in this thesis, the metabolic profiles of adipogenic and osteogenic cells share many commonalities, this is likely due to the fact that differentiation into any lineage requires similar activation of genes and proteins (Godoy et al. 2018).

Upon analysis of these data, both the adipogenic and osteogenic metabolome were shown to cluster together. Differentiation into both of these stem cell lineages has been shown (see chapters 5 and 6) to cause the release of factors capable of triggering activation of MCF7 spheroid model. Thus, further investigation into the potential mechanism of activation through metabolic changes was investigated. Recent data has identified metabolic remodelling of cancer cells as being very influential, not just in dormancy of cancer cells but also reawakening. Historic reasoning behind the altered metabolic state of cancer cells was termed 'Warburg metabolism' (Urbano 2021; Otto Warburg, Wind, and Negelein, 1927.), however recent studies have underlined how cancer cells have largely adaptive, heterogenous metabolic preferences (Pranzini, Raugei, and Taddei 2022). Shown to shift and adapt based on the needs of the cell.

Upon pathway analysis, pathways such as the arginine and proline metabolism pathway emerged as a potential mechanism of activation. Arginine is known to be vitally important for several aspects of cellular behaviour, including cell proliferation, cell signalling, immunity and biosynthesis of amino acids and growth factors (Qiu et al. 2014). Arginine is essential as it is also necessary for the synthesis of important intermediary molecules such as ornithine, agmatine and NO (nitric oxide) (Coradduzza et al. 2022). These molecules are vitally important, as both ornithine and agmatine are necessary for the synthesis of putrescine, an essential intermediary for the production of polyamines, which in turn are essential for cell proliferation and growth (C. T. Cheng et al. 2018a; Patil et al. 2016).

Metabolic data analysis identified the upregulated secretion of certain metabolites, with ornithine being present at nearly 3-fold increase when compared with the MSC control. As ornithine can be both generated from and regenerate arginine through the urea cycle (Fujimi et al. 2020), the large overexpression in the adipo and osteo media is indicative of an altered pathway. Ornithine is also essential for cell growth as described above. Specifically in cancer cells ornithine is seen to fuel tumour cells to generate polyamines essential for growth (J. Li et al. 2020). Thus, the observed increase in secretion of ornithine into the conditioned media by both the adipo and osteo cell lineages

is likely influential in the observed proliferation increase of conditioned media treated spheroids.

While cells have the intrinsic ability to synthesis arginine through relevant metabolic pathways, cancer has been observed to under ‘arginine starvation’ or ‘arginine addiction’ whereby cancer cells are dependent on an external source of arginine (C. T. Cheng et al. 2018b). Starving cancer cells, specifically breast and prostate cancer cells, of arginine was shown to have far reaching effects on the cells, including global transcriptional suppression of metabolic genes (Qiu et al. 2014; C. T. Cheng et al. 2018a; Patil et al. 2016). This thesis shows that treatment of MCF7 spheroids with regular DMEM/FCS media (see methods) supplemented with 0.775mM ornithine triggered an increase in proliferation when compared with regular DMEM control. Thus, the introduction of excess ornithine in the conditioned media may be important in the reawakening of the dormant breast cancer cells, as it provides fuel for both cell growth and the renewal of arginine.

7.3 Limitations of the project

7.3.1 Bone Marrow Cell Types

This project utilizes the model described previously to investigate dormant breast cancer and its relationship with differentiated stem cells. This model has uses in the field as it is simplistic in its design and is capable of relatively high throughput testing of signalling factors. However, it is not without its drawbacks, most notably is the fact this model does not account for the other cell types present within the bone marrow. Although this project was focused on differentiated MSCs as a source of signalling factors to influence dormant MCF7 model, HSCs are present within the bone marrow, in close localisation with resident MSCs in vivo. These cells are capable of self-renewal and differentiation into blood lineage cells, while also are partially responsible for the maintenance of the stem cell niche (Szade et al. 2018; Morrison and Scadden 2014).

Other cells such as fibroblasts or cancer-associated fibroblasts (CAFs) also have a profound effect on tumours in vivo, these cells are ultimately derived from MSCs (Denu et al. 2016). As immune cells they have been shown to play an integral part in the clearance of invading bccs into the bone marrow (Mukaida, Zhang, and Sasaki 2020).

The addition of multiple cell types to the culture however results in several issues. Most notably of which is the need of different cell types to be cultured in distinct cell culture media. However, the addition of several cell types into the culture would give more information about the relationship between disseminated bccs and their colonised environment. However, concessions would have to be made as regards to the media used to culture the cells, with physiology of the cells likely being impacted by culture in sub-optimal growth media.

7.3.2 Differing Disease Conditions

The model described in this thesis recreated several conditions, namely MSC secretions, adipocyte secretions and osteoblast secretions. However, it is likely the patients suffering from this disease will have differing states of bone marrow health. One such factor that is very likely to cause alterations in the bone marrow microenvironment is age, with aged patients being far more likely to be osteoporotic (Byrne, Summers, and McDonald 2019). Osteoporosis is a disease characterised by systemic bone loss, ultimately causing increased fragility of bone. This increased fragility often leads to issues such as fractures, as bone fractures would occur more regularly in osteoporotic patients, so too would bone repair (Pisani et al. 2016). It has been shown in this thesis that MSCs differentiated into osteoblast lineage secrete factors capable of reactivating the dormant breast cancer cell model. Thus, an observed increase in bone repair would likely result in the release of factors capable of triggering reactivation of dormant breast cancer.

7.3.3 Biomaterials

The use of biomaterials to trigger differentiation in MSCs could yield interesting results, comparing the biomaterials PEA/FN/GF differentiation media with that induced by supplemented media. However, upon upscaling this procedure, differentiation of MSCs could not be achieved. Previous studies have shown that at smaller working surface areas (specifically coverslips) the PEA/FN/GF model of growth factor inducted differentiation is effective (Llopis-Hernández et al. 2016), however upscaling was unsuccessful. Previous studies have shown that the biomaterials coating is effective when coated into coverslips, this thesis investigated the upscaling of this procedure into tissue culture flasks. XPS and AFM readings were taken for each sample (taken from 24 well Corning plate and T75 Corning tissue culture flask), both showed the FN nanonetworks after FN coating. Both also showed sufficient binding of growth factors and presentation of cell binding sites, verified with ELISA. However, despite this the biomaterials model did not cause differentiation of MSCs. One possible explanation is that the MSCs were still proliferating when seeded into the flask (proliferating cells resist differentiation (Ruijtenberg and van den Heuvel 2016b)), this could potentially be remedied by seeding at a higher cell density so there is less room for cells to expand.

7.4 Future Work

Based on results obtained in this thesis, potential further work is discussed below.

As addressed in the limitation subchapter (7.3), the model described in this thesis although useful in its simplicity is hindered by its ability to replicate conditions in vivo. A method that could be utilized in order to more closely mimic the in vivo conditions is the use of a hydrogel insert (potentially collagen based). A hydrogel insert can be tuned to mimic the bone marrow microenvironment, allowing for a more representative model (Pradhan and Slater 2019). The density of hydrogels can be altered to suit needs; thus, experiments could be designed so that hydrogels could be used to allow the co-

culture of bone marrow related cells with MCF7 spheroids. This would allow for a more accurate model, whereby the secreted factors originating from the MSCs, osteoblasts and adipocytes could directly influence the MCF7 spheroids over time. This has been shown in other cell types to be extremely informative as to inform on the cross play between cell types (Scalzone et al. 2019).

Along with the use of hydrogels to more accurately mimic in vivo conditions, the co-culture of MSCs with other cell types present in the bone marrow niche would be very informative as to the combinative effect of the total secretome of this culture. In this thesis, the secretome of MSCs, osteoblast and adipocytes were assessed for its ability to trigger the activation of the dormant breast cancer cell mass model. Undoubtably, however, the co-culture of these cells with other cells presents in the bone microenvironment such as HSCs and fibroblasts would further influence the total metabolites present in conditioned media. This would in turn provide a more accurate representation of the total metabolites present in the bone marrow niche in vivo.

Although the metabolomics experiments described in this thesis were useful in identifying potential triggers of reactivation through secreted metabolites, the changes in metabolism undergone by the MCF7 spheroids themselves was not assessed. Future experiments could revolve around the analysis of MCF7 spheroid cellular metabolism after treatment with conditioned media and individual metabolites. As this would be more informative in regard to the mechanisms of reactivation as opposed to the triggers of dormant breast cancer cell reawakening and inform of any switches to or from OXPHOS/glycolysis.

Recent data has suggested the role of EVs and EV cargo in the reawakening of breast cancer (Casson et al. 2018). Most studies have focused on the contents and effect of MSC derived EVs on dormant breast cancer cell models. Future experiments could be designed so that EVs could be isolated from MSCs as well as osteoblasts and adipocytes, these isolated EVs could then be characterised and used in the treatment of the dormant breast cancer cell model. Total EVs could also be potentially isolated from co-cultures described above, giving further insight into the triggers and mechanisms surrounding the dormancy of breast cancer cells in the bone marrow.

The biomaterials model could potentially provide very interesting information, as it could illuminate the indirect effect of growth factors present in the bone marrow on the dormant phenotype of invading BCCs. As this project focused on the plasma polymerisation of PEA onto the tissue culture surface, future experiments could be designed whereby the tissue culture surface would be coated with PEA using the more traditional and gold standard method of spin coating (Alba-Perez et al. 2020d). Along with changing the method of coating, alterations could be made in the seeding concentrations of both fibronectin and growth factors. An altered concentration of fibronectin used to coat the PEA could result in altered FN network densities which could in turn influence the effectiveness of the model to trigger differentiation through the presentation of growth factors (Vanterpool et al. 2014; Alba-Perez et al. 2020d).

7.5 Conclusion

Over recent years much research has been done into the phenomenon of breast cancer dormancy, however large gaps in knowledge still exist and further research much be done to fill those gaps. This thesis describes a cheap, simple model of dormant breast cancer cell masses. These spheroids are easily produced and can be used for a variety of assays, including viability assays, drug screening, and gene expression analysis. In addition, the model allows for the study of the mechanisms that regulate dormancy and reactivation of breast cancer cells, which could help the development of new therapeutics. The use of this model in high throughput screening could greatly accelerate the discovery of novel drugs and biomarkers for breast cancer dormancy, ultimately leading to improved patient outcomes. However, more research needs to be conducted in order to make the model more clinically relevant, such as the development of a co-culture system with MSCs or perhaps other bone marrow resident cells, so that observations can be made in real time allowing for a more accurate representation of the disease.

List of References

Agrawal, Ganesh Kumar, Nam Soo Jwa, Marc Henri Lebrun, Dominique Job, and Randeep Rakwal. 2010. 'Plant Secretome: Unlocking Secrets of the Secreted Proteins'. *Proteomics*. https://doi.org/10.1002/pmic.200900514.

Ahirwar, Dinesh K., Mohd W. Nasser, Madhu M. Ouseph, Mohamad Elbaz, Maria C. Cuitiño, Raleigh D. Kladney, Sanjay Varikuti, et al. 2018. 'Fibroblast-Derived CXCL12 Promotes Breast Cancer Metastasis by Facilitating Tumor Cell Intravasation'. *Oncogene* 37 (32): 4428–42. https://doi.org/10.1038/s41388-018-0263-7.

Al-Awsi, Ghaidaa Raheem Lateef, Fahad Alsaikhan, Ria Margiana, Irfan Ahmad, Indrajit Patra, Mazin A.A. Najm, Ghulam Yasin, et al. 2023. 'Shining the Light on Mesenchymal Stem Cell-Derived Exosomes in Breast Cancer'. *Stem Cell Research and Therapy*. BioMed Central Ltd. https://doi.org/10.1186/s13287-023-03245-3.

Alba-Perez, Andres, Vineetha Jayawarna, Peter G. Childs, Matthew J. Dalby, and Manuel Salmeron-Sanchez. 2020a. 'Plasma Polymerised Nanoscale Coatings of Controlled Thickness for Efficient Solid-Phase Presentation of Growth Factors'. *Materials Science and Engineering C* 113 (January): 110966. https://doi.org/10.1016/j.msec.2020.110966.

———. 2020b. 'Plasma Polymerised Nanoscale Coatings of Controlled Thickness for Efficient Solid-Phase Presentation of Growth Factors'. *Materials Science and Engineering C* 113 (January): 110966. https://doi.org/10.1016/j.msec.2020.110966.

———. 2020c. 'Plasma Polymerised Nanoscale Coatings of Controlled Thickness for Efficient Solid-Phase Presentation of Growth Factors'. *Materials Science and Engineering C* 113 (August). https://doi.org/10.1016/j.msec.2020.110966.

———. 2020d. 'Plasma Polymerised Nanoscale Coatings of Controlled Thickness for Efficient Solid-Phase Presentation of Growth Factors'. *Materials Science and Engineering C* 113 (August). https://doi.org/10.1016/j.msec.2020.110966.

Alberghina, L., and D. Gaglio. 2014. 'Redox Control of Glutamine Utilization in Cancer'. *Cell Death and Disease* 5 (12). https://doi.org/10.1038/cddis.2014.513.

Al-Nedawi, Khalid, Brian Meehan, Johann Micallef, Vladimir Lhotak, Linda May, Abhijit Guha, and Janusz Rak. 2008. 'Intercellular Transfer of the Oncogenic Receptor EGFRvIII by Microvesicles Derived from Tumour Cells'. *Nature Cell Biology* 10 (5): 619–24. https://doi.org/10.1038/ncb1725.

Anand, Sushma, Monisha Samuel, Sharad Kumar, and Suresh Mathivanan. 2019. 'Ticket to a Bubble Ride: Cargo Sorting into Exosomes and Extracellular Vesicles'. *Biochimica et Biophysica Acta - Proteins and Proteomics* 1867 (12): 140203. https://doi.org/10.1016/j.bbapap.2019.02.005.

Ashrafian, Houman, Linda O'Flaherty, Julie Adam, Violetta Steeples, Yuen Li Chung, Phil East, Sakari Vanharanta, et al. 2010. 'Expression Profiling in Progressive Stages of Fumarate-Hydratase Deficiency: The Contribution of Metabolic Changes to Tumorigenesis'. *Cancer Research* 70 (22): 9153–65. https://doi.org/10.1158/0008-5472.CAN-10-1949.

Babst, Markus. 2011. ‘MVB Vesicle Formation: ESCRT-Dependent, ESCRT-Independent and Everything in Between’. *Current Opinion in Cell Biology* 23 (4): 452–57. https://doi.org/10.1016/j.ceb.2011.04.008.

Baghban, Roghayyeh, Leila Roshangar, Rana Jahanban-Esfahlan, Khaled Seidi, Abbas Ebrahimi-Kalan, Mehdi Jaymand, Saeed Kolahian, Tahereh Javaheri, and Peyman Zare. 2020. ‘Tumor Microenvironment Complexity and Therapeutic Implications at a Glance’. *Cell Communication and Signaling*. BioMed Central Ltd. https://doi.org/10.1186/s12964-020-0530-4.

Beer, Katharina B., and Ann Marie Wehman. 2017. ‘Mechanisms and Functions of Extracellular Vesicle Release in Vivo—What We Can Learn from Flies and Worms’. *Cell Adhesion and Migration* 11 (2): 135–50. https://doi.org/10.1080/19336918.2016.1236899.

Blache, Ulrich, Edward R. Horton, Tian Xia, Erwin M. Schoof, Lene H. Blicher, Angelina Schönenberger, Jess G. Snedeker, Ivan Martin, Janine T. Erler, and Martin Ehrbar. 2019. ‘Mesenchymal Stromal Cell Activation by Breast Cancer Secretomes in Bioengineered 3D Microenvironments’. *Life Science Alliance* 2 (3): 1–15. https://doi.org/10.26508/lsa.201900304.

Bliss, Sarah A., Garima Sinha, Oleta A. Sandiford, Lisa M. Williams, Daniel J. Engelberth, Khadidiatou Guiro, Leidy L. Isenalumhe, et al. 2016. ‘Mesenchymal Stem Cell-Derived Exosomes Stimulate Cycling Quiescence and Early Breast Cancer Dormancy in Bone Marrow’. *Cancer Research* 76 (19): 5832–44. https://doi.org/10.1158/0008-5472.CAN-16-1092.

Bobrie, Angélique, Sophie Krumeich, Fabien Reyal, Chiara Recchi, Luis F. Moita, Miguel C. Seabra, Matias Ostrowski, and Clotilde Théry. 2012. ‘Rab27a Supports Exosome-Dependent and -Independent Mechanisms That Modify the Tumor Microenvironment and Can Promote Tumor Progression’. *Cancer Research* 72 (19): 4920–30. https://doi.org/10.1158/0008-5472.CAN-12-0925.

Bonifacino, Juan S., and Benjamin S. Glick. 2004. ‘The Mechanisms of Vesicle Budding and Fusion’. *Cell* 116 (2): 153–66. https://doi.org/10.1016/S0092-8674(03)01079-1.

Boyd, Norman F., Lisa J. Martin, Michael Bronskill, Martin J. Yaffe, Neb Duric, and Salomon Minkin. 2010. ‘Breast Tissue Composition and Susceptibility to Breast Cancer’. *Journal of the National Cancer Institute* 102 (16): 1224–37. https://doi.org/10.1093/jnci/djq239.

Boyle, William J, W Scott Simonet, and David L Lacey. 2003. ‘And Activation’ 423 (May): 337–42.

Bragado, Paloma, Yeriel Estrada, Falguni Parikh, Sarah Krause, Carla Capobianco, Hernan G. Farina, Denis M. Schewe, and Julio A. Aguirre-Ghiso. 2013. ‘TGF-B2 Dictates Disseminated Tumour Cell Fate in Target Organs through TGF-ß-RIII and P38α/ß Signalling’. *Nature Cell Biology* 15 (11): 1351–61. https://doi.org/10.1038/ncb2861.

Braun, Stephan, Klaus Pantel, Peter Müller, Wolfgang Janni, Florian Hepp, Christina R.M. Kentenich, Stephan Gastroph, et al. 2000. ‘Cytokeratin-Positive Cells in the Bone Marrow and Survival of Patients with Stage I, II, or III Breast Cancer’. *New England Journal of Medicine* 342 (8): 525–33. https://doi.org/10.1056/NEJM200002243420801.

Budczies, Jan, Carsten Denkert, Berit M. Müller, Scarlet F. Brockmöller, Frederick Klauschen, Balazs Györffy, Manfred Dietel, et al. 2012. ‘Remodeling of Central Metabolism in Invasive Breast Cancer Compared to Normal Breast Tissue - a GC-TOFMS Based Metabolomics Study’. *BMC Genomics* 13 (1). https://doi.org/10.1186/1471-2164-13-334.

Bushnell, Grace G., Abhijeet P. Deshmukh, Petra den Hollander, Ming Luo, Rama Soundararajan, Dongya Jia, Herbert Levine, Sendurai A. Mani, and Max S. Wicha. 2021a. 'Breast Cancer Dormancy: Need for Clinically Relevant Models to Address Current Gaps in Knowledge'. *Npj Breast Cancer*. Nature Research. https://doi.org/10.1038/s41523-021-00269-x.

———. 2021b. 'Breast Cancer Dormancy: Need for Clinically Relevant Models to Address Current Gaps in Knowledge'. *Npj Breast Cancer*. Nature Research. https://doi.org/10.1038/s41523-021-00269-x.

Byrne, Niall M., Matthew A. Summers, and Michelle M. McDonald. 2019. 'Tumor Cell Dormancy and Reactivation in Bone: Skeletal Biology and Therapeutic Opportunities'. *JBMR Plus*. Blackwell Publishing Ltd. https://doi.org/10.1002/jbm4.10125.

Caillat, Christophe, Sourav Maity, Nolwenn Miguet, Wouter H. Roos, and Winfried Weissenhorn. 2019. 'The Role of VPS4 in ESCRT-III Polymer Remodeling'. *Biochemical Society Transactions* 47 (1): 441–48. https://doi.org/10.1042/BST20180026.

Cao, Yangchun, Shimin Liu, Kai Liu, Imtiaz Hussain Raja Abbasi, Chuanjiang Cai, and Junhu Yao. 2019. 'Molecular Mechanisms Relating to Amino Acid Regulation of Protein Synthesis'. *Nutrition Research Reviews* 32 (2): 183–91. https://doi.org/10.1017/S0954422419000052.

Cappariello, Alfredo, and Nadia Rucci. 2019. 'Tumour-Derived Extracellular Vesicles (EVs): A Dangerous "Message in a Bottle" for Bone'. *International Journal of Molecular Sciences* 20 (19). https://doi.org/10.3390/ijms20194805.

Casson, Jake, Owen G. Davies, Carol Anne Smith, Matthew J. Dalby, and Catherine C. Berry. 2018. 'Mesenchymal Stem Cell-Derived Extracellular Vesicles May Promote Breast Cancer Cell Dormancy'. *Journal of Tissue Engineering* 9 (December). https://doi.org/10.1177/2041731418810093.

Chan, Mun Yew Patrick, and Serene Lim. 2010. 'Predictors of Invasive Breast Cancer in Ductal Carcinoma in Situ Initially Diagnosed by Core Biopsy'. *Asian Journal of Surgery* 33 (2): 76–82. https://doi.org/10.1016/S1015-9584(10)60013-9.

Chandrasekaran, Siddarth. 2012. 'Gather Round: In Vitro Tumor Spheroids as Improved Models of in Vivo Tumors'. *Journal of Bioengineering & Biomedical Science* 02 (04). https://doi.org/10.4172/2155-9538.1000e109.

Charrin, Stéphanie, Stéphanie Jouannet, Claude Boucheix, and Eric Rubinstein. 2014. 'Tetraspanins at a Glance'. *Journal of Cell Science* 127 (17): 3641–48. https://doi.org/10.1242/jcs.154906.

Chen, Anan, Dingding Wang, Xueting Liu, Shuilian He, Zhihong Yu, and Ju Wang. 2012. 'Inhibitory Effect of BMP-2 on the Proliferation of Breast Cancer Cells'. *Molecular Medicine Reports* 6 (3): 615–20. https://doi.org/10.3892/mmr.2012.962.

Chen, Chen, Shujie Zhao, Anand Karnad, and James W. Freeman. 2018. 'The Biology and Role of CD44 in Cancer Progression: Therapeutic Implications'. *Journal of Hematology and Oncology* 11 (1): 1–23. https://doi.org/10.1186/s13045-018-0605-5.

Chen, Meng Ting, He Fen Sun, Yang Zhao, Wen Yan Fu, Li Peng Yang, Shui Ping Gao, Liang Dong Li, Hong Lin Jiang, and Wei Jin. 2017. 'Comparison of Patterns and Prognosis among Distant Metastatic Breast Cancer Patients by Age Groups: A SEER Population-Based Analysis'. *Scientific Reports* 7 (1). https://doi.org/10.1038/s41598-017-10166-8.

Cheng, Chun Ting, Yue Qi, Yi Chang Wang, Kevin K. Chi, Yiyin Chung, Ching Ouyang, Yun Ru Chen, et al. 2018a. 'Arginine Starvation Kills Tumor Cells through Aspartate Exhaustion and Mitochondrial Dysfunction'. *Communications Biology* 1 (1). https://doi.org/10.1038/s42003-018-0178-4.

———. 2018b. 'Arginine Starvation Kills Tumor Cells through Aspartate Exhaustion and Mitochondrial Dysfunction'. *Communications Biology* 1 (1). https://doi.org/10.1038/s42003-018-0178-4.

Cheng, Zhe A., Andres Alba-Perez, Cristina Gonzalez-Garcia, Hannah Donnelly, Virginia Llopis-Hernandez, Vineetha Jayawarna, Peter Childs, et al. 2018. 'Nanoscale Coatings for Ultralow Dose BMP-2-Driven Regeneration of Critical-Sized Bone Defects'. *Advanced Science* 1800361. https://doi.org/10.1002/advs.201800361.

Chernomordik, Leonid V., Grigorii B. Melikyan, and Yurii A. Chizmadzhev. 1987. 'Biomembrane Fusion: A New Concept Derived from Model Studies Using Two Interacting Planar Lipid Bilayers'. *BBA - Reviews on Biomembranes* 906 (3): 309–52. https://doi.org/10.1016/0304-4157(87)90016-5.

Chong Seow Khoon, Mark. 2015. 'Experimental Models of Bone Metastasis: Opportunities for the Study of Cancer Dormancy'. *Advanced Drug Delivery Reviews* 94: 141–50. https://doi.org/10.1016/j.addr.2014.12.007.

Cieślikowski, Wojciech A., Joanna Budna-Tukan, Monika Świerczewska, Agnieszka Ida, Michał Hrab, Agnieszka Jankowiak, Martine Mazel, et al. 2020. 'Circulating Tumor Cells as a Marker of Disseminated Disease in Patients with Newly Diagnosed High-Risk Prostate Cancer'. *Cancers* 12 (1). https://doi.org/10.3390/cancers12010160.

Clements, Miranda E., and Rachelle W. Johnson. 2019a. 'Breast Cancer Dormancy in Bone'. *Current Osteoporosis Reports*. Current Medicine Group LLC 1. https://doi.org/10.1007/s11914-019-00532-y.

———. 2019b. 'Breast Cancer Dormancy in Bone'. *Current Osteoporosis Reports*. Current Medicine Group LLC 1. https://doi.org/10.1007/s11914-019-00532-y.

Cohen, S., and R. Levi-Montalcini. 1956. 'A Nerve Growth-Stimulating Factor Isolated From Snake Venom'. *Proceedings of the National Academy of Sciences* 42 (9): 571–74. https://doi.org/10.1073/pnas.42.9.571.

Cook, Leah M., Gemma Shay, Arturo Aruajo, and Conor C. Lynch. 2014. 'Integrating New Discoveries into the "Vicious Cycle" Paradigm of Prostate to Bone Metastases'. *Cancer and Metastasis Reviews* 33 (2–3): 511–25. https://doi.org/10.1007/s10555-014-9494-4.

Coradduzza, Donatella, Tatiana Solinas, Emanuela Azara, Nicola Culeddu, Sara Cruciani, Angelo Zinellu, Serenella Medici, Margherita Maioli, Massimo Madonia, and Ciriaco Carru. 2022. 'Plasma Polyamine Biomarker Panels: Agmatine in Support of Prostate Cancer Diagnosis'. *Biomolecules* 12 (4). https://doi.org/10.3390/biom12040514.

Cosentino, Giulia, Ilaria Plantamura, Elda Tagliabue, Marilena V. Iorio, and Alessandra Cataldo. 2021. 'Breast Cancer Drug Resistance: Overcoming the Challenge by Capitalizing on MicroRNA and Tumor Microenvironment Interplay'. *Cancers*. MDPI AG. https://doi.org/10.3390/cancers13153691.

Costa, Elisabete C., Duarte de Melo-Diogo, André F. Moreira, Marco P. Carvalho, and Ilídio J. Correia. 2018. 'Spheroids Formation on Non-Adhesive Surfaces by Liquid Overlay Technique: Considerations and Practical Approaches'. *Biotechnology Journal*. Wiley-VCH Verlag. https://doi.org/10.1002/biot.201700417.

Crane, Genevieve M., Elise Jeffery, and Sean J. Morrison. 2017. 'Adult Haematopoietic Stem Cell Niches'. *Nature Reviews Immunology*. Nature Publishing Group. https://doi.org/10.1038/nri.2017.53.

Cruzat, Vinicius, Marcelo Macedo Rogero, Kevin Noel Keane, Rui Curi, and Philip Newsholme. 2018. 'Glutamine: Metabolism and Immune Function, Supplementation and Clinical Translation'. *Nutrients*. MDPI AG. https://doi.org/10.3390/nu10111564.

Cui, X., Y. Hartanto, and H. Zhang. 2017. 'Advances in Multicellular Spheroids Formation'. *Journal of the Royal Society Interface*. Royal Society. https://doi.org/10.1098/rsif.2016.0877.

Curi, R., C. J. Lagranha, S. Q. Doi, D. F. Sellitti, J. Procopio, T. C. Pithon-Curi, M. Corless, and P. Newsholme. 2005. 'Molecular Mechanisms of Glutamine Action'. *Journal of Cellular Physiology*. https://doi.org/10.1002/jcp.20339.

Delston, R. B., K. A. Matatall, Y. Sun, M. D. Onken, and J. W. Harbour. 2011. 'P38 Phosphorylates Rb on Ser567 by a Novel, Cell Cycle-Independent Mechanism That Triggers Rb-Hdm2 Interaction and Apoptosis'. *Oncogene* 30 (5): 588–99. https://doi.org/10.1038/onc.2010.442.

Denu, Ryan A., Steven Nemcek, Debra D. Bloom, A. Daisy Goodrich, Jaehyup Kim, Deane F. Mosher, and Peiman Hematti. 2016. 'Fibroblasts and Mesenchymal Stromal/Stem Cells Are Phenotypically Indistinguishable'. *Acta Haematologica* 136 (2): 85–97. https://doi.org/10.1159/000445096.

Dioufa, Nikolina, Amanda M. Clark, Bo Ma, Colin H. Beckwitt, and Alan Wells. 2017. 'Bi-Directional Exosome-Driven Intercommunication between the Hepatic Niche and Cancer Cells'. *Molecular Cancer* 16 (1): 1–14. https://doi.org/10.1186/s12943-017-0740-6.

Dolatshahi-Pirouz, A., T. Jensen, M. Foss, J. Chevallier, and F. Besenbacher. 2009. 'Enhanced Surface Activation of Fibronectin upon Adsorption on Hydroxyapatite'. *Langmuir* 25 (5): 2971–78. https://doi.org/10.1021/la803142u.

Dominiak, Agnieszka, Beata Chełstowska, Wioletta Olejarz, and Grażyna Nowicka. 2020. 'Communication in the Cancer Microenvironment as a Target for Therapeutic Interventions'. *Cancers*. MDPI AG. https://doi.org/10.3390/cancers12051232.

Dominici, M., K. Le Blanc, I. Mueller, I. Slaper-Cortenbach, F. C. Marini, D. S. Krause, R. J. Deans, A. Keating, D. J. Prockop, and E. M. Horwitz. 2006. 'Minimal Criteria for Defining Multipotent Mesenchymal Stromal Cells. The International Society for Cellular Therapy Position Statement'. *Cytotherapy* 8 (4): 315–17. https://doi.org/10.1080/14653240600855905.

Donnarumma, Elvira, Danilo Fiore, Martina Nappa, Giuseppina Roscigno, Assunta Adamo, Margherita Iaboni, Valentina Russo, et al. 2017. 'Cancer-Associated Fibroblasts Release Exosomal MicroRNAs That Dictate an Aggressive Phenotype in Breast Cancer'. *Oncotarget* 8 (12): 19592–608. https://doi.org/10.18632/oncotarget.14752.

Donnelly, Hannah, Manuel Salmeron-Sanchez, and Matthew J. Dalby. 2018. 'Designing Stem Cell Niches for Differentiation and Self-Renewal'. *Journal of the Royal Society Interface* 15 (145). https://doi.org/10.1098/rsif.2018.0388.

Doyle, Laura, and Michael Wang. 2019. 'Overview of Extracellular Vesicles, Their Origin, Composition, Purpose, and Methods for Exosome Isolation and Analysis'. *Cells* 8 (7): 727. https://doi.org/10.3390/cells8070727.

D'Souza-Schorey Crislyn, C., and James W. Clancy. 2012. 'Tumor-Derived Microvesicles: Shedding Light on Novel Microenvironment Modulators and

Prospective Cancer Biomarkers'. *Genes and Development* 26 (12): 1287–99. https://doi.org/10.1101/gad.192351.112.

Dunn, Warwick B., and David I. Ellis. 2005. 'Metabolomics: Current Analytical Platforms and Methodologies'. *TrAC - Trends in Analytical Chemistry* 24 (4): 285–94. https://doi.org/10.1016/j.trac.2004.11.021.

Eagle, Harry, Vance I Oyama, Mina Levy, Clara L Horton, and Ralph Fleischman. n.d. 'THE GROWTH RESPONSE OF MAMMALIAN CELLS IN TISSUE CULTURE TO L-GLUTAMINE AND L-GLUTAMIC ACID'.

Ehninger, Armin, and Andreas Trumpp. 2011. 'The Bone Marrow Stem Cell Niche Grows up: Mesenchymal Stem Cells and Macrophages Move In'. *Journal of Experimental Medicine* 208 (3): 421–28. https://doi.org/10.1084/jem.20110132.

Elkhenany, Hoda, Lisa Amelse, Andersen Lafont, Shawn Bourdo, Marc Caldwell, Nancy Neilsen, Enkeleda Dervishi, et al. 2015. 'Graphene Supports in Vitro Proliferation and Osteogenic Differentiation of Goat Adult Mesenchymal Stem Cells: Potential for Bone Tissue Engineering'. *Journal of Applied Toxicology* 35 (4): 367–74. https://doi.org/10.1002/jat.3024.

Endo, Hiroko, and Masahiro Inoue. 2019. 'Dormancy in Cancer'. *Cancer Science*. Blackwell Publishing Ltd. https://doi.org/10.1111/cas.13917.

Erson, Philip P, and " Brooklyn. n.d. 'OTTO WARBURG : "ON THE ORIGIN OF CANCER CELLS"'.

———. n.d. 'OTTO WARBURG : "ON THE ORIGIN OF CANCER CELLS"'.

Fantin, V. R., and P. Leder. 2006. 'Mitochondriotoxic Compounds for Cancer Therapy'. *Oncogene*. https://doi.org/10.1038/sj.onc.1209599.

Fantin, Valeria R., Julie St-Pierre, and Philip Leder. 2006. 'Attenuation of LDH-A Expression Uncovers a Link between Glycolysis, Mitochondrial Physiology, and Tumor Maintenance'. *Cancer Cell* 9 (6): 425–34. https://doi.org/10.1016/j.ccr.2006.04.023.

Fares, Jawad, Mohamad Y. Fares, Hussein H. Khachfe, Hamza A. Salhab, and Youssef Fares. 2020. 'Molecular Principles of Metastasis: A Hallmark of Cancer Revisited'. *Signal Transduction and Targeted Therapy*. Springer Nature. https://doi.org/10.1038/s41392-020-0134-x.

Fatima, Farah, and Muhammad Nawaz. 2017. 'Nexus between Extracellular Vesicles, Immunomodulation and Tissue Remodeling: For Good or for Bad?' *Annals of Translational Medicine* 5 (6): 1–6. https://doi.org/10.21037/atm.2017.03.71.

Fluegen, Georg, Alvaro Avivar-Valderas, Yarong Wang, Michael R. Padgen, James K. Williams, Ana Rita Nobre, Veronica Calvo, et al. 2017. 'Phenotypic Heterogeneity of Disseminated Tumour Cells Is Preset by Primary Tumour Hypoxic Microenvironments'. *Nature Cell Biology* 19 (2): 120–32. https://doi.org/10.1038/ncb3465.

Fujimi, Takahiko J., Yoshihiro Mezaki, Takahiro Masaki, Ayasa Tajima, Mariko Nakamura, Akira Yoshikawa, Noriyuki Murai, et al. 2020. 'Investigation of the Effects of Urea Cycle Amino Acids on the Expression of ALB and CEBPB in the Human Hepatocellular Carcinoma Cell Line FLC-4'. *Human Cell* 33 (3): 590–98. https://doi.org/10.1007/s13577-020-00383-1.

Galipeau, Jacques, Mauro Krampera, John Barrett, Francesco Dazzi, Robert J. Deans, Joost DeBruijn, Massimo Dominici, et al. 2015. 'International Society for Cellular Therapy Perspective on Immune Functional Assays for Mesenchymal Stromal Cells as Potency Release Criterion for Advanced Phase Clinical Trials'. *Cytotherapy* 18 (2): 151–59. https://doi.org/10.1016/j.jcyt.2015.11.008.

Gauthier, Sébastien A., Rocío Pérez-González, Ajay Sharma, Fang Ke Huang, Melissa J. Alldred, Monika Pawlik, Gurjinder Kaur, Stephen D. Ginsberg, Thomas A. Neubert, and Efrat Levy. 2017. 'Enhanced Exosome Secretion in Down Syndrome Brain - a Protective Mechanism to Alleviate Neuronal Endosomal Abnormalities'. *Acta Neuropathologica Communications* 5 (1): 65. https://doi.org/10.1186/s40478-017-0466-0.

Gee, Elaine P.S., Donald E. Ingber, and Collin M. Stultz. 2008. 'Fibronectin Unfolding Revisited: Modeling Cell Traction-Mediated Unfolding of the Tenth Type-III Repeat'. *PLoS ONE* 3 (6). https://doi.org/10.1371/journal.pone.0002373.

Ghajar, Cyrus M. 2015. 'Metastasis Prevention by Targeting the Dormant Niche'. *Nature Reviews Cancer* 15 (4): 238–47. https://doi.org/10.1038/nrc3910.

Ghajar, Cyrus M., Héctor Peinado, Hidetoshi Mori, Irina R. Matei, Kimberley J. Evason, Hélène Brazier, Dena Almeida, et al. 2013. 'The Perivascular Niche Regulates Breast Tumour Dormancy'. *Nature Cell Biology* 15 (7): 807–17. https://doi.org/10.1038/ncb2767.

Gilligan, Katie E., and Róisín M. Dwyer. 2020. 'Extracellular Vesicles for Cancer Therapy: Impact of Host Immune Response'. *Cells* 9 (1): 224. https://doi.org/10.3390/cells9010224.

Gimbrone, Michael A., Stephen B. Leapman, Ramzi S. Cotran, and Judah Folkman. 1972. 'Tumor Dormancy in Vivo by Prevention of Neovascularization'. *Journal of Experimental Medicine* 136 (2): 261–76. https://doi.org/10.1084/jem.136.2.261.

Giusti, Ilaria, Marianna Di Francesco, Sandra D'Ascenzo, Maria Grazia Palmerini, Guido Macchiarelli, Gaspare Carta, and Vincenza Dolo. 2018. 'Ovarian Cancer-Derived Extracellular Vesicles Affect Normal Human Fibroblast Behavior'. *Cancer Biology and Therapy* 19 (8): 722–34. https://doi.org/10.1080/15384047.2018.1451286.

Godoy, Patricio, Wolfgang Schmidt-Heck, Birte Hellwig, Patrick Nell, David Feuerborn, Jörg Rahnenführer, Kathrin Kattler, Jörn Walter, Nils Blüthgen, and Jan G. Hengstler. 2018. 'Assessment of Stem Cell Differentiation Based on Genome-Wide Expression Profiles'. *Philosophical Transactions of the Royal Society B: Biological Sciences*. Royal Society Publishing. https://doi.org/10.1098/rstb.2017.0221.

Gomis, Roger R., and Sylwia Gawrzak. 2017. 'Tumor Cell Dormancy'. *Molecular Oncology* 11 (1): 62–78. https://doi.org/10.1016/j.molonc.2016.09.009.

Gong, Xue, Chao Lin, Jian Cheng, Jiansheng Su, Hang Zhao, Tianlin Liu, Xuejun Wen, and Peng Zhao. 2015. 'Generation of Multicellular Tumor Spheroids with Microwell-Based Agarose Scaffolds for Drug Testing'. *PLoS ONE* 10 (6). https://doi.org/10.1371/journal.pone.0130348.

Gonzalez, Hugo, Catharina Hagerling, and Zena Werb. 2018. 'Roles of the Immune System in Cancer: From Tumor Initiation to Metastatic Progression'. *Genes and Development* 32 (19–20): 1267–84. https://doi.org/10.1101/GAD.314617.118.

Graham, Nicola, and Bin Zhi Qian. 2018. 'Mesenchymal Stromal Cells: Emerging Roles in Bone Metastasis'. *International Journal of Molecular Sciences* 19 (4). https://doi.org/10.3390/ijms19041121.

Grange, Cristina, Marta Tapparo, Federica Collino, Loriana Vitillo, Christian Damasco, Maria Chiara Deregibus, Ciro Tetta, Benedetta Bussolati, and Giovanni Camussi. 2011. 'Microvesicles Released from Human Renal Cancer Stem Cells Stimulate Angiogenesis and Formation of Lung Premetastatic

Niche'. *Cancer Research* 71 (15): 5346–56. https://doi.org/10.1158/0008-5472.CAN-11-0241.

Green, Toni M., Mary L. Alpaugh, Sanford H. Barsky, Germana Rappa, and Aurelio Lorico. 2015. 'Breast Cancer-Derived Extracellular Vesicles: Characterization and Contribution to the Metastatic Phenotype'. *BioMed Research International* 2015. https://doi.org/10.1155/2015/634865.

Guan, Xiaoying, Xiaoli Guan, Chi Dong, and Zuoyi Jiao. 2020. 'Rho GTPases and Related Signaling Complexes in Cell Migration and Invasion'. *Experimental Cell Research* 388 (1): 447–57. https://doi.org/10.1016/j.yexcr.2020.111824.

Gunti, Sreenivasulu, Austin T.K. Hoke, Kenny P. Vu, and Nyall R. London. 2021. 'Organoid and Spheroid Tumor Models: Techniques and Applications'. *Cancers*. MDPI AG. https://doi.org/10.3390/cancers13040874.

Hadjidakis, Dimitrios J., and Ioannis I. Androulakis. 2006. 'Bone Remodeling'. *Annals of the New York Academy of Sciences* 1092: 385–96. https://doi.org/10.1196/annals.1365.035.

Han, Se Jik, Sangwoo Kwon, and Kyung Sook Kim. 2021. 'Challenges of Applying Multicellular Tumor Spheroids in Preclinical Phase'. *Cancer Cell International*. BioMed Central Ltd. https://doi.org/10.1186/s12935-021-01853-8.

Hankins, Hannah M., Ryan D. Baldridge, Peng Xu, and Todd R. Graham. 2015. 'Role of Flippases, Scramblases and Transfer Proteins in Phosphatidylserine Subcellular Distribution'. *Traffic* 16 (1): 35–47. https://doi.org/10.1111/tra.12233.

Hanoun, Maher, Maria Maryanovich, Anna Arnal-Estapé, and Paul S. Frenette. 2015. 'Neural Regulation of Hematopoiesis, Inflammation, and Cancer'. *Neuron*. Cell Press. https://doi.org/10.1016/j.neuron.2015.01.026.

Hanson, Phyllis I., and Anil Cashikar. 2012. 'Multivesicular Body Morphogenesis'. *Annual Review of Cell and Developmental Biology* 28 (1): 337–62. https://doi.org/10.1146/annurev-cellbio-092910-154152.

Harding, C., J. Heuser, and P. Stahl. 1983. 'Receptor-Mediated Endocytosis of Transferrin and Recycling of the Transferrin Receptor in Rat Reticulocytes.' *The Journal of Cell Biology* 97 (2): 329–39. https://doi.org/10.1083/jcb.97.2.329.

Heiden, Matthew G. Vander. 2011. 'Targeting Cancer Metabolism: A Therapeutic Window Opens'. *Nature Reviews Drug Discovery*. https://doi.org/10.1038/nrd3504.

Heiden, Matthew G.Vander, Lewis C. Cantley, and Craig B. Thompson. 2009. 'Understanding the Warburg Effect: The Metabolic Requirements of Cell Proliferation'. *Science*. https://doi.org/10.1126/science.1160809.

Henderson, Brian, Sean Nair, Jaqueline Pallas, and Mark A. Williams. 2011. 'Fibronectin: A Multidomain Host Adhesin Targeted by Bacterial Fibronectin-Binding Proteins'. *FEMS Microbiology Reviews* 35 (1): 147–200. https://doi.org/10.1111/j.1574-6976.2010.00243.x.

Hernández-Barranco, Alberto, Laura Nogués, and Héctor Peinado. 2021. 'Could Extracellular Vesicles Contribute to Generation or Awakening of "Sleepy" Metastatic Niches?' *Frontiers in Cell and Developmental Biology*. Frontiers Media S.A. https://doi.org/10.3389/fcell.2021.625221.

Hsu, Chieh, Yuichi Morohashi, Shin Ichiro Yoshimura, Natalia Manrique-Hoyos, Sang Yong Jung, Marcel A. Lauterbach, Mostafa Bakhti, et al. 2010. 'Regulation of Exosome Secretion by Rab35 and Its GTPase-Activating

Proteins TBC1D10A-C'. *Journal of Cell Biology* 189 (2): 223–32. https://doi.org/10.1083/jcb.200911018.

Hu, Fen, Xiangzhi Meng, Qi Tong, Lin Liang, Rong Xiang, Tianhui Zhu, and Shuang Yang. 2013. 'BMP-6 Inhibits Cell Proliferation by Targeting MicroRNA-192 in Breast Cancer'. *Biochimica et Biophysica Acta - Molecular Basis of Disease* 1832 (12): 2379–90. https://doi.org/10.1016/j.bbadis.2013.08.011.

Hu, Lifang, Chong Yin, Fan Zhao, Arshad Ali, Jianhua Ma, and Airong Qian. 2018. 'Mesenchymal Stem Cells: Cell Fate Decision to Osteoblast or Adipocyte and Application in Osteoporosis Treatment'. *International Journal of Molecular Sciences* 19 (2). https://doi.org/10.3390/ijms19020360.

Huang, Peide, Anan Chen, Weiyi He, Zhen Li, Guanglin Zhang, Zhong Liu, Ge Liu, Xueting Liu, Shuilian He, and Gang Xiao. 2017. 'BMP-2 Induces EMT and Breast Cancer Stemness through Rb and CD44'. *Nature Publishing Group*, no. March. https://doi.org/10.1038/cddiscovery.2017.39.

Hüsemann, Yves, Jochen B. Geigl, Falk Schubert, Piero Musiani, Manfred Meyer, Elke Burghart, Guido Forni, et al. 2008. 'Systemic Spread Is an Early Step in Breast Cancer'. *Cancer Cell* 13 (1): 58–68. https://doi.org/10.1016/j.ccr.2007.12.003.

Int, Pergamon. 1997. 'MOLECULES IN FOCUS Fibronectin'. *J. Biochem. Cell Biol.* Vol. 29.

Inwald, E. C., M. Klinkhammer-Schalke, F. Hofstädter, F. Zeman, M. Koller, M. Gerstenhauer, and O. Ortmann. 2013. 'Ki-67 Is a Prognostic Parameter in Breast Cancer Patients: Results of a Large Population-Based Cohort of a Cancer Registry'. *Breast Cancer Research and Treatment* 139 (2): 539–52. https://doi.org/10.1007/s10549-013-2560-8.

Isola, Allison L., and Suzie Chen. 2017. 'Extracellular Vesicles: Important Players in Immune Homeostasis'. *Annals of Translational Medicine* 5 (Suppl 1): 2–3. https://doi.org/10.21037/atm.2017.03.76.

Ito, Takeshi, Yoko Hamazaki, Akifumi Takaori-Kondo, and Nagahiro Minato. 2017. 'Bone Marrow Endothelial Cells Induce Immature and Mature B Cell Egress in Response to Erythropoietin'. *CELL STRUCTURE AND FUNCTION*. Vol. 42.

Jabalee, James, Rebecca Towle, and Cathie Garnis. 2018. 'The Role of Extracellular Vesicles in Cancer: Cargo, Function, and Therapeutic Implications'. *Cells* 7 (8): 93. https://doi.org/10.3390/cells7080093.

Jahanban-Esfahlan, Rana, Khaled Seidi, Masoud H. Manjili, Ali Jahanban-Esfahlan, Tahereh Javaheri, and Peyman Zare. 2019. 'Tumor Cell Dormancy: Threat or Opportunity in the Fight against Cancer'. *Cancers* 11 (8): 1–23. https://doi.org/10.3390/cancers11081207.

Jahangiri, Leila, and Tala Ishola. 2022. 'Dormancy in Breast Cancer, the Role of Autophagy, LncRNAs, MiRNAs and Exosomes'. *International Journal of Molecular Sciences*. MDPI. https://doi.org/10.3390/ijms23095271.

Jahn, Reinhard, and Richard H. Scheller. 2006. 'SNAREs - Engines for Membrane Fusion'. *Nature Reviews Molecular Cell Biology* 7 (9): 631–43. https://doi.org/10.1038/nrm2002.

Johnson, Helen E., David Broadhurst, Royston Goodacre, and Aileen R. Smith. 2003. 'Metabolic Fingerprinting of Salt-Stressed Tomatoes'. *Phytochemistry* 62 (6): 919–28. https://doi.org/10.1016/S0031-9422(02)00722-7.

Johnstone, R. M., M. Adam, J. R. Hammond, L. Orr, and C. Turbide. 1987. 'Vesicle Formation during Reticulocyte Maturation. Association of Plasma Membrane Activities with Released Vesicles (Exosomes).' *Journal of Biological Chemistry* 262 (19): 9412–20.

Jóźwiak, Paweł, Ewa Forma, Magdalena Bryś, and Anna Krześlak. 2014. 'O-GlcNAcylation and Metabolic Reprograming in Cancer'. *Frontiers in Endocrinology*. Frontiers Media S.A. https://doi.org/10.3389/fendo.2014.00145.

Justus, Calvin R., Edward J. Sanderlin, and Li V. Yang. 2015. 'Molecular Connections between Cancer Cell Metabolism and the Tumor Microenvironment'. *International Journal of Molecular Sciences*. MDPI AG. https://doi.org/10.3390/ijms160511055.

Kadler, Karl E., Adele Hill, and Elizabeth G. Canty-Laird. 2008. 'Collagen Fibrillogenesis: Fibronectin, Integrins, and Minor Collagens as Organizers and Nucleators'. *Current Opinion in Cell Biology*. https://doi.org/10.1016/j.ceb.2008.06.008.

Kajimoto, Taketoshi, Taro Okada, Satoshi Miya, Lifang Zhang, and Shun Ichi Nakamura. 2013. 'Ongoing Activation of Sphingosine 1-Phosphate Receptors Mediates Maturation of Exosomal Multivesicular Endosomes'. *Nature Communications* 4. https://doi.org/10.1038/ncomms3712.

Kapałczyńska, Marta, Tomasz Kolenda, Weronika Przybyła, Maria Zajączkowska, Anna Teresiak, Violetta Filas, Matthew Ibbs, Renata Bliźniak, Łukasz Łuczewski, and Katarzyna Lamperska. 2018. '2D and 3D Cell Cultures – a Comparison of Different Types of Cancer Cell Cultures'. *Archives of Medical Science* 14 (4): 910–19. https://doi.org/10.5114/aoms.2016.63743.

Keselowsky, Benjamin G, David M Collard, and Andrés J García. 2003. 'Surface Chemistry Modulates Fibronectin Conformation and Directs Integrin Binding and Specificity to Control Cell Adhesion'.

Khamis, Zahraa I., Ziad J. Sahab, and Qing-Xiang Amy Sang. 2012. 'Active Roles of Tumor Stroma in Breast Cancer Metastasis'. *International Journal of Breast Cancer* 2012: 1–10. https://doi.org/10.1155/2012/574025.

Khandare, Jayant, and Tamara Minko. 2006. 'Polymer-Drug Conjugates: Progress in Polymeric Prodrugs'. *Progress in Polymer Science (Oxford)*. https://doi.org/10.1016/j.progpolymsci.2005.09.004.

Kim, Kwang-Soo, Ji-In Park, Nuri Oh, Hyeon-Ju Cho, Ji-Hoon Park, and Kyung-Soon Park. 2019. 'ELK3 Expressed in Lymphatic Endothelial Cells Promotes Breast Cancer Progression and Metastasis through Exosomal MiRNAs'. *Scientific Reports* 9 (1): 8418. https://doi.org/10.1038/s41598-019-44828-6.

Konoshenko, Maria Yu, Evgeniy A. Lekchnov, Alexander V. Vlassov, and Pavel P. Laktionov. 2018. 'Isolation of Extracellular Vesicles: General Methodologies and Latest Trends'. *BioMed Research International* 2018. https://doi.org/10.1155/2018/8545347.

Krüger-Genge, Anne, Anna Blocki, Ralf Peter Franke, and Friedrich Jung. 2019. 'Vascular Endothelial Cell Biology: An Update'. *International Journal of Molecular Sciences*. MDPI AG. https://doi.org/10.3390/ijms20184411.

Lane, Steven W., David A. Williams, and Fiona M. Watt. 2014. 'Modulating the Stem Cell Niche for Tissue Regeneration'. *Nature Biotechnology* 32 (8): 795–803. https://doi.org/10.1038/nbt.2978.

Langley, Robert R., and Isaiah J. Fidler. 2007. 'Tumor Cell-Organ Microenvironment Interactions in the Pathogenesis of Cancer Metastasis'. *Endocrine Reviews* 28 (3): 297–321. https://doi.org/10.1210/er.2006-0027.

Lawson, Michelle A., Michelle M. McDonald, Natasa Kovacic, Weng Hua Khoo, Rachael L. Terry, Jenny Down, Warren Kaplan, et al. 2015. 'Osteoclasts Control Reactivation of Dormant Myeloma Cells by Remodelling the Endosteal Niche'. *Nature Communications* 6 (May): 1–15. https://doi.org/10.1038/ncomms9983.

Lázaro-Ibáñez, Elisa, Cecilia Lässer, Ganesh Vilas Shelke, Rossella Crescitelli, Su Chul Jang, Aleksander Cvjetkovic, Anaís García-Rodríguez, and Jan Lötvall. 2019. 'DNA Analysis of Low- and High-Density Fractions Defines Heterogeneous Subpopulations of Small Extracellular Vesicles Based on Their DNA Cargo and Topology'. *Journal of Extracellular Vesicles* 8 (1). https://doi.org/10.1080/20013078.2019.1656993.

Lebelo, Maphuti T., Anna M. Joubert, and Michelle H. Visagie. 2019. 'Warburg Effect and Its Role in Tumourigenesis'. *Archives of Pharmacal Research*. Pharmaceutical Society of Korea. https://doi.org/10.1007/s12272-019-01185-2.

Lee, Chanbin, Minju Kim, Jinsol Han, Myunghee Yoon, and Youngmi Jung. 2021. 'Mesenchymal Stem Cells Influence Activation of Hepatic Stellate Cells, and Constitute a Promising Therapy for Liver Fibrosis'. *Biomedicines*. MDPI. https://doi.org/10.3390/biomedicines9111598.

Lee, Hyuk, Hongsuk Park, Hyeong Sup Yu, Kun Na, Kyung Taek Oh, and Eun Seong Lee. 2019. 'Dendritic Cell-Targeted Ph-Responsive Extracellular Vesicles for Anticancer Vaccination'. *Pharmaceutics* 11 (2): 1–13. https://doi.org/10.3390/pharmaceutics11020054.

Leiss, Michael, Karsten Beckmann, Amparo Girós, Mercedes Costell, and Reinhard Fässler. 2008. 'The Role of Integrin Binding Sites in Fibronectin Matrix Assembly in Vivo'. *Current Opinion in Cell Biology*. https://doi.org/10.1016/j.ceb.2008.06.001.

Lenglet, Aurélie, Sophie Liabeuf, Sandra Bodeau, Loïc Louvet, Aurélien Mary, Agnès Boullier, Anne Sophie Lemaire-Hurtel, et al. 2016. 'N-Methyl-2-Pyridone-5-Carboxamide (2PY) — Major Metabolite of Nicotinamide: An Update on an Old Uremic Toxin'. *Toxins*. MDPI AG. https://doi.org/10.3390/toxins8110339.

Lerouge, S., J. P. Decruppe, and C. Humbert. 1998. 'Shear Banding in a Micellar Solution under Transient Flow'. *Physical Review Letters* 81 (24): 5457–60. https://doi.org/10.1103/PhysRevLett.81.5457.

Leslie-Barbick, Julia E., Jennifer E. Saik, Daniel J. Gould, Mary E. Dickinson, and Jennifer L. West. 2011. 'The Promotion of Microvasculature Formation in Poly(Ethylene Glycol) Diacrylate Hydrogels by an Immobilized VEGF-Mimetic Peptide'. *Biomaterials* 32 (25): 5782–89. https://doi.org/10.1016/j.biomaterials.2011.04.060.

Li, Jiajing, Yan Meng, Xiaolin Wu, and Yuxin Sun. 2020. 'Polyamines and Related Signaling Pathways in Cancer'. *Cancer Cell International*. BioMed Central Ltd. https://doi.org/10.1186/s12935-020-01545-9.

Li, Lian Tao, Guan Jiang, Qian Chen, and Jun Nian Zheng. 2015. 'Predic Ki67 Is a Promising Molecular Target in the Diagnosis of Cancer (Review)'. *Molecular Medicine Reports*. Spandidos Publications. https://doi.org/10.3892/mmr.2014.2914.

Li, Shuling, Yi Peng, Eric D. Weinhandl, Anne H. Blaes, Karynsa Cetin, Victoria M. Chia, Scott Stryker, Joseph J. Pinzone, John F. Acquavella, and Thomas J. Arneson. 2012. 'Estimated Number of Prevalent Cases of Metastatic Bone Disease in the US Adult Population'. *Clinical Epidemiology* 4 (1): 87–93. https://doi.org/10.2147/CLEP.S28339.

Liberti, Maria V., and Jason W. Locasale. 2016. 'The Warburg Effect: How Does It Benefit Cancer Cells?' *Trends in Biochemical Sciences*. Elsevier Ltd. https://doi.org/10.1016/j.tibs.2015.12.001.

Liu, Yewei, Ting Yin, Yuanbo Feng, Marlein Miranda Cona, Gang Huang, Jianjun Liu, Shaoli Song, et al. 2015. 'Mammalian Models of Chemically Induced

Primary Malignancies Exploitable for Imaging-Based Preclinical Theragnostic Research.' *Quantitative Imaging in Medicine and Surgery* 5 (5): 708–70829. https://doi.org/10.3978/j.issn.2223-4292.2015.06.01.

Liu, Yijun, and Teng Ma. 2015. 'Metabolic Regulation of Mesenchymal Stem Cell in Expansion and Therapeutic Application'. *Biotechnology Progress* 31 (2): 468–81. https://doi.org/10.1002/btpr.2034.

Llopis-Hernández, Virginia, Marco Cantini, Cristina González-García, Zhe A. Cheng, Jingli Yang, Penelope M. Tsimbouri, Andrés J. García, Matthew J. Dalby, and Manuel Salmerón-Sánchez. 2016. 'Material-Driven Fibronectin Assembly for High-Efficiency Presentation of Growth Factors'. *Science Advances* 2 (8): 1–11. https://doi.org/10.1126/sciadv.1600188.

López de Andrés, Julia, Carmen Griñán-Lisón, Gema Jiménez, and Juan Antonio Marchal. 2020. 'Cancer Stem Cell Secretome in the Tumor Microenvironment: A Key Point for an Effective Personalized Cancer Treatment'. *Journal of Hematology and Oncology*. BioMed Central Ltd. https://doi.org/10.1186/s13045-020-00966-3.

Lunt, Sophia Y., and Matthew G. Vander Heiden. 2011a. 'Aerobic Glycolysis: Meeting the Metabolic Requirements of Cell Proliferation'. *Annual Review of Cell and Developmental Biology* 27: 441–64. https://doi.org/10.1146/annurev-cellbio-092910-154237.

———. 2011b. 'Aerobic Glycolysis: Meeting the Metabolic Requirements of Cell Proliferation'. *Annual Review of Cell and Developmental Biology* 27: 441–64. https://doi.org/10.1146/annurev-cellbio-092910-154237.

———. 2011c. 'Aerobic Glycolysis: Meeting the Metabolic Requirements of Cell Proliferation'. *Annual Review of Cell and Developmental Biology* 27: 441–64. https://doi.org/10.1146/annurev-cellbio-092910-154237.

Lv, Feng Juan, Rocky S. Tuan, Kenneth M.C. Cheung, and Victor Y.L. Leung. 2014. 'Concise Review: The Surface Markers and Identity of Human Mesenchymal Stem Cells'. *Stem Cells*. Wiley-Blackwell. https://doi.org/10.1002/stem.1681.

Machlus, Kellie R., and Joseph E. Italiano. 2013. 'The Incredible Journey: From Megakaryocyte Development to Platelet Formation'. *Journal of Cell Biology*. https://doi.org/10.1083/jcb.201304054.

Malhotra, Vivek. 2013. 'Unconventional Protein Secretion: An Evolving Mechanism'. *EMBO Journal*. https://doi.org/10.1038/emboj.2013.104.

Manuel Iglesias, Juan, Izaskun Beloqui, Francisco Garcia-Garcia, Olatz Leis, Alejandro Vazquez-Martin, Arrate Eguiara, Silvia Cufi, et al. 2013. 'Mammosphere Formation in Breast Carcinoma Cell Lines Depends upon Expression of E-Cadherin'. *PLoS ONE* 8 (10). https://doi.org/10.1371/journal.pone.0077281.

Mao, Yong, and Jean E. Schwarzbauer. 2005. 'Fibronectin Fibrillogenesis, a Cell-Mediated Matrix Assembly Process'. *Matrix Biology*. Elsevier. https://doi.org/10.1016/j.matbio.2005.06.008.

Mariotto, Angela B., Ruth Etzioni, Marc Hurlbert, Lynne Penberthy, and Musa Mayer. 2017. 'Estimation of the Number of Women Living with Metastatic Breast Cancer in the United States'. *Cancer Epidemiology Biomarkers and Prevention* 26 (6): 809–15. https://doi.org/10.1158/1055-9965.EPI-16-0889.

Martin, T. John. 2014. 'Bone Biology and Anabolic Therapies for Bone: Current Status and Future Prospects'. *Journal of Bone Metabolism* 21 (1): 8. https://doi.org/10.11005/jbm.2014.21.1.8.

Martino, Mikaël M., and Jeffrey A. Hubbell. 2010. 'The 12th–14th Type III Repeats of Fibronectin Function as a Highly Promiscuous Growth Factor-

Binding Domain'. *The FASEB Journal* 24 (12): 4711–21. https://doi.org/10.1096/fj.09-151282.
Massagué, Joan, and Anna C. Obenauf. 2016. 'Metastatic Colonization by Circulating Tumour Cells'. *Nature*. Nature Publishing Group. https://doi.org/10.1038/nature17038.
McNeil, Paul L., and Richard A. Steinhardt. 1997. 'Loss, Restoration, and Maintenance of Plasma Membrane Integrity'. *Journal of Cell Biology* 137 (1): 1–4. https://doi.org/10.1083/jcb.137.1.1.
Mehta, Geeta, Amy Y. Hsiao, Marylou Ingram, Gary D. Luker, and Shuichi Takayama. 2012. 'Opportunities and Challenges for Use of Tumor Spheroids as Models to Test Drug Delivery and Efficacy'. *Journal of Controlled Release* 164 (2): 192–204. https://doi.org/10.1016/j.jconrel.2012.04.045.
Méndez-Ferrer, Simón, and Claire Fielding. 2020. 'Neuronal Regulation of Bone Marrow Stem Cell Niches'. *F1000Research*. F1000 Research Ltd. https://doi.org/10.12688/f1000research.22554.1.
Metzger, Wolfgang, Daniela Sossong, Annick Bächle, Norbert Pütz, Gunther Wennemuth, Tim Pohlemann, and Martin Oberringer. 2011. 'The Liquid Overlay Technique Is the Key to Formation of Co-Culture Spheroids Consisting of Primary Osteoblasts, Fibroblasts and Endothelial Cells'. *Cytotherapy* 13 (8): 1000–1012. https://doi.org/10.3109/14653249.2011.583233.
Miglietta, F., M. Bottosso, G. Griguolo, M. V. Dieci, and V. Guarneri. 2022. 'Major Advancements in Metastatic Breast Cancer Treatment: When Expanding Options Means Prolonging Survival'. *ESMO Open*. Elsevier B.V. https://doi.org/10.1016/j.esmoop.2022.100409.
Miller, Donald M., Shelia D. Thomas, Ashraful Islam, David Muench, and Kara Sedoris. 2012. 'C-Myc and Cancer Metabolism'. *Clinical Cancer Research*. https://doi.org/10.1158/1078-0432.CCR-12-0977.
Miller, Iain, Mingwei Min, Chen Yang, Chengzhe Tian, Sara Gookin, Dylan Carter, and Sabrina L. Spencer. 2018. 'Ki67 Is a Graded Rather than a Binary Marker of Proliferation versus Quiescence'. *Cell Reports* 24 (5): 1105-1112.e5. https://doi.org/10.1016/j.celrep.2018.06.110.
Moreira, Joana, A. Catarina Vale, and Natália M. Alves. 2021. 'Spin-Coated Freestanding Films for Biomedical Applications'. *Journal of Materials Chemistry B*. Royal Society of Chemistry. https://doi.org/10.1039/d1tb00233c.
Morrison, Sean J., and David T. Scadden. 2014. 'The Bone Marrow Niche for Haematopoietic Stem Cells'. *Nature*. https://doi.org/10.1038/nature12984.
Morrissey, Meghan, Elliott Hagedorn, and David Sherwood. 2013. 'Cell Invasion through Basement Membrane: The Netrin Receptor DCC Guides the Way'. *Worm* 2 (3): e26169. https://doi.org/10.4161/worm.26169.
Mukaida, Naofumi, Di Zhang, and So Ichiro Sasaki. 2020. 'Emergence of Cancer-Associated Fibroblasts as an Indispensable Cellular Player in Bone Metastasis Process'. *Cancers*. MDPI AG. https://doi.org/10.3390/cancers12102896.
Mulcahy, Laura Ann, Ryan Charles Pink, and David Raul Francisco Carter. 2014. 'Routes and Mechanisms of Extracellular Vesicle Uptake'. *Journal of Extracellular Vesicles* 3 (1). https://doi.org/10.3402/jev.v3.24641.
Muralidharan-Chari, Vandhana, James Clancy, Carolyn Plou, Maryse Romao, Philippe Chavrier, Graca Raposo, and Crislyn D'Souza-Schorey. 2009. 'ARF6-Regulated Shedding of Tumor Cell-Derived Plasma Membrane Microvesicles'. *Current Biology* 19 (22): 1875–85. https://doi.org/10.1016/j.cub.2009.09.059.

Muralidharan-Chari, Vandhana, James W. Clancy, Alanna Sedgwick, and Crislyn D'Souza-Schorey. 2010. 'Microvesicles: Mediators of Extracellular Communication during Cancer Progression'. *Journal of Cell Science* 123 (10): 1603–11. https://doi.org/10.1242/jcs.064386.

Nakazawa, Michael S., Brian Keith, and M. Celeste Simon. 2016. 'Oxygen Availability and Metabolic Adaptations'. *Nature Reviews Cancer*. Nature Publishing Group. https://doi.org/10.1038/nrc.2016.84.

Nath, Sritama, and Gayathri R. Devi. 2016. 'Three-Dimensional Culture Systems in Cancer Research: Focus on Tumor Spheroid Model'. *Pharmacology and Therapeutics*. Elsevier Inc. https://doi.org/10.1016/j.pharmthera.2016.03.013.

Neophytou, Christiana M., Theodora Christina Kyriakou, and Panagiotis Papageorgis. 2019. 'Mechanisms of Metastatic Tumor Dormancy and Implications for Cancer Therapy'. *International Journal of Molecular Sciences*. MDPI AG. https://doi.org/10.3390/ijms20246158.

Neve, Anna, Addolorata Corrado, and Francesco Paolo Cantatore. 2011. 'Osteoblast Physiology in Normal and Pathological Conditions'. *Cell and Tissue Research* 343 (2): 289–302. https://doi.org/10.1007/s00441-010-1086-1.

Niel, Guillaume van, Ptissam Bergam, Aurelie Di Cicco, Ilse Hurbain, Alessandra Lo Cicero, Florent Dingli, Roberta Palmulli, et al. 2015. 'Apolipoprotein E Regulates Amyloid Formation within Endosomes of Pigment Cells'. *Cell Reports* 13 (1): 43–51. https://doi.org/10.1016/j.celrep.2015.08.057.

Niel, Guillaume van, Stéphanie Charrin, Sabrina Simoes, Maryse Romao, Leila Rochin, Paul Saftig, Michael S. Marks, Eric Rubinstein, and Graça Raposo. 2011. 'The Tetraspanin CD63 Regulates ESCRT-Independent and -Dependent Endosomal Sorting during Melanogenesis'. *Developmental Cell* 21 (4): 708–21. https://doi.org/10.1016/j.devcel.2011.08.019.

Niel, Guillaume Van, Gisela D'Angelo, and Graça Raposo. 2018. 'Shedding Light on the Cell Biology of Extracellular Vesicles'. *Nature Reviews Molecular Cell Biology* 19 (4): 213–28. https://doi.org/10.1038/nrm.2017.125.

O'Loghlen, Ana. 2018. 'Role for Extracellular Vesicles in the Tumour Microenvironment'. *Philosophical Transactions of the Royal Society B: Biological Sciences* 373 (1737). https://doi.org/10.1098/rstb.2016.0488.

Ono, Makiko, Nobuyoshi Kosaka, Naoomi Tominaga, Yusuke Yoshioka, Fumitaka Takeshita, Ryou-u Takahashi, Masayuki Yoshida, Hitoshi Tsuda, Kenji Tamura, and Takahiro Ochiya. 2014. 'Exosomes from Bone Marrow Mesenchymal Stem Cells Contain a MicroRNA That Promotes Dormancy in Metastatic Breast Cancer Cells' 7 (332).

Ostrowski, Matias, Nuno B. Carmo, Sophie Krumeich, Isabelle Fanget, Graça Raposo, Ariel Savina, Catarina F. Moita, et al. 2010. 'Rab27a and Rab27b Control Different Steps of the Exosome Secretion Pathway'. *Nature Cell Biology* 12 (1): 19–30. https://doi.org/10.1038/ncb2000.

Otto Warburg, BY, Franz Wind, and N Negelein. n.d. 'THE METABOLISM OF TUMORS IN THE BODY'.

———. n.d. 'THE METABOLISM OF TUMORS IN THE BODY'.

Paggetti, Jerome, Franziska Haderk, Martina Seiffert, Bassam Janji, Ute Distler, Wim Ammerlaan, Yeoun Jin Kim, et al. 2015. 'Exosomes Released by Chronic Lymphocytic Leukemia Cells Induce the Transition of Stromal Cells into Cancer-Associated Fibroblasts'. *Blood* 126 (9): 1106–17. https://doi.org/10.1182/blood-2014-12-618025.

Pakdel, Mehrshad. 2014. ‘The Dynamic Assembly and Disassembly of the ESCRT Machinery’, 1–35.

Pankov, Roumen, and Kenneth M. Yamada. 2002. ‘Fibronectin at a Glance’. *Journal of Cell Science* 115 (20): 3861–63. https://doi.org/10.1242/jcs.00059.

Parfitt, A. M. 2002. ‘Targeted and Nontargeted Bone Remodeling: Relationship to Basic Multicellular Unit Origination and Progression’. *Bone* 30 (1): 5–7. https://doi.org/10.1016/S8756-3282(01)00642-1.

Patil, M. D., J. Bhaumik, S. Babykutty, U. C. Banerjee, and D. Fukumura. 2016. ‘Arginine Dependence of Tumor Cells: Targeting a Chink in Cancer’s Armor’. *Oncogene*. Nature Publishing Group. https://doi.org/10.1038/onc.2016.37.

Pedersen, Rikke Nørgaard, Buket Öztürk Esen, Lene Mellemkjær, Peer Christiansen, Bent Ejlertsen, Timothy Lee Lash, Mette Nørgaard, and Deirdre Cronin-Fenton. 2022. ‘The Incidence of Breast Cancer Recurrence 10-32 Years after Primary Diagnosis’. *Journal of the National Cancer Institute* 114 (3): 391–99. https://doi.org/10.1093/jnci/djab202.

Peng, Jin, Yumiko Yoshioka, Masaki Mandai, Noriomi Matsumura, Tsukasa Baba, Ken Yamaguchi, Junzo Hamanishi, et al. 2016. ‘The BMP Signaling Pathway Leads to Enhanced Proliferation in Serous Ovarian Cancer-A Potential Therapeutic Target’. *Molecular Carcinogenesis* 55 (4): 335–45. https://doi.org/10.1002/mc.22283.

Pfrieger, Frank W., and Nicolas Vitale. 2018. ‘Thematic Review Series: Exosomes and Microvesicles: Lipids as Key Components of Their Biogenesis and Functions Cholesterol and the Journey of Extracellular Vesicles’. *Journal of Lipid Research* 59 (12): 2255–61. https://doi.org/10.1194/jlr.R084210.

Phan, Tri Giang, and Peter I. Croucher. 2020. ‘The Dormant Cancer Cell Life Cycle’. *Nature Reviews Cancer* 20 (7): 398–411. https://doi.org/10.1038/s41568-020-0263-0.

Pinto, Bárbara, Ana C. Henriques, Patrícia M.A. Silva, and Hassan Bousbaa. 2020. ‘Three-Dimensional Spheroids as in Vitro Preclinical Models for Cancer Research’. *Pharmaceutics*. MDPI AG. https://doi.org/10.3390/pharmaceutics12121186.

Piper, Robert C., and David J. Katzmann. 2007. ‘Biogenesis and Function of Multivesicular Bodies’. *Annual Review of Cell and Developmental Biology* 23 (1): 519–47. https://doi.org/10.1146/annurev.cellbio.23.090506.123319.

Pisani, Paola, Maria Daniela Renna, Francesco Conversano, Ernesto Casciaro, Marco Di Paola, Eugenio Quarta, Maurizio Muratore, and Sergio Casciaro. 2016. ‘Major Osteoporotic Fragility Fractures: Risk Factor Updates and Societal Impact’. *World Journal of Orthopedics*. Baishideng Publishing Group Co. https://doi.org/10.5312/wjo.v7.i3.171.

Poi-I-S, Jennifer R, and D Campbell. 1996. ‘Structure and Function of Fibronectin Modules’. *Matrix Biology*. Vol. 15.

Pradhan, Shantanu, and John H. Slater. 2019. ‘Tunable Hydrogels for Controlling Phenotypic Cancer Cell States to Model Breast Cancer Dormancy and Reactivation’. *Biomaterials* 215 (January): 119177. https://doi.org/10.1016/j.biomaterials.2019.04.022.

Pranzini, Erica, Giovanni Raugei, and Maria Letizia Taddei. 2022. ‘Metabolic Features of Tumor Dormancy: Possible Therapeutic Strategies’. *Cancers* 14 (3): 547. https://doi.org/10.3390/cancers14030547.

Price, Trevor T., Monika L. Burness, Ayelet Sivan, Matthew J. Warner, Renee Cheng, Clara H. Lee, Lindsey Olivere, et al. 2016. ‘Dormant Breast Cancer Micrometastases Reside in Specific Bone Marrow Niches That Regulate Their

Transit to and from Bone'. *Science Translational Medicine* 8 (340). https://doi.org/10.1126/scitranslmed.aad4059.

Pulze, Laura, Terenzio Congiu, Tiziana A.L. Brevini, Annalisa Grimaldi, Gianluca Tettamanti, Paola D'antona, Nicolò Baranzini, Francesco Acquati, Federico Ferraro, and Magda de Eguileor. 2020a. 'Mcf7 Spheroid Development: New Insight about Spatio/Temporal Arrangements of TNTS, Amyloid Fibrils, Cell Connections, and Cellular Bridges'. *International Journal of Molecular Sciences* 21 (15): 1–24. https://doi.org/10.3390/ijms21155400.

———. 2020b. 'Mcf7 Spheroid Development: New Insight about Spatio/Temporal Arrangements of TNTS, Amyloid Fibrils, Cell Connections, and Cellular Bridges'. *International Journal of Molecular Sciences* 21 (15): 1–24. https://doi.org/10.3390/ijms21155400.

Qiu, Fuming, Yun Ru Chen, Xiyong Liu, Cheng Ying Chu, Li Jiuan Shen, Jinghong Xu, Shikha Gaur, et al. 2014. 'Cancer: Arginine Starvation Impairs Mitochondrial Respiratory Function in ASS1-Deficient Breast Cancer Cells'. *Science Signaling* 7 (319). https://doi.org/10.1126/scisignal.2004761.

Raghavan, Shreya, Pooja Mehta, Eric N Horst, Maria R Ward, Katelyn R Rowley, and Geeta Mehta. n.d. 'Comparative Analysis of Tumor Spheroid Generation Techniques for Differential in Vitro Drug Toxicity'. www.impactjournals.com/oncotarget/.

Rameshwar, Pranela. 2010. 'Breast Cancer Cell Dormancy in Bone Marrow: Potential Therapeutic Targets within the Marrow Microenvironment'. *Expert Review of Anticancer Therapy*. https://doi.org/10.1586/ERA.10.3.

Raposo, Graça, Hans W. Nijman, Willem Stoorvogel, Richtje Leijendekker, Clifford V. Harding, Cornelis J.M. Melief, and Hans J. Geuze. 1996. 'B Lymphocytes Secrete Antigen-Presenting Vesicles'. *Journal of Experimental Medicine* 183 (3): 1161–72. https://doi.org/10.1084/jem.183.3.1161.

Reed, John C. 2000. 'Mechanisms of Apoptosis'. *The American Journal of Pathology* 157 (5): 1415–30. https://doi.org/10.1016/s0002-9440(10)64779-7.

Reznik, Ed, Augustin Luna, Bülent Arman Aksoy, Eric Minwei Liu, Konnor La, Irina Ostrovnaya, Chad J. Creighton, A. Ari Hakimi, and Chris Sander. 2018. 'A Landscape of Metabolic Variation across Tumor Types'. *Cell Systems* 6 (3): 301-313.e3. https://doi.org/10.1016/j.cels.2017.12.014.

Richards, K. E., A. E. Zeleniak, M. L. Fishel, J. Wu, L. E. Littlepage, and R. Hill. 2017. 'Cancer-Associated Fibroblast Exosomes Regulate Survival and Proliferation of Pancreatic Cancer Cells'. *Oncogene* 36 (13): 1770–78. https://doi.org/10.1038/onc.2016.353.

Rodríguez-Pérez, E., A. Lloret Compañ, M. Monleón Pradas, and C. Martínez-Ramos. 2016. 'Scaffolds of Hyaluronic Acid–Poly(Ethyl Acrylate) Interpenetrating Networks: Characterization and In Vitro Studies'. *Macromolecular Bioscience*, August, 1147–57. https://doi.org/10.1002/mabi.201600028.

Rosenberg, Nahum, Orit Rosenberg, and Michael Soudry. 2012. 'Osteoblasts in Bone Physiology – Mini Review'. *Rambam Maimonides Medical Journal* 3 (2). https://doi.org/10.5041/rmmj.10080.

Rucci, Nadia. 2008. 'Molecular Biology of Bone Biology'. *Clinical Cases in Mineral and Bone Metabolism* 5 (1): 49–56.

Ruijtenberg, Suzan, and Sander van den Heuvel. 2016a. 'Coordinating Cell Proliferation and Differentiation: Antagonism between Cell Cycle Regulators and Cell Type-Specific Gene Expression'. *Cell Cycle*. Taylor and Francis Inc. https://doi.org/10.1080/15384101.2015.1120925.

———. 2016b. ‘Coordinating Cell Proliferation and Differentiation: Antagonism between Cell Cycle Regulators and Cell Type-Specific Gene Expression’. *Cell Cycle*. Taylor and Francis Inc. https://doi.org/10.1080/15384101.2015.1120925.

Sahana, Jayashree, Mohamed Zakaria Nassef, Markus Wehland, Sascha Kopp, Marcus Krüger, Thomas J. Corydon, Manfred Infanger, Johann Bauer, and Daniela Grimm. 2018. ‘Decreased E-Cadherin in MCF7 Human Breast Cancer Cells Forming Multicellular Spheroids Exposed to Simulated Microgravity’. *Proteomics* 18 (13): 1–10. https://doi.org/10.1002/pmic.201800015.

Sakurai, Satoshi, Yasuo Okada, and Izumi Mataga. 2011. ‘Inhibitory Effects of Glycerol on Growth and Invasion of Human Oral Cancer Cell Lines’. *Journal of Hard Tissue Biology* 20 (1): 37–46.

Sandiford, Oleta A., Robert J. Donnelly, Markos H. El-Far, Lisa M. Burgmeyer, Garima Sinha, Sri Harika Pamarthi, Lauren S. Sherman, et al. 2021. ‘Mesenchymal Stem Cell-Secreted Extracellular Vesicles Instruct Stepwise Dedifferentiation of Breast Cancer Cells into Dormancy at the Bone Marrow Perivascular Region’. *Cancer Research* 81 (6): 1567–82. https://doi.org/10.1158/0008-5472.CAN-20-2434.

Savina, Ariel, Marcelo Furlán, Michel Vidal, and Maria I. Colombo. 2003. ‘Exosome Release Is Regulated by a Calcium-Dependent Mechanism in K562 Cells’. *Journal of Biological Chemistry* 278 (22): 20083–90. https://doi.org/10.1074/jbc.M301642200.

Scalzone, Annachiara, Ana M. Ferreira, Chiara Tonda-Turo, Gianluca Ciardelli, Kenny Dalgarno, and Piergiorgio Gentile. 2019. ‘The Interplay between Chondrocyte Spheroids and Mesenchymal Stem Cells Boosts Cartilage Regeneration within a 3D Natural-Based Hydrogel’. *Scientific Reports* 9 (1). https://doi.org/10.1038/s41598-019-51070-7.

Scheel, Christina, and Robert A. Weinberg. 2012. ‘Cancer Stem Cells and Epithelial-Mesenchymal Transition: Concepts and Molecular Links’. *Seminars in Cancer Biology* 22 (5–6): 396–403. https://doi.org/10.1016/j.semcancer.2012.04.001.

Schömel, Nina, Lisa Gruber, Stephanie J. Alexopoulos, Sandra Trautmann, Ellen M. Olzomer, Frances L. Byrne, Kyle L. Hoehn, et al. 2020. ‘UGCG Overexpression Leads to Increased Glycolysis and Increased Oxidative Phosphorylation of Breast Cancer Cells’. *Scientific Reports* 10 (1). https://doi.org/10.1038/s41598-020-65182-y.

Schömel, Nina, Sarah E. Hancock, Lisa Gruber, Ellen M. Olzomer, Frances L. Byrne, Divya Shah, Kyle L. Hoehn, et al. 2019. ‘UGCG Influences Glutamine Metabolism of Breast Cancer Cells’. *Scientific Reports* 9 (1). https://doi.org/10.1038/s41598-019-52169-7.

Scully, Olivia Jane, Boon-huat Bay, George Yip, and Yingnan Yu. 2012. ‘Breast Cancer Metastasis’ 320: 311–20.

Sedgwick, Alanna E., James W. Clancy, M. Olivia Balmert, and Crislyn D’Souza-Schorey. 2015. ‘Extracellular Microvesicles and Invadopodia Mediate Non-Overlapping Modes of Tumor Cell Invasion’. *Scientific Reports* 5 (April): 1–14. https://doi.org/10.1038/srep14748.

Sharma, Shikhar, Theresa K. Kelly, and Peter A. Jones. 2009. ‘Epigenetics in Cancer’. *Carcinogenesis* 31 (1): 27–36. https://doi.org/10.1093/carcin/bgp220.

Shaul, Yoav D., Elizaveta Freinkman, William C. Comb, Jason R. Cantor, Wai Leong Tam, Prathapan Thiru, Dohoon Kim, et al. 2014. ‘Dihydropyrimidine

Accumulation Is Required for the Epithelial-Mesenchymal Transition'. *Cell* 158 (5): 1094–1109. https://doi.org/10.1016/j.cell.2014.07.032.

Shiozawa, Yusuke, Elisabeth A Pedersen, Aaron M Havens, Younghun Jung, Anjali Mishra, Jeena Joseph, Jin Koo Kim, et al. 2011. 'Human Prostate Cancer Metastases Target the Hematopoietic Stem Cell Niche to Establish Footholds in Mouse Bone Marrow'. *The Journal of Clinical Investigation* 121. https://doi.org/10.1172/JCI43414DS1.

Shupp, Alison B., Alexus D. Kolb, Dimpi Mukhopadhyay, and Karen M. Bussard. 2018. 'Cancer Metastases to Bone: Concepts, Mechanisms, and Interactions with Bone Osteoblasts'. *Cancers* 10 (6): 1–37. https://doi.org/10.3390/cancers10060182.

Singh, Mohini, Nicolas Yelle, Chitra Venugopal, and Sheila K. Singh. 2018. 'EMT: Mechanisms and Therapeutic Implications'. *Pharmacology and Therapeutics* 182 (August 2017): 80–94. https://doi.org/10.1016/j.pharmthera.2017.08.009.

Singh, Purva, Cara Carraher, and Jean E. Schwarzbauer. 2010. 'Assembly of Fibronectin Extracellular Matrix'. *Annual Review of Cell and Developmental Biology*. https://doi.org/10.1146/annurev-cellbio-100109-104020.

Sinn, Hans Peter, and Hans Kreipe. 2013. 'A Brief Overview of the WHO Classification of Breast Tumors, 4th Edition, Focusing on Issues and Updates from the 3rd Edition'. *Breast Care* 8 (2): 149–54. https://doi.org/10.1159/000350774.

Smittenaar, C. R., K. A. Petersen, K. Stewart, and N. Moitt. 2016. 'Cancer Incidence and Mortality Projections in the UK until 2035'. *British Journal of Cancer* 115 (9): 1147–55. https://doi.org/10.1038/bjc.2016.304.

Sobecki, Michal, Karim Mrouj, Alain Camasses, Nikolaos Parisis, Emilien Nicolas, David Llè Res, Franç Ois Gerbe, et al. 2016. 'The Cell Proliferation Antigen Ki-67 Organises Heterochromatin'. https://doi.org/10.7554/eLife.13722.001.

Sobhani, A, Aligholi Sobhani, Neda Khanlarkhani, Maryam Baazm, Farzaneh Mohammadzadeh, Atefeh Najafi, Shayesteh Mehdinejadiani, and Fereydoon Sargolzaei Aval. 2017. 'Multipotent Stem Cell and Current Application'. *Acta Med Iran*. Vol. 55.

Song, Pingping, Katarina Trajkovic, Taiji Tsunemi, and Dimitri Krainc. 2016. 'Parkin Modulates Endosomal Organization and Function of the Endo-Lysosomal Pathway'. *Journal of Neuroscience* 36 (8): 2425–37. https://doi.org/10.1523/JNEUROSCI.2569-15.2016.

Song, Young Hye, Christine Warncke, Sung Jin Choi, Siyoung Choi, Aaron E. Chiou, Lu Ling, Han Yuan Liu, et al. 2017. 'Breast Cancer-Derived Extracellular Vesicles Stimulate Myofibroblast Differentiation and pro-Angiogenic Behavior of Adipose Stem Cells'. *Matrix Biology* 60–61: 190–205. https://doi.org/10.1016/j.matbio.2016.11.008.

Sosa, Maria Soledad, Alvaro Avivar-Valderas, Paloma Bragado, Huei Chi Wen, and Julio A. Aguirre-Ghiso. 2011. 'ERK1/2 and P38α/ß Signaling in Tumor Cell Quiescence: Opportunities to Control Dormant Residual Disease'. *Clinical Cancer Research*. https://doi.org/10.1158/1078-0432.CCR-10-2574.

Sosa, Maria Soledad, Falguni Parikh, Alexandre Gaspar Maia, Yeriel Estrada, Almudena Bosch, Paloma Bragado, Esther Ekpin, et al. 2015. 'NR2F1 Controls Tumour Cell Dormancy via SOX9- and RARß-Driven Quiescence Programmes'. *Nature Communications* 6 (January). https://doi.org/10.1038/ncomms7170.

Sosnoski, Donna M., Robert J. Norgard, Cassidy D. Grove, Shelby J. Foster, and Andrea M. Mastro. 2015. 'Dormancy and Growth of Metastatic Breast Cancer Cells in a Bone-like Microenvironment'. *Clinical and Experimental Metastasis* 32 (4): 335–44. https://doi.org/10.1007/s10585-015-9710-9.

Sprott, Mark Robert. 2019. 'Surface Functionalisation of Poly L-Lactic Acid to Control Protein Organisation and Growth Factor Presentation in Tissue Engineering'. http://eleanor.lib.gla.ac.uk/record=b3366163%0Ahttp://theses.gla.ac.uk/74292/1/2019SprottPhD.pdf%0Ahttp://theses.gla.ac.uk/74292/.

Sprott, Mark Robert, Gloria Gallego-Ferrer, Matthew J. Dalby, Manuel Salmerón-Sánchez, and Marco Cantini. 2019. 'Functionalization of PLLA with Polymer Brushes to Trigger the Assembly of Fibronectin into Nanonetworks'. *Advanced Healthcare Materials* 8 (3). https://doi.org/10.1002/adhm.201801469.

Sreedhar, Annapoorna, and Yunfeng Zhao. 2018. 'Dysregulated Metabolic Enzymes and Metabolic Reprogramming in Cancer Cells'. *Biomedical Reports*. Spandidos Publications. https://doi.org/10.3892/br.2017.1022.

Sun, Linchong, Libing Song, Qianfen Wan, Gongwei Wu, Xinghua Li, Yinghui Wang, Jin Wang, et al. 2015. 'CMyc-Mediated Activation of Serine Biosynthesis Pathway Is Critical for Cancer Progression under Nutrient Deprivation Conditions'. *Cell Research* 25 (4): 429–44. https://doi.org/10.1038/cr.2015.33.

Sun, Xiaoming, and Paul D. Kaufman. 2018. 'Ki-67: More than a Proliferation Marker'. *Chromosoma*. Springer Science and Business Media Deutschland GmbH. https://doi.org/10.1007/s00412-018-0659-8.

Sun, Yanan, Xiaoyun Mao, Chuifeng Fan, Chong Liu, Ayao Guo, Shu Guan, Quanxiu Jin, Bo Li, Fan Yao, and Feng Jin. 2014. 'CXCL12-CXCR4 Axis Promotes the Natural Selection of Breast Cancer Cell Metastasis'. *Tumor Biology* 35 (8): 7765–73. https://doi.org/10.1007/s13277-014-1816-1.

Suzuki, Sayuri, Jun Namiki, Shinsuke Shibata, Yumi Mastuzaki, and Hideyuki Okano. 2010. 'The Neural Stem/Progenitor Cell Marker Nestin Is Expressed in Proliferative Endothelial Cells, but Not in Mature Vasculature'. *Journal of Histochemistry and Cytochemistry* 58 (8): 721–30. https://doi.org/10.1369/jhc.2010.955609.

Szade, Krzysztof, Gunsagar S. Gulati, Charles K.F. Chan, Kevin S. Kao, Masanori Miyanishi, Kristopher D. Marjon, Rahul Sinha, Benson M. George, James Y. Chen, and Irving L. Weissman. 2018. 'Where Hematopoietic Stem Cells Live: The Bone Marrow Niche'. *Antioxidants and Redox Signaling*. Mary Ann Liebert Inc. https://doi.org/10.1089/ars.2017.7419.

Takahashi, Hiroki, Takuya Morimoto, Naotake Ogasawara, and Shigehiko Kanaya. 2011. 'AMDORAP: Non-Targeted Metabolic Profiling Based on High-Resolution LC-MS'. *BMC Bioinformatics* 12 (June). https://doi.org/10.1186/1471-2105-12-259.

Théry, Clotilde, Matias Ostrowski, and Elodie Segura. 2009. 'Membrane Vesicles as Conveyors of Immune Responses'. *Nature Reviews Immunology* 9 (8): 581–93. https://doi.org/10.1038/nri2567.

Thissen, H. 2016. *Plasma-Based Surface Modification for the Control of Biointerfacial Interactions. Biosynthetic Polymers for Medical Applications*. Elsevier Ltd. https://doi.org/10.1016/B978-1-78242-105-4.00005-5.

Tjalsma, Harold, Albert Bolhuis, Jan D H Jongbloed, Sierd Bron, Jan Maarten, and Van Dijl. 2000. 'Signal Peptide-Dependent Protein Transport in Bacillus

Subtilis: A Genome-Based Survey of the Secretome'. *MICROBIOLOGY AND MOLECULAR BIOLOGY REVIEWS*. Vol. 64.

Todorova, Dilyana, Stéphanie Simoncini, Romaric Lacroix, Florence Sabatier, and Françoise Dignat-George. 2017. 'Extracellular Vesicles in Angiogenesis'. *Circulation Research* 120 (10): 1658–73. https://doi.org/10.1161/CIRCRESAHA.117.309681.

Trajkovic, K. 2008. 'Ceramide Triggers Budding of Exosome Vesicles into Multivesicular Endosomes (Science (1244))'. *Science* 320 (5873): 179. https://doi.org/10.1126/science.320.5873.179.

Tricarico, Christopher, James Clancy, and Crislyn D'Souza-Schorey. 2017. 'Biology and Biogenesis of Shed Microvesicles'. *Small GTPases* 8 (4): 220–32. https://doi.org/10.1080/21541248.2016.1215283.

Tsai, Hui Hsu Gavin, Che Ming Chang, and Jian Bin Lee. 2014. 'Multi-Step Formation of a Hemifusion Diaphragm for Vesicle Fusion Revealed by All-Atom Molecular Dynamics Simulations'. *Biochimica et Biophysica Acta - Biomembranes* 1838 (6): 1529–35. https://doi.org/10.1016/j.bbamem.2014.01.018.

Tsuzuki, Shunsuke, Sun Hee Park, Matthew R. Eber, Christopher M. Peters, and Yusuke Shiozawa. 2016. 'Skeletal Complications in Cancer Patients with Bone Metastases'. *International Journal of Urology*. Blackwell Publishing. https://doi.org/10.1111/iju.13170.

Umezu, Tomohiro, Hiroko Tadokoro, Kenko Azuma, Seiichiro Yoshizawa, Kazuma Ohyashiki, and Junko H. Ohyashiki. 2014. 'Exosomal MiR-135b Shed from Hypoxic Multiple Myeloma Cells Enhances Angiogenesis by Targeting Factor-Inhibiting HIF-1'. *Blood* 124 (25): 3748–57. https://doi.org/10.1182/blood-2014-05-576116.

Urbano, Ana M. 2021. 'Otto Warburg: The Journey towards the Seminal Discovery of Tumor Cell Bioenergetic Reprogramming'. *Biochimica et Biophysica Acta - Molecular Basis of Disease*. Elsevier B.V. https://doi.org/10.1016/j.bbadis.2020.165965.

Valadi, Hadi, Karin Ekström, Apostolos Bossios, Margareta Sjöstrand, James J. Lee, and Jan O. Lötvall. 2007. 'Exosome-Mediated Transfer of MRNAs and MicroRNAs Is a Novel Mechanism of Genetic Exchange between Cells'. *Nature Cell Biology* 9 (6): 654–59. https://doi.org/10.1038/ncb1596.

Vanterpool, Frankie A., Marco Cantini, F. Philipp Seib, and Manuel Salmerón-Sánchez. 2014. 'A Material-Based Platform to Modulate Fibronectin Activity and Focal Adhesion Assembly'. *BioResearch Open Access* 3 (6): 286–96. https://doi.org/10.1089/biores.2014.0033.

Vater, Corina, Philip Kasten, and Maik Stiehler. 2011. 'Culture Media for the Differentiation of Mesenchymal Stromal Cells'. *Acta Biomaterialia*. Elsevier Ltd. https://doi.org/10.1016/j.actbio.2010.07.037.

Vélez-Cruz, Renier, and David G. Johnson. 2017. 'The Retinoblastoma (RB) Tumor Suppressor: Pushing Back against Genome Instability on Multiple Fronts'. *International Journal of Molecular Sciences* 18 (8). https://doi.org/10.3390/ijms18081776.

Vienken J. 2008. 'TESTING BIOMATERIALS FOR APPLICATION IN ARTIFICIAL ORGANS: IMPACT OF PROCEDURES, DONOR AND PATIENT PROPERTIES'. *Contributions, Sec. Biol. Med. Sci* 2: 25–37.

Vinci, Maria, Carol Box, and Suzanne A. Eccles. 2015. 'Three-Dimensional (3D) Tumor Spheroid Invasion Assay'. *Journal of Visualized Experiments* 2015 (99). https://doi.org/10.3791/52686.

Vishnoi, Monika, Sirisha Peddibhotla, Wei Yin, Antonio T. Scamardo, Goldy C. George, David S. Hong, and Dario Marchetti. 2015. 'The Isolation and Characterization of CTC Subsets Related to Breast Cancer Dormancy'. *Scientific Reports* 5 (December). https://doi.org/10.1038/srep17533.

Walker, Nykia D., Jimmy Patel, Jessian L. Munoz, Madeleine Hu, Khadidiatou Guiro, Garima Sinha, and Pranela Rameshwar. 2016. 'The Bone Marrow Niche in Support of Breast Cancer Dormancy'. *Cancer Letters* 380 (1): 263–71. https://doi.org/10.1016/j.canlet.2015.10.033.

Wallace, Dorothy I., and Xinyue Guo. 2013. 'Properties of Tumor Spheroid Growth Exhibited by Simple Mathematical Models'. *Frontiers in Oncology* 3 MAR. https://doi.org/10.3389/fonc.2013.00051.

Wandinger-Ness, Angela, and Marino Zerial. 2014. 'Rab Proteins and the Compartmentalization of the Endosomal System'. *Cold Spring Harbor Perspectives in Biology* 6 (11): a022616. https://doi.org/10.1101/cshperspect.a022616.

Wang, Hong-xia, and Olivier Gires. 2019. 'Tumor-Derived Extracellular Vesicles in Breast Cancer : From Bench to Bedside'. *Cancer Letters* 460 (June): 54–64. https://doi.org/10.1016/j.canlet.2019.06.012.

Wang, Jianhua, Robert Loberg, and Russell S. Taichman. 2006. 'The Pivotal Role of CXCL12 (SDF-1)/CXCR4 Axis in Bone Metastasis'. *Cancer and Metastasis Reviews*. https://doi.org/10.1007/s10555-006-9019-x.

Wang, Leo D., and Amy J. Wagers. 2011. 'Dynamic Niches in the Origination and Differentiation of Haematopoietic Stem Cells'. *Nature Reviews Molecular Cell Biology*. https://doi.org/10.1038/nrm3184.

Wang, Lingling, Shizhen Zhang, and Xiaochen Wang. 2021. 'The Metabolic Mechanisms of Breast Cancer Metastasis'. *Frontiers in Oncology* 10 (January): 1–21. https://doi.org/10.3389/fonc.2020.602416.

Wang, Miao, and Randal J. Kaufman. 2016. 'Protein Misfolding in the Endoplasmic Reticulum as a Conduit to Human Disease'. *Nature*. Nature Publishing Group. https://doi.org/10.1038/nature17041.

Weiswald, Louis Bastien, Dominique Bellet, and Virginie Dangles-Marie. 2015a. 'Spherical Cancer Models in Tumor Biology'. *Neoplasia (United States)*. Neoplasia Press, Inc. https://doi.org/10.1016/j.neo.2014.12.004.

———. 2015b. 'Spherical Cancer Models in Tumor Biology'. *Neoplasia (United States)*. Neoplasia Press, Inc. https://doi.org/10.1016/j.neo.2014.12.004.

Whiteside, T. L. 2008. 'The Tumor Microenvironment and Its Role in Promoting Tumor Growth'. *Oncogene*. https://doi.org/10.1038/onc.2008.271.

Wiebe, J P, and C J Dinsdale. 1991. 'INHIBITION OF CELL PROLIFERATION BY GLYCEROL'. *Life Sciences*. Vol. 48.

Wise, David R, Ralph J Deberardinis, Anthony Mancuso, Nabil Sayed, Xiao-Yong Zhang, Harla K Pfeiffer, Ilana Nissim, et al. 2008. 'Myc Regulates a Transcriptional Program That Stimulates Mitochondrial Glutaminolysis and Leads to Glutamine Addiction'. www.pnas.org/cgi/content/full/.

Wishart, David. 2022. 'Metabolomics and the Multi-Omics View of Cancer'. *Metabolites* 12 (2). https://doi.org/10.3390/metabo12020154.

Witsch, Esther, Michael Sela, and Yosef Yarden. 2010. 'Roles for Growth Factors in Cancer Progression'. *Physiology* 25 (2): 85–101. https://doi.org/10.1152/physiol.00045.2009.

Wu, Rongrong, Masanori Oshi, Mariko Asaoka, Yoshihisa Tokumaru, Takashi Ishikawa, and Kazuaki Takabe. 2022. 'E12550 Publication Only Association of NR2F1, a Tumor Dormancy Marker, with Cancer Cell Proliferation and Lymph

Node Metastasis, and Expression in Cancer-Associated Fibroblasts in Breast Cancer'.

Xie, Feihu, Shi Feng, Huayu Yang, and Yilei Mao. 2019. 'Extracellular Vesicles in Hepatocellular Cancer and Cholangiocarcinoma'. *Annals of Translational Medicine* 7 (5): 86–86. https://doi.org/10.21037/atm.2019.01.12.

Xu, Feng, and Steven L. Teitelbaum. 2013. 'Osteoclasts: New Insights'. *Bone Research* 1 (1): 11–26. https://doi.org/10.4248/BR201301003.

Yakavets, Ilya, Aurelie Francois, Alice Benoit, Jean Louis Merlin, Lina Bezdetnaya, and Guillaume Vogin. 2020. 'Advanced Co-Culture 3D Breast Cancer Model for Investigation of Fibrosis Induced by External Stimuli: Optimization Study'. *Scientific Reports* 10 (1). https://doi.org/10.1038/s41598-020-78087-7.

Ye, Jun, Dang Wu, Pin Wu, Zhigang Chen, and Jian Huang. 2014. 'The Cancer Stemcell Niche: Cross Talk between Cancer Stemcells and Their Microenvironment'. *Tumor Biology*. Kluwer Academic Publishers. https://doi.org/10.1007/s13277-013-1561-x.

Yetkin-Arik, Bahar, Ilse M.C. Vogels, Patrycja Nowak-Sliwinska, Andrea Weiss, Riekelt H. Houtkooper, Cornelis J.F. Van Noorden, Ingeborg Klaassen, and Reinier O. Schlingemann. 2019. 'The Role of Glycolysis and Mitochondrial Respiration in the Formation and Functioning of Endothelial Tip Cells during Angiogenesis'. *Scientific Reports* 9 (1). https://doi.org/10.1038/s41598-019-48676-2.

Yin, Tong, and Linheng Li. 2006. 'Review Series The Stem Cell Niches in Bone'. *Journal of Clinical Investigation* 116 (5): 1195–1201. https://doi.org/10.1172/JCI28568.the.

Yixin Yao, Wei Dai. 2014. 'Genomic Instability and Cancer Yixin'. *J Carcinog Mutagen*. 5: 1–3. https://doi.org/10.4172/2157-2518.1000165.Genomic.

Yuan, Peng, Benling Xu, Chengzheng Wang, Chengjuan Zhang, Miaomiao Sun, and Long Yuan. 2016. 'Ki-67 Expression in Luminal Type Breast Cancer and Its Association with the Clinicopathology of the Cancer'. *Oncology Letters* 11 (3): 2101–5. https://doi.org/10.3892/ol.2016.4199.

Zajac, Olivier, Joel Raingeaud, Fotine Libanje, Celine Lefebvre, Dora Sabino, Isabelle Martins, Pétronille Roy, et al. 2018. 'Tumour Spheres with Inverted Polarity Drive the Formation of Peritoneal Metastases in Patients with Hypermethylated Colorectal Carcinomas'. *Nature Cell Biology* 20 (3): 296–306. https://doi.org/10.1038/s41556-017-0027-6.

Zhang, Xiang H.F., Mario Giuliano, Meghana V. Trivedi, Rachel Schiff, and C. Kent Osborne. 2013. 'Metastasis Dormancy in Estrogen Receptor-Positive Breast Cancer'. *Clinical Cancer Research* 19 (23): 6389–97. https://doi.org/10.1158/1078-0432.CCR-13-0838.

Zhang, Xuefeng, Shideh Kazerounian, Mark Duquette, Carole Perruzzi, Janice A. Nagy, Harold F. Dvorak, Sareh Parangi, and Jack Lawler. 2009. 'Thrombospondin-1 Modulates Vascular Endothelial Growth Factor Activity at the Receptor Level'. *The FASEB Journal* 23 (10): 3368–76. https://doi.org/10.1096/fj.09-131649.

Zhao, Shuang, S. Laura Chang, Jennifer J. Linderman, Felix Y. Feng, and Gary D. Luker. 2014. 'A Comprehensive Analysis of CXCL12 Isoforms in Breast Cancer1,2'. *Translational Oncology* 7 (3): 429–38. https://doi.org/10.1016/j.tranon.2014.04.001.

Zheng, Jie. 2012. 'Energy Metabolism of Cancer: Glycolysis versus Oxidative Phosphorylation (Review)'. *Oncology Letters*. https://doi.org/10.3892/ol.2012.928.

Zhou, Xiaohe, Tao Li, Yufei Chen, Nannan Zhang, Pengli Wang, Yingying Liang, Melissa Long, et al. 2019. 'Mesenchymal Stem Cell.Derived Extracellular Vesicles Promote the in Vitro Proliferation and Migration of Breast Cancer Cells through the Activation of the ERK Pathway'. *International Journal of Oncology* 54 (5): 1843–52. https://doi.org/10.3892/ijo.2019.4747.

Zhu, Jiajun, and Craig B. Thompson. 2019. 'Metabolic Regulation of Cell Growth and Proliferation'. *Nature Reviews Molecular Cell Biology*. Nature Publishing Group. https://doi.org/10.1038/s41580-019-0123-5.